# Investigating the human

# locus coeruleus-norepinephrine system

# *in vivo*:

## Discussions on the anatomy, involvement in cognition and clinical applications

**Klodiana Tona**

Designing of cover and chapters: Sofia Vasili

Cover synthesis: K.D. Tona

Printing: Ocelotos Publishing, 55 Vatatzi str., Athens Greece



ISBN: 978-960-564-970-8

This work was funded by a Consolidator Grant from the European Research Council (ERC; GA 283314-NOREPI). The funders had no role in study design, data collection and analysis, decision to publish, or preparation of the manuscript. The authors report no conflicts of interest.

# Investigating the human locus coeruleus-norepinephrine system *in vivo:* Discussions on the anatomy, involvement in cognition and clinical applications

Proefschrift

ter verkijging van

de graad van Doctor aan de Universiteit Leiden,

op gezag van Rector Magnificus, Prof.mr. C.J.J.M. Stolker

volgens besluit van het College voor Promoties

te verdedigen op donderdag10 September 2020

klokke: 11:15 uur

door

Klodiana Tona

geboren te Kamenitsa

in 1985

**Promotoren**

Prof. dr. S.T. Nieuwenhuis

Prof. dr. B.U. Forstmann

**Promotiecommissie**

Prof. dr. M. Mather (University of Southern California, USA)

Prof. dr. S.A.R.B. Rombouts

Dr. E.J. Hermans (Radboud University, The Netherlands)

*Στους γονείς και την οικογένεια μου.*

*Δεν υπάρχουν λόγια που να μπορούν να εκφράσουν την ευγνωμοσύνη και τον σεβασμό που τρέφω για αυτούς.*

*Ti printsãe shi soia amea.*

*Zboarãli nu-nj agiungu tas sã spun vrearea shi tinjia tsi lu port.*

*To my parents and family.*

*No words exist that could sufficiently describe the gratitude and respect I owe to them.*

*Aan mijn ouders en familie.*

*Er bestaan geen woorden die voldoende de dankbaarheid en het respect kunnen beschrijven dat ik ze verschuldigd ben.*

**Contents**

# Chapter 1

# General Introduction

## The LC-NE system: Functions and malfunctions

The neuromodulator norepinephrine (NE) is involved in multiple cognitive processes including attention, learning, and emotions, and has been shown to be disturbed in psychiatric and neurological disorders such as anxiety disorder, post-traumatic stress disorder (PTSD), Alzheimer's disease, and schizophrenia. Most of the NE released in the brain originates from the locus coeruleus (LC), a brainstem nucleus with noradrenergic projections to multiple brain regions. This neuroanatomical formation of the noradrenergic system makes it well suited to rapidly and globally modulate brain function in response to changes in the environment, when cognitive flexibility and increased attention are required, such as when confronted with an important or life-threatening stimulus. Arousal, vigilance and cognitive flexibility in these situations increase the chances of survival and prepare the organism for immediate action. Nonetheless, if this state of arousal and vigilance is prolonged, as it happens in cases of chronic stress, the same mechanism becomes problematic and can lead to disorders such as anxiety disorder and PTSD, instead of being beneficial for survival. Therefore the LC-NE system can be functional and promote survival or be malfunctional and convert into the driving mechanism behind a disorder.

## The LC-NE system: Norepinephrine

Norepinephrine (NE), also called noradrenaline, is a catecholamine that functions as a neurotransmitter, neuromodulator and hormone in the brain and body. In the brain, NE is produced mainly by the brainstem nucleus LC. Outside the brain, NE is used as a neurotransmitter by sympathetic ganglia located near the spinal cord or ganglia located in the chest, abdomen and other visceral organs (Hamill, Shapiro, & Vizzard, 2012) and is released into the bloodstream by the adrenal glands in the kidneys. The later provides the name to NE, given that "norepinephrine" (from Greek) and "noradrenaline" (from Latin) means "alongside the kidneys". Regardless of where it is released, NE binds to and activates adrenergic receptors located on the cell surface. As a "classical neurotransmitter", NE transfers information to the postsynaptic neuron. In addition, NE modulates effects produced by other neurotransmitters such as glutamate and gamma amino butyric acid (GABA), and it is this latter function that makes NE a "neuromodulator".

As a neurotransmitter, neuromodulator and hormone, NE plays a crucial role in the function of cognition and the sympathetic nervous system. Indeed, many sympathomimetic drugs (compounds which mimic the effects of endogenous agonists of the sympathetic nervous system) are used to treat high blood pressure (e.g., beta-blockers) but at the same time have effects on brain and cognition (e.g., beta-blockers can impede the consolidation or retrieval of traumatic memories; (Kroes et al., 2016; Lonergan, Olivera-Figueroa, Pitman, & Brunet, 2013).

## Norepinephrine: Structure, biosynthesis and receptor types

NE is synthesized from the amino acid tyrosine in the adrenal medulla and postganglionic neurons of the sympathetic nervous system. Tyrosine converts to dopamine mainly in the cytoplasm while dopamine converts to NE mainly inside the neurotransmitter vesicles (Musacchio, 1975). The metabolic pathway is:

Phenylalanine → Tyrosine → L-DOPA → Dopamine → Norepinephrine

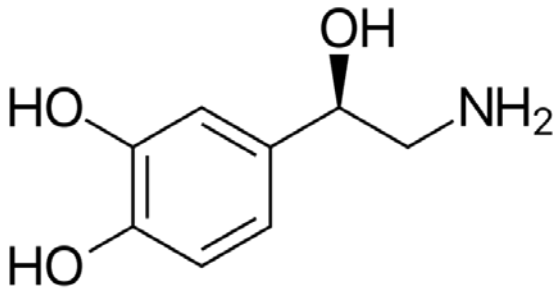


**Figure 1.** Chemical diagram of the structure of a norepinephrine molecule.

NE effects occur after its binding to noradrenergic receptors. To date, two receptor types have been identified: alpha receptors (divided into subtypes α1 and α2) and beta receptors (divided into subtypes β1, β2, and β3; Rang, 2014). All these receptors are G protein-coupled receptors. After its release, NE is cleared from the synaptic cleft by the NE transporter (NET). In **Chapter 6**, we use the NE transporter blocker atomoxetine in order to manipulate NE levels in healthy human participants.

**The central LC-NE system: The LC-NE system in the brain**

The LC is located in the brainstem, adjacent to the 4th ventricle. It is a bilateral structure, meaning that there are two LCs in the brain: one at each side of the floor of the 4th ventricle. Although there is a large interindividual variability regarding the exact size and location of the LC, it is estimated that the LC contains approximately 15,000 neurons in each hemisphere of a healthy adult brain (Mather, Clewett, Sakaki, & Harley, 2016). Although this size is as small as a grain of rice (Mouton, Pakkenberg, Gundersen, & Price, 1994), the LC has a substantial influence on brain function due to its wide, ascending, projections to forebrain and midbrain regions such as amygdala, thalamus, hippocampus, basal ganglia, the cortex, and the cerebellum (Aston-Jones, Foote, & Bloom, 1984). At the same time, the LC has connections to the spinal cord (Sara & Bouret, 2012). All these projections make the LC the dominant source of NE in the central nervous system (i.e., the brain and the spinal cord).

**The central LC-NE system: Connecting forebrain, midbrain, brainstem and the periphery**

The LC in the brain is activated in parallel with the autonomic system in the body. NE released in the forebrain facilitates attention, processing and cognitive flexibility. Central activation of neuromodulatory neurons in concert with peripheral arousal (related to LC via the spinal cord, the vagus nerve, the nucleus tractus solitarius (NTS), the PGi and

from the paraventricular nucleus of the hypothalamus) prepare the organism for a reorientation or reset of cortical networks and an adaptive response (Nieuwenhuis, De Geus, & Aston-Jones, 2011; Sara & Bouret, 2012; Valentino & Van Bockstaele, 2008).

In case of a confrontation with important stimuli or in situations of stress and fear, the high NE levels manifest both at a higher cognitive level by modulating forebrain regions involved in sensory processing, attention and vigilance, and at a more peripheral level, by preparing the body for the fight-and-flight response and controlling autonomic responses (Valentino & Van Bockstaele, 2008). In **Chapters 4, 5 and 6** we examine the involvement of the LC-NE system in higher-order cognition (cognitive flexibility and tasks that require attention and cognitive control) as well as its relation with peripheral measures (pupil dilation, cortisol, alpha-amylase). In addition, in **Chapter 6**, we use stress in order to manipulate NE levels in healthy human participants.

**LC-NE system in the periphery: The peripheral autonomic nervous system (the sympatho-adrenomedullary system)**

The peripheral autonomic nervous system (ANS) is activated in parallel to the centrally-acting LC-NE system and these two systems together co-ordinate the reaction of the brain and body, especially in stressful or threatening situations, when rapid reaction may be needed. The ANS is divided into a sympathetic system, which promotes action, and a parasympathetic system, which facilitates relaxation. These two sub-systems interact with each other and function in an antagonistic or (in some cases) in a synergetic fashion. Activation of the sympathetic limb of the sympatho-adrenomodulatory axis leads to increased levels of epinephrine (from the adrenal medula) and NE (from sympathetic nerve ends). Peripheral epinephrine acts on the central LC-NE system through activation of the vagal afferents to the NTS, and from there to the LC. Another pathway that might explain the relatively fast response of the LC is the input that the LC receives from the dorsal horn of the spinal cord (Cedarbaum & Aghajanian, 1978).

Except from the above-mentioned afferent pathways, there are also efferent pathways which send information from the LC towards brain nuclei and the periphery. The LC has an output to sympathetic and parasympathetic preganglionic neurons of the intermediolateral cell column of the spinal cord, and innervates other autonomic nuclei, such as the Edinger-Westphal nucleus, the paraventricular nucleus, the caudal raphe, and the rostroventrolateral medulla. The LC also projects to the dorsal and ventral horns of the spinal cord, respectively (Bouret & Sara, 2004; Hancock & Fougerousse, 1976; Jones & Yang, 1985; Leong, Shieh, & Wong, 1984; Samuels & Szabadi, 2008a). The parallel activation of the centrally acting LC-NE system and the ANS facilitate an organism's fast response to a stimulus (e.g., threat) and prepare the body for the relevant response (flight-or-fight; flight-or-fight; Sara & Bouret, 2012; Valentino & Van Bockstaele, 2008).

**LC-NE system in the periphery: The hypothalamic–pituitary–adrenal axis**

Aside from its involvement in ANS regulation, the LC is also involved in neuroendocrine function by projections to the neuroendocrine cells of the hypothalamic–pituitary–adrenal

(HPA) axis. The HPA axis is activated in parallel to the ANS but the activation of this system is slower and has longer-lasting effects. As part of this axis, the paraventricular nucleus of the hypothalamus is activated, which secretes corticotropin-releasing hormone and arginine vasopressin. These hormones act on the anterior pituitary to promote the secretion of adrenocorticotropic hormone, which stimulates the adrenal cortex to initiate the synthesis and release of corticosteroids (cortisol in humans; cortisol in humans; Oyola & Handa, 2017; van Bodegom, Homberg, & Henckens, 2017). In **Chapters 5 and 6**, we assess biomarkers and hormones involved in ANS and HPA-axis regulation (i.e., alpha-amylase and cortisol).

**LC-NE system in the periphery: The vagus nerve**

LC activity is also linked with that of the tenth cranial nerve (also called "the vagus nerve" – meaning "the nerve that wanders" in Latin). The vagus nerve is the longest nerve in our body and communicates the state of the viscera to the brain and vice versa. The vagus nerve innervates the brain and its auricular branch innervates the external auditory canal and parts of the external ear. In the rest of the body, the main part of the vagus nerve travels down and innervates the viscera (i.e., internal organs: heart, spleen, kidneys, liver, stomach, lungs, small intestines and colon; i.e., internal organs: heart, spleen, kidneys, liver, stomach, lungs, small intestines and colon; Berthoud & Neuhuber, 2000; Ruffoli et al., 2011; Waldman, 2009; Yuan & Silberstein, 2016). Importantly, the vagus nerve projects to the NTS, which in turn projects directly and indirectly to the LC (Berridge & Waterhouse, 2003). Animal studies have found that vagus nerve stimulation (VNS) increased the firing rate of NE neurons in the LC (Dorr & Debonnel, 2006; Raedt et al., 2011; Roosevelt, Smith, Clough, Jensen, & Browning, 2006), and increased NE levels in the prefrontal cortex (Follesa et al., 2007), basolateral amygdala (Hassert, Miyashita, & Williams, 2004), and cerebrospinal fluid (Martlé et al., 2015). Importantly, this increase in NE levels occurred in a dose-dependent manner, and returned to baseline after termination of VNS (Raedt et al., 2011; Roosevelt et al., 2006).

To date, activation of the vagus nerve happens invasively via a surgical procedure using a pacemaker-like device (vagus nerve stimulation, VNS) or non-invasively via the stimulation of the auricular brunch of the vagus nerve on the ear, using an iPod-like device (transcutaneous VNS, tVNS). In **Chapter 5** we use tVNS to monitor the noradrenergic, arousal-related effects of tVNS and validate the impact of this technique on the LC-NE system. In **Chapter 6**, we use tVNS at different levels of stimulation intensity in order to differentially manipulate NE levels in healthy human participants.

**LC-NE system in the periphery: Alpha-amylase, cortisol and pupil responses**

Adrenaline, noradrenaline and cortisol are the three major hormones that are secreted in situations of high arousal and elevated stress, and that are related to the LC-NE system (Bremner, 2006). The adrenergic and the corticosteroid systems influence each other as they are both part of the HPA axis, and part of systems that influence each other in

situations of high arousal and elevated stress—the sympathetic-adrenomedullary system and the HPA axis. This interaction has been presented in detail above.

As already mentioned, cortisol is a glucocorticoid stress hormone that correlates with HPA-axis activation (Bosch et al., 2009; Hill, Taylor, Harmer, & Cowen, 2003; Oyola & Handa, 2017; van Bodegom et al., 2017). Salivary cortisol is mediated by noradrenergic inputs to the hypothalamus (Bosch et al., 2009; Dunn, Swiergiel, & Palamarchouk, 2004; Hill et al., 2003) and is sensitive to pharmacologically induced changes in central NE activity (Chamberlain, Muller, Cleary, Robbins, & Sahakian, 2007; Warren, Wilson, et al., 2017). Thus, cortisol can index LC-NE activity. Salivary alpha-amylase (SAA) is a digestive enzyme that is released by the saliva glands in response to local sympathetic nervous system activity (Bosch, Veerman, de Geus, & Proctor, 2011). SAA is a proxy marker of sympathetic-adreno-medullary activation (Bosch et al., 2009; Bosch et al., 2011) and, given that this system is directly activated by central NE, SAA has been suggested as a biomarker of central NE activity (Ehlert, Erni, Hebisch, & Nater, 2006; Speirs, Herring, Cooper, Hardy, & Hind, 1974; van Stegeren, Rohleder, Everaerd, & Wolf, 2006; Warren, van den Brink, Nieuwenhuis, & Bosch, 2017). SAA secretion is increased during stress and correlates with blood plasma NE during arousing activities such as exercise (Bosch et al., 1996; Chatterton, Vogelsong, Lu, Ellman, & Hudgens, 1996).

In **Chapter 5** we assess levels of cortisol and SAA in order to monitor the noradrenergic, arousal-related effects of tVNS and validate the potential of this technique to modulate the LC-NE system. Consecutively, in **Chapter 6**, we asses cortisol and alpha-amylase as a biomarker of LC-NE activity after tVNS, a pharmacological, and a stress manipulation.

Studies of primates and rodents show that LC activity correlates with baseline pupil diameter (Joshi, Li, Kalwani, & Gold, 2016; Reimer et al., 2014) and the magnitude of task-evoked pupil dilations (Aston-Jones & Cohen, 2005; Joshi et al., 2016; Varazzani, San-Galli, Gilardeau, & Bouret, 2015). In line with this, fMRI studies in humans have shown that BOLD activity in the LC covaries with pupil size at rest and during simple decision-making tasks (de Gee et al., 2017; Murphy, Vandekerckhove, & Nieuwenhuis, 2014). The relationship between pupil size and LC may be mediated by activity in the rostral ventrolateral medulla, which projects to the LC and also innervates the peripheral sympathetic ganglia regulating the pupil (Nieuwenhuis, De Geus, et al., 2011). Based on these findings, many studies have used stimulus-evoked pupil dilation as an indirect measure of phasic activity of the human LC-NE system (e.g., Einhäuser, Stout, Koch, & Carter, 2008; Gilzenrat, Nieuwenhuis, Jepma, & Cohen, 2010; Jepma & Nieuwenhuis, 2010). We report pupil dilation as a biomarker of LC-NE activity after administration of a loud noise (accessory stimulus; **Chapter 4**) and after tVNS (**Chapter 5**).

In short, given that this dissertation aimed to investigate the LC-NE system in a holistic manner and from different perspectives, we assessed biomarkers in the body (periphery) that have been linked with the activation of the LC-NE system and its involvement in arousal, stress and cognition.

## LC-NE system in the brain & the periphery: Functions

The LC-NE system exerts its action in the brain and body via neuronal (electrical) but also neurochemical and hormonal pathways. It influences the brain via the connections it has with multiple brain regions, and it influences the periphery via the connections it has with other brainstem nuclei, the spinal cord, and the vagus nerve; but also due to the involvement of the LC-NE system in two systems that are well studied in the stress literature: the fast and rapidly activated peripheral ANS and the slower activated HPA axis. It therefore comes as no surprise that there is a great similarity between conditions that activate the LC in the brain and conditions that activate the sympathetic nervous system in the periphery: the LC mobilizes the brain for action while the sympathetic system mobilizes the body.

The LC-NE system is put into action to face environmental challenges, in parallel with the recruitment of the ANS, which responds to homeostatic challenges, stressors, and other stimuli that are important for the organism, and in turn determines general arousal level. The autonomic activation promotes the physiological response, whereas the LC promotes an efficient and appropriate cognitive response through its action in the forebrain. In this way, the LC-NE system plays and important role in cognition and in the orienting reflex, which includes physiological responses such as changes in pupil dilation and heart rate, activated by arousing or motivationally significant stimuli or unexpected changes in the environment (Nieuwenhuis, De Geus, et al., 2011; Pfaff, Martin, & Faber, 2012; Sara & Bouret, 2012).

A significant number of studies have aimed to illuminate these functions of the LC-NE system, but due to technical and anatomical challenges, a large part of this research has been limited to animal subjects or computational models. Research conducted in the context of this PhD dissertation aims to bridge the gap between animal studies and theoretical/computational frameworks by acquiring data in human subjects.

## Physiology: The LC exhibits two modes of activity

Studies in non-human primates have suggested that the LC has two distinct modes of discharge: a phasic and a tonic mode (Aston-Jones & Cohen, 2005). During bursts of phasic discharge, LC neurons fire in a highly synchronized manner as a consequence of direct electrical coupling between individual neurons of the LC (Ishimatsu & Williams, 1996). During the tonic discharge, the LC shows a constant background activity characterized by non-synchronicity, uncoupling, and random bursts (Usher, Cohen, Servan-Schreiber, Rajkowski, & Aston-Jones, 1999).

The two types of discharge influence each other in a way that the magnitude of phasic discharge is related to the level of ongoing tonic discharge. Phasic discharge is optimal at moderate levels of tonic discharge and is diminished in situations where tonic discharge is low (e.g., in slow-wave sleep) or when tonic discharge surpasses a moderate level (e.g., in stress; e.g. in stress; Aston-Jones, Rajkowski, & Cohen, 2000; Usher et al., 1999; Valentino & Van Bockstaele, 2008).

The two modes of discharge are related to different types of contexts and behavior. High phasic discharge in the LC is observed when the animal is shown a stimulus that is salient or motivationally significant. Strong tonic discharge occurs in situations of distractible behavior or stress. It has been suggested that there is an inverted-U relation between LC activity and task performance, similar to the classical Yerkes-Dodson relationship between arousal and performance (Aston-Jones, Rajkowski, & Cohen, 1999). Performance is poor at very low levels of LC tonic discharge when the organisms is non-alert. It becomes optimal at moderate LC tonic activity (phasic LC mode; when the phasic discharge is high but tonic is moderate). Finally, performance becomes poor at high levels of tonic LC activity (tonic mode, when tonic activity is high but phasic activity is diminished; Aston-Jones & Cohen, 2005; Aston-Jones et al., 1999).

The fact that the LC exhibits a dual mode of activity has inspired influential theories about how the LC-NE system affects cognition and behavior. These theories are briefly presented below.

**Theories regarding effects of the LC-NE system on cognition and behavior**

***The adaptive gain theory***

The adaptive gain theory suggests that the role of the LC is to regulate global neural gain in order to maximize utility in a given context. It does so by balancing the trade-off between tonic and phasic activity. For instance, by gradually shifting between tonic and phasic modes of activity, the LC regulates the trade-off between exploration and exploitation. The LC phasic mode promotes exploitative behavior by facilitating processing of task-relevant information (through the phasic response) but at the same time filtering out irrelevant stimuli (through relatively low tonic activity). In this mode, the organism is highly concentrated on the ongoing task and harvests rewards that this action offers. In contrast, the LC tonic mode promotes distractibility and disengagement from the task. This facilitates exploration and search for alternative, perhaps more productive, behaviors.

Thus, according to the adaptive gain theory, changes in the mode of LC activity orchestrate shifts in behaviors in line with environmental requirements, in order to maximize utility in a specific context (Aston-Jones & Cohen, 2005; Usher et al., 1999).

***The network reset theory***

As mentioned above, the LC-NE system is activated in response to salient stimuli. According to the network reset theory, when these stimuli are detected, the LC sends a phasic “reset” signal that reorganizes neural networks to facilitate behavioral and cognitive shifts in a way that promotes optimal behavioral performance (Hermans et al., 2011; Sara, 2009; Sara & Bouret, 2012). In **Chapter 5,** we test whether the LC-NE system is involved in cognitive shifts by assessing task switching, a pure form of cognitive flexibility.

### *The unexpected uncertainty theory*

Yu and Dayan (2005) suggest that NE signals unforeseen changes of task context, signaled by strongly unexpected observations. This 'unexpected uncertainty' originates from changes in environmental parameters that require an appropriate update of predictions about the environment, and thus a change in behavior. In contrast, according to this theory, the neuromodulator acetylcholine signals known ('expected') uncertainty in a given task context.

### *The glutamate amplifies noradrenergic effects (GANE) theory*

Based on the 'glutamate amplifies noradrenergic effects' (GANE) theory, the LC-NE system promotes neural representations of goal-relevant information through the 'ignition' of local hotspots that contain the neurotransmitter glutamate. High-priority perceptual representations are favored over low-priority representations due to the collaborating action and timely release of glutamate and phasic NE (Mather, Clewett, Sakaki, & Harley, 2015). Local glutamate–NE effects occur in parallel to more broad-scale actions, resulting in a "winner-takes-more / loser-takes-less" dynamic: high-priority items are even more likely to be remembered, whereas low-priority items are even more likely to be forgotten.

### *The LC-NE system and stress theory*

Although not falling under the category of a "typical" theory, work performed by Valentino and Van Bockstaele regarding the LC-NE system under stress, is very relevant for the research presented in this dissertation, and thus merits acknowledgement in this section. Valentino and Van Bockstaele (2008) draw a link between the dual modes of LC activity (tonic or phasic) and the stress context. Interactions between stress-related neurotransmitters that act on LC neurons regulate shifts between these modes of discharge in response to a stressor and make the LC-NE system a key player in behavioral and cognitive aspects of stress response.

During periods of elevated tonic LC activity, such as in life-threatening situations, phasic responses are diminished in order to facilitate a shift towards an exploratory mode. This response is optimal in a challenging environment and enhances chances for survival, so the ability of LC neurons to switch between phasic and tonic activity would be advantageous for rapidly modifying behavior in response to a stressor or after stress cessation.

The mode of LC activity is modulated by afferent, stress-released neurotransmitters, especially excitatory amino acids, corticotropin-releasing hormone and endogenous opioids secreted onto LC neurons. By biasing the activity of LC neurons towards a particular mode of discharge, these chemicals can favor advantageous behaviors in specific situations. On the other hand, LC neurons, through changes in their discharge rate, facilitate the cognitive and behavioral branches of the stress response.

The theories mentioned above, are to a large extent complementary to each other and extend the adaptive gain theory to different contexts and enriched perspectives. The theories agree that the LC-NE system promotes behavioral adaptation to the demands of the environment. However, each of them focuses on different mechanistic aspects of the way in which NE coordinates such behavioral adaptations.

**This dissertation: Holistic approach**

When studying brain and cognition, researchers tend to segregate the different parts in order to be able to study the system of interest, but it is important to always return to the holistic level in the end. The beauty of human cognition is that it functions by bringing different levels together in harmony and in a holistic approach: from cell, to synapse, from neuron to neuromodulatory networks, from central neuromodulators to hormones that are secreted in the body, from anatomy to physiology and cognition.

Therefore, this dissertation approaches human cognition and the study of the LC-NE system in a holistic manner. To this end, all chapters are written by taking into consideration theoretical knowledge about the LC-NE system with regard to brain anatomy, cognitive functions, neuromodulation (mainly NE), physiological responses, and clinical applications. Each chapter concentrates on one of these factors to a higher degree but all the other factors are also involved or assessed in some way. The first two chapters deal mainly with the anatomy of the LC, yet there is always a link with the other factors and especially the clinical application of MRI scans and LC integrity as a biomarker for neurological and psychiatric diseases. The last three chapters concentrate on cognition and physiology (pupil responses, P300 component of ERP), but always taking into consideration the structural connections of the LC-NE system. Finally, the last two chapters have a clinical approach and collectively deal with clinical applications of tVNS (medical device), alpha-amylase, cortisol, physiological responses, stress, and pharmacology.

Below there is a brief description of the next chapters and an introduction to the studies performed for this PhD dissertation, where a holistic approach in cognitive and clinical neuroscience is applied.

**Chapter 2: In vivo visualization of the locus coeruleus in humans: Quantifying the test-retest reliability**

Visualization of the LC has been based mainly on ex vivo material (i.e., material of donors after their death) because in vivo localization (in living humans) has been a very difficult enterprise. The reasons for this difficulty are technical and anatomical in nature.

Regarding the technical challenges, there is a need for specific technological advancements, and these have only recently taken place. Until recently the available MRI scans were not able to visualize small brainstem nuclei. This means that no matter how hard the researcher of the past would have tried to visualize and map the LC and other small brainstem nuclei in living humans, such an enterprise was simply impossible

because the timing was not right: one is dependent on technological advances and special MRI scans that require a long time to develop and implement in brain research.

Regarding the anatomical challenges, the LC is difficult to map due to its small size and big inter-individual variability in location and size. Additionally, it is located in parts of the brain that are very challenging to visualize in living humans with MRI scanners (i.e., located close to the vessels and the 4th ventricle that pulsate when blood or cerebrospinal fluid is rushing). This motion creates noise in the visualization in anatomical scans and is particularly problematic in the case of functional MRI (fMRI), which is more sensitive to such motion, rendering co-registration of functional and structural scans almost impossible. Additionally the cerebrospinal fluid running through the 4th ventricle might create noisy signal that can be wrongly perceived as genuine brain activity (i.e., the researcher is detecting noise originating from cerebrospinal fluid but thinks that it is BOLD activity). Finally, MRI research has mainly focused on the cortex and largely ignored the brainstem. Only recently there have been more advances towards this direction (Forstmann, de Hollander, van Maanen, Alkemade, & Keuken, 2017).

Recent developments in neuroimaging methods and scanning protocols have made possible the visualization of the LC by the adaptation of a T1-weighted turbo spin echo (TSE) scan sequence for 3T MRI, which is thought to be sensitive to neuromelanin (Keren et al., 2015; Sasaki et al., 2006), a pigment that is produced in catecholaminergic neurons and exists in large quantities in the LC (Fedorow et al., 2005).

Since the initial publication, numerous studies have used this scanning protocol for visualizing the LC in a variety of applications (Astafiev, Snyder, Shulman, & Corbetta, 2010; Clewett et al., 2016; Keren, Lozar, Harris, Morgan, & Eckert, 2009; Murphy, Vandekerckhove, et al., 2014; Sasaki et al., 2008; Takahashi et al., 2015). Importantly, given that LC dysfunction plays an important role in cognitive and neurodegenerative disorders, such as Parkinson's and Alzheimer's disease (Grudzien et al., 2007; Mravec, Lejavova, & Cubinkova, 2014) and monoamine-related psychiatric disorders such as anxiety, depression (Ressler & Nemeroff, 1999; Schramm, McDonald, & Limbird, 2001) and schizophrenia (van Kammen & Kelley, 1991), it has been suggested that TSE scans may be used as a diagnostic tool for tracking the progression of these disorders or as a biomarker for differential diagnosis. Importantly, this requires a reliable and robust scan protocol that allows delineation of the LC in a reproducible manner across different time points and by different raters/clinicians. Otherwise, there is risk of wrong diagnosis or fallacious treatment plan decisions, with possible deleterious effects for the patient. Aside from its use as a tool for monitoring pathological changes in LC structure, the TSE sequence is also used to identify the LC for region-of-interest analyses in fMRI studies. Both applications require that the contrast generation process is robust and reproducible, and that the scans allow accurate delineation of the LC. Despite its frequent use, to date no study has investigated the reproducibility and inter-observer variability of the LC masks identified using the TSE scan sequence.

In Chapter 2 we aimed to quantify the test-retest reliability of LC imaging by assessing stability of the TSE contrast of the LC across two independent scan sessions and by quantifying its intra- and inter-rater reliability. Additionally, we combined all TSE scans of our study and created a probabilistic LC atlas that quantifies the variability of this structure and can facilitate the spatial localization of the LC in standardized (MNI) space.

We found moderate reproducibility and scan-rescan stability, indicating that the localization and segmentation of the LC in vivo is a challenging, but reliable enterprise. However, clinical or longitudinal studies should be carried out carefully. Our probabilistic atlas results show substantial variability in the spatial location of the LC. In the current atlas (freely available from http://www.nitrc.org/projects/prob_lc_3t) we adopted a quantification approach, resulting in probabilistic information on where the LC is located. This information can, for instance, be used to weigh the measured fMRI signal with the probability of it originating from the LC. It is the first probabilistic atlas for the LC and one of the few attempts to map the brainstem, a field that deserves more attention and is promising to turn the brainstem from a "terra incognita" into a fully mapped and understood region in the future (Forstmann et al., 2017).

**Chapter 3: Paving the path for better visualization for the LC: Quantifying the contrast of the human locus coeruleus in vivo at 7 Tesla MRI.**

As discussed above, the important role that the LC plays in cognition and its use as a biomarker for assessment of neurodegenerative disorders necessitate accurate visualization of the LC. To date the most frequently used scan at 3T scanners is a T1-weighted TSE scan sequence (e.g., Betts, Cardenas-Blanco, Kanowski, Jessen, & Düzel, 2017; Clewett et al., 2016; de Gee et al., 2017; Keren et al., 2009; Liu et al., 2017). In Chapter 2, we made an attempt to assess the robustness of visualization of the LC at a 3T scanner using this TSE sequence. In Chapter 3, we made a step to further improve LC visualization by using an ultra-high field (7T) MRI scanner. We hypothesized that imaging at higher magnetic field strength might provide a solution to the challenges involved in LC imaging. Higher magnetic field strength increases signal-to-noise ratio and allows imaging at a higher spatial resolution (Cho et al., 2014; Sclocco, Beissner, Bianciardi, Polimeni, & Napadow, 2017; van der Zwaag, Schafer, Marques, Turner, & Trampel, 2016). This, in turn, results in smaller partial volume effects, which in itself can help to improve contrast and thereby detectability (de Hollander, Keuken, & Forstmann, 2015; Kneeland, Shimakawa, & Wehrli, 1986).

Additionally, we examined a number of sequences whose utility for LC imaging has been implied by prior literature. We measured the LC contrast in vivo for these 7T sequences and compared the obtained contrast measures to a frequently used sequence at 3T MRI.

The results indicate that several of the 7T sequences provide detectable contrast between the LC and surrounding tissue. Of the tested sequences, a T1-weighted sequence with spectral presaturation inversion recovery (SPIR) seems the most promising method for visualizing the LC at ultra-high-field MRI. This sequence provides similar contrast of the

LC as the 3T sequence commonly used, but at a higher spatial resolution and with isotropic voxels. The isotropic voxels at 7T are an important advantage given the small size of the LC. Finally, although there is no clear benefit in contrast, a potential advantage of using SPIR is the relatively short acquisition time, which may be desirable in clinical settings to minimize subject motion.

To conclude, in Chapter 3 we made a first step towards the improvement of visualization of the LC in a 7 Tesla MRI scanner. We are the first ones to compare these scan sequences in 7T and develop a TSE scan sequence version for the 7T. Future work can utilize this work and proceed to further development and improvement of MRI scans in order to achieve better visualization of the LC at 3 T, 7T and maybe higher magnetic field scanners.

**Chapter 4: The accessory stimulus effect is mediated by phasic arousal: a pupillometry study**

As highlighted above, the LC-NE system plays an important role in arousal. Different levels of induced arousal can have beneficial or detrimental effects on cognitive functioning and performance (usually according to an inverted U-shaped function; Yerkes & Dodson, 1908). A phenomenon that has been linked with arousal and positive cognitive performance is the accessory stimulus (AS) effect. It has been shown that people respond faster and more accurately in reaction time (RT) tasks when a visual imperative stimulus is immediately preceded by a task-irrelevant accessory stimulus (AS) presented in a different (e.g., auditory) perceptual modality, compared to when the imperative stimulus is presented alone. Although the information processing stage(s) that benefit from the AS remain debated, there seems to be a consensus that the AS effect is caused by a brief surge of arousal. Indeed, both pioneering and more recent studies have used the terms immediate arousal effect (Hackley & Valle-Inclán, 1999; Kiesel & Miller, 2007; Sanders, 1975) and automatic alertness/arousal (Posner, Klein, Summers, & Buggie, 1973) to refer to the AS effect. Despite the common inference that the AS effect is mediated by a phasic arousal response, there is only some indirect evidence to support this idea.

In Chapter 4, we exploited pupil dilation as a common index of phasic arousal (Beatty & Lucero-Wagoner, 2000) and LC activity (Joshi et al., 2016; Murphy, Vandekerckhove, et al., 2014; Varazzani et al., 2015) and examined its relationship with the AS effect. Participants carried out a demanding choice reaction time task with accessory stimuli occurring on 25% of the trials.

Results showed that participants exhibited the typical AS effect, and the accessory stimuli evoked a reliable early pupil dilation on top of the more protracted dilation associated with the imperative stimulus. Variation in reaction times on AS trials was selectively associated with pupil dilation during the early time window within which the AS had an effect, such that particularly large AS-evoked dilations were associated with especially fast responses. These results provide the first evidence for the long-standing assumption that the AS effect is mediated by AS-evoked phasic arousal.

**Chapter 5: The neuromodulatory and hormonal effects of transcutaneous vagus nerve stimulation as evidenced by salivary alpha-amylase, salivary cortisol, pupil diameter, and the P3 event-related potential**

As mentioned above, activity of the LC-NE system is linked to the activity of the vagus nerve, and the vagus nerve can be stimulated in an invasive and non-invasive manner. Invasive VNS is a promising treatment for depression (George & Aston-Jones, 2010; Nemeroff et al., 2006; Vonck et al., 2014) and epilepsy (Ellrich, 2011; Kraus et al., 2013) that likely exerts part of its therapeutic effect by increasing NE release from the LC. tVNS can be achieved by delivering electrical impulses to the auricular branches of the vagus nerve, which are situated close to the surface of the skin of the outer ear (Ellrich, 2011). fMRI studies in healthy humans demonstrate that tVNS elicits widespread changes in cortical and brainstem activity (Frangos, Ellrich, & Komisaruk, 2015; Kraus et al., 2007; Kraus et al., 2013; Yakunina, Kim, & Nam, 2017). In light of the clinical potential of tVNS, it would be valuable to establish if tVNS, like invasive VNS, affects NE, using relatively inexpensive and easy-to-use biomarkers of NE. In Chapter 5, we evaluate the effect of tVNS on NE levels using three accepted biomarkers and one putative biomarker of central NE activity: salivary alpha-amylase (SAA), salivary cortisol, pupil size, and the P3 component of the event-related brain potential (ERP), respectively.

The connection between LC-NE activity and SAA, salivary cortisol, and pupil size has been described above. Regarding the P3 component of the event-related brain potential, it has been suggested that the phasic changes in cortical NE levels are associated with the scalp-recorded P3 component (Chmielewski, Muckschel, Ziemssen, & Beste, 2017; De Taeye et al., 2014; Murphy, Robertson, Balsters, & O'Connell R, 2011; Neuhaus et al., 2007; Nieuwenhuis, Aston-Jones, & Cohen, 2005; Warren & Holroyd, 2012; Warren, Tanaka, & Holroyd, 2011; Wolff, Mückschel, Ziemssen, & Beste, 2018). Events that lead to increased phasic firing of the LC also lead to increased P3 amplitude (Nieuwenhuis et al., 2005). Noradrenergic drugs influence P3 amplitude in both animals (Swick, Pineda, & Foote, 1994) and humans (Brown et al., 2016; Brown, van der Wee, van Noorden, Giltay, & Nieuwenhuis, 2015; de Rover et al., 2015), and lesion of the LC eliminates the P3 in monkeys (Pineda, Foote, & Neville, 1987). Of interest here, the amplitude of the P3 is increased by invasive VNS (De Taeye et al., 2014; Neuhaus et al., 2007; Schevernels et al., 2016).

Despite the common inference that the tVNS effect, similarly to the invasive VNS effect, is mediated by increasing central NE activity, there is only some indirect, limited evidence to support this idea. To explore the claim that tVNS increases central NE, in Chapter 5 we assess SAA, salivary cortisol, pupil size and P3 amplitude across three experiments.

Results show that tVNS significantly increased SAA and salivary cortisol, but did not affect P3 amplitude nor pupil size. These findings suggest that SAA and cortisol, but not pupil size and P3 amplitude, can be used to monitor the arousal-related effects of tVNS.

## Chapter 6: Noradrenergic regulation of cognitive flexibility: No effects of stress, transcutaneous vagus nerve stimulation and atomoxetine on task-switching in humans

Cognitive flexibility allows us to adaptively switch between different responsibilities in important domains of our daily life. Previous work has suggested an important role for the LC-NE system in modulating several forms of cognitive flexibility, possibly by global modulation of gain and corresponding levels of decision noise (Aston-Jones & Cohen, 2005; Kane et al., 2017; Warren, Wilson, et al., 2017). However, it is still unknown whether NE levels are also critical for task switching (Kehagia, Cools, Barker, & Robbins, 2009; Kehagia, Murray, & Robbins, 2010), which requires the dynamic transformation of task-set representations from trial to trial.

In Chapter 6, we addressed this question by examining cued task-switching performance after manipulating activity of the LC-NE system using stress induction, tVNS at moderate and high intensity, and administration of the selective NE blocker atomoxetine.

None of the manipulations affected cognitive flexibility, leaving the size of the switch costs and the preparation effect unaffected. The findings were highly consistent, suggesting that NE is not involved in the cognitive flexibility required to switch between relatively abstract rules and sets of stimulus-response mappings. Task-switching performance reflects a complex mix of cognitive control and bottom-up dynamics of task-set representations. Our findings suggest that NE does not affect either of these aspects of cognitive flexibility.

Although stress induction, tVNS and atomoxetine also affect other neuromodulator systems, and the three manipulations do not affect the LC-NE system in a similar way, if task switching is crucially dependent on activity of the LC-NE system, one would expect effects of (some of) these manipulations on task switching performance – which we did not find.

# Chapter 2

# In vivo visualization of the locus coeruleus in humans: Quantifying the test-retest reliability

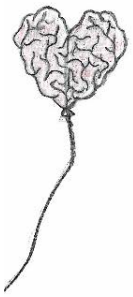

This chapter is published as: Tona, K.D., Keuken, M.C., de Rover, M., Lakke, E., Forstmann, B.U., Nieuwenhuis, S., & van Osch, M.J.P. (2017). In vivo visualization of the locus coeruleus in humans: Quantifying the test-retest reliability. Brain Structure and Function, 222, 4203-4217.

**Abstract**

The locus coeruleus (LC) is a brainstem nucleus involved in important cognitive functions. Recent developments in neuroimaging methods and scanning protocols have made it possible to visualize the human LC in vivo by utilizing a $T_1$-weighted turbo spin echo (TSE) scan. Despite its frequent use and its application as a biomarker for tracking the progress of monoaminergic-related neurodegenerative diseases, no study to date has investigated the reproducibility and inter-observer variability of LC identification using this TSE scan sequence. In this paper, we aim to quantify the test-retest reliability of LC imaging by assessing stability of the TSE contrast of the LC across two independent scan sessions and by quantifying the intra- and interrater reliability of the TSE scan. Additionally, we created a probabilistic LC atlas which can facilitate the spatial localization of the LC in standardized (MNI) space. Seventeen healthy volunteers participated in two scanning sessions with a mean intersession interval of 2.8 months. We found that for intra-rater reliability the mean Dice coefficient ranged between 0.65 and 0.74; and inter-rater reliability ranged between 0.54 and 0.64, showing moderate reproducibility. The mean LC contrast was 13.9% (*SD* 3.8) and showed scan-rescan stability (ROI approach: ICC = 0.63; maximum intensity approach: ICC = 0.53). We conclude that localization and segmentation of the LC in vivo is a challenging, but reliable enterprise, although clinical or longitudinal studies should be carried out carefully.

## Introduction

Recent developments in neuroimaging methods and scanning protocols have made possible what had been challenging for many years: the visualization of the human brainstem nucleus locus coeruleus (LC) in vivo. The LC is a small nucleus in the brainstem involved in a range of important cognitive functions. The visualization of the LC has been made possible by the adaptation of a $T_1$-weighted turbo spin echo (TSE) scan sequence for 3-Tesla MRI, which is thought to be sensitive to neuromelanin (Keren et al., 2015; Sasaki et al., 2006). Neuromelanin is a pigment that is produced in catecholaminergic neurons and exists in large quantities in the LC (Fedorow et al., 2005). With this adapted TSE sequence, a hyperintense signal was observed in locations closely corresponding to the bilateral LC in the upper pontine tegmentum (Naidich et al., 2009; Sasaki et al., 2006).

Since the initial publication, numerous studies have used this scanning protocol for visualizing the LC in a variety of applications (Astafiev et al., 2010; Clewett et al., 2016; Keren et al., 2009; Murphy, O'Connell, O'Sullivan, Robertson, & Balsters, 2014; Sasaki et al., 2008; Takahashi et al., 2015). Importantly, given that LC dysfunction plays an important role in cognitive and neurodegenerative disorders, such as Parkinson's and Alzheimer's disease (Grudzien et al., 2007; Mravec et al., 2014), multiple system atrophy, and monoamine-related psychiatric disorders such as depression (Ressler & Nemeroff, 1999; Schramm et al., 2001) and schizophrenia (van Kammen & Kelley, 1991), it has been suggested that TSE scans may be used as a diagnostic tool for tracking the progression of these disorders (Matsuura et al., 2013; Ohtsuka et al., 2013; Sasaki et al., 2008; Sasaki et al., 2006; Takahashi et al., 2015), as a biomarker for the efficacy of attention-related pharmaceutical treatments (Keren et al., 2009) or as a biomarker for differential diagnosis of parkinsonian disorders (e.g. differentiate Parkinson's disease from multiple system atrophy) (Matsuura et al., 2013). Importantly, this requires a reliable and robust scan protocol that allows delineation of the LC in a reproducible manner across different time points and by different raters/clinicians. Otherwise, there is risk of wrong diagnosis or fallacious treatment plan decisions, with possible deleterious effects for the patient. Aside from its use as a tool for monitoring pathological changes in LC structure, the TSE sequence is also used to identify the LC for region-of-interest (ROI) analyses in functional MRI studies. Both applications require that the contrast generation process is robust and reproducible, and that the scans allow accurate delineation of the LC. However, despite its frequent use, to date no study has investigated the reproducibility and inter-observer variability of the LC masks identified using the TSE scan sequence.

We aimed to quantify the test-retest reliability of LC imaging by assessing stability of the TSE contrast of the LC across two independent scan sessions and by quantifying its intra- and interrater reliability. Additionally, we combined all TSE scans of our study and created a probabilistic LC atlas that quantifies the variability of this structure and can facilitate the spatial localization of the LC in standardized (MNI) space. This

complements the LC map previously developed by Keren and colleagues (Keren et al., 2009), which is only based on the voxels with maximum signal intensity.

## Methods

### *Participants*

Seventeen healthy volunteers (10 females; age range: 19-24 years; mean age = 20.9 years; SD = 1.7) participated in two scanning sessions with a mean intersession interval of 2.8 months. Only healthy, right-handed participants without a history of neurological or psychiatric problems were included (based on self-report questionnaires). The study was approved by the medical ethics committee of the Leiden University Medical Center. All participants gave written informed consent prior to their inclusion in the study, and received monetary compensation for their participation.

### *MRI acquisition parameters*

During both MRI scan sessions, the participants underwent a whole-brain 3D $T_1$-weighted (Grabner et al., 2006) and a brainstem-zoomed $T_1$-weighted turbo spin echo (TSE) structural scan (Sasaki et al., 2006) in a 3 Tesla-TX Philips scanner equipped with a 32-channel head coil. The whole-brain volume (field of view (FOV): 224 x 177.33 x 168 mm; 140 slices; 0.87 x 0.87 x 1.2 mm; TR: 9.7ms; TE: 4.5 ms; flip angle $8^o$; acquisition matrix: 192 x 152; scan duration: 4.9 min) was used to facilitate co-registration between scan sessions and subsequent normalization to the standard 0.5-mm MNI template. The TSE scan sequence was used to detect the LC and had similar sequence parameters as the ones reported in prior literature (FOV: 180 x 180 x 22.95 mm; 14 slices; reconstruction resolution 0.35 x 0.35 x 1.5 mm, gap of 10%; TSE factor: 3; TR: 500 ms; TE: 10 ms; flip angle $90^o$; acquisition matrix: 256 x 204; scan duration: 7 min) (see Figure 1 for an example).

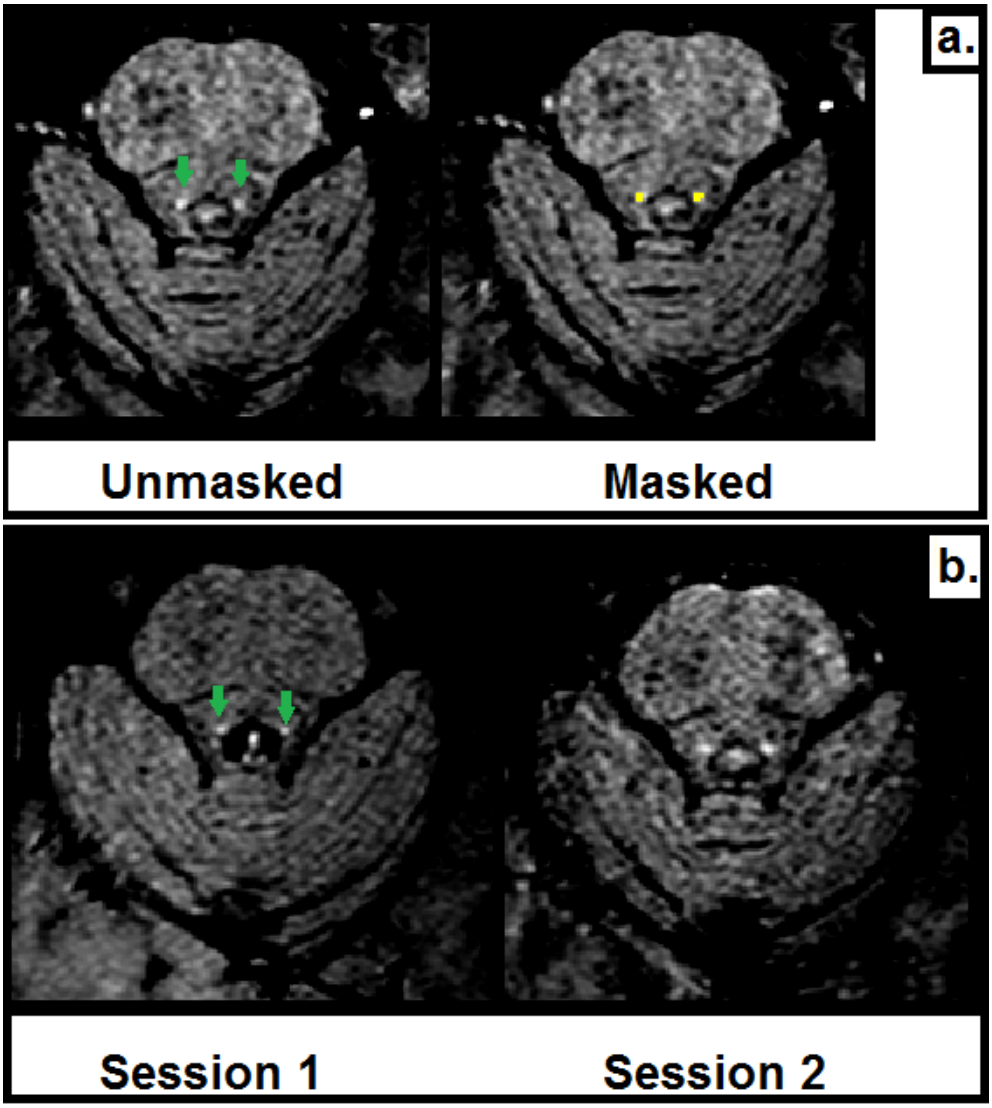


**Figure 1.** A) Example TSE scan (right and left LC) from one participant in the same session with (right image) and without (left image) the manually segmented LC mask overlaid. B) Example TSE scans (right and left LC) from one participant in session 1 and session 2. Green arrows indicate the LC.

### *Segmentation protocol*

Before segmentation started, the data was first anonymized by replacing the participant identifier by a random number. The LC was then manually segmented twice on the TSE images by two independent raters using FSLview (FSL 5.0.8; Smith et al., 2004). The interval between segmentation 1 and segmentation 2 was at least two weeks. The two raters performed the parcellation after being trained by a neuroanatomist and by using a rigorous parcellation protocol (see Appendix below for details). The order of segmentation was randomized between raters and across segmentation sessions. A similar protocol was used for the parcellation of the middle cerebral peduncle (brachium pontis; MCP) which functioned as control ROI for the contrast analysis, with the only difference that parcellation was performed by only one rater and that the LC masks were overlaid while segmenting the control ROI to guarantee that the control ROI was included on all slices in which the LC was present. To make sure that the control ROI captured as much

variance as possible, the MCP mask consisted of approximately double the number of voxels of the LC ROI. The MCP was chosen as a control ROI because it is a large structure, extends to both the left and right side of the brainstem, and is a relatively homogeneous region of voxels that show a signal intensity comparable to surrounding tissue of the LC.

*Registration to standard stereotactic MNI space*

All registration steps were performed using FSL (5.0.8.; Jenkinson, Beckmann, Behrens, Woolrich, & Smith, 2012). Figure 2 provides an overview of the employed registration pipeline. First, the TSE slab volumes were linearly registered to the $T_1$-weighted whole-brain volume using FLIRT by means of correlation ratio, 6 degrees of freedom, and trilinear interpolation. The linearly registered TSE slabs were then non-linearly optimized to the $T_1$ whole-brain volume using the standard settings in FNIRT. To avoid nonlinear misregistration due to the smaller coverage of the TSE scan in the slice selection direction ("z-direction"), the $T_1$ whole-brain volume was masked in the z-direction. This was done by first masking the $T_1$ whole-brain volume with the linearly registered TSE volume. The masked $T_1$ volume was subsequently binarized and dilated with a box kernel of 9 voxels in width, centered on each voxel. This resulted in a binary mask which was used to mask the original $T_1$ whole-brain volume, resulting in a $T_1$ reduced FOV. Visual inspection of the individual registrations suggested that this procedure resulted in a good correspondence across scan sessions.

The $T_1$ whole-brain volumes were linearly registered to the MNI 0.5-mm template using correlation ratio and 12 degrees of freedom. The linearly registered $T_1$ whole-brain volume was then non-linearly optimized to the MNI 0.5-mm template using the standard settings in FNIRT. All registrations were visually inspected in FSLview. For the TSE slab volume to $T_1$ whole brain volume registration the following landmarks were checked for alignment: fourth ventricle floor, the top indentation of the pons, and the bilateral cerebellar superior peduncle. The landmarks that were additionally checked for the $T_1$ whole brain to MNI registration were the corpus callosum and the lateral ventricles.

All LC masks were transformed to either whole-brain or standard MNI space by combining the linear transformation matrices with the non-linear deformation fields to reduce the number of interpolations.

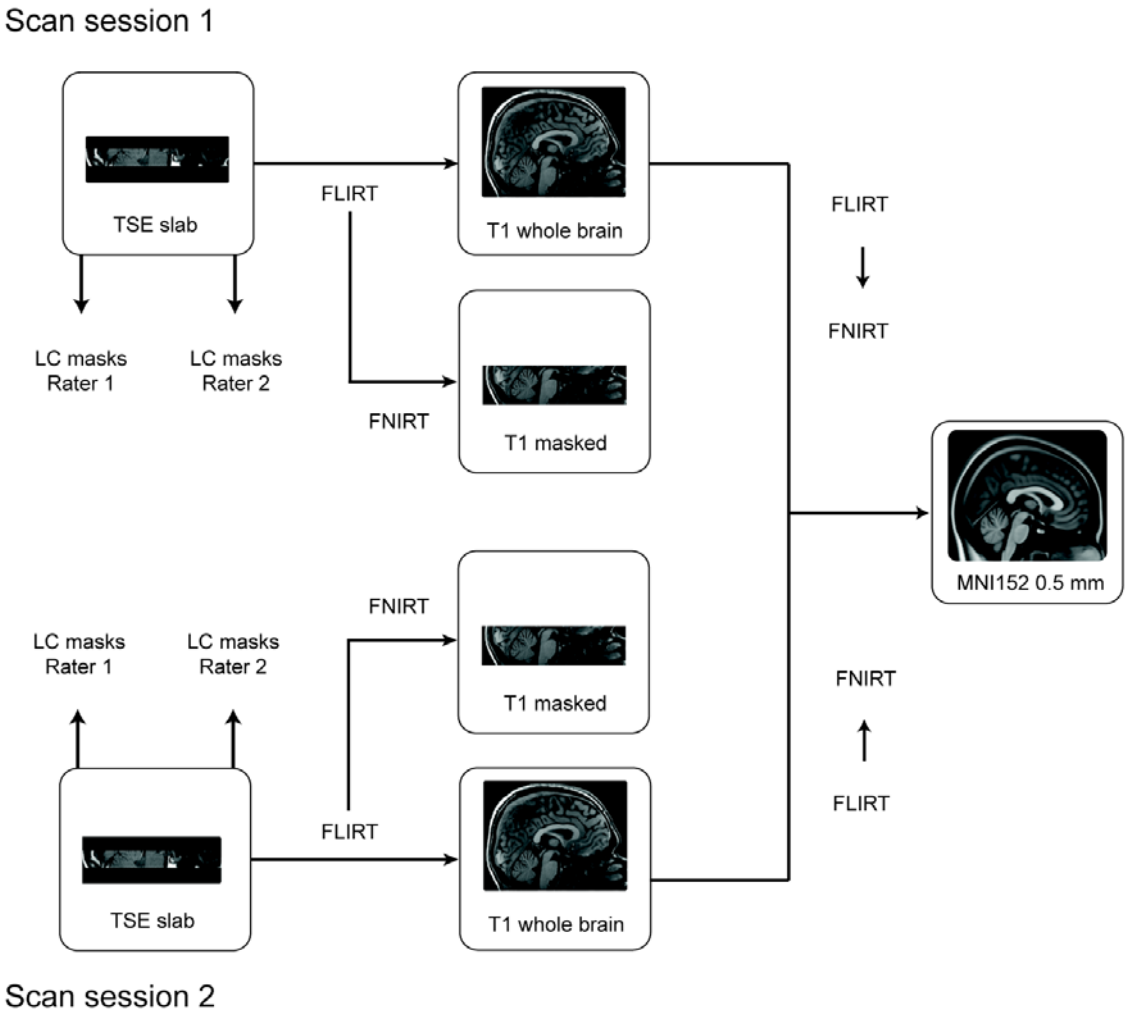


**Figure 2.** Overview of the registration protocol. The TSE slab was linearly registered to the T1 whole-brain volume, after which the TSE slab was nonlinearly optimized to the cropped T1 volume. The T1 whole-brain volume was first linearly and then non-linearly registered to the MNI 0.5-mm template. The LC masks were directly registered to MNI space by combining the linear transformation matrix and non-linear warp field. The arrows show the registration steps conducted to transfer the individual masks into MNI standard space.

*Creation of the probabilistic LC atlas in MNI space*

Given the small size and anatomical variability in size and location, it is crucial that an LC atlas incorporates this variability (Fernandes, Regala, Correia, & Goncalves-Ferreira, 2012). Previous work by Keren et al. (2009) resulted in an LC atlas, but this was based on a non-homogeneous group in terms of age, the LC was identified by extracting slice-wise the voxel with the maximum intensity in each slice, and the atlas does not contain probabilistic information. Instead we used the conjunction masks of the LC (over observers, scan and segmentation sessions), based on a homogeneous group which is more representative of most experimental studies in psychology and neuroscience (Chiao, 2009; Henrich, Heine, & Norenzayan, 2010), adopted a ROI segmentation approach, and preserved the probabilistic information at the spatial level. The probabilistic atlas was created by adding the individual conjunction masks, which were registered to MNI space

in a similar way as in previous work (Keuken & Forstmann, 2015). The intensities in the resulting probability atlas indicate the amount of spatial overlap in the LC across participants.

***LC volume estimates***

All volume estimations of the LC were carried out in native TSE space and were based on different levels of strictness. We report volume estimates based on the segmentations of the individual raters ("entire LC volume"). In addition, we report volume estimates based on the conjunction masks ("conjunction volume"). These conjunction masks are considerably more conservative because they only incorporate the voxels that both raters agreed upon.

***Reproducibility of measured contrast***

*ROI analysis:* The average LC signal intensity was extracted per hemisphere from the conjunction LC masks using the FSL Utilities toolbox (5.0.8.; Jenkinson et al., 2012). Mean signal intensity of the MCP was taken as an internal calibration measurement (control ROI). Subsequently, the contrast of the LC (from now on called "$LC_{contrast\ ratio}$") was calculated per hemisphere based on the following relative contrast formula: $LC_{contrast\ ratio} = [(SI_{LC} - SI_{MCP}) / SI_{MCP}]$ (Haacke & Brown, 2014) where $SI_{LC}$ and $SI_{MCP}$ refer to the mean signal within the LC and the MCP ROIs, respectively.

*Maximum intensity voxel analysis:* Since the mean signal intensity in the ROI depends on the selected ROI which was manually drawn on the same images and is therefore in itself dependent on the contrast in the images, a maximum intensity voxel analysis was used as an additional, alternative method for measuring the contrast. This approach, which mirrors prior literature (Keren et al., 2009), is less conservative and less dependent on the LC boundary definition but also less robust in terms of statistics. For this analysis, the same formula for contrast assessment was employed as above, but now using the peak voxel intensity of the right LC, left LC, and MCP, respectively (i.e., maximum intensity within the ROI). For the MCP, the maximum intensity voxel was taken from the same slice as that containing the maximum LC voxel intensity.

***Statistical analyses***

Statistical analyses were conducted using R (version 3.2.4; R Development Core Team, 2008) and SPSS software (version 23; IBM Corp. Armonk, NY). The segmentation protocol resulted in a total of 272 LC masks (17 participants x 2 scan sessions x 2 bilateral LC masks x 2 segmentation sessions x 2 raters), which led to the calculation of the following reliability measures:

a) inter-rater reliability between rater 1 and rater 2 (first segmentation session)

b) inter-rater reliability between rater 1 and rater 2 (second segmentation session)

c) intra-rater reliability for rater 1 (first and second segmentation session)

d) intra-rater reliability for rater 2 (first and second segmentation session).

*Inter-rater reliability and volume estimates*

Dice's coefficient (Dice, 1945) and the conjunction volume in $mm^3$ of the LC-segmented masks were used as indices of the inter- and intra-rater reliability. To assess intra-rater reliability, the Dice coefficients and the volume values expressing the difference between segmentation sessions 1 and 2 were analyzed using repeated-measures ANOVAs with rater (rater 1 vs. rater 2), scan session (first vs. second), segmentation session (first vs. second), and hemisphere (left vs. right) as within-subject factors. To assess inter-rater reliability (volume of the overlap between segmentations of rater 1 and 2), the relevant Dice coefficients and volume values were analyzed using repeated-measures ANOVAs with scan session (first vs. second), segmentation session (first vs. second), and hemisphere (left vs. right) as within-subject factors.

*The entire volume estimates*

For the entire LC mask estimates, volume values were analyzed using repeated-measures ANOVAs with rater (first vs. second), scan session (first vs. second), segmentation session (first vs. second), and hemisphere (left vs. right) as within-subject factors.

Data were controlled for equality of error variance and Greenhouse-Geisser correction was applied whenever the assumption of sphericity was violated. In these cases, we report corrected *p* values and uncorrected degrees of freedom.

*Reproducibility of LC contrast*

First, it was tested whether the LC indeed provided positive contrast with respect to the surrounding tissue. To this end, groupwise distributions for each term were subjected to one-sample t-tests (two-tailed) to test whether they were significantly different than 1 at the group level. Subsequently, for both the ROI analysis and the maximum-intensity analysis, the following analyses were performed: first, the mean and intensity range of the contrast were determined for the left and right LC, separately for sessions 1 and 2. Second, the correlation between the contrasts of the left and right LC was determined. And finally, the intraclass correlation coefficient (ICC) was calculated to assess test-retest reliability. The ICC was calculated using a two-way mixed model with measures of absolute agreement (McGraw & Wong, 1996).

## Results

### *Dice coefficient*

For two participants one or more Dice coefficients were zero. These participants were excluded from the intensity analyses given that not all conjunction masks were available.

For intra-rater reliability the mean Dice coefficient for the different scans, segmentation sessions and hemispheres ranged between 0.65 and 0.74; inter-rater reliability ranged between 0.54 – 0.64, showing moderate reproducibility (see Table 1 for the Dice

coefficients). The intra-rater reliability did not differ between raters ($F_{(1,16)}$ = 0.07, $p$ = 0.79), scan sessions within the same participant ($F_{(1,16)}$ = 0.67, $p$ = 0.42), and hemispheres ($F_{(1,16)}$ = 0.65, $p$ = 0.43), nor was there any interaction between these variables. Likewise, inter-rater reliability did not differ between scan sessions ($F_{(1,16)}$ = 0.90, $p$ = 0.36), segmentation session ($F_{(1,16)}$ = 1.54, $p$ = 0.23), and hemispheres ($F_{(1,16)}$ = 0.45, $p$ = 0.51), nor was there any interaction between these variables.

***LC volume***

The volume of the individual segmented LC masks had a mean of 9.53 $mm^3$ (SD 3.83 $mm^3$) and ranged between 0.82 – 25.29 $mm^3$. The mean volume was 7.96 $mm^3$ (range 3.26 $mm^3$ – 14.28 $mm^3$) for rater 1 and 11.11 $mm^3$ (range 0.82 $mm^3$ – 25.29 $mm^3$) for rater 2. The largest LC mask volume reported across all sessions and raters was 25.29 $mm^3$ and the smallest 0.82 $mm^3$. The LC volume was stable across scan sessions ($F_{(1,16)}$ = 0.10, $p$ = 0.92). There were, however, significant main effects of rater ($F_{(1,16)}$ = 27.55, $p$ < 0.001), segmentation session ($F_{(1,16)}$ = 5.29, $p$ = 0.035), and hemisphere ($F_{(1,16)}$ = 6.19, $p$ = 0.024). The volumes of the LC of rater 2 were consistently larger than those of rater 1, rater 1 became more stringent during the second segmentation session (i.e., decreasing the volume of the LC mask), and the right hemisphere (mean 9.91 $mm^3$; SD 3.81) was larger than the left (9.15; SD 3.82). Similar results were found when looking at the conjunction volume, except for the fact that the intra-rater volume estimates of the LC were stable across scan sessions ($F_{(1,16)}$ = 0.08, $p$ = 0.78) and hemispheres ($F_{(1,16)}$ = 0.88, $p$ = 0.36). Finally, the inter-rater volumes of the LC did not differ between scan sessions ($F_{(1,16)}$ = 0.10, $p$ = 0.75), segmentation sessions ($F_{(1,16)}$ = 2.24, $p$ = 0.15), and hemispheres ($F_{(1,16)}$ = 4.38, $p$ = 0.53) for the conjunction volume.

**Table 1.** The mean (SD) conjunction volume in $mm^3$ and Dice coefficient of the LC inter- and intra-rater masks.

| | | Segmentation session | Scan session | Conj.Volume $mm^3$ | Dice coefficient |
|---|---|---|---|---|---|
| Inter-rater | Left | 1 | 1 | 5.78 (2.11) | 0.60 (0.15) |
| | Right | 1 | 1 | 6.31 (1.98) | 0.63 (0.14) |
| | Overall | 1 | 1 | 6.05 (2.03) | 0.62 (0.14) |
| | Left | 1 | 2 | 5.60 (2.94) | 0.54(0.25) |
| | Right | 1 | 2 | 6.54 (2.82) | 0.58 (0.18) |
| | Overall | 1 | 2 | 6.07 (2.87) | 0.56 (0.21) |
| | Left | 2 | 1 | 5.55(1.69) | 0.62(0.13) |
| | Right | 2 | 1 | 6.20 (1.74) | 0.64 (0.14) |
| | Overall | 2 | 1 | 5.88 (1.72) | 0.63 (0.13) |
| | Left | 2 | 2 | 5.41(1.94) | 0.62(0.19) |
| | Right | 2 | 2 | 5.58 (1.85) | 0.58 (0.18) |
| | Overall | 2 | 2 | 5.49 (1.87) | 0.60 (0.18) |
| Intra-rater 1 | Left | 1-2 | 1 | 5.34 (1.25) | 0.69 (0.08) |
| | Right | 1-2 | 1 | 6.14 (1.16) | 0.73 (0.09) |
| | Overall | 1-2 | 1 | 5.74 (1.26) | 0.71 (0.09) |
| | Left | 1-2 | 2 | 5.21 (1.79) | 0.68 (0.19) |
| | Right | 1-2 | 2 | 5.65 (2.19) | 0.67 (0.20) |
| | Overall | 1-2 | 2 | 5.43 (1.98) | 0.68 (0.19) |
| Intra-rater 2 | Left | 1-2 | 1 | 8.17 (3.57) | 0.74 (0.15) |
| | Right | 1-2 | 1 | 7.76 (3.08) | 0.68 (0.17) |
| | Overall | 1-2 | 1 | 7.97 (3.29) | 0.71 (0.16) |
| | Left | 1-2 | 2 | 7.71 (3.31) | 0.68 (0.23) |
| | Right | 1-2 | 2 | 8.18 (3.14) | 0.65 (0.19) |
| | Overall | 1-2 | 2 | 7.95 (3.19) | 0.66 (0.21) |

### *Probabilistic atlas of the LC*

The overlap of the LC masks across participants was calculated using the non-linearly optimized inter-rater masks in MNI space (following following following following Diedrichsen et al., 2011). The values in the resulting probability atlas indicate for each voxel the percentage of participants for which that voxel contained the segmented LC. The maximum percentage overlap varied across segmentation and scan sessions and ranged between 28% and 36% (mean: 33%; SD: 3.2; see Figure 3 for an overview of LC probability atlas). The non-linear atlases of the LC per scan session are freely available (www.nitrc.org/projects/prob_lc_3t; reviewers can have access to the atlas already by following this link: https://www.dropbox.com/s/7h33nlnho5mxsid/LC_prob_atlas_mni05.zip?dl=0).

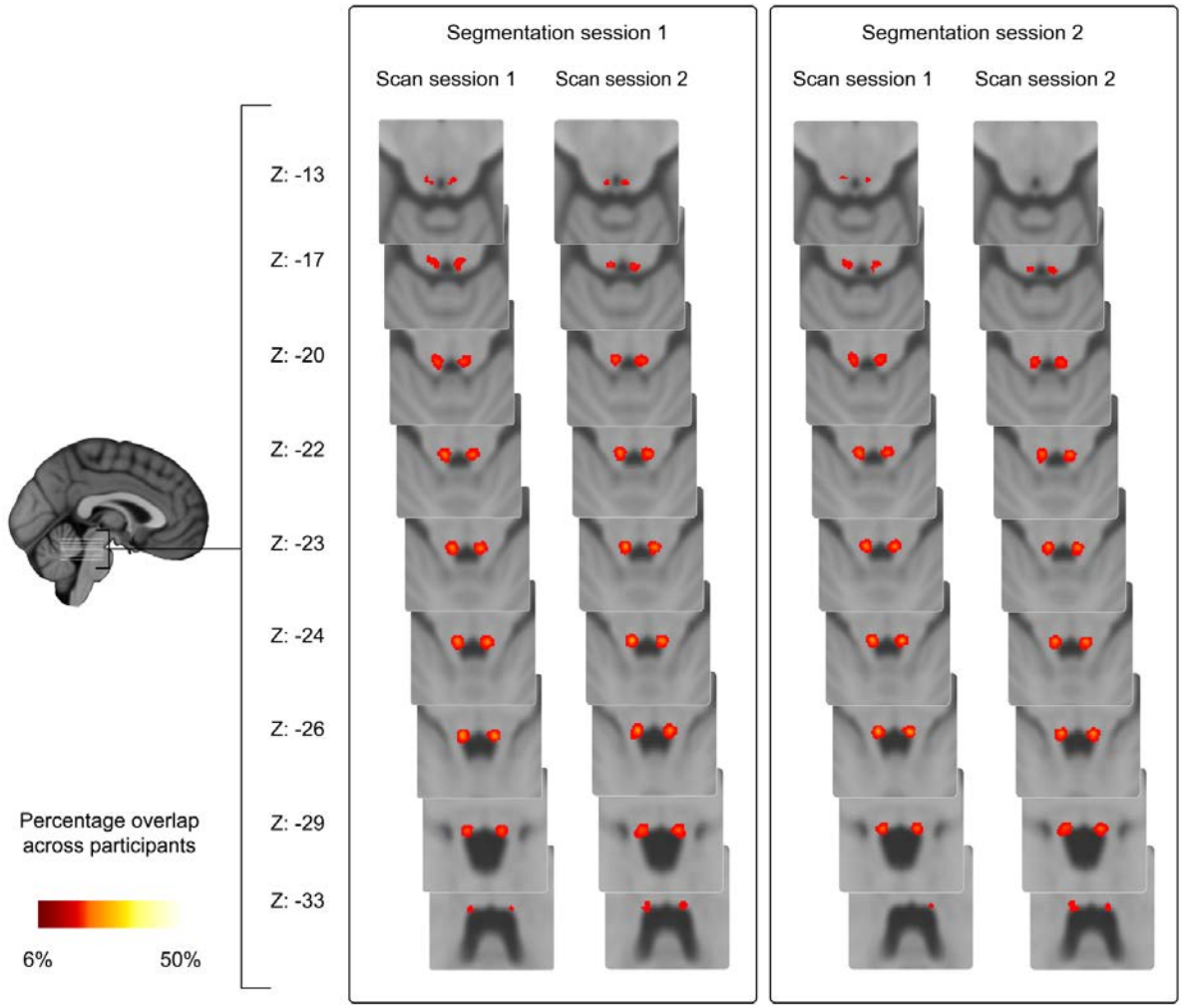


**Figure 3.** Overview of LC probability atlas. The color intensity indicates the percentage overlap across the 17 participants. The z coordinates are in MNI space

### *Test-retest reliability of the MRI contrast*

Control analyses showed that the $LC_{contrast\ ratio}$ for each participant in the first and second scan sessions and right and left hemispheres was significantly larger from 1 both for the ROI and maximum intensity approach ($p < .001$)

In the ROI analysis the mean $LC_{contrast\ ratio}$ was 13.9% (SD 3.8; Figure 4a). The $LC_{contrast\ ratio}$ did not differ between scan sessions, but there was a lateralization effect, with the $LC_{contrast\ ratio}$ in the right LC being significantly higher than that in the left LC in both scan sessions (session 1: $t(14) = 3.78$, $p = .002$; session 2: $t(14) = 3.43$, $p = .004$; Figure 4a). The minimum $LC_{contrast\ ratio}$ observed over all participants and all sessions was 4.5%. However, the range in $LC_{contrast\ ratio}$ (4.5% – 32.4%) was wide. A high correlation was observed between the $LC_{contrast\ ratio}$ of the right and left LC for scan session 1 ($r = .57$, $p = .026$), but not for session 2 ($r = .07$, $p = .82$); Figure 4b). Finally, a moderate ICC was found for the $LC_{contrast\ ratio}$ between scan session 1 and 2 (ICC = 0.63), with the left LC showing a higher ICC than the right LC (Figure 4c; left LC: ICC = 0.71; right LC: ICC = 0.36).

Regarding the maximum intensity approach, similar to the ROI approach, $LC_{contrast\ ratio}$ in the right LC was higher than in the left LC, but this time it did not reach significance (session 1: $p = .20$; session 2: $p = .058$; Figure 5a). Also, contrary to the findings of the ROI approach, in the maximum intensity approach there was no correlation between the contrast of the right and left LC for either scan session (session 1: $r = .36$, $p = .19$; session 2: $r = .003$, $p = .99$; Figure 5b) and the ICC for the contrast between session 1 and 2 was lower than the ICC of the ROI approach (Figure 5c; ICC = 0.53; left LC: ICC = 0.45; right LC: ICC = 0.51).

There was no correlation between inter-rater reliability and $LC_{contrast\ ratio}$. Dice coefficient did not correlate with ROI $LC_{contrast\ ratio}$ (session 1: $r = -.10$, $p = .59$; session 2: $r = -.38$, $p = .84$), or maximum intensity $LC_{contrast\ ratio}$ (session 1: $r = -.06$, $p = .74$; session 2: $r = .03$, $p = .86$). LC conjunction volume did not correlate with ROI $LC_{contrast\ ratio}$ (session 1; $r = .04$, $p = .82$; session 2: $r = -.10$, $p = .58$), or maximum intensity $LC_{contrast\ ratio}$ (session 1: $r = .08$, $p = .66$; session 2: $r = -.09$, $p = .64$).

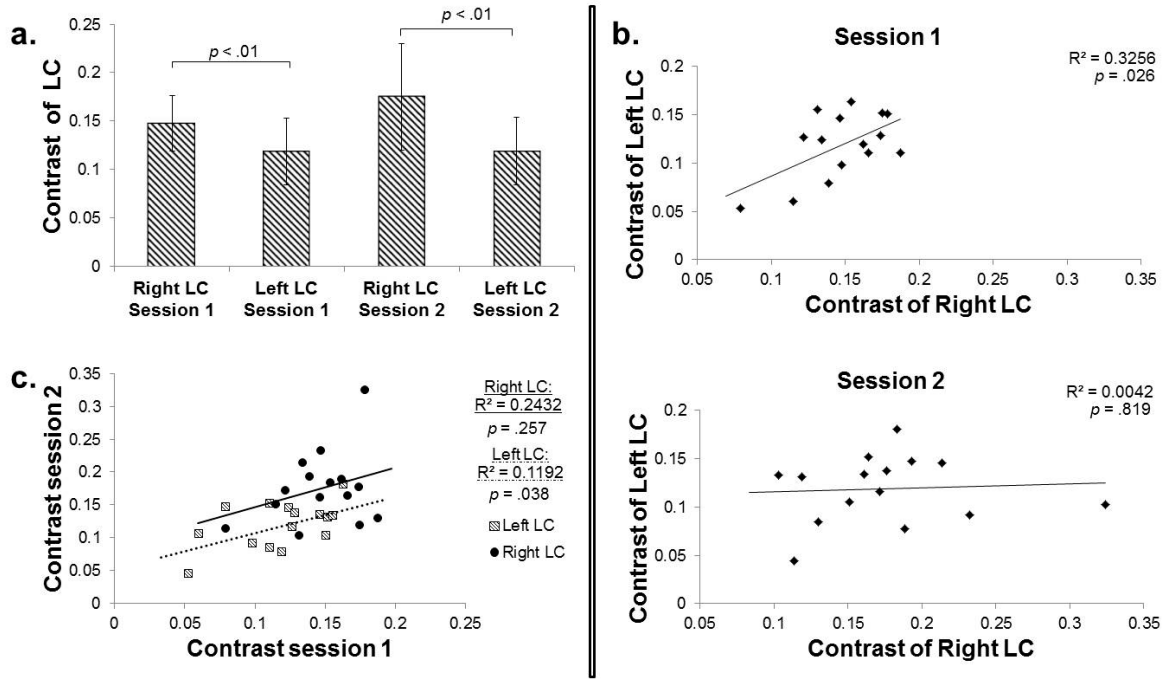


**Figure 4.** ROI analysis examining the test-retest reliability of the MRI contrast. A) Contrast of the right and left LC for the first (left) and second scan session (right). Bars indicate mean ± standard deviation. B) Correlation between right and left LC contrast of the first (top) and second (bottom) scan session. C) Correlation between contrast of first and second scan session.

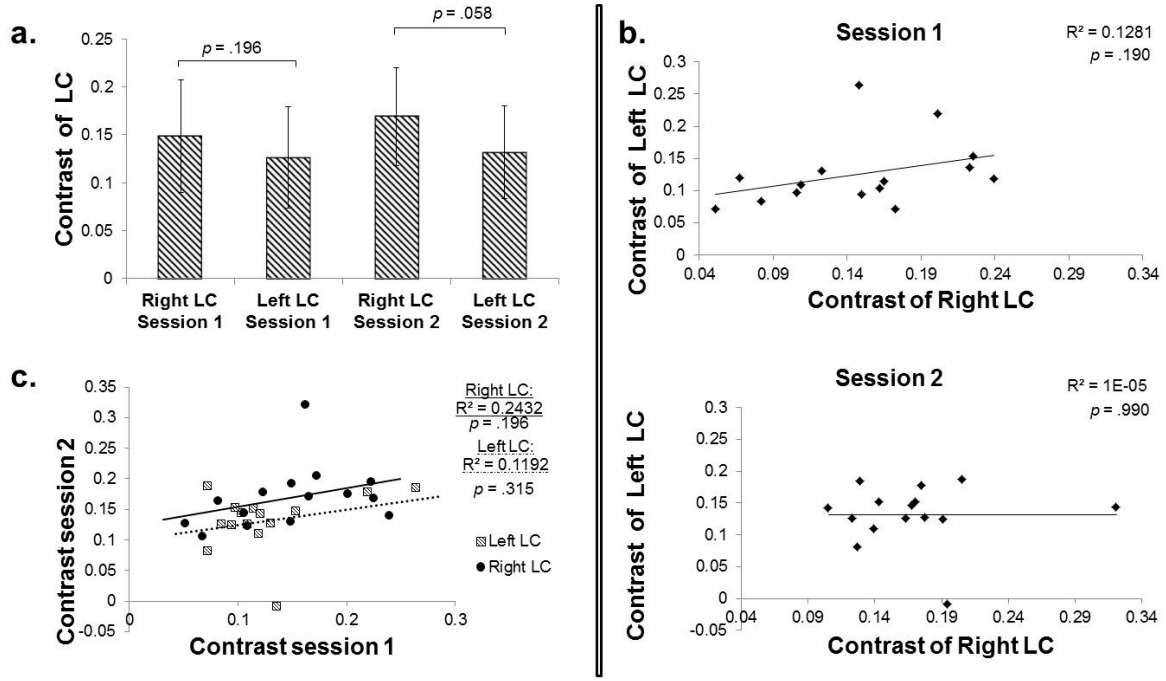


**Figure 5.** Maximum intensity voxel analysis examining the test-retest reliability of the MRI contrast. A) Contrast of the right and left LC for the first (left) and second session (right). Bars indicate mean ± standard deviation. B) Correlation between right and left LC contrast of the first (top) and second (bottom) session. C) Correlation between contrast of first and second session.

## Discussion

The most important findings of this study are threefold: first, there was a moderate scan-rescan reliability of the TSE scan in visualising the LC; second, the LC volume estimated with the TSE scan appears to be smaller than volumes reported in ex vivo studies; and third, we observed a lateralization effect in terms of LC volume and intensity.

### *Scan-rescan reliability*

There was a moderate scan-rescan reliability of the LC. Taking into consideration the challenges of imaging the LC due to its location and small volume and the fact that these reliability indexes are similar to other, bigger structures located in less susceptible parts of the brain (e.g. the amygdala, reliability of 0.67-0.89 for automated segmentation and 0.75 for manual; Bartzokis et al., 1993; R. A. Morey et al., 2010), we conclude that localization and segmentation of the LC in vivo is a challenging but reliable enterprise.

The moderate inter- and intra-rater reliability (as assessed with the Dice coefficient) shows moderate reproducibility of the TSE scan in terms of LC visualization. This reliability was stable across the two raters, the two scan sessions, the two segmentation sessions and the two hemispheres. A stable inter-rater and inter-segmentation session reliability is an indication that the raters performed the segmentation in a reliable manner. The moderately stable scan-to-scan reliability has implications for longitudinal studies and suggests that this scan can be applied to the same participant more than once with a moderate confidence that it will lead to the same result. Our evaluations are limited to two scanning sessions, but future research can investigate the reliability of the TSE scan in multiple sessions.

This is the first study that was designed to assess TSE scan reliability of the LC, but there are two other studies of which the results are pertinent to this topic. The intra-rater values reported in these studies are higher than those reported here (0.89 – 0.94 and 0.98 – 0.99 for Ohtsuka et al., 2013 and Takahashi et al., 2015, respectively, and 0.65 – 0.74 for our study). This discrepancy can be explained by methodological differences. More concretely, we assessed intra-rater agreement using Dice coefficients and masks that were manually segmented in each individual's native space, whereas Ohtsuka et al. (2013) and Takahashi et al. (2015) report intra-observer agreement using an ICC approach (instead of Dice coefficient) and a fixed 1-mm or 2-mm diameter circle for LC segmentation. The approach of employing fixed diameter for the ROI segmentation is not optimal for assessing reliability because it entails the risk of losing part of the LC or of misattributing surrounding tissues to the LC. Indeed, as already mentioned, although histological studies show that the LC is 2.0-2.5 mm wide, there is a substantial variability in the LC shape. Additionally, this approach utilizes a fixed circle that is smaller than the actual size of the LC, thus it might capture a region where the LC signal is at its maximum and bias the intra-rater values towards the high end of the scale. Finally, in Takahashi et al. (2015), one rater performed the segmentation three times and the in

between interval was shorter than in this study (one week vs. at least two weeks), while in Ohtsuka et al. (2013) the segmentation interval is not mentioned.

Regarding the scan-to-scan reproducibility, a third study should be mentioned: Langley and colleagues report higher reproducibility values for the scan-rescan magnetization transfer contrast (ICC= 0.76) and a mean Dice coefficient of 0.63 for the delineation of the LC scan-to-scan volumes (Langley, Huddleston, Liu, & Hu, 2016). However, our findings cannot be directly compared with the results of this study, because Langley and colleagues utilized a different MRI sequence: a gradient echo pulse scan. It has been argued that this sequence, similar to the TSE sequence, is sensitive to the presence of neuromelanin (Chen et al., 2014; Langley et al., 2016). In addition, there are also methodological differences between the two studies in terms of: a) segmentation procedure (no manual segmentation of the mask), b) ROI definition (LC contrast extraction based on a fixed 3-mm diameter circle placed over the left and the right LC, and consecutive exclusion of the voxels that were 4 standard deviations above the mean intensity of the reference ROI), c) definition of LC intensity assessment, and d) scan-to-scan session interval (both scanning sessions were on the same day).

***LC volume***

The volume of the individual-rater LC masks was 9.53 $mm^3$ on average (SD 3.83) and ranged between 0.82 – 25.29 $mm^3$ (per hemisphere). There is a discrepancy in the post-mortem literature regarding the exact size and location of the LC, and there seem to be large inter-individual differences in LC cell distribution (Afshar, Watkins, & Yap, 1978; Fernandes et al., 2012; German et al., 1988; see Table 2). However, the volume found in our study is smaller than one would expect based on post-mortem studies (see Table 2). A similar LC volume was reported with another type of neuromelanin MRI sequence, the gradient echo pulse scan (Chen et al., 2014). The reason why MRI scans lead to decreased LC volume estimates compared to post-mortem estimates is not clear, but we speculate that the discrepancy might be due to the following reasons: a) methodological MRI factors, such as the possibility that current neuromelanin MRI scans might not be very sensitive, and an improvement of these scan sequences might lead to better volume estimations; b) the homogeneity of the sample in terms of age span (e.g., young/homogenous vs. old/nonhomogeneous population); and c) partial volume effects. We will discuss each of these factors in turn.

**Table 2.** Estimation of human LC volume based on prior post mortem literature.

| Reference | LC length in mm | LC width in mm | LC height in mm | Volume in $mm^2$ (Reported) | Volume in $mm^3$ (Estimated) | LC region |
|---|---|---|---|---|---|---|
| German et al., 1988 | 13-17 | 2.5 | 2.5 | 17.2 to 32.8 | 3.14 x $(1.25)^2$ x 15 = 73.59 | Entire LC |
| | 7.2 | 2.5 | 2.5 | | 35.26 | "core" LC only |
| Fernandes et al., 2012 | 14.5 | 2.5 | 2 | | 3.14 x 1.56 x 14.5 = 71 | Entire LC |
| | 11 (80% of cases) | 2.5 | 2 | | 3.14 x 1.56 x 11= 53.88 | "core" LC only |
| | 10 (90% of cases) | 2.5 | 2 | | 3.14 x 1.56 x 10 = 48.98 | "core" LC only |
| | 7.5 (100% of cases) | 2.5 | 2 | | 3.14 x 1.56 x 7.5 = 36.74 | "core" LC only |
| Afshar et al., 1978 | 10 | 1.28 | 1.23 | | 3.14 x 1.63 x 10 = 51.44 | Entire LC |
| | 6 (100% of cases) | 1.04 | 1.10 | | 3.14 x 1.21 x 6 = 22.81 | "core LC" only |

LC length, width and height as provided/estimated by German et al.,1998, Fernandes et al., 2012, and Afshar et al., 1978. LC volume estimation of the entire and the "central/core part" of the LC (where the neuromelanin concentration is higher and there is higher overlap between participants). For German et al. the "core area" corresponds to 3 slices where the number of the LC cells are substantially high; for Fernandes et al., and for Afshar et al., this area corresponds to the part of the LC that is common for every case (present and shared by the 100% of the cases). These core LC volume values are closer to the LC volume as shown by the TSE scan in our study where the largest mask that we segmented was 25.29 $mm^3$.

Regarding the first point, it has been argued that the TSE scan can visualize the LC because, similar to histological methods, it is sensitive to the neuromelanin pigments that exist in the LC cells (Keren et al., 2009; Keren et al., 2015; Sasaki et al., 2006). Histological and MRI studies show that neuromelanin concentration is highly dense in the center ("core") of the LC and more spread in the rostral and caudal extremities. For Keren et al., the elevated signal in the (in vivo) TSE scan corresponded to the location of greatest LC neuron density as reported in the post mortem LC study by German et al. (1988) (Keren et al., 2009; Keren et al., 2015). For Fernandes et al. (2012), and for Afshar et al. (1978), this area corresponds to the part of the LC that is common for every case (present and shared by the 100% of the cases; see Table 2). This might mean that the TSE scan captures mainly the "core" region of the LC or cannot fully capture the part where the LC cell distribution is less dense. If the TSE scan cannot capture the entire size of the LC, it will substantially reduce the volume of the LC compared to the size reported in histological studies. Although the exact volume of this highly dense, "core" region of the LC is not mentioned in prior studies, it can be estimated based on the information provided in the papers. Based on this information, we estimate that the core region of the LC is approximately 35 $mm^3$ for German et al. 37 $mm^3$ for Fernandes et al. and 23 $mm^3$ for Afshar et al. (see Table 2). These core LC volume values are closer to the LC volume reported in our study, although still a factor three larger than the measured volumes.

As far as age is concerned, although not all studies support this finding (Fernandes et al., 2012; Mouton et al., 1994; Takahashi et al., 2015), post-mortem and in vivo MRI studies show that changes in size or intensity occur to the LC structure with age (Clewett et al., 2016; German et al., 1988; Keren et al., 2009; Lohr & Jeste, 1988; Manaye, McIntire, Mann, & German, 1995; Ohtsuka et al., 2013; Shibata et al., 2006; Vijayashankar & Brody, 1979; Zecca et al., 2004). It has also been argued that neuromelanin concentrations increase with age (Mann & Yates, 1974; Zecca et al., 2004). If that is the case, the inclusion of young participants in our study might have resulted in smaller LC volumes due to lower levels of neuromelanin. Future research concentrating on reproducibility of the TSE scan in elder participants, employing similar methods as in the current study, can help address this question.

Finally, partial volume effects might play a role too. Indeed, when imaging a small and thin brain structure like the LC, the volume can be underestimated, for example due to loss of visualization of the upper or lower part of the LC (Hoffman, Huang, & Phelps, 1979; Vos, Jones, Viergever, & Leemans, 2011). Yet, the use of high contrast, high spatial resolution sequence, similar to the one used here, decreases these effects, leading to increased visualization of the tissue, less mixing of signals coming from different regions, and sharper definition of the individual tissue (Kneeland et al., 1986).

***LC contrast***

The range in $LC_{contrast\ ratio}$ (4.5% – 32.4%) was wide, suggesting a large inter-subject variation in visualization of the LC (Figure 4a). Our results are similar to Takahashi et al. (2015), who, by using a TSE sequence, report an LC contrast range of 6.24-20.94%

(median 14.35%) for healthy volunteers and a significant drop of LC contrast in patients with mild cognitive impairment and Alzheimer's disease. The $LC_{contrast\ ratio}$ did not differ between scan sessions 1 and 2, suggesting that the scan is reliable and can be used in longitudinal studies. Yet, the fact that the reliability is moderate and that a high correlation was observed between the $LC_{contrast\ ratio}$ of the right and left LC only for scan session 1 but not for session 2 (Figure 4b), suggests that changes in signal intensities over time should be interpreted with caution. The mean $LC_{contrast\ ratio}$ for the peak voxel analysis (14.4%) was similar to the mean $LC_{contrast\ ratio}$ of the ROI analysis (13.9%). However, similar to Keren et al. (2009), and contrary to the ROI approach, we found no significant lateralization effect in the peak voxel approach. This suggests that the peak approach might not be sensitive enough to detect the effect due to its limited coverage and decreased robustness.

***Lateralization effect***

Our results of the LC volume and ROI intensity analysis suggest an LC lateralization with the right LC being larger and of higher intensity than the left LC. This lateralization effect was not reported before and the majority of LC studies highlight its bilateral hemispheric symmetry (Chan-Palay & Asan, 1989; Fernandes et al., 2012; German et al., 1988; Keren et al., 2009; Ohm, Busch, & Bohl, 1997; Vijayashankar & Brody, 1979). However, German et al. (1988) mention that "although there is a bilateral symmetry, the two sides do not appear identical" and report that the total horizontal area of the left LC is smaller than that of the right LC for one of the five cases. Keren et al. (2009) found that "the LCs are not perfectly symmetrical in peak or in the variance of the peak location". When the same authors employed 7T MRI (using a RARE-INV MR scanning sequence), the asymmetry became more obvious (note the hemispheric asymmetry in size and shape of the putative LC contrast through slices 5-7 in Fig 4, pp. 6; note the hemispheric asymmetry in size and shape of the putative LC contrast through slices 5-7 in Fig 4, pp. 6; note the hemispheric asymmetry in size and shape of the putative LC contrast through slices 5-7 in Fig 4, pp. 6; note the hemispheric asymmetry in size and shape of the putative LC contrast through slices 5-7 in Fig 4, pp. 6; Keren et al., 2015). In line with our study, Keren et al. (2015) show elevated contrast in the right LC in comparison to the left side at least for one subject (see Fig. 5; Keren at al., 2015).

It is important to note that lateralization in the brainstem has not been investigated in detail for two reasons. First, until the discovery of the ability of the TSE scan to generate LC-specific contrast, it was not possible to image the monoamine brainstem nuclei in vivo. Second, it has been a common approach in MRI methods to investigate lateralization effects in the cortex, but to perceive the brainstem and the LC as one single midline structure (e.g., Morey et al., 2010; Ohtsuka et al., 2013; Takahashi et al., 2015). However, lateralization effects have been reported for other brain structures that exist in pairs (e.g., the amygdalae and the hippocampi; Baas, Aleman, & Kahn, 2004; Cahill, Uncapher, Kilpatrick, Alkire, & Turner, 2004; Frings et al., 2006; Iglói, Doeller, Berthoz, Rondi-Reig, & Burgess, 2010).

Finally, technical explanations of the observed lateralization effects, such as RF-asymmetry, cannot be ruled out. For example, Zwanenburg et al. reported signal asymmetries in FLAIR scans due to RF-inhomogeneities (Zwanenburg, Visser, Hendrikse, & Luijten, 2013). Taking into consideration that lateralization effects play an important role in brain function, future studies should further investigate whether our finding of LC lateralization can be replicated, and if this lateralization also exists for LC function.

### *The LC probability atlas*

Our results show substantial variability in the spatial location of the LC, given that the maximum percentage overlap was only 36%.

There is only one in vivo atlas of the human LC published to date (Keren et al., 2009). The atlas described in this study differs on three crucial aspects from that atlas: segmentation method, sample type, and information. Contrary to the atlas by Keren et al. (2009) the entire visible LC was segmented, providing a more extensive coverage of the LC. This aspect of our approach is more relevant for fMRI studies in which the extent of activation refers to multiple voxels instead of peak coordinates; an fMRI study that uses a peak approach atlas entails the risk that the cluster of activation extending outside the LC map is missed. Additionally, in the current atlas we adopted a quantification approach and we provide the probabilistic information on where the LC is located. This information can, for instance, be used to weigh the measured fMRI signal with the probability of it originating from the LC. Finally, our LC atlas is based on a homogeneous sample of young participants, which is more representative of and relevant for most experimental studies in psychology and neuroscience, given that the majority of (fMRI) studies in cognitive neuroscience are based on healthy young volunteers (Chiao, 2009; Henrich et al., 2010).

Although the probability LC atlas can be used as an ROI for the LC in future studies, it should be noted that the use of an atlas is always less anatomically precise than the individually determined masks. Given that our TSE scanning protocol is relatively short (7 min), and covers a large region in the brainstem, with a relatively high spatial resolution (0.34x0.34x1.5mm), we recommend to include such a structural scan during the data acquisition phase (in this study we also provide a relevant segmentation protocol to assist in the creation of individual LC masks, see Appendix below). If this is, however, not feasible, one could consider to use the probability atlas.

A strong aspect of the LC atlas, as mentioned above, is the homogeneous sample on which it was based. But one limitation is the small size of this sample.

Another limitation refers to the TSE scan which has a limited coverage of the brainstem due to the compromise between signal-to-noise ratio and increased resolution. Although our study has a larger coverage than other studies, it still does not provide full coverage,

making planning of the imaging volume somewhat troublesome during the acquisition. By planning the volume perpendicular to the brainstem, by utilizing anatomical landmarks such as the fourth ventricle and the inferior colliculus, we were successful in always including the LC into the imaged volume.

Finally, an additional limitation of the TSE scan is the voxel size of 0.35x0.35x1.5mm which might be considered relatively big for such a small structure as the LC. Initial pilot scans with a smaller voxel size were tested but showed substantial loss of image quality. A possible explanation for this is that the increased acquisition time resulted in more motion artifacts.

## Appendix

### *Segmentation Protocol of LC masks*

- The raters were trained by a neuroanatomist and discussed which guidelines should be followed when parcellating the LC. This discusision led to the creation of this segmentation protocol.
- Before segmentation started, the data was first anonymized by replacing the participant identifier by a random number.
- The order of segmentation was randomized between raters and across segmentation sessions

The segmentation protocol of LC masks was based on the following steps:

1. In order to correctly spot the LC, the fourth ventricle and the pontomedullary junction were used as anatomical landmarks. The LC is approximately located in the following region:

   3.2 ± 0.3 mm from the midline

   1.1 ± 0.2 mm under the fourth ventricle

   18.5 ± 1.5 mm apart from the pontomedullary junction

2. After the identification of the LC, the raters zoomed in at a point that got a good image of both the right and the left LC.
3. The contrast of the image was consecutively optimized per individual in such a way that the LC had the highest contrast with the surroundings and the borders were well defined. The same contrast intensity was kept for both LCs and the minimum and maximum values of the contrast were notated for each participant.
4. To ensure accuracy, segmentation was performed by consulting three dimensions for the images (axial, sagittal, and coronal) but was mainly based on the axial slice.
5. The starting point for the segmentation was the axial slice in which the LC voxel intensity was more pronounced and the raters had a good image of both LCs.

Segmentation started in this scan after zooming into a single LC. The zooming level was kept such that the raters could still see at least half of the fourth ventricle.

6. The segmentation of the LC continued upwards until no hyperintensity region could be discerned that is in line with previous slices. When the rostral part of the LC was completed, raters continued with the caudal slices.

There are two possible problems with segmenting the LC:

   a. In dorsal direction one might encounter two hyper-intense clusters which both can be considered as a continuum of the previous slice. At the most rostral end of the LC, at the level of the inferior colliculus, the one closest to the pons *(=lateral cluster)* is most likely the trochlear nerve (Naidich et

al. 2009). At more caudal levels, where the inferior colliculus is not in plane yet, the one closest to the fourth ventricle *(=medial cluster)* is most likely the trochlear nerve (Keren et al. 2009; Naidich et al. 2009). For this reason, the hyper-intense cluster towards the pons (=lateral cluster), was selected by the raters as the LC, unless it was at the level of the inferior colliculus.

b. In caudal direction one might encounter a 'gap' in the LC. When segmenting the LC in axial view there might be a moment where there is no clearly visible LC. However, in the following slices in caudal one might start to identify hyper-intense spots that might correspond to the LC. The raters being aware of literature that shows the existence of subcureleus region caudally to the LC (Ehrminger et al., 2016; Paxinos & Feng Huang, c1995), and that the number of LC neuromalanin neurons decrease at a caudal level and increase again at the very last caudal part of the LC (German et al., 1988), were careful and reached the following agreement prior the segmentation:

    a) *If the gap was only 1 slice thick and in one or several adjacent slices in caudal direction, the hyperintense regions could be identified; two masks were saved: one containing the extra caudal slices (but left the gap open; this was done only if the caudal hyper intense cluster seemed to be a continuity of the cluster prior to the gap, not if it was obviously a different structure with a different location) and one without (in the second case the raters stopped the segmentation prior to the gap).*
    b) *If the gap is larger than 1 slice; the segmentation of the LC stopped.*

7. In the cases where the raters were in doubt, and for the cases where the two raters largely disagreed (i.e., the interrater for that participant was 2 standard deviations from the mean), the atlas and literature (and if necessary a neuroanatomist) was consulted to identify the problematic areas. Data from these participants were segmented again and this was the final mask for those participants.

Segmentation Protocol of control ROI (MCP) masks

A similar protocol was used for the parcellation of the middle cerebral peduncle (brachium pontis; MCP) which functioned as control ROI for the contrast analysis, with the only difference that parcellation was performed by only one rater and that the LC masks were overlaid while segmenting the control ROI to guarantee that the control ROI was included on all slices in which the LC was present. To make sure that the control ROI captured as much variance as possible, the MCP mask consisted of approximately double the number of voxels of the LC ROI. The MCP was chosen as a control ROI because it is

a large structure, extends to both the left and right side of the brainstem, and is a relatively homogeneous region of voxels that show a signal intensity comparable to surrounding tissue of the LC.

A practical description of the MCP segmentation protocol is the following:

1. To ensure accuracy, segmentation was performed by consulting three orientations of the images (axial, sagittal, and coronal) but was mainly based on the axial slice.
2. The starting point for the MCP segmentation was the axial slice in which the LC-mask was located and the brainstem was at its widest.
3. In order to detect the starting point of the MCP segmentation, a horizontal line was drawn through the brainstem at the level that the brainstem is at its widest
4. Starting from either the left or right side of the brainstem (counterbalanced segmentation order of hemisphere), the outermost pixel on this line was identified that was fully inside the brainstem.
5. Moving 14 voxels medially along this horizontal line, one reaches a region that is approximately the center of the MCP, which was adopted as the MCP mask center voxel (because the MCP is a large structure, this point always represented white matter and was approximately at the center of MCP, but the data was also checked carefully by the researcher and adjusted accordingly if necessary).
6. Taking this voxel as the center of the MCP mask, a rectangular mask with a size of 8 x 8 voxels was created around this central voxel. This was taken as the MCP mask for that particular slice.
7. The segmentation of the MCP continued to the next axial slices: first upwards until the point that the LC mask would end. When the rostral part of the MCP was completed, the rater continued with the caudal slices.
8. The same was done for the other side of the brainstem (the order of hemispheres was counterbalanced).
9. In this way a control ROI similar to the LC was created but with the voxels being double the number of the LC voxels (the LC was usually 4 voxels per slice).

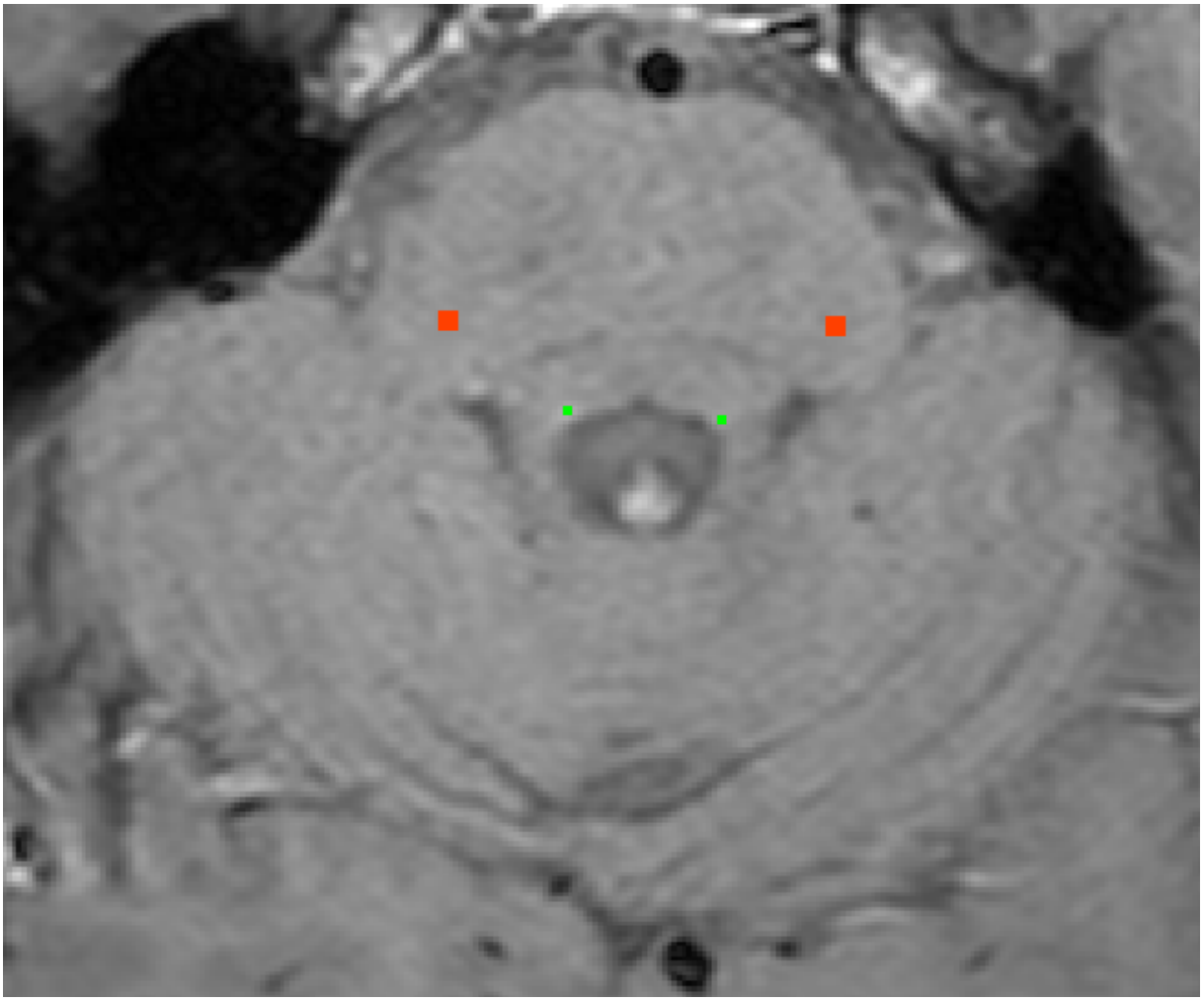

**Appendix Figure 1**. Example TSE scan with the manually segmented mask overlaid: right and left LC (radiological convention, in green) and MCP-control ROI (in red).

# Chapter 3

# Paving the path for better visualization for the LC:

# Visualizing the human locus coeruleus *in vivo* at 7 Tesla MRI

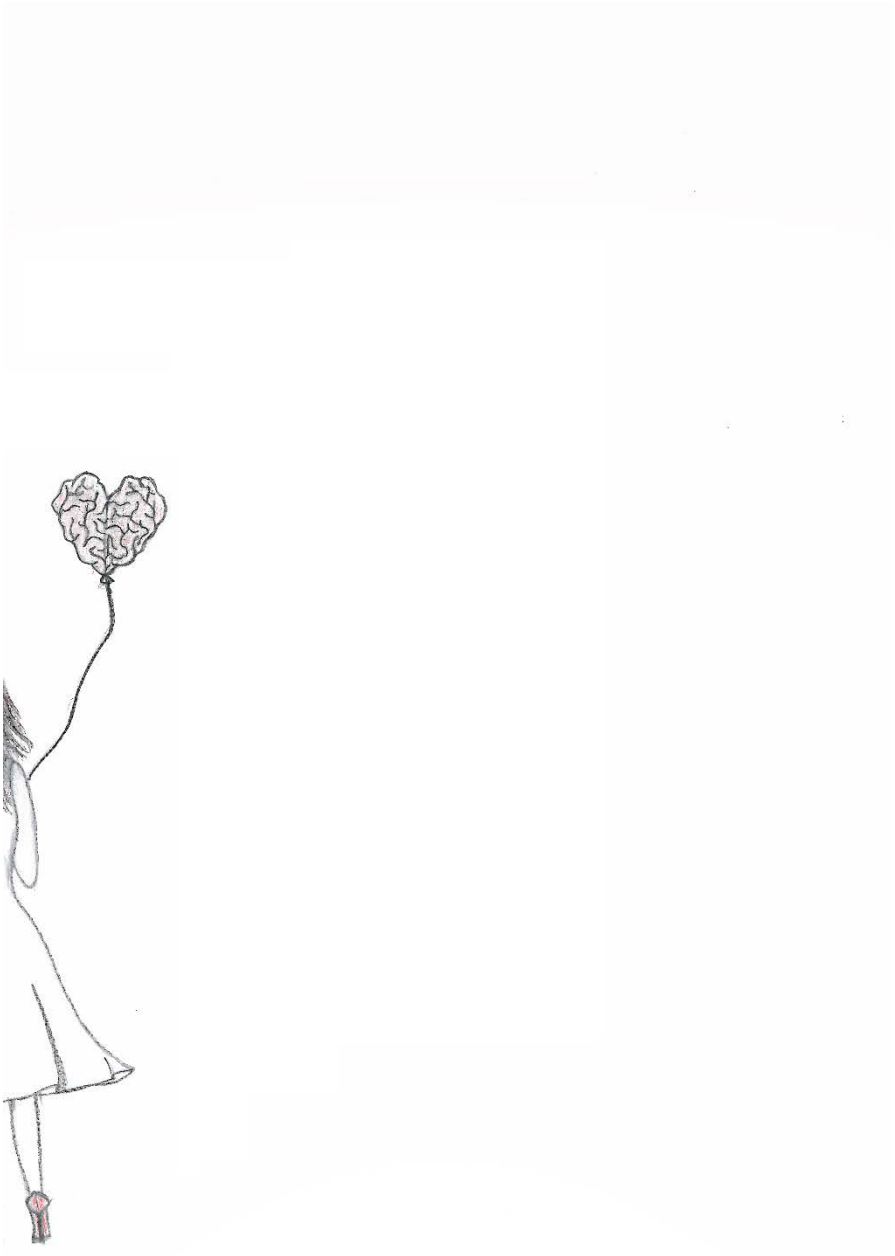

This chapter is published as: Tona, K.D., van Osch, M.J.P., Nieuwenhuis, S., & Keuken, M.C. (2019). Visualizing the human locus coeruleus in vivo at 7 Tesla MRI. PLoS ONE, 14: e0209842.

**Abstract**

The locus coeruleus is a small brainstem nucleus which contains neuromelanin cells and is involved in a number of cognitive functions such as attention, arousal and stress, as well as several neurological and psychiatric disorders. Locus coeruleus imaging *in vivo* is generally performed using a $T_1$-weighted turbo spin echo MRI sequence at 3 Tesla (T). However, imaging at high magnetic field strength can increase the signal-to-noise ratio and offers the possibility of imaging at higher spatial resolution. Therefore, in the present study we explored the possibility of visualizing the locus coeruleus at 7T. To this end, twelve healthy volunteers participated in three scanning sessions: two with 3T MRI and one with 7T MRI. The volumes of the first 3T session were used to segment the locus coeruleus, whereas the volumes of the second 3T and the 7T session were used to quantify the contrast of the locus coeruleus with several reference regions across eight different structural sequences. The results indicate that several of the 7T sequences provide detectable contrast between the locus coeruleus and surrounding tissue. Of the tested sequences, a $T_1$-weighted sequence with spectral presaturation inversion recovery (SPIR) seems the most promising method for visualizing the locus coeruleus at ultra-high field MRI. While there is insufficient evidence to prefer the 7T SPIR sequence over the 3T TSE sequence, the isotropic voxels at 7T are an important advantage when visualizing small structures such as the locus coeruleus.

## Introduction

The locus coeruleus (LC) is a brainstem nucleus that is involved in important cognitive functions such as attention, arousal and stress (Aston-Jones & Cohen, 2005). Also LC atrophy has been connected to disorders such as Alzheimer's and Parkinson's disease (Gesi et al., 2000; Kelly et al., 2017). The important role that the LC plays in cognition and its use as a biomarker for assessment of neurodegenerative disorders (Matsuura et al., 2013; Ohtsuka et al., 2013; Sasaki et al., 2008; Sasaki et al., 2006) necessitate accurate visualization of the LC.

Recently, a $T_1$-weighted FLASH sequence has been used to image the LC at 3T (Betts et al., 2017). However, to date the most frequently used scan at 3T scanners is a $T_1$-weighted TSE scan sequence (e.g. Betts et al., 2017; Clewett et al., 2016; de Gee et al., 2017; Keren et al., 2009; Liu et al., 2017). Such a TSE sequence is thought to be sensitive to neuromelanin, a pigment that is produced in catecholaminergic neurons and that exists in large quantities in the LC (Fedorow et al., 2005). Indeed, the TSE scan shows enhanced contrast between neuromenalin-rich structures such as the LC and surrounding brain tissue (Keren et al., 2015; Sasaki et al., 2006). The LC contrast is thought to be attributed to a number of tissue properties which selectively influence the MRI contrast mechanisms. The presence of neuromelanin alone can result in paramagnetic $T_1$-shortening effects (Bolding et al., 2013). Paramagnetic ions such as those of iron and copper found in the LC are expected to contribute to T2 and T2* contrast (Lee et al., 2016; McRobbie, Moore, Graves, & Prince, 2017; Priovoulos et al., 2017).

While the TSE sequence has moderate test-retest reliability for visualizing the LC at 3T (Tona et al., 2017), the voxel dimensions generally acquired are highly anisotropic, which hinders the accurate visualization of the LC (Wonderlick et al., 2009). We hypothesized that imaging at higher magnetic field strength might provide a solution to the challenges involved in LC imaging. Higher magnetic field strength increases signal-to-noise ratio and allows imaging at a higher spatial resolution (Cho et al., 2014; Sclocco et al., 2017; van der Zwaag et al., 2016). This, in turn, results in smaller partial volume effects, which in itself can help to improve contrast and thereby detectability (de Hollander et al., 2015; Kneeland et al., 1986).

However, it is well-known that MRI properties of tissue are field-strength-dependent (van der Zwaag et al., 2016) and that the TSE sequence is specific absorption rate (SAR) intensive (Hennig, Nauerth, & Friedburg, 1986). Therefore, it is uncertain whether sequences that have been proven successful at 3T, such as the TSE scan, will also provide the best contrast for visualization of the LC at higher field strengths. To address this issue, we studied the contrast of the LC for a number of 7T MRI sequences that have proven to provide detailed anatomical information in the brainstem at 7T (Keuken, Isaacs, Trampel, van der Zwaag, & & Forstmann, in press) or which have been suggested for imaging neuromelanin or catecholamine-related structures such as the LC and the nigrosome substructures of the substantia nigra (Blazejewska et al., 2013; Duyn et al.,

2007; Haacke, Mittal, Wu, Neelavalli, & Cheng, 2009; Versluis et al., 2010). See also methods for more details on the scan sequences and choice rationale.

Our aim was to explore whether there are 7T scan sequences that can achieve adequate contrast for imaging the LC. For reference, we also included the standard TSE sequence used at 3T. The results indicate that several of the 7T sequences provide detectable contrast between the locus coeruleus and surrounding tissue. Of the tested sequences, a $T_1$-weighted sequence with spectral presaturation inversion recovery (SPIR) seems the most promising method for visualizing the locus coeruleus at ultra-high field MRI.

## Methods

### *Participants*

Twelve healthy volunteers (mean age 23 years old; SD: 1.7) participated in three scanning sessions: two at 3T MRI and one at 7T MRI (the two 3T scan sessions were initally acquired to assess reproducibility of the TSE scan at 3T MRI; results published in the two 3T scan sessions were initally acquired to assess reproducibility of the TSE scan at 3T MRI; results published in the two 3T scan sessions were initally acquired to assess reproducibility of the TSE scan at 3T MRI; results published in the two 3T scan sessions were initally acquired to assess reproducibility of the TSE scan at 3T MRI; results published in Tona et al., 2017). All participants were healthy, right-handed and without a history of neurological or psychiatric problems as assessed by self-report questionnaires. The study was approved by the medical ethics committee of the Leiden University Medical Center. All participants provided written informed consent prior to their inclusion in the study (in accordance with the Declaration of Helsinki), and received monetary compensation for their participation.

### *Choice of MRI scan sequences*

The following scan sequences for 7T MRI were included in this study. Details about each scanning protocol are provided in the section “MRI acquisition parameters”.

*a.* TSE sequence (TSE 7T): this sequence closely resembles the neuromelanin-sensitive scan as commonly employed at 3T (Sasaki et al., 2006; Tona et al., 2017). Minor adaptations were necessary to allow the usage of this scan at 7T, mainly due to specific absorption rate limits.

*b.* High-resolution TSE sequence (HR-TSE 7T): this scan is similar to the previous TSE scan but at a higher spatial resolution, with a higher in-plane resolution, as well as a continuous coverage (no slice gap) in the z-direction, which was achieved via acquisition in four packages of interleaving slices.

*c.* High-resolution $T_2$*-weighted sequence: this scan is commonly used at 7T for detection of iron deposition, presence of deoxyhemoglobin, or other sources of magnetic susceptibility variations (HR-T2*; HR-T2*; HR-T2*; HR-T2*; Duyn et al., 2007; Versluis et al., 2010). For this scan, both the magnitude and phase

of the MRI signal were recorded, which allows the reconstruction of three image types:

- The magnitude image (HR-$T_2$* magnitude).
- The unwrapped phase image (HR-$T_2$* phase unwrapped) for which a high-pass filter was applied to exclude low spatial-frequency variations of the phase due to macroscopic magnetic field differences.
- The susceptibility-weighted images (HR-$T_2$* SWI), based on the multiplication of the magnitude image with a filtered version of the unwrapped phase image, as originally proposed to enhance venous structures (Haacke et al., 2009).

*d.* $T_1$-weighted scan with spectral presaturation with inversion recovery sequence (SPIR): this scan has previously been used in Parkinson's disease patients at 7T to directly visualize nigrosome substructures of the substantia nigra by utilizing the presence of iron and neuromelanin in this structure (Blazejewska et al., 2013). SPIR is a hybrid technique which nulls the fat magnetization by means of a fat-selective radio frequency pulse and spoiler gradient. Due to the fact that the SPIR pulse is off-resonance with respect to the water peak, this pulse exhibits some magnetization transfer (MT) effects on the contrast (Blazejewska et al., 2013).

*e.* A whole-brain 3D $T_1$-weighted (MPRAGE) sequence. This is a widely-used pulse sequence for anatomical imaging in MRI with contrast originating from $T_1$ relaxation time differences.

Furthermore, at 3T we acquired the $T_1$-weighted TSE structural scan that has been used to accentuate neuromelanin rich structures (Keren et al., 2015; Sasaki et al., 2006). The TSE scan from the first 3T scan session was used to manually segment the LC according to the segmentation protocol described in Tona et al., (Tona et al., 2017). This LC mask was used to localize the LC in the 7T images and in the TSE image of the second 3T scan session. The TSE scan from session 2 was used to extract the 3T TSE signal and provided the reference value for the contrast extraction at 7T. Because the 3T TSE from session 2 is separate from the scans which were used to create the LC masks (first 3T TSE scan session), a comparison between the contrasts at 3T and 7T can be made while trying to avoid biases towards the sequence of the scan on which the mask was drawn.

***MRI acquisition parameters***

***3 Tesla MRI*** Two scanning sessions took place at a 3T-TX Philips scanner equipped with a 32-channel head coil. During both scan sessions, the participants underwent a whole-brain 3D $T_1$-weightedsequence (3T whole-brain T1; field of view (FOV): 224 x 177.33 x 168 mm; 140 slices; resolution 0.87 x 0.87 x 1.2 mm; repetition time (TR): 9.7ms; echo time (TE): 4.5 ms; flip angle $8^o$; acquisition matrix: 192 x 152; time of acquisition (TA): 4 min 9 s) and a brainstem-zoomed $T_1$-weighted TSE structural scan (Sasaki et al., 2006). The TSE scan sequence was used to detect the LC and had similar sequence parameters as the ones reported in prior literature (Liu et al., 2017) (FOV: 180 x 180 x 22.95 mm; 14

slices; acquisition resolution 0.70 x 0.80 x 1.5 mm, reconstruction resolution (through the use of zero padding) 0.35 x 0.35 x 1.5 mm, gap of 10%; TSE factor: 3; repetition time (TR): 500 ms; echo time (TE): 10 ms; flip angle $90^{o}$; acquisition matrix: 256 x 204; time of acquisition (TA): 7 min). For more details about the 3T methods see Tona *et al.* (2017).

***7 Tesla MRI*** The 7T MRI session was performed on a whole-body Achieva Philips scanner equipped with a 32-channel head coil. During this scan session, the participants underwent a whole-brain 3D $T_1$-weighted scan (FOV: 246 x 246 x 174 mm; 249 slices; 0.69 x 0.69 x 0.69 mm; TR: 4.5 ms; TE: 2.0 ms; flip angle $7^{o}$; acquisition matrix: 352 x 353; TI = 1600 ms; sagittal orientation; TA: 8 min 26 s).

We acquired a TSE scan with parameters as similar as possible to the 3T scan (TSE 7T; FOV: 180 x 180 x 9.75 mm; 6 slices;0.70 x 0.87 x 1.5 mm; slice gap: 0.15 mm; TR: 500 ms; TE: 10 ms; flip angle $90^{o}$; acquisition matrix: 265 x 204; transverse orientation; TSE factor 3; TA: 6 min 54 s).A TSE scan with higher spatial resolution was locally optimized (HR-TSE 7T; FOV: 180 x 180 x 13 mm; 12 slices acquired in 4 interleaved packages; slice gap: 0 mm; 0.44 x 0.44 x 2 mm; TR: 550 ms; TE: 8.4 ms; flip angle $90^{o}$; acquisition matrix: 400 x 400; TA: 14 min 47 s).

Finally, we obtained a high-resolution $T_2$*-weighted scan (HR-$T_2$*; FOV: 240 x 180 x 50 mm; 46 slices; 0.23 x 0.23 x 1 mm; slice gap: 0.1 mm; TR: 1766 ms; TE: 25.2 ms; flip angle $60^{o}$; transverse orientation; acquisition matrix: 1000 x 750; TA: 10 min 09 s) and a T1-weighted SPIR scan (FOV: 180 x 180 x 7.2 mm; 12 slices; 0.60 x 0.60 x 0.60 mm; TR: 9.9 ms; TE: 5.3 ms; flip angle $35^{o}$; transverse orientation; acquisition matrix: 300 x 294; offset frequency: 1053 Hz; pulse magnitude: 6.17 mT; TA: 7 min 16 s). T*otal scan duration was approximately 60 minutes. All 3T and 7T sequences were acquired in transverse direction.* We chose not to match the sequences on resolution or FOV because, if we would have chosen the lowest common denominator across the sequences, this would have severely limited the capabilities of a number of sequences. In the end, we chose specific, optimal, scan parameters per sequence which have been shown to be successful in depicting subcortical structures . See Table 1 for a summary of the main scan parameters and Fig 1 for an overview of the different contrasts.

**Table 1.** Overview of the scan parameters used to extract the LC contrast.

| MR parameter | TSE 3T | TSE 7T | HR-TSE 7T | HR-$T_2$* - magnitude | HR-$T_2$* - phase unwrapped | HR-$T_2$* - SWI | SPIR | Whole-brain $T_1$ |
|---|---|---|---|---|---|---|---|---|
| Field strength | 3 T | 7 T | 7 T | 7 T | 7 T | 7 T | 7 T | 7 T |
| Acq. Res. | 0.70x0.88x1.5 | 0.70x0.87x1.5 | 0.44x0.44x2 | 0.23x0.23x1 | 0.23x0.23x1 | 0.23x0.23x1 | 0.6x0.6x0.6 | 0.69x0.69x0.69 |
| Rec. Res. | 0.35x0.35x1.5 | 0.35x0.35x1.65 | 0.35x0.35x1.0 | 0.23x0.23x1 | 0.23x0.23x1 | 0.23x0.23x1 | 0.56x0.56x0.6 | 0.64x0.64x0.69 |
| TE | 10 ms | 10 ms | 8.4 ms | 25.2 ms | 25.2 ms | 25.2 ms | 5.3 ms | 2.0 ms |
| TR | 500 ms | 500 ms | 550 ms | 1766 ms | 1767ms | 1767ms | 9.9 ms | 4.5 ms |
| Flip angle | 90$^o$ | 90$^o$ | 90$^o$ | 60$^o$ | 60$^o$ | 60$^o$ | 35$^o$ | 7$^o$ |
| Matrix size | 256 x 204 | 265 x 204 | 400 x 400 | 1000 x 750 | 1000 x 750 | 1000 x 750 | 300 x 294 | 352 x 353 |
| Number of slices | 14 | 6 | 12 | 46 | 46 | 46 | 12 | 249 |
| Acquisition time | 7min | 6min54s | 14min47s | 10min09s | 10min09s | 10min09s | 7min16s | 8min26s |
| Total number of subjects | 12 | 12 | 12 | 12 | 11 | 11 | 12 | 12 |

All DICOM scans were exported to NIfTI using dcm2nii as implemented in MRIcron (V. 2014; Rorden & Brett, 2000). Due to technical reasons the HR-$T_2$* unwrapped-phase and SWI scans are missing for one participant. Acq. Res: acquired resolution; Rec. Res: Reconstructed resolution; TE: echo time; TR: repetition time.

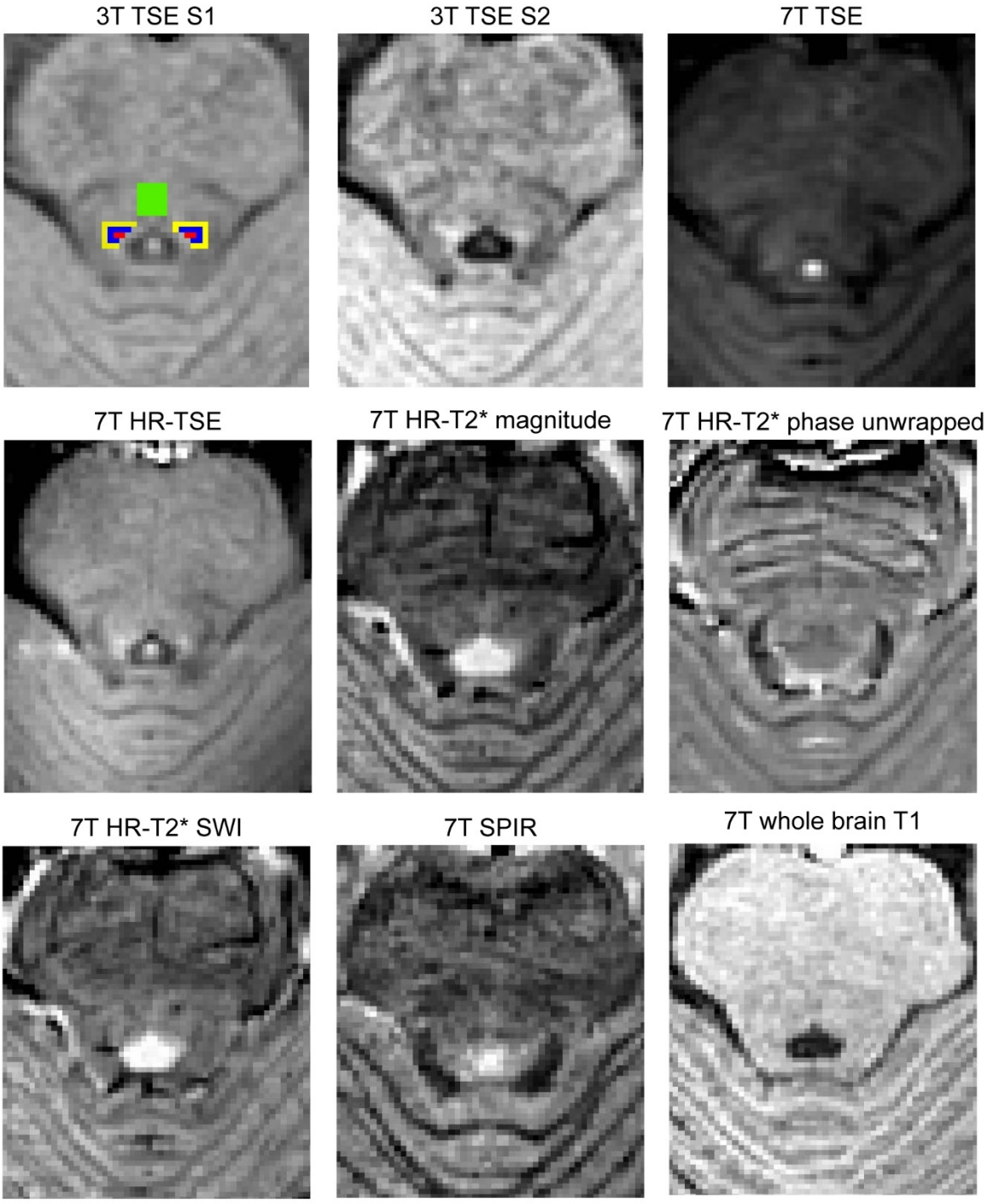


**Figure 1.** Visual representation of the contrast as obtained from the different scan sequences for a representative participant. The LC masks obtained from the 3T TSE scan in session 1 (S1) are depicted in red (masks of two raters were combined). Blue color indicates voxels that are directly adjacent to the LC mask (plus1). Yellow indicates voxels located two voxels away from the LC mask (plus2). Green color refers to the pontine tegmantum ROI (pt). The other panels show the other eight sequences acquired in this study. All scans were linearly registered to the 7T whole-brain $T_1$ scan to enable visualization of the same brain region. The contrast levels for each sequence were normalized using the quickLUT tool in MIPAV. This tool was used to set the image contrast based on the highest and lowest values in an identical region across sequences.

***Selection of field of view (FOV) for the slab scans***

The field of view (FOV) for the slab acquisitions was selected by two authors (KDT and MvO) after training by a neuroanatomist, extensive piloting and consultation of the literature. During the 3T acquisition the FOV was set perpendicular to the LC and covered the entire LC region (see Tona et al.;  Tona et al., 2017). For the 7T acquisition the same experts selected the FOV based not only on knowledge about LC position and anatomy but also by having the previously acquired 3T LC scan (of the same participant) as well as its planning relative to the survey scans available at the MRI console during the planning procedure. In this manner, maximum consistency was achieved for the LC localization between and within subjects but also between scanning sessions and different scans.

***Extent of the LC captured by the slab scans***

Due to the SAR limitation, the 7T slab scans can suffer from a limited coverage. The priority of this study was to achieve higher contrast and resolution in order to visualize the LC. This came at the expense of brain coverage and the ability to capture the entire rostrocaudal extent of the LC. Specifically, the average percentage of the rostrocaudal extent of the LC (compared to the 3T TSE manual delineation) was 84% (SD 13%) for the 7T TSE sequence, 93% (SD 15%) for the 7T HR-TSE sequence, 100% for the 7T HR T2* slabs, and 60% (SD 27%) for the 7T SPIR sequence.

***Registration procedures***

*Registration of 3T to 7T dataset*

All registration steps were done on a single-subject level and performed using FSL (5.0.8.; Jenkinson et al., 2012). The slab of 3T TSE imaging slices was linearly registered to the 7T $T_1$-weighted whole-brain volume using FLIRT by means of mutual information, 6 degrees of freedom, and trilinear interpolation. This was done for both 3T TSE volumes. Subsequently, the LC mask of the first scan session at 3T (manually segmented twice by two raters, i.e. 4 segmentations in total) was registered to the 7T whole-brain scan by using the transformation matrix and nearest neighbour interpolation. The 3T LC masks of the first 3T TSE scan session (2 raters X 2 segmentation sessions) were combined and thresholded to create a conjunction mask that contained only voxels that were identified as LC in 3 out of the 4 masks. This conjunction mask was consecutively used as an ROI for measuring the contrast of the LC for all 7T scans, as well as for the second scan session at 3T. Next, two additional masks were created by expanding the LC masks with plus 1 and plus 2 voxels using a 2D box kernel, while excluding the LC mask. Finally, the fourth ventricle was manually segmented on the 3T TSE scan in native space of the first scan session. This was done to ensure that none of the employed masks included any voxels located within the fourth ventricle. Finally, two additional masks were created by expanding the LC masks with plus 1 and plus 2 voxels using a 2D box kernel, while excluding the LC mask. To provide comparable contrast with previous work (Mather et al., 2017; Matsuura et al., 2013; Miyoshi et al., 2013) an additional control

region was created in the pontine tegmentum. For all axial slices that contained the LC mask, a region of approximately 4.0 x 4.0 mm was identified in the center of the pontine tegmentum. The resulting LC and control region ROIs can be seen in Fig 1.

*Registration of 7T dataset*

The 7T scans were co-registered to the 7T whole-brain scan using 6 degrees of freedom, mutual information, and trilinear interpolation, except for the 7T TSE scan, for which mutual information failed and normalized correlation was used instead. All 3T and 7T registrations were visually inspected in FSLview by checking the following landmarks for alignment: fourth ventricle floor, the top indentation of the pons, and the bilateral cerebellar superior peduncle. See Fig. S1 for examples of the registration accuracy.

## Analysis

### *Signal extraction*

To measure the contrast of the LC, not only the signal intensity within the LC mask was determined, but also the signal intensity in its immediate surroundings. In more detail, for each image registered to the 7T whole-brain T1-weighted image, we extracted the median signal within the LC ROI, the median signal within the voxels directly adjacent to the LC mask (LC plus 1), and the median signal within the region that is two voxels away from the LC mask (LC plus 2). We also extracted the median signal from the pt ROI.

We included the plus 1 and plus 2 control regions as these ROIs reflect the borders that are of direct interest when parcellating the LC. The reason why we include two different control regions adjacent to the LC (plus 1 and plus 2) was to control for partial volume effects. Given the underlying anatomy of the LC, which has a dense core of neurons and then a diluted area around it (Fernandes et al., 2012; German et al., 1988; Keren et al., 2015), it is likely that the directly adjacent voxels (plus 1) still contain parts of the LC.

The pontine tegmentum control region was included because it facilitates comparisons with prior literature and because this ROI is not sensitive to LC-partial volume effects. However, it should be noted that this pons control ROI is not homogenous as it encompasses elements of the pontine reticular formation (i.e., the nucleus raphe pontines and nucleus reticularis tegmentipontis). In addition, the pons control ROI contains both longitudinally and transversely oriented fibre tracts (the tectospinal and decussating trigemino-thalamic tracts respectively) see, e.g., brain atlases such (Nieuwenhuys, Voogd, & van Huijzen, 2013) and (DeArmond, Fusco, & Dewey, 1974).

In our main analysis we registered all the LC masks and MRI sequences to the corresponding whole brain 7T $T_1$-weighted image. The advantage of this approach is that it allows us to compare the exact same locations across the different sequences. A limitation however is that it entails a registration step which results in implicit smoothing. Therefore, in addition to the main analysis, the LC masks were projected to each individual sequence native space using the combined transformation matrices.

***Contrast ratio estimation***

The contrast of the LC was calculated per hemisphere based on the following relative contrast formulas:

$$LC\ contrast\ 1 = \frac{LC - LC\ plus\ 1}{LC\ plus\ 1} * 100$$

$$LC\ contrast\ 2 = \frac{LC\ - LC\ plus\ 2}{LC\ plus\ 2} * 100$$

$$LC\ contrast\ pt = \frac{LC\ - PT}{PT} * 100$$

where *LC* is the median intensity within the LC ROI, *LC plus 1* is the median intensity in the control region that is one voxel adjacent to the LC ROI, *LC plus 2* is the median intensity in the control region that is two voxels away from the LC ROI and *PT* is the median intensity in the pontine tegmentum control region. To test whether the left and right LC had similar contrast we calculated the Pearson correlation coefficient per contrast and sequence.

The LC contrasts were first calculated for each hemisphere and then averaged, since we had no a-priori hypothesis regarding hemispheric differences in contrast ratio. This resulted in a total of eight contrast values per subject: one for the reference 3T TSE scan and seven for the 7T scans.

***Data preprocessing and Bayesian statistics***

The LC contrast 1 and LC contrast 2 were first calculated per hemisphere separately, and subsequently averaged over hemispheres, resulting in a total of eight contrast values per subject: one for the reference 3T TSE scan and seven for the 7T scans. An outlier rejection criterion of three times the interquartile range was subsequently used to test for outliers.

All sequences were compared in a quantitative statistical manner. Bayesian one-sample t-tests using a Cauchy prior of 0.707 were utilized to quantify whether the LC contrasts differed significantly from zero. The one-sample t-tests were carried out using JASP (JASP Team, 2017). The benefit of using Bayesian statistics is that it allows the quantification of evidence for the null hypothesis ($H_0$: the intensity of the LC does not differ from the adjacent voxels) versus the alternative hypothesis ($H_1$: the intensity of the LC does differ from the adjacent voxels). We used the labels as proposed by Jeffreys (1961) and edited by Wetzels and Wagemakers (Wetzels & Wagenmakers, 2012). Table 2 shows this suggested evidence categorization for the $BF_{10}$, but note that these labels are only used to facilitate the interpretation of the evidence and should not zealously be adhered to.

**Table 2.** Suggested categories for interpreting the Bayes factors.

| Bayes factor $BF_{10}$ | | | Interpretation |
|---|---|---|---|
| | > | 100 | Decisive evidence for $H_1$ |
| 30 | - | 100 | Very strong evidence for $H_1$ |
| 10 | - | 30 | Strong evidence for $H_1$ |
| 3 | - | 10 | Substantial evidence for $H_1$ |
| 1 | - | 3 | Anecdotal evidence for $H_1$ |
| | 1 | | No evidence |
| 1/3 | - | 1 | Anecdotal evidence for $H_0$ |
| 1/10 | - | 1/3 | Substantial evidence for $H_0$ |
| 1/30 | - | 1/10 | Strong evidence for $H_0$ |
| 1/100 | - | 1/30 | Very strong evidence for $H_0$ |
| | < | 1/100 | Decisive evidence for $H_0$ |

The scans for which the one-sample t-tests indicated strong or more ($BF_{10} > 10.0$) evidence in favor of $H_1$ were then statistically compared with each other in a JZS Bayesian mixed effect model with contrast ratio as the dependent variable, contrast level and sequence type as the independent variables, and subjects as the random factor. This analysis and the follow-up post-hoc Bayesian paired t-tests were carried out using the Bayes Factor package (R. D. Morey & Rouder, 2013; Rouder, Morey, Speckman, & Province, 2012) as implemented in R ( V. 3.2.4; R-Development_Core_Team, 2013). For the paired t-tests, subjects were excluded if they had a missing value due to outlier rejection in any of the tested scans.

### *Data availability*

All extracted data from the MRI sequences and code used to analyse the data are made available on https://osf.io/83r9j/?view_only=a9e469fac61e4731a5e1cb7ade3ab9a2.

## Results

### *Descriptives*

After registration of the various images the median signal was extracted for the LC and the surrounding control regions, and the contrasts were calculated. The summary statistics are provided in Table 3. Note that while the 7T HR-$T_2$*-magnitude sequence had the smallest contrast, on average it had the highest left-right contrast consistency. Other sequences that had a high left-right contrast consistency were the 7T SPIR and 3T TSE sequence. Also note that depending on the control region, the left-right contrast consistency varied substantially within and between sequences. To visualize the contrast

of the different types of scans, a representative subject was selected for whom, for a single slice and profile line, the signal intensity was extracted and plotted (see Fig 2). The descriptive results were very similar when the contrast was extracted in native scan space (see Table S1 and Fig. S2)

**Table 3.** Summary statistics of the estimated LC contrasts for each scan sequence.

| | | LC contrast 1 | | | LC contrast 2 | | | LC contrast pt | | |
|---|---|---|---|---|---|---|---|---|---|---|
| | N(contrast 1/2/pt) | Avg. median | IQR | Cor. L/R | Avg. median | IQR | Cor. L/R | Avg. median | IQR | Cor. L/R |
| 3T TSE | 12/12/12 | 4.39 | 1.63 | 0.68 | 8.58 | 1.66 | 0.47 | 9.06 | 2.43 | 0.47 |
| 7T TSE | 12/12/12 | 2.91 | 3.27 | 0.50 | 7.51 | 3.69 | 0.48 | 9.44 | 9.35 | -0.25 |
| 7T HR-TSE | 12/12/12 | 2.36 | 2.32 | 0.26 | 5.51 | 1.46 | 0.13 | 6.40 | 7.18 | -0.40 |
| 7T HR-$T_2$* - magnitude | 11/11/9 | -0.20 | 0.16 | 1.0 | -0.36 | 0.32 | 1.0 | -0.42 | 0.38 | 1.0 |
| 7T HR-$T_2$* - phase unwrapped | 11/10/9 | -44.72 | 100.46 | 0.35 | 19.92 | 179.54 | 0.19 | -21.72 | 150.43 | 0.74 |
| 7T HR-$T_2$* - SWI | 9/8/7 | -0.51 | 0.39 | 0.68 | 0.83 | 0.53 | 0.23 | 1.03 | 0.71 | 0.26 |
| 7T SPIR | 12/12/12 | 5.60 | 2.60 | 0.68 | 11.90 | 4.70 | 0.60 | 7.49 | 5.41 | 0.40 |
| 7T whole brain $T_1$ | 12/12/12 | 1.32 | 2.77 | 0.23 | -0.66 | 3.02 | -0.15 | 1.85 | 4.42 | -0.32 |

N: the number of participants after outlier rejection. Avg. Median: average median. Cor. L/R: Pearson correlation coefficient between the left and right hemisphere contrast. Note that for the $T_2$*-based contrasts one participant was missing due to technical reasons; IQR: interquartile range; pt: pontine tegmentum.

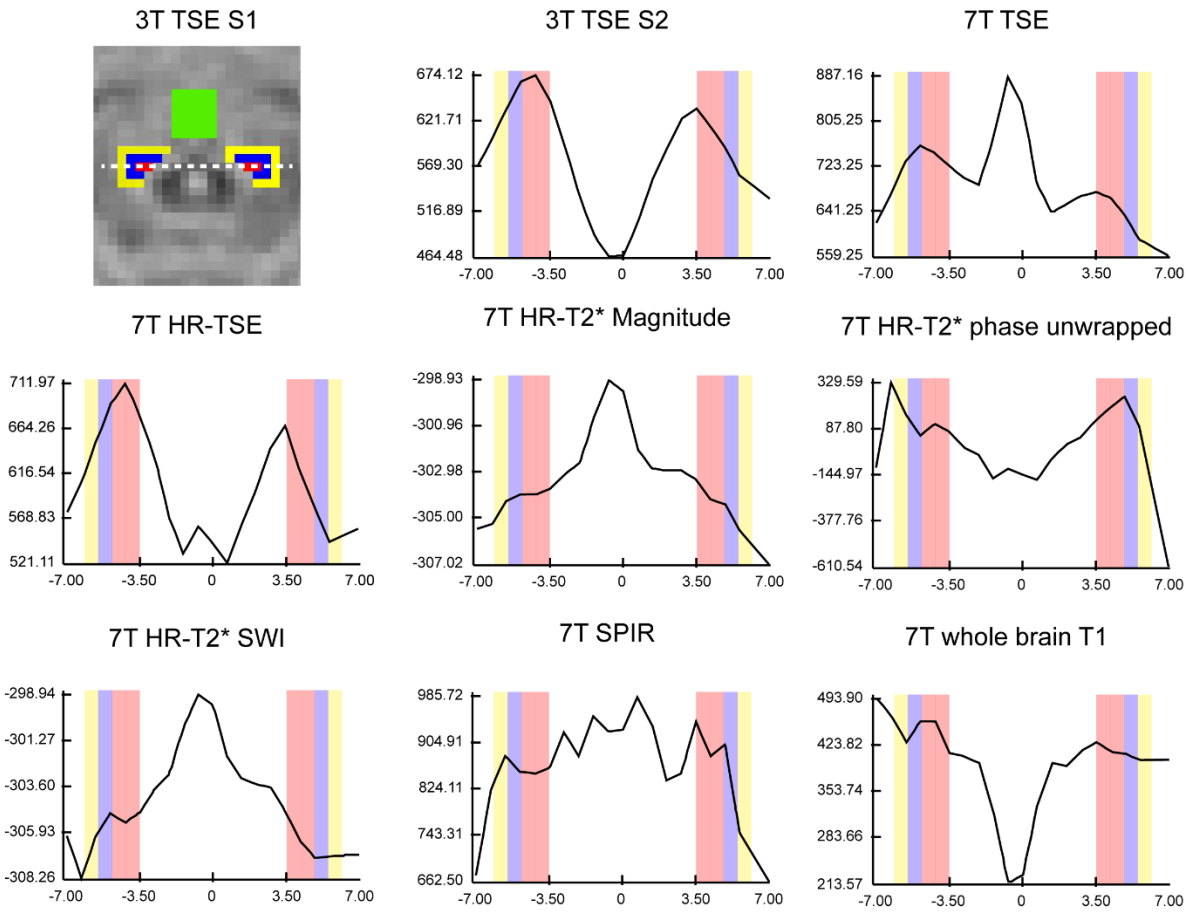


**Figure 2.** A scan intensity profile figure. The black intensity line shows the change of intensity for a single subject along the dotted line as indicated in the 3T TSE scan of the first session (S1). All intensity values were extracted from the same axial level of the LC across contrasts. The participant and axial level is identical to Fig 1. The point 0 of the x-axis corresponds to the middle of the 4th ventricle, the red bars correspond to the LC mask, the blue and yellow bars correspond respectively to the ROIs of LC plus 1 and LC plus 2. Contrary to this approach (scan intensity profile; which includes only the voxels on the line), the statistical analyses included the median of the entire LC mask, which makes those analyses less susceptible to noise.

### *Contrast between the LC and the surrounding tissue*

Our first goal was to test whether the different sequences provide any contrast between the LC and the surrounding tissue. To this end, a Bayesian one-sample t-test was used to test whether any of the 8 scan sequences provided a contrast which is different from zero. Fig 3 and Table 4 provide the results for all contrast definitions: LC contrast 1, LC contrast 2, and LC contrast PT.

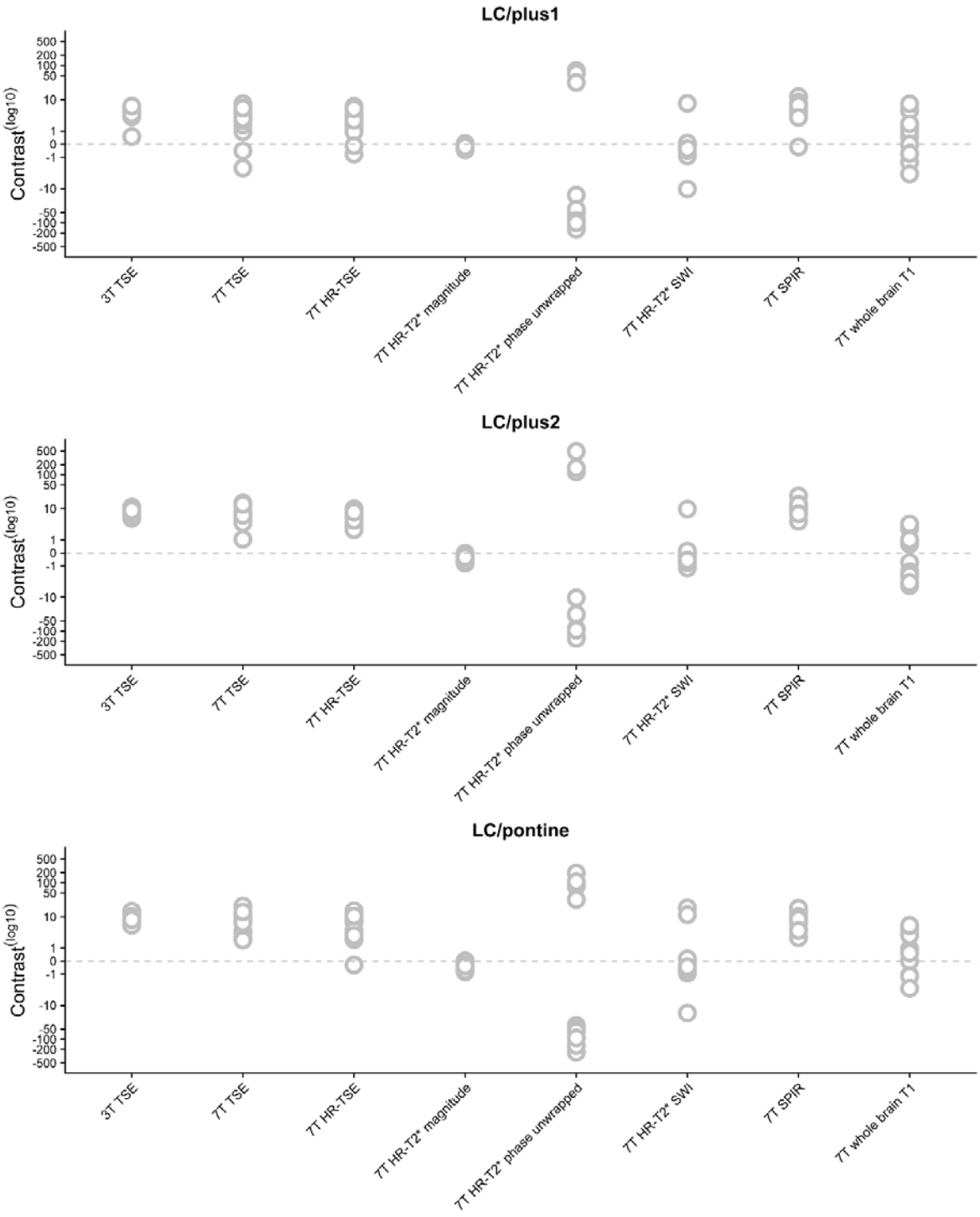


**Figure 3.** Contrast ratios per scan, separately for each participant. The top panel illustrates the contrast per sequence between the LC and the directly adjacent voxels (LC/plus1). The middle panel illustrates the contrast between the LC and the region which is two voxels removed from the LC (LC/plus2). Finally, in the lower panel, the contrast between the LC and the pontine is shown (LC/pontine). Each circle corresponds to a single subject.

Bayes factors indicated strong or more evidence ($BF_{10} > 10.0$) in favour of the hypothesis that there is a contrast different from zero between the LC and the surrounding tissue for the following sequences: 3T TSE, 7T TSE, 7T HR-TSE,7T HR-$T_2$*-magnitude, and the 7T SPIR. All of these scans showed a positive contrast (i.e., higher signal intensity for LC

than the surroundings) except for the HR-$T_2$*-magnitude sequence, which on average displayed a lower intensity within the LC (see Fig 3 and Table 4). As these five sequences had a $BF_{10}$ higher than 10.0 for all three contrasts, they were included in the mixed effect model to compare the contrast between sequences. For a proper comparison between the contrasts of the different scans, the 7T HR-$T_2$* magnitude contrast scores were inverted by multiplying with -1 for all further analyses. The results are very similar when the signal was extracted in native scan space (Table S2).

**Table 4.** Results of the Bayesian one-sample t-tests examining which scans deliver a detectable contrast between the LC and surrounding tissue.

| Comparison | N(contrast 1/2/pt) | LC contrast 1 $BF_{10}$ | LC contrast 2 $BF_{10}$ | LC contrast pt $BF_{10}$ |
|---|---|---|---|---|
| 3T TSE ≠ 0 | 12/12/12 | 13.4e3 | 2.98e6 | 1.72e4 |
| 7T TSE ≠ 0 | 12/12/12 | 12.8 | 546 | 118.56 |
| 7T HR-TSE ≠ 0 | 12/12/12 | 18.4 | 12.1e3 | 57.68 |
| 7T HR-T2* - magnitude ≠ 0 | 11/11/11 | 72.7 | 86.2 | 139.18 |
| 7T HR-T2*-phase unwrapped ≠ 0 | 11/10/10 | 1.24 | 0.32 | 0.35 |
| 7T HR-T2* - SWI ≠ 0 | 9/8/10 | 0.34 | 0.40 | 0.33 |
| 7T SPIR ≠ 0 | 11/11/11 | 183 | 1.36e3 | 66.11 |
| 7T whole brain T1 ≠ 0 | 12/12/12 | 0.70 | 0.42 | 1.72 |

N: the number of participants after outlier rejection.

The reader is referred to Table 2 for an interpretation of the resulting Bayes factor.

### *Mixed effect model to compare the sequences*

A JZS Bayesian mixed effect model (R. D. Morey & Rouder, 2015; Rouder et al., 2012) with default prior scales revealed that the model with main effects of scan sequence and contrast ratio, as well as an interaction between those variables, is preferred above the model without the interaction effect by a Bayes factor of 21.02. The data therefore provide strong evidence that the contrast between the LC and the surrounding tissue is influenced by sequence type, distance from the LC, as well as an interaction between the two factors.

Post-hoc pairwise comparisons among the five sequences showed decisive evidence that the 7T HR-$T_2$* magnitude sequence provides lower contrast than the other four sequences, so this 7T sequence can be discarded (Table 5). The remaining six comparisons yielded three noteworthy findings. First, the results (LC contrast 2) show strong evidence that of the remaining three 7T sequences the SPIR sequence provides higher contrast than the two sequences that were based on the 3T TSE sequence: 7T TSE

and 7T-HR TSE. Second, the results of all contrasts provide insufficient evidence ($BF_{10}$ close to 1.0) to determine whether the SPIR sequence has different or similar contrast as the 3T TSE sequence (see Fig 4 for visualization of the SPIR contrast and Fig S3 for the SPIR visualization for all subjects included in the study). Third, and perhaps counterintuitively, we find strong to very strong evidence that the 3T TSE sequence provides higher contrast for the LC with the direct surrounding tissue than the high-resolution 7T TSE sequence. The results are very similar when the signal was extracted in native scan space (Table S3). This quantitative comparison of contrast was based on the median value of the intensity within the LC masks and control region. However, given that the intensity values within the LC masks may be highly variable, we also provide the (median/(within ROI IQR) ratio within the LC mask for each scan and participant. The results of these extra analyses provide an estimate of "within LC mask"- contrast variability, are in line with the results mentioned here and can be found on Table S4.

**Table 5.** The post-hoc Bayesian paired t-tests examining whether there was a difference in contrast between sequences, for LC contrast 1, LC contrast 2 and LC contrast pt separately.

| Comparison | N | $BF_{10}$ for LC contrast 1 | $BF_{10}$ for LC contrast 2 | $BF_{10}$ for LC contrast pt |
|---|---|---|---|---|
| 3T TSE – 7T TSE | 12 | 1.19 | 0.42 | 0.29 |
| **3T TSE** – 7T HR-TSE | 12 | 15.04* | 40.81* | 0.85 |
| **3T TSE** – 7T HR-T2* magnitude | 11 | 3547.95* | 1.01e+6* | 9.7e+4 |
| 3T TSE – 7T SPIR | 11 | 0.55 | 1.98 | 0.56 |
| 7T TSE – 7T HR-TSE | 12 | 0.33 | 0.90 | 2.37 |
| **7T TSE** – 7T HR-T2* magnitude | 11 | 6.00 | 152.59* | 63.13 |
| **7T HR-TSE** – 7T HR-T2* magnitude | 11 | 8.10 | 1326.17* | 23.55 |
| **7T SPIR** – 7T HR-T2* magnitude | 10 | 68.09* | 422.07* | 27.24 |
| **7T SPIR** – 7T TSE | 11 | 1.78 | 13.33* | 0.36 |
| **7T SPIR** –7T HR-TSE | 11 | 2.71 | 12.76* | 0.36 |

N: the number of participants after outlier rejection. For comparisons with strong evidence for a difference in contrast (*$BF_{10}$ > 10.0), bold-faced sequence has the higher contrast. Pt: pontine tegmentum. The reader is referred to Table 2 for an interpretation of the resulting Bayes factor.

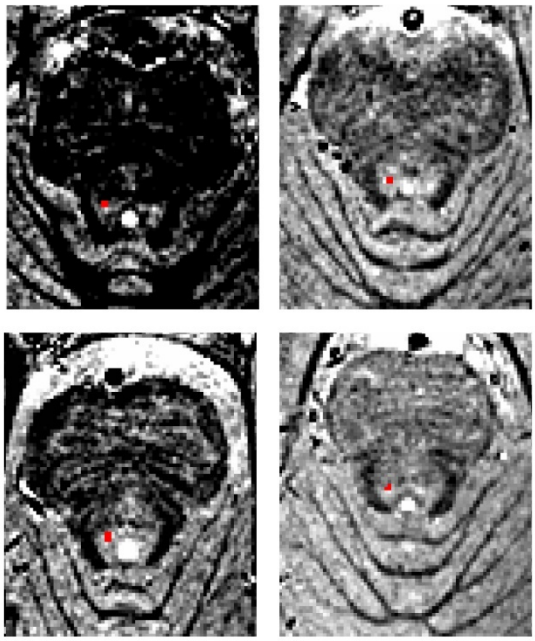

**Figure 4.** Visualizing the SPIR contrast. For four participants the 7T SPIR volumes in native space are highlighted. The red voxels correspond to the LC as identified on a 3T TSE scan from scan session 1 and registered to the 7T SPIR volume. The contrast levels were set using the min/max values directly surrounding the LC mask.

## Discussion

In this study we measured the LC contrast *in vivo* for a number of 7T sequences and compared the obtained contrast measures to a frequently used sequence at 3T. The Bayesian one-sample t-tests indicated that the 3T TSE, 7T TSE, 7T HR-TSE, 7T HR-$T_2$*-magnitude, and the 7T SPIR sequences are able to provide significant contrast for visualizing the LC. The statistical analyses also suggested that, of the 7T sequences included in this study, SPIR provides higher contrast than the sequences that were directly based on the 3T TSE sequence. Based on the statistical test, one should conclude that there is not sufficient evidence to state whether the SPIR sequence provides similar, stronger or weaker contrast than the 3T TSE sequence. Further research, preferably with a larger sample size, is needed to address that question. A benefit of the 7T SPIR over the 3T TSE sequence is that, given a similar acquisition time, the 7T sequence has isotropic voxels which are approximately 4 times as small in volume as the voxel size of the 3T TSE scan employed in this study. There are clear advantages of isotropic voxels for edge detection, and therefore volume estimates, of small brain areas (Wonderlick et al., 2009). However due to SAR limitations the SPIR scan did not cover the entire brain. This leads to some limitations that we further comment on in the limitation section. Recent efforts by Priovoulos et al. (2017) have been successful in visualizing the LC using a MT-weighted FLASH sequence with 0.4 x 0.4 x 0.5mm resolution at 7T, whereas Betts et al. (2017) visualized the LC using a $T_1$-weighted FLASH sequence with 0.75mm isotropic resolution at 3T. The advantage of those sequences is that they were able to visualize the entire rostrocaudal extent of the LC. Unfortunately, these efforts were unknown when our data were acquired. While the choice of sequences in the current study might be less optimal than the sequences by Priovoulos et al. (2017) and Betts et al. (2017), our results complement these efforts by directly quantifying the LC contrast with a number of control regions in a Bayesian framework. Additionally, we examined a number of

sequences whose utility for LC imaging has been highlighted by prior literature whereas these sequences were not tested by Priovoulos et al. (2017) and Betts et al. (2017), e.g. 7T TSE, 7T HR-$T_2$* - magnitude, 7T HR-$T_2$*-phase unwrapped, 7T HR-$T_2$* - SWI. In summary, our study confirms that a MT-weighted (by exploiting the SPIR module in our protocol) FLASH sequence seems the most appropriate method for LC scanning at 7 Tesla.

There has been an ongoing discussion about whether the LC signal intensity should be normalized to a reference region and if so, which region would be most suitable (Liu et al. 2017). Here, we normalized the LC intensity with three different reference regions: the voxels directly adjacent to the LC, two voxels away from the LC mask, and a frequently used area in the pontine tegmentum. The mixed effect model results showed that the contrast between the LC and surrounding tissue is influenced by sequence type, distance from the LC, as well as an interaction between the two factors, suggesting that the LC contrast with the surrounding tissue increases when the control region is not taken directly adjacent to the LC. Given the underlying anatomy of the LC, which has a dense core of neurons, this result can be explained by partial volume effects which are smaller as the distance between the core LC and surrounding tissue increases, and thus result in a larger contrast. For segmentation purposes the LC contrast with the plus 1 and plus 2 reference region seems the most relevant as it entails the border that one wants to identify. The LC contrast with the pontine tegmentum control region seems to be most relevant for comparing our results with previous work (Liu et al. 2017). But a cautionary note should be made, because it is known that the pontine tegmentum shows age-related changes in intensity, which complicates comparisons between LC contrasts normalized with such a reference region over a wide age range (Keren et al., 2009), (Clewett et al., 2016). The choice of the control region also has an influence on hemispheric contrast consistency. As shown in Table 3, depending on which control region is used, the correlation coefficient between the left and right LC contrast can vary substantially. This effect of control region should be taken into account when interpreting the various reports on hemisphere difference in LC intensity (e.g., Betts et al., 2017; Dahl et al., 2018; Keren et al., 2015; Tona et al., 2017)

***Potential contrast mechanism of 7T SPIR sequence***

Of the seven 7T sequences we tested, SPIR was found to give the highest contrast between the LC and the surrounding tissue. Here we discuss the potential underlying contrast mechanism of this sequence. It has been argued that the origin of MRI contrast in neuromelanin imaging is based on the combination of a number of factors: presence of neuromelanin, but also iron and copper, as well as the occurrence of magnetization transfer (MT) effects (Chen et al., 2014; Keren et al., 2015; Nakane, Nihashi, Kawai, & Naganawa, 2008; Ogisu et al., 2013; Priovoulos et al.; Trujillo et al., 2016). Although the primary use of a SPIR pulse is to suppress the signal from fat, this pulse does introduce some MT effects into the contrast as the pulse is off-resonance with respect to the water peak (Del Grande et al., 2014). Besides the $T_1$ component in the employed SPIR sequence, the MT contribution in combination with $T_1$-weighting might be the reason

why the SPIR sequence was found to be the most promising sequence for LC imaging at 7T. Indeed, in line with our results, a recently published study shows that MT-weighted sequences can deliver sufficient contrast to visualize the LC *in vivo* at 7T (Priovoulos et al., 2017). However, other recent work imaging phantoms with different concentrations of iron and synthetic melanin, indicates that the presence of melanin with or without iron does not lead to direct MT effects (Trujillo et al., 2016). Instead any reduction in MT ratio (MTR) is due to $T_1$ effects of the free water pool. Thus, the MTR can be indirectly reduced in the presence of melanin-iron complexes, as a result of $T_1$ shortening. Based on the current results as well as previous results (Priovoulos et al., 2017; Trujillo et al., 2016) it seems likely that MT play an important role in LC imaging, along with other factors that determine the contrast (e.g., $T_1$ effects).

***Limitations***

This study has a few limitations. The first is that we did not randomize the order of scan sequences over the subjects, which might have resulted in more motion artifacts in the later scans (Forstmann et al., 2017). However, it should be noted that the 7T SPIR sequence, which was the most promising 7T sequence, was always acquired last. Additionally it is important to state that the employed sequences in this study or in literature are mainly sensitive but not exclusively sensitive to neuromelanin. Contrast in the scans is therefore likely to differ between sequences as well as between field strengths. Another limitation pertains to the choice of 6 degrees of freedom for all registration steps. The rationale for this choice was that all registration steps were done in a "within-subject" fashion (inter-subject analysis) and that we did not want to incorporate different scaling factors for registration analysis applied to different datasets. While all registration steps were visually inspected and several examples of registration accuracy are given in the Fig. S1, it might still be the case that different geometric distortions between field strengths resulted in subtle misalignments (see for instance (Duchin, Abosch, Yacoub, Sapiro, & Harel, 2012). As a result, due to the concatenation of two 3T towards 7T transformation matrices, it might explain why the number of outliers for the 3T TSE sequence in native space is higher than in 7T $T_1$-space. Another limitation is that we did not acquire quantitative MRI (qMRI) sequences. There are several benefits of qMRI ($T_1$, $T_2$, $T_2$*, PD, MT etc) over standard weighted sequences as the values are standardized and allow for direct comparison between centers (Weiskopf et al., 2013). Another advantage of qMRI is that a physical meaning can be assigned to the intensity of the voxel, which can then be linked to the underlying mechanism contributing to the contrast (Weiskopf, Mohammadi, Lutti, & Callaghan, 2015). Contrary to the SPIR sequence, which was not optimized to maximize MT effects, the acquisition of qMT volumes would have allowed for a direct quantification of the contribution of MT to the LC contrast. Another limitation is that the CNR comparisons were only performed on young participants. It is known that the level of neuromelanin in young adults is lower than in elderly (Mann & Yates, 1974; Zecca et al., 2004). Such age-related changes in the tissue property might influence the generalizability of our results and should be considered when including different age groups.

It should also be noted that the recently published sequences by Priovoulos et al. (includes 7T sequences) and Betts et al. (includes 3T sequences) were not included in our set of sequences, since these studies were only published after our data collection. Sequences in our protocol resembled their settings, but were slightly different. Moreover, our results complement their efforts by directly quantifying the LC contrast with a number of control regions in a Bayesian framework. Additionally, we examined a number of sequences whose utility for LC imaging has been suggested by prior literature but were not tested by Priovoulos and Betts; e.g. 7T TSE, 7T HR-$T_2$* - magnitude, 7T HR-$T_2$*-phase unwrapped, 7T HR-$T_2$* - SWI. In summary, our study confirms arguments by Priovoulos et al. and Betts et al. that a MT-weighted (by exploiting the SPIR module in our protocol) FLASH sequence seems the most appropriate method for LC scanning at 7 Tesla.

Additionally, while all registration steps were visually inspected and several examples are given in the Fig. S1, it might still be the case that different geometric distortions between field strengths resulted in subtle misalignments (see for instance Duchin et al., 2012). As a result, due to the concatenation of two 3T towards 7T transformation matrices, it might explain why the number of outliers for the 3T TSE sequence in native space is higher than in 7T $T_1$-space.

***Suggestions for future directions***

Future studies should further optimize the SPIR sequence to allow for manual segmentation of the LC and improve the coverage of the rostrocaudal extent of the LC, for example with multiband MRI. Another possibility that future studies might consider is to potentially increase the SPIR contrast by modifying the suppression pulse amplitude, the off-resonance frequency and time between suppression and excitation. Additionally, some of the SNRs for the 7T images are lower than the 3T (see Table S4), which might indicate that the increase in resolution costs more SNR than is gained by moving to 7T. Therefore, future studies comparing 3T with 7T could incorporate a design where the SNR is kept constant between the two modalities by finding the exact resolution on the 7T that would match the SNR at 3T and then compare the detectability of the LC.

***Conclusion***

In conclusion, by quantitatively comparing the contrast of the LC with the surrounding tissue for a number of sequences, we have identified a promising SPIR-based sequence. This sequence provides similar contrast of the LC as the 3T sequence commonly used, but at a higher spatial resolution (compared to the 3T TSE scan used in the majority of studies) and with isotropic voxels. The isotropic voxels at 7T should be considered an important advantage given the small size of the LC. Finally, although there is no clear benefit in contrast, a potential advantage of using SPIR is the relatively short acquisition time, which may be desirable in clinical settings to minimize subject motion.

## Supporting Information

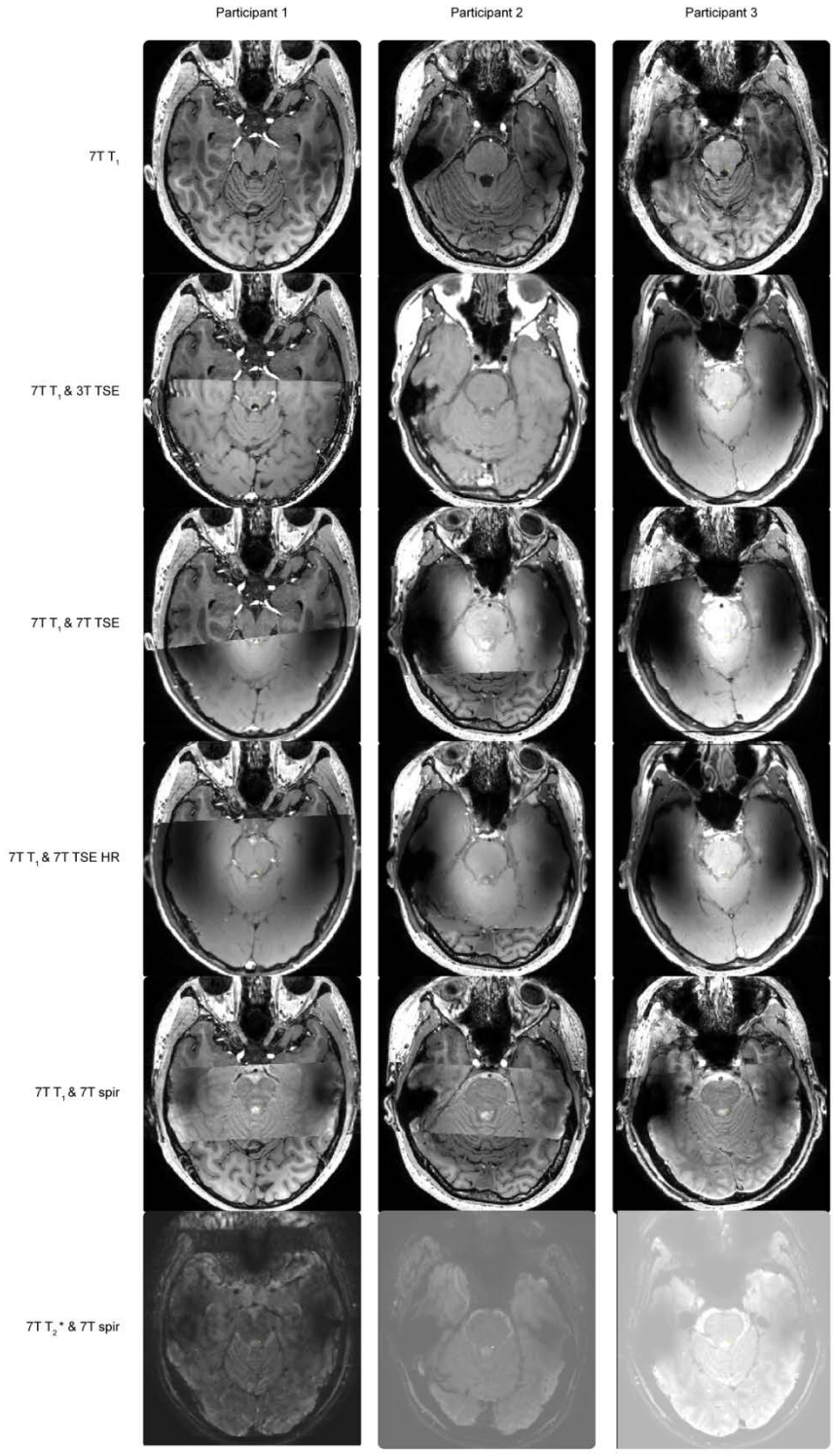


**Figure S1.**

*Registration accuracy of the different sequences to 7T $T_1$ whole brain. As can be noted by the skull contour, sulci patterns and borders of the 4$^{th}$ ventricle, the registration employing 6 DoF was successful between the different sequences and the 7T $T_1$ whole brain volume. The yellow pixels directly adjunct to the 4$^{th}$ ventricle correspond to the locus coeruleus in the left hemisphere.*

In the main text the LC masks and MRI sequences were all registered to the corresponding 7T $T_1$-weighted image. This registration step does however result in implicit smoothing and partial voluming effects. Therefore, in addition to the main analysis, the LC masks were projected to each individual sequence native space using the combined transformation matrices. As is shown below, the results in native space are very similar to the results in 7T $T_1$ space.

**Table S2.** *Summary statistics of the estimated LC contrasts for each scan sequence in native scan space.*

| | | LC contrast 1 | | LC contrast 2 | | LC contrast PT | |
|---|---|---|---|---|---|---|---|
| | N (contrast 1/2/pt) | Average median | IQR | Average median | IQR | Average median | IQR |
| 3T TSE | 12/10/11 | 6.49 | 2.08 | 11.04 | 0.91 | 10.62 | 2.6 |
| 7T TSE | 12/12/12 | 3.01 | 4.31 | 8.06 | 4.47 | 10.46 | 8.11 |
| 7T HR-TSE | 12/12/12 | 3.39 | 4.36 | 6.46 | 3.47 | 7.68 | 8.39 |
| 7T HR-$T_2$* - magnitude | 11/11/11 | -0.21 | 0.13 | -0.38 | 0.26 | -0.46 | 0.31 |
| 7T HR-$T_2$* - phase unwrapped | 11/11/11 | -60.85 | 118.63 | 22.6 | 262.09 | -99.2 | 231.40 |
| 7T HR-$T_2$* - SWI | 10/8/9 | 1.75 | 0.48 | 0.93 | 0.71 | 3.69 | 0.75 |
| 7T SPIR | 11/11/11 | 6.02 | 2.5 | 12.23 | 6.38 | 7.65 | 4.42 |
| 7T whole brain $T_1$ | 12/12/12 | 1.32 | 2.77 | -0.66 | 3.02 | 1.85 | 4.42 |

*N: the number of participants after outlier rejection, note that for the $T_2$* based contrasts one participant was missing due to technical reasons; IQR: interquartile range; pt: pontine tegmentum.*

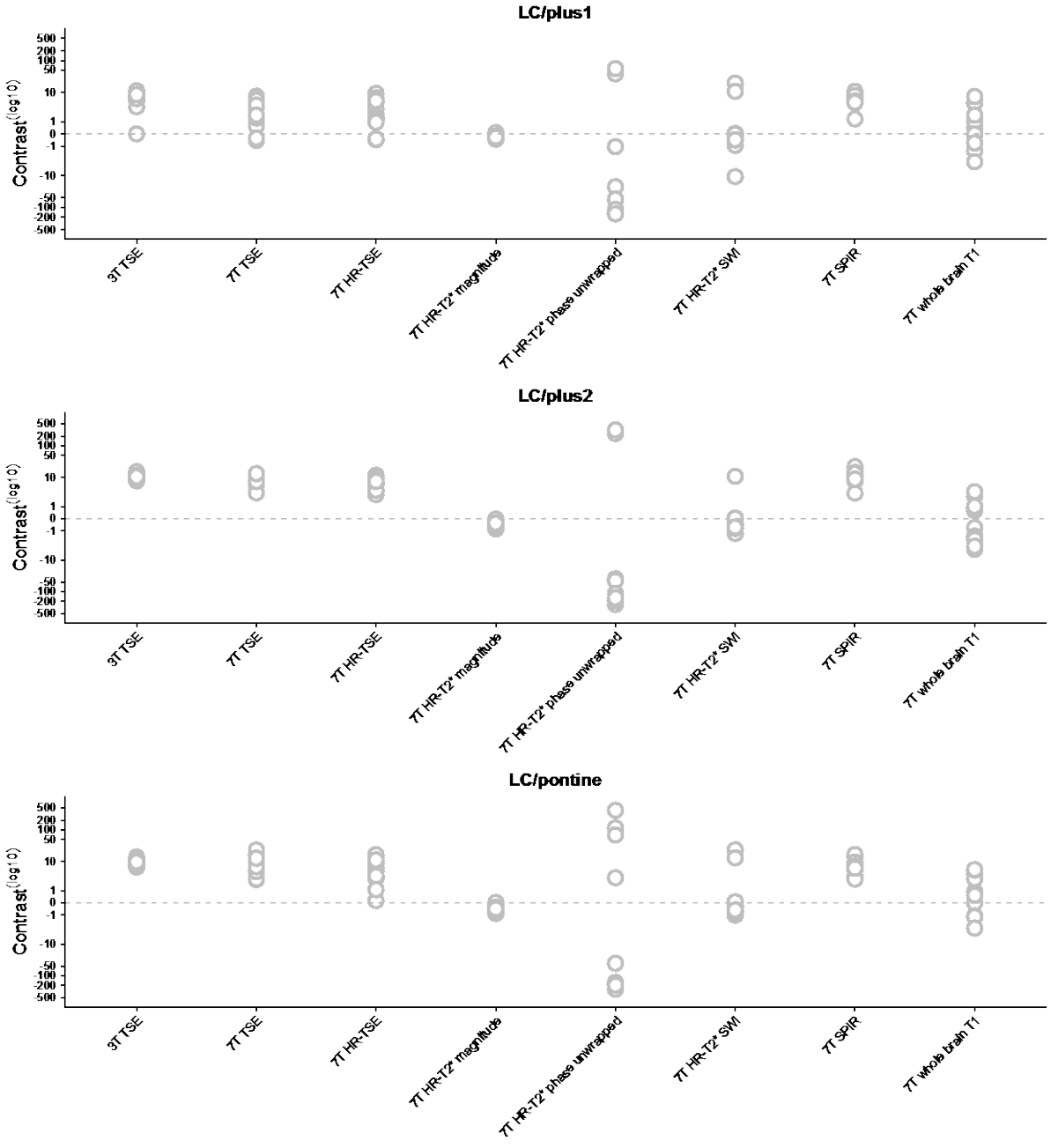


**Figure S2**. *Contrast ratios per scan in native scan space, separately for each participant.*

**Table S2.** *Results of the Bayesian one-sample t-tests examining which scans deliver a detectable contrast between the LC and surrounding tissue. Contrast is extract in native scanner space.*

| Comparison | N (contrast 1/2/pt) | LC contrast 1 $BF_{10}$ | LC contrast 2 $BF_{10}$ | LC contrast PT $BF_{10}$ |
|---|---|---|---|---|
| 3T TSE ≠ 0 | 12/10/11 | 3372.54 * | 460533.1 * | 925874.1 * |
| 7T TSE ≠ 0 | 12/12/12 | 16.28 * | 5060.3 * | 235.62 * |
| 7T HR-TSE ≠ 0 | 12/12/12 | 16.16 * | 6232.48 * | 60.04 * |
| 7T HR-$T_2$* - magnitude ≠ 0 | 11/11/11 | 55.74 * | 84.99 * | 178.52 * |
| 7T HR-$T_2$*-phase unwrapped ≠ 0 | 11/11/11 | 3.06 | 0.31 | 0.54 |
| 7T HR-$T_2$* - SWI ≠ 0 | 10/8/9 | 0.38 | 0.4 | 0.6 |
| 7T SPIR ≠ 0 | 11/11/11 | 2363.7 * | 1687.39 * | 159.27 * |
| 7T whole brain $T_1$ ≠ 0 | 12/12/12 | 0.7 | 0.42 | 1.72 |

*N: the number of participants after outlier rejection.*

Similar to the results in 7T $T_1$ space, the Bayesian one-sample t-tests indicate strong or more evidence (BF10>10.0) in favour of the hypothesis that there is a contrast different from zero between the LC and the surrounding tissue for the 3T TSE, 7T TSE, 7T HR-TSE, 7T HR-$T_2$*-magnitude, and the 7T SPIR. Statistically significant values (BF10>10.0) are also indicated by asterisk "*".

A JZS Bayesian mixed effect model (R. D. Morey & Rouder, 2015; Rouder et al., 2012) with default prior scales revealed that the model with main effects of scan sequence and contrast ratio, as well as an interaction between those variables, is preferred above the model without the interaction effect by a Bayes factor of 55.10. The data therefore provide very strong evidence that the contrast between the LC and the surrounding tissue is influenced by sequence type, control region, as well as an interaction between the two factors.

Post-hoc pairwise comparisons among the five sequences showed that, similar to the results in 7T $T_1$ space, the $T_2$*-magnitude image provides lower contrast that the other four sequences (Table S3). The overall pattern of the remaining results is very similar to the results obtained in 7T $T_1$ space (Table 5 versus Table S3).

**Table S3.** *The post-hoc Bayesian paired t-tests examining whether there was a difference in contrast between sequences, for LC contrast 1 and LC contrast 2 separately.*

| Comparison | N | $BF_{10}$ for LC contrast 1 | $BF_{10}$ for LC contrast 2 | $BF_{10}$ for LC contrast pt |
|---|---|---|---|---|
| 3T TSE – 7T TSE | 9 | 18.16 * | 2.14 | 0.33 |
| 3T TSE – 7T HR-TSE | 9 | 43.61 * | 41.95 * | 0.7 |
| 3T TSE – 7T HR-$T_2$* magnitude | 8 | 2620.32 * | 250573.9 * | 110713.3 * |
| 3T TSE – 7T SPIR | 8 | 0.51 | 0.36 | 30.92 * |
| 7T TSE – 7T HR-TSE | 12 | 0.30 | 0.58 | 1.74 |
| 7T TSE – 7T HR-$T_2$* magnitude | 11 | 8.71 | 1190.95 * | 179.98 * |
| 7T HR-TSE – 7T HR-$T_2$* magnitude | 11 | 8.82 | 784.67 * | 20.51 * |
| 7T SPIR – 7T HR-$T_2$* magnitude | 10 | 739.33 * | 503.21 * | 53.22 * |
| 7T SPIR – 7T TSE | 11 | 2.14 | 6.54 | 0.52 |
| 7T SPIR – 7T HR-TSE | 11 | 1.19 | 4.15 | 0.30 |

*N: the number of participants after outlier rejection.*

The Bayesian paired t-tests indicate strong or more evidence (BF10>10.0) in favour of the hypothesis that there is a difference in contrast between sequences for LC contrast 1 and LC contrast 2 separately. Statistically significant values (BF10>10.0) are also indicated by asterisk "*".

**Table S4.** *Within LC mask contrast variability. The quantitative comparison of contrast was based on the median value of the intensity within the LC masks and control region. However, given that the intensity values within the LC masks may be highly variable, we also provide the (median/(within ROI IQR) ratio within the LC mask for each scan and participant. Results are reported separately for each hemisphere. Analysis was done in native space. "–" indicates missing data either due to FoV placement (SPIR) or technical reasons (SWI, phase unwrapped)*

| Median/IQR (per hemisphere) | | | | | | | | | | | | | | |
|---|---|---|---|---|---|---|---|---|---|---|---|---|---|---|
| Scan | Hemisphere | 1 | 2 | 3 | 4 | 5 | 6 | 7 | 8 | 9 | 10 | 11 | 12 | Average |
| 3T TSE | Left | 15.6 | 9.6 | 12.4 | 10.6 | 15.2 | 20.9 | 19.2 | 18.1 | 21.4 | 19.2 | 17.4 | 11.6 | 15.9 |
| | Right | 15.8 | 12.4 | 14.0 | 12.4 | 22.9 | 17.6 | 12.8 | 12.1 | 17.6 | 11.5 | 19.0 | 17.1 | 15.4 |
| 7T TSE | Left | 9.9 | 5.7 | 8.7 | 10.3 | 14.1 | 21.1 | 12.2 | 12.4 | 12.2 | 16.8 | 10.6 | 8.8 | 11.9 |
| | Right | 17.9 | 13.7 | 10.5 | 17.0 | 25.2 | 28.2 | 19.0 | 17.7 | 7.1 | 8.6 | 28.9 | 8.5 | 16.9 |
| 7T HR-TSE | Left | 7.0 | 8.8 | 10.0 | 5.6 | 11.1 | 13.4 | 6.6 | 11.5 | 14.5 | 16.2 | 8.7 | 10.4 | 10.3 |
| | Right | 7.7 | 12.9 | 12.8 | 7.0 | 7.4 | 9.2 | 11.8 | 13.4 | 14.3 | 8.9 | 9.5 | 13.6 | 10.7 |
| 7T HR-T2* - magnitude | Left | -116.2 | -197.1 | -248.7 | -131.6 | -219.1 | -165.0 | -198.8 | -165.5 | 4.9 | -180.6 | -284.5 | -165.1 | -172.3 |
| | Right | -131.6 | -132.0 | -220.8 | -123.1 | -246.1 | -197.8 | -198.5 | -198.1 | 6.4 | -219.5 | -180.7 | -165.0 | -167.2 |
| 7T HR-T2* - phase unwrapped | Left | 0.2 | -0.1 | 0.5 | 0.4 | -0.5 | 0.5 | 0.2 | 0.5 | 0.1 | -0.1 | 0.0 | - | 0.2 |
| | Right | 0.8 | 0.6 | 0.5 | 0.0 | -0.2 | 0.1 | 0.2 | 0.6 | -0.3 | -0.1 | -0.4 | - | 0.2 |
| 7T HR-T2* - SWI | Left | 0.8 | 7.4 | -124.9 | -76.3 | -219.3 | -110.5 | 5.0 | -117.1 | -110.5 | -221.4 | 1.1 | - | -87.8 |
| | Right | 0.2 | 3.2 | -142.5 | -94.1 | -151.7 | -132.2 | 4.5 | -153.0 | -197.7 | -153.0 | 2.4 | - | -92.2 |
| 7T SPIR | Left | 12.1 | 7.8 | 9.4 | 8.4 | 45.3 | 6.3 | 8.6 | 10.5 | 10.8 | 12.9 | 9.7 | 23.5 | 13.8 |
| | Right | 10.1 | 6.1 | 5.6 | 10.0 | 5.1 | 12.0 | 7.3 | 7.6 | 9.9 | 14.7 | 7.7 | - | 8.7 |
| 7T whole brain T1 | Left | 15.3 | 7.6 | 10.0 | 7.8 | 10.7 | 19.8 | 12.0 | 11.0 | 13.0 | 10.9 | 12.7 | 11.3 | 11.8 |
| | Right | 11.7 | 11.5 | 16.8 | 5.2 | 6.8 | 12.9 | 8.0 | 11.9 | 12.0 | 12.3 | 10.1 | 6.1 | 10.4 |

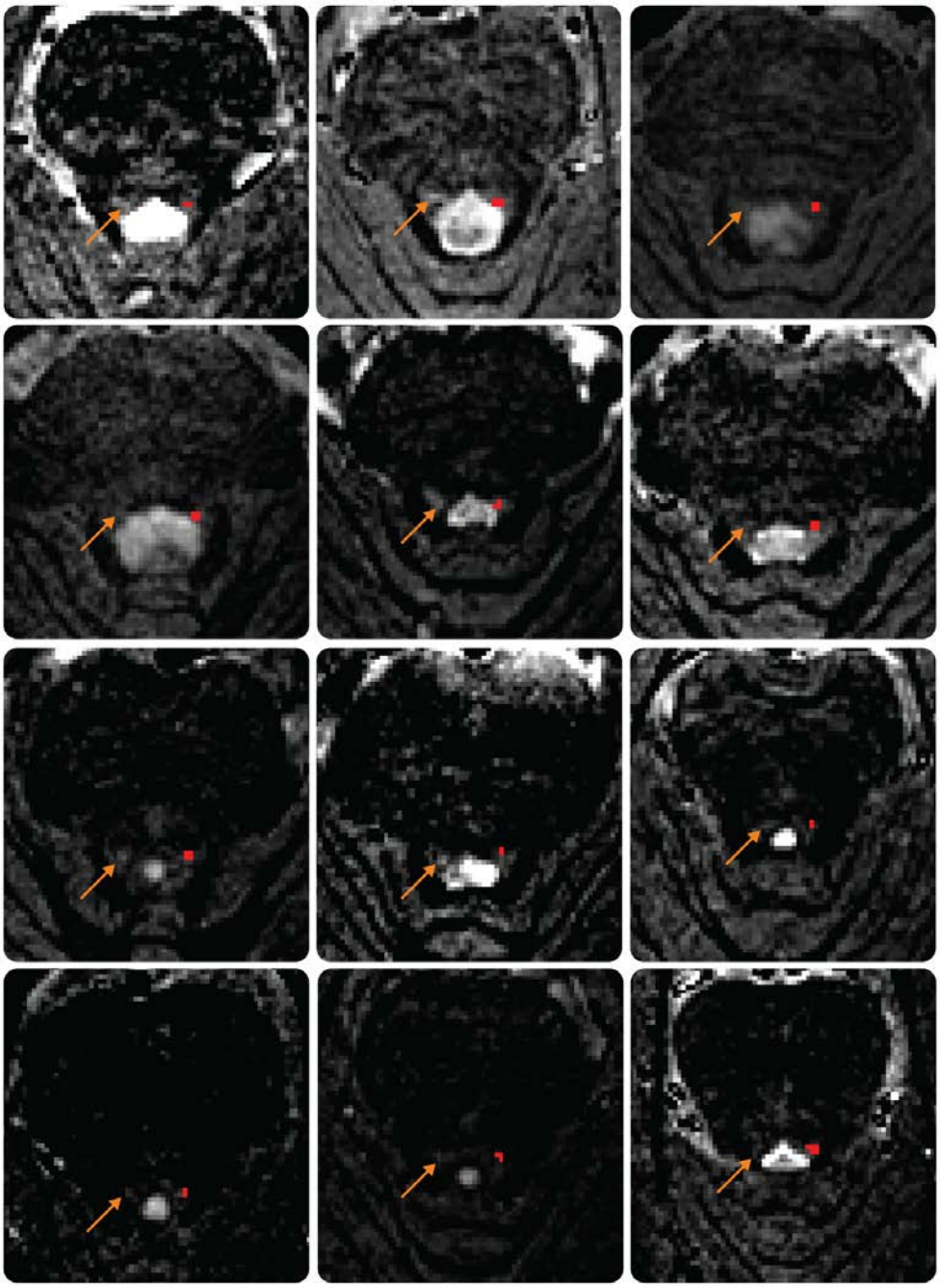

**Figure S3.** *Depiction of 7T SPIR sequence in native space for each participant separately. For all participants, an axial slice of the 7T SPIR sequence is shown in native space. The red voxels correspond to the left LC as identified on a 3T TSE scan from scan session 1 and registered to the 7T SPIR volume. The contrast levels were set using the min/max values directly surrounding the LC mask. The arrow indicates the location of the right LC.*

# Chapter 4

# The accessory stimulus effect is mediated by phasic arousal: a pupillometry study

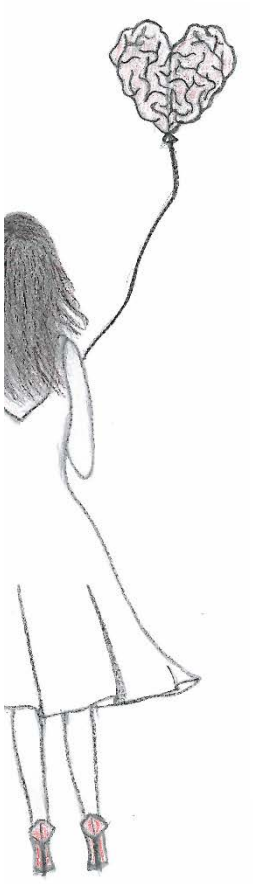

This chapter is published as: Tona, K.D., Murphy, P.R., Brown, S.B., & Nieuwenhuis, S. (2016). The accessory stimulus effect is mediated by phasic arousal: a pupillometry study. Psychophysiology, 53, 1108-1113.

**Abstract**

People usually respond faster to a visual stimulus when it is immediately preceded by a task-irrelevant, auditory accessory stimulus (AS). This AS effect occurs even in choice reaction time tasks, despite the fact that the AS carries no information about the correct response. Researchers often assume that the AS effect is mediated by a phasic arousal burst evoked by the AS, but direct evidence for that assumption is lacking. We conducted a pupillometry study to directly test the phasic arousal hypothesis. Participants carried out a demanding choice reaction time task with accessory stimuli occurring on 25% of the trials. Pupil diameter, a common index of arousal, was measured throughout the task. Standard analyses of task performance and pupil diameter showed that participants exhibited the typical AS effect, and that accessory stimuli evoked a reliable early pupil dilation on top of the more protracted dilation associated with the imperative stimulus. Moreover, regression analyses at the single-trial level showed that variation in reaction times on AS trials were selectively associated with pupil dilation during the early time window within which the AS had an effect, such that particularly large AS-evoked dilations were associated with especially fast responses. These results provide the first evidence that the AS effect is mediated by AS-evoked phasic arousal.

## Introduction

It has been shown that people respond faster in reaction time (RT) tasks when a visual imperative stimulus is immediately preceded by a task-irrelevant *accessory stimulus* (AS) presented in a different (e.g., auditory) perceptual modality, compared to when the imperative stimulus is presented alone. This AS effect occurs even in choice RT tasks, despite the fact that the AS carries no information about the correct response (Bernstein, Clark, & Edelstein, 1969; Hackley & Valle-Inclan, 1998; Posner et al., 1973; Sanders, 1975) Furthermore, an AS tends to speed up reactions without a concomitant reduction in accuracy, suggesting that the AS effect does not reflect a speed-accuracy-trade-off (Brown, van Steenbergen, Kedar, & Nieuwenhuis, 2014; Hackley & Valle-Inclán, 1999; Jepma, Wagenmakers, Band, & Nieuwenhuis, 2009; but see Posner at al., 1973).

Although the information processing stage(s) that benefit from the AS remain debated (Brown, Tona, et al., 2015; Hackley & Valle-Inclán, 1999; Jepma et al., 2009; Sanders, 1980), there seems to be a consensus that the AS effect is caused by a brief surge of arousal (i.e., phasic arousal; Bertelson & Tisseyre, 1969; Lawrence & Klein, 2013; Posner et al., 1973; Sanders, 1980). Indeed, both pioneering and more recent studies have used the terms "immediate arousal effect (Hackley & Valle-Inclán, 1999; Kiesel & Miller, 2007; Sanders, 1975) and "automatic alertness/arousal" (Posner et al., 1973) to refer to the AS effect. Despite the common inference that the AS effect is mediated by a phasic arousal response, there is only some indirect evidence to support this idea. The AS effect is stronger for auditory than for visual accessory stimuli (Bertelson & Tisseyre, 1969), and scales with the intensity of auditory accessory stimuli (Bernstein, Chu, Briggs, & Schurman, 1973; Stahl & Rammsayer, 2005). Furthermore, the AS effect is larger under conditions of temporal uncertainty, presumably characterized by relatively low arousal and thus offering more room for a phasic arousal effect (Hackley et al., 2009; Sanders, 1980). The time course of the AS effect, indexed by the effect of the stimulus onset asynchrony between AS and imperative stimulus, has also been argued to be consistent with a phasic arousal effect (Bertelson & Tisseyre, 1969).

We recently tested the phasic arousal hypothesis by examining the effect of clonidine, an α2–adrenergic agonist, on the AS effect (Brown, Tona, et al., 2015). Clonidine administration led to decreased blood pressure and increased simple reaction times, consistent with reduced arousal. Yet, we also observed that clonidine increased the size of the AS effect. Although at first glance this finding seems at odds with the phasic arousal hypothesis, an important distinction is that the primary effect of clonidine is to decrease tonic/baseline arousal levels (Arnsten, Steere, & Hunt, 1996; Samuels & Szabadi, 2008b), whereas the phasic noradrenaline-mediated arousal response may be preserved or even enhanced (Aston-Jones & Cohen, 2005). We concluded in this study that the clonidine-related reduction in general alertness provided greater scope for compensatory AS-induced performance improvements that were mediated by the phasic arousal response (Brown, Tona, et al., 2015). However, because this argument relies on several

assumptions about the effect of clonidine administration, a further, more direct test of the phasic arousal hypothesis is warranted.

Here, we exploited pupil dilation as a common index of phasic arousal (Beatty & Lucero-Wagoner, 2000), and examined its relationship with the AS effect. Participants carried out a four-choice Simon task with accessory stimuli occurring on 25% of the trials. Pupil diameter was measured throughout the task. Trials were separated by long and variable intervals to allow the pupil response to develop, and to minimize preparation for the next stimulus, thus increasing the impact of the AS (Hackley et al., 2009; Sanders, 1980). Finally, the AS was presented almost simultaneously with the imperative stimulus (30 ms prior to the stimulus; Hackley & Valle-Inclan, 1998; Jepma et al., 2009). This time period is too short for the AS to serve as a cue for the participant to start voluntary preparation. Indeed it has been shown that at stimulus onset asynchronies shorter than 200 ms, the endogenous effect of a preceding cue signal is minimal (Lawrence & Klein, 2013).

Our hypothesis was threefold: first, at the behavioral level, we expected that participants would exhibit the typical AS effect. Second, we expected that accessory stimuli would evoke a reliable transient pupil dilation on top of the dilation associated with the imperative stimulus. This would imply that the AS causes a phasic increase in arousal. Finally, we tested a critical prediction of the phasic arousal hypothesis, which capitalized on the trial-to-trial variability in the size of AS-evoked pupil dilation: RTs on AS trials should be negatively correlated with the size of the AS-evoked pupil dilation. That is, large-dilation trials, reflecting increased phasic arousal, should be associated with faster responses.

## Method

### *Participants*

Twenty-eight volunteers (19 women; aged: 19-27 years; mean age = 21 years) participated in a 1-hour experimental session and were given €6.50 or course credits in return. The study was approved by the local ethics committee and only healthy participants with no neurological or psychiatric history were included.

### *Task*

Participants performed a four-choice Simon task implemented in E-Prime (Psychology Software tools, Sharpsburg). Their task was to identify an imperative stimulus and classify it by pressing one of four keys on a QWERTY keyboard (a, z, k, m). To induce the Simon effect, the four keys had a similar spatial configuration as the four screen locations where the stimuli could appear (Figure 1).

The task consisted of 240 experimental trials that were presented in two blocks of 120 trials. No feedback on response accuracy was provided during the actual task. Half of the trials were congruent, meaning that the stimulus appeared in a location that matched the required response. The other half of the trials were incongruent, meaning that the stimulus

appeared in one of the other three locations. The AS – a loud tone (800 Hz, 77 dB, 150 ms), which started 30 ms prior to the onset of the imperative stimulus – was presented binaurally through headphones and accompanied two of the four possible stimuli in 50% of the trials on which those stimuli were presented. The trials in which these stimuli were accompanied by an AS will be referred to as "AS trials", whereas the trials in which these stimuli were not accompanied by an AS are referred to as "no-AS trials". The other two stimuli were never accompanied by an AS. Trials on which these stimuli were presented are referred to as "filler trials". The filler trials were included in the study design in order to reduce the overall proportion of AS trials and to minimize habituation to the AS. The two stimuli that were followed by an AS varied across participants in a counterbalanced fashion.

Each trial started with a fixation cross (occupying 0.2° of the visual angle), presented for 3600-4100 ms with a mean duration of 3850 ms, and surrounded by four placeholder frames (each of which occupied 28.3° of the visual angle; Figure 1). Next, the imperative stimulus, one of four adjusted Glagolitic characters (characters of an early Slavic/Cyrillic script developed in the 9$^{th}$ century AD by the Greek Byzantine monk Cyril; occupying on average 9.5° of the visual angle) appeared in one of the frames (Figure 1). The stimulus was presented for 1000ms, after which the next trial started.

Throughout the task, colors from the Teufel colors set were used to ensure isoluminance and avoid luminance-related changes in pupil size: the background was slate-blue (RGB code:166,160,198) and the stimuli, the placeholder frames and the fixation cross were salmon (217,152,158). Additionally, each of the four Glagolitic stimuli consisted of the same number of salmon pixels.

Participants were told that they would occasionally hear a loud tone that was not relevant to the task. They were encouraged to ignore the tone and complete the task by responding as quickly and accurately as possible. They were also instructed to blink as little as possible and keep their eyes on the fixation cross while performing the task. The stimuli were presented in close proximity to the cross, in such a way that the participants could detect and categorize their identity while maintaining fixation. All four possible stimulus positions had the same distance from the fixation cross (7.6°).

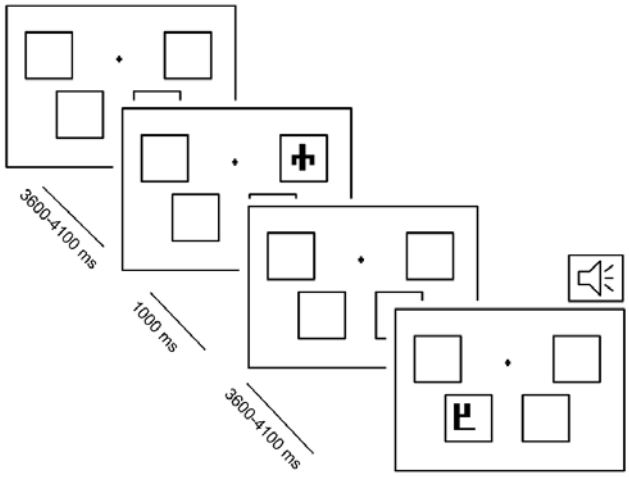


**Figure 1**. Overview of the trial procedure in the four-choice Simon task. The stimuli were isoluminant (see Method for actual colors). Accessory stimuli started 30 ms prior to the onset of the imperative stimulus, could accompany two of the four possible stimuli, and occurred on 25% of all trials.

### *Procedure*

The study was conducted in a dimly-lit room. The session started with a block of trials that facilitated measurement of the pupil response to the AS in the absence of the visual stimuli. While the participant was looking at the fixation cross, the AS was presented at pseudorandom time points. Specifically, the temporal spacing of accessory stimuli was similar to that in the actual task: On seven out of the 28 'trials' an AS was presented (referred to below as "AS-only trials"); on the remaining 21 trials no AS was presented ("null trials"). No visual stimuli were presented, except for a fixation cross that remained on the screen, and participants were not required to respond to the AS in any way.

Next, to learn the stimulus-response mappings participants performed 80 practice trials in which the stimuli were presented in the center of the screen and feedback on response accuracy was presented after each trial. Following this practice block, participants performed an additional 16 practice trials with the Simon task described above. Finally, the 240 experimental trials were administered.

### *Pupil recordings and pre-processing*

Participants were seated at a distance of 60 cm from a 17-inch monitor on which stimuli were presented. Pupil diameter was recorded continuously at 60 Hz using a Tobii T120 eye tracker (Tobii Technology, Stockholm, Sweden).

We performed a trial-averaged and a single-trial analysis where pupil dilation was defined as the mean pupil diameter during a 300-500 ms period (early time window) or a 500-2500 ms period (late time window) following stimulus onset, relative to a 200-ms prestimulus baseline (see Results for rationale).

Pupil data were analyzed using custom-made macros in BrainVision Analyzer (BrainVision Analyzer 2.0, Brain Products GmbH). Linear interpolation was applied to artifacts such as blinks and missing data (during the interval between -200 and 2500 ms after stimulus onset). In a second phase, trials containing a large number of interpolated data points (i.e., less than 50% valid data points in the interval of interest) were excluded from the analysis (17.0% and 15.6% of the trials for the early and late time windows, respectively).

### *Data analysis*

Data from three participants were excluded due to technical failure of the eye tracker or a high proportion of invalid eye-tracking data (>50% trials discarded). Data from three other participants were excluded due to low overall response accuracy rates (62.9%, 75.0%, 58.8%), which resulted in fewer than 20 trials in one or more cells of the design. For the remaining 22 participants, trials were excluded from the behavioral and pupil data analysis if the RT was longer than 1000 ms (6.2% of the trials).

Correct RT, accuracy and pupil dilation were analyzed using repeated-measures ANOVAs with AS presence (AS vs. no-AS) and congruency (congruent vs. incongruent trials) as within-subject factors. The AS-only trials were not included in any of the analyses. Greenhouse-Geisser correction was applied whenever the assumption of sphericity was violated. In these cases we report corrected *p* values and uncorrected degrees of freedom. Partial eta-squared values are reported as measures of effect size.

To investigate whether AS-related pupil dilation can predict RT on AS trials, we performed a within-subject, multiple-regression analysis on the single-trial RT data, separately for the early and for late window. More specifically, we fitted the following linear regression model:

$$RT = \beta_0 + \beta_1 * Congruency + \beta_2 * Pupil + \beta_3 * (Congruency * Pupil)$$

where *RT* indicates reaction times, *Congruency* is a binary indicator variable representing single-trial congruency (coded as 1 = congruent, 0 = incongruent), *Pupil* represents single-trial pupil dilation, and the final term represents the interaction between the *Congruency* and *Pupil* predictors.

This approach yielded $\beta$ weights that indicated the extent to which each factor predicted the RTs. Standardized $\beta$ coefficients were extracted for each term and participant and group-wise distributions for each term were subjected to one-sample *t* tests (two-tailed) to test whether they were significantly different than zero at the group level. A similar analysis was conducted for the no-AS trials.

## Results

### *Behavior*

Mean correct RTs and response accuracies for each cell of the study design are reported in Table 1. The behavioral results showed a standard congruency effect: RTs were shorter for congruent trials (674 ms) than for incongruent trials (725 ms), $F(1,21) = 98.6$, $p < .001$, $\eta^2_p = .824$, and response accuracy was higher for congruent trials (96.3%) than for incongruent trials (92.6%), $F(1,21) = 22.7$, $p < .001$, $\eta^2_p = .519$. Furthermore, we found a typical AS effect on RT: AS trials were associated with shorter RTs (686 ms) than no-AS trials (713 ms), $F(1,21) = 30.7$, $p < .001$, $\eta^2_p = .594$. There was no main effect of AS presence on accuracy, ($p = .83$), and no interaction between AS presence and congruency for either RTs ($p = .97$) or accuracy ($p = .92$).

**Table 1.** Mean correct reaction times and standard deviations for each task condition.

| | Congruent | | Incongruent | | Congruency | AS | Congruent | Incongruent |
|---|---|---|---|---|---|---|---|---|
| | AS | No-AS | AS | No- AS | effect | effect | filler | filler |
| *RT (ms)* | 660 | 687 | 712 | 738 | 51 | 27 | 670 | 727 |
| *SD* | 63 | 73 | 68 | 76 | 24 | 23 | 55 | 54 |
| *Accuracy (%)* | 96.4 | 96.1 | 92.6 | 92.5 | 3.7 | 0.2 | 96.8 | 92.4 |
| *SD* | 3.8 | 3.8 | 3.5 | 5.3 | 3.6 | 4.1 | 3.4 | 5.6 |

### *Pupil diameter*

Figure 2 shows the grand-average pupil waveforms for the task conditions of interest. Comparison of the waveforms suggests that the effects of AS presence and target congruency have distinct time courses. The difference between the AS and no-AS waveforms, and the time course of the AS-only waveform, suggest that the AS effect is particularly strong soon after onset of the imperative stimulus (300-500 ms). This AS-related effect on pupil diameter — larger dilation on AS than no-AS trials — is consistent with previous research showing increased pupil dilation after alerting stimuli (Geva, Zivan, Warsha, & Olchik, 2013). In contrast, the effect of congruency, driven by processing of the content of the imperative stimulus, only develops after this early time period and lasts much longer. To confirm this impression, we performed separate analyses for mean pupil size in an early time window (300-500 ms) and in a late time window (500-2500 ms). For the early time window, the results showed an effect of AS presence, $F(1,21) = 24.9$, $p < .001$, $\eta^2_p = .542$, but no effect of congruency, $F(1,21) = 0.6$, $p = .43$, $\eta^2_p = .030$. In contrast, for the late time window, there was no effect of AS presence, $F(1,21) = 0.8$, $p = .37$, $\eta^2_p = .039$, but consistent with previous research (van Steenbergen & Band, 2013) there was an effect of congruency, $F(1,21) = 4.7$, $p = .042$, $\eta^2_p = .182$. These results suggest that the pupil dilation related to the AS can be isolated from the pupil dilation related to the visual target (as indexed by the congruency effect).

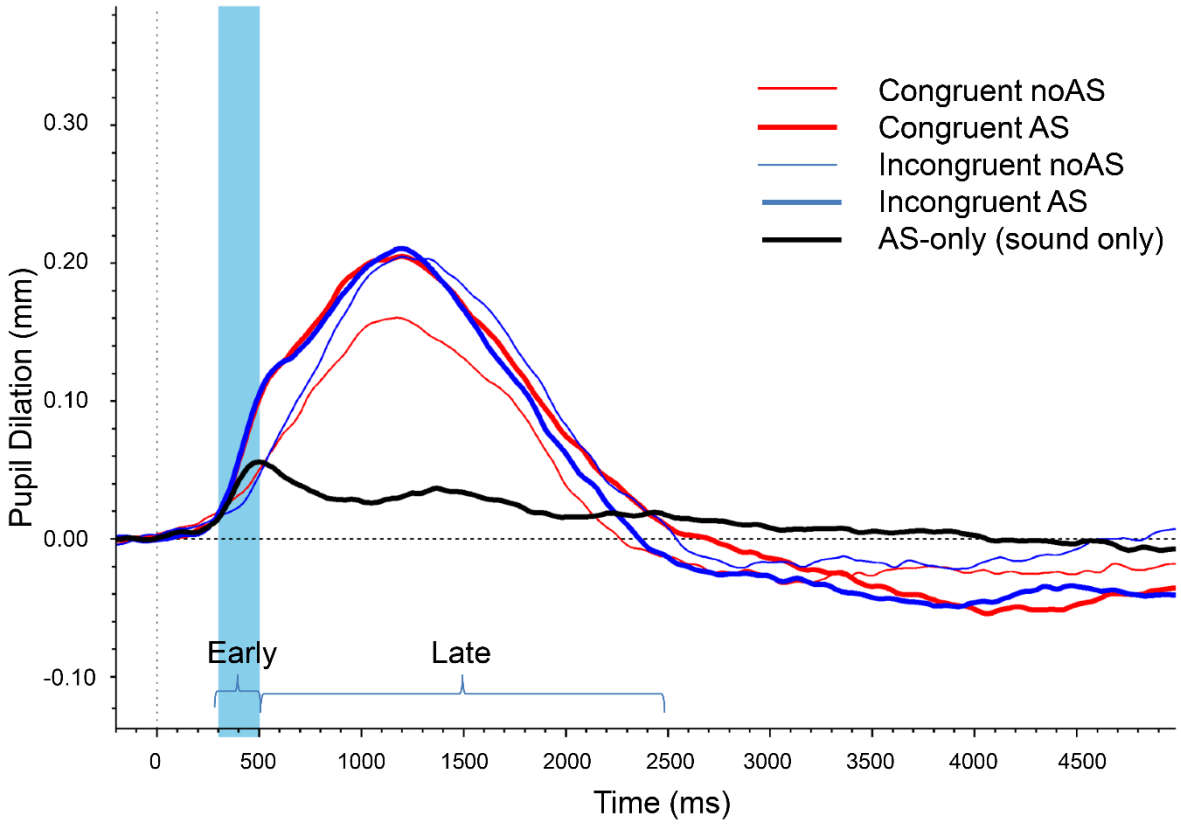


**Figure 2.** Effects of AS presence and congruency on grand-averaged pupil responses. Time 5 0 corresponds to the onset of the visual target stimulus. AS-only waveforms were obtained in a separate block.

### *Pupil-RT correlations*

To investigate whether AS-related pupil dilation can predict RT on AS trials, we carried out a single-trial regression analysis (see Methods). For the early time window, congruency, $t(21) = 8.5$, $p < .001$, and pupil dilation, $t(21) = -2.9$, $p = .009$, were significant predictors of RT, while their interaction was not, $t(21) = 1.7$, $p = .11$. The significant negative relationship between pupil dilation and RT (Figure 3) supports the hypothesis that the AS effect on RT is mediated by a phasic arousal response. In contrast, for the late time window the only significant predictor was congruency, $t(21) = 7.3$, $p < .001$. The contributions of pupil dilation, $t(21) = 1.0$, $p = .33$, and the interaction between pupil dilation and congruency, $t(21) = 1.0$, $p = .35$, were not significant. However, it is important to note that, although not statistically significant, the relationship between RT and pupil dilation during the late time window was positive in direction, which contrasts with the negative relationship for the earlier measurement window. This corroborates the notion that the significant pupil-RT relationship for the early time window is driven by AS-evoked pupil dilation, not by pupil dilation associated with processing of the visual target.

An equivalent analysis for the no-AS trials yielded no significant contribution to RT of pupil dilation during the early time window, $t(21) = -1.2$, $p = .23$, potentially suggesting that AS presentation was a prerequisite for observation of a reliable negative relationship

between early pupil dilation and RT. However, the direction of the relationship was the same on both AS and no-AS trials, and the relatively low trial counts at our disposal prevented the construction of more complex multi-factorial regression models that would facilitate an appropriate statistical test of any pupil by AS-presence interaction effect. In the Discussion we will consider the implications of this issue.

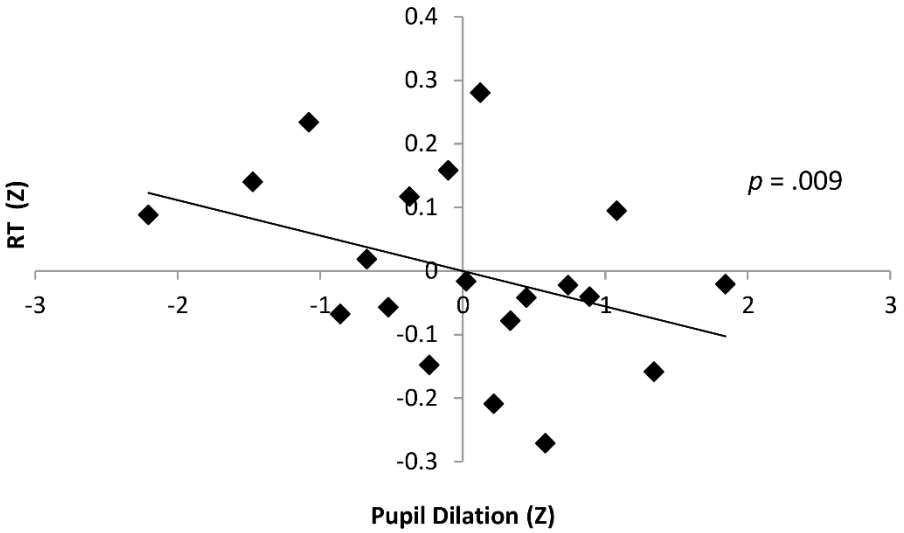


**Figure 3.** Scatter plot illustrating the negative relationship between ASrelated pupil dilation in the early window (300–500 ms) and correct RT on AS trials. Points reflect means of data that were z-scored for each participant separately, pooled across participants, and grouped into 20 five-percentile bins.

### *Control analysis: the AS effect does not reflect associative learning between AS and S-R pairs*

Given that the AS in our task was associated with only 2 of the 4 stimulus-response (S-R) pairs, it is possible that participants implicitly learned this relationship. In this case, the AS effect on RT could reflect the fact that the presentation of the AS constrained the number of S-R pairs that could be presented, thus allowing participants to selectively prepare for these S-R pairs. To rule out this possibility, we performed the following control analysis: we divided the RT trials into four chronological bins (each of which contained 60 trials), and computed the AS effect for each of these bins. We reasoned that if the AS effect in our task reflects (in part) an experience-based associative-learning effect, then the AS effect should increase over time.

The mean AS effects in the four bins were 18, 30, 18 and 35 ms. A one-way repeated-measures ANOVA revealed that these values did not significantly differ from each other, $F(3,63) = 0.8$, $p = .50$, $\eta^2_p = .036$, suggesting that any associative learning between AS occurrence and S-R pairs did not substantially contribute to the AS effect. These results uphold our key conclusion that the AS effect reflects a genuine effect of increased phasic arousal.

## Discussion

The AS effect is often assumed to be driven by a phasic arousal response to the AS. However, direct evidence for the phasic arousal hypothesis is lacking. In the current pupillometry study participants exhibited the typical behavioral AS effect, and the accessory stimuli evoked reliable pupil dilation on top of the dilation associated with the imperative stimulus. Importantly, and in line with the phasic arousal hypothesis, the RTs on AS trials were negatively correlated with the size of the AS-evoked pupil dilation: large-dilation trials, reflecting particularly strong phasic arousal evoked by the AS, were associated with particularly fast responses. A relationship that was opposite in direction, though not reliable, was observed between RT and the temporally extended pupil dilation evoked by the imperative stimulus, suggesting that our primary finding was specifically due to the AS. These results provide the first straightforward evidence that the AS effect is mediated by AS-evoked phasic arousal.

RTs on no-AS trials were also negatively correlated with pupil dilation in the interval from 300 to 500 ms after the stimulus, although this relationship did not approach statistical significance. Even if this finding reflects a genuine relationship that could be revealed with greater statistical power, we believe it would not pose a challenge for our central argument. Variability in the magnitude of early pupil dilation on no-AS trials might reflect spontaneous variability in baseline arousal or variability in the alerting effect caused by stimulus onset, before any higher-level processing of stimulus content has taken place. Such sources of arousal may influence RT in the same way as AS-evoked arousal does, but less strongly. The ensuing single-trial relationship between early pupil dilation and RT would further emphasize our argument that the AS effect on RT is driven by the robust difference in phasic arousal between AS trials and no-AS trials, as revealed by the trial-averaged early pupil dilation effect in Figure 2.

Although the information processing stage(s) that benefit from the AS have long been debated (Bernstein, Rose, & Ashe, 1970; Hackley & Valle-Inclán, 1999; Posner, 1978; Sanders, 1980), recent electrophysiological and computational modeling evidence suggests that the AS increases perceptual sensitivity and reduces the time needed for target encoding (Brown, Tona, et al., 2015; Jepma et al., 2009). In reaction-time tasks such as the Simon task employed presently, the earlier onset of the evidence accumulation process that results from faster stimulus encoding would translate to faster responses (Nieuwenhuis & de Kleijn, 2013; Seibold, Bausenhart, Rolke, & Ulrich, 2011). Moreover, in psychophysics tasks in which target stimuli are only briefly presented, it would ensure that evidence can accumulate to a higher level before the target is masked, resulting in higher response accuracy (Brown, Tona, et al., 2015; Nieuwenhuis & de Kleijn, 2013; Seifried, Ulrich, Bausenhart, Rolke, & Osman, 2010).

We consider two ways in which AS-related phasic arousal might cause this improvement in task performance through an effect on perceptual encoding. First, the AS may speed up perception through an arousal-evoked phase reset. Electrophysiological studies have shown that the momentary phase of neural oscillations at target onset is an important trial-

by-trial predictor of perceptual and attentional variability (Van Rullen, Busch, Drewes, & Dubois, 2011). Response errors, which are known to evoke a phasic arousal response (including pupil dilation; Hajcak, McDonald, & Simons, 2003; Murphy, van Moort, & Nieuwenhuis, 2016) lead to a phase reset of slow neural oscillations (van den Brink, Wynn, & Nieuwenhuis, 2014). Therefore, it seems possible that accessory stimuli improve performance by resetting oscillatory phase to an optimal value for processing of an immediately subsequent target (Diederich, Schomburg, & Colonius, 2012). Such an AS-evoked phase reset may be especially beneficial in tasks in which variability in interstimulus intervals prevents spontaneous entrainment of neural rhythms (cf. van den Brink et al., 2014), a notion consistent with the finding of larger AS effects when target onset is less predictable (Hackley et al., 2009; Sanders, 1980).

Second, the AS effect on behavior may be mediated by an arousal-related transient increase in neural gain. Increased arousal, including fluctuations in pupil size, is thought to be associated with global modulations in neural gain (Aston-Jones & Cohen, 2005; Clewett et al., 2016; Eldar, Cohen, & Niv, 2013; Vinck, Batista-Brito, Knoblich, & Cardin, 2015), a multiplicative change in the input-to-output function of a neuron (Servan-Schreiber, Printz, & Cohen, 1990). Thus, an AS may elicit a phasic increase in neural gain that, when occurring just before target onset, boosts neural responsivity and expedites the processing of that target, equivalent to a speeding up of perceptual encoding. Arousal-related changes in gain are likely to be regulated by neuromodulator systems such as the locus coeruleus-norepinephrine system. The brainstem nucleus locus coeruleus exhibits a rapid increase in activity in response to salient stimuli, including task-irrelevant intense auditory stimuli (Grant, Aston-Jones, & Redmond, 1988), and the consequent phasic increase in norepinephrine release increases neural gain. In recent research we have found that norepinephrine-mediated increases in gain enhance the precision of cortical perceptual representations (Frangos, Ellrich, & Komisaruk, 2014). Several researchers have proposed that the AS effect and related phasic alerting effects are mediated by phasic norepinephrine release (Fernandez-Duque & Posner, 1997; Hackley & Valle-Inclán, 1999, 2003). Although direct evidence is still lacking, the current findings provide indirect evidence for this hypothesis, given that recent studies have found correlations between LC activity and pupil diameter (Joshi et al., 2016; Murphy, O'Connell, et al., 2014; Varazzani et al., 2015).

It is worth noting that the two accounts discussed above are not mutually exclusive: Bursts of LC firing can reset the phase of ongoing low-frequency oscillations, thus influencing cortical excitability and sensory processing (Safaai, Neves, Eschenko, Logothetis, & Panzeri, 2015), while the phase of ongoing low-frequency oscillations can reflect fluctuations in neural gain (Lakatos, Karmos, Mehta, Ulbert, & Schroeder, 2008).

To conclude, our study utilized pupillometry methods to provide important new evidence for the long-standing assumption that the AS effect is mediated by phasic arousal. A limitation of our findings is that they are correlational in nature and thus do not provide definitive evidence for the causal role of such phasic arousal. Future studies should

examine whether experimenter-controlled phasic arousal bursts (e.g., optogenetically induced in animals), of a size comparable to those evoked by accessory stimuli, facilitate task performance in a similar way.

# Chapter 5

# The neuromodulatory and hormonal effects of transcutaneous vagus nerve stimulation as evidenced by salivary alpha-amylase, salivary cortisol, pupil diameter, and the P3 event-related potential

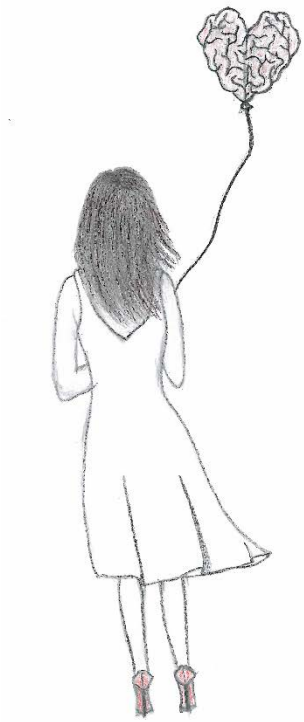

This chapter is published as: Warren, C.M., Tona, K.D., Ouwerkerk, L., van Paridon, J., Poletiek, F., van Steenbergen, H., Bosch, J.A., & Nieuwenhuis, S. (2019). The neuromodulatory and hormonal effects of transcutaneous vagus nerve stimulation as evidenced by salivary alpha amylase, salivary cortisol, pupil diameter, and the P3 event-related potential. Brain Stimulation, 12, 635-642.

**Abstract**

Transcutaneous vagus nerve stimulation (tVNS) is a new, non-invasive technique being investigated as an intervention for a variety of clinical disorders, including epilepsy and depression. tVNS is thought to exert its therapeutic effect by increasing central norepinephrine (NE) activity. Salivary alpha amylase (SAA) is a digestive enzyme released in response to sympathetic nervous system activation. Salivary cortisol is a stress hormone that marks activation of the hypothalamic-pituitary-adrenal axis. Pupil size is correlated with activity of NE-releasing neurons in the locus coeruleus. The P3 event-related potential may reflect phasic changes in cortical NE levels. In order to test for an impact of tVNS on arousal-related neuromodulatory and hormonal systems, we applied tVNS in concert with assessment of salivary alpha amylase and cortisol, pupil size, and electroencephalogram (EEG) recordings. Across three experiments, we applied real and sham tVNS to 24 (Exp. 1A), 20 (Exp. 1B), and 17 (Exp. 2) healthy participants while they performed a set of simple stimulus-discrimination tasks. Before and after the task, as well as during one break, participants provided saliva samples and had their pupil size recorded. The EEG was recorded and assessed throughout the task. tVNS significantly increased SAA and salivary cortisol, but did not affect P3 amplitude nor pupil size. These findings suggest that that SAA and cortisol, but not pupil size and P3 amplitude, can be used to monitor the arousal-related effects of tVNS.

## Introduction

Invasive vagus nerve stimulation (VNS) is a somewhat promising treatment for depression (George & Aston-Jones, 2010; Nemeroff et al., 2006; Vonck et al., 2014) and epilepsy (Ellrich, 2011; Kraus et al., 2013) that likely exerts part of its therapeutic effect by increasing norepinephrine (NE) release from the locus coeruleus (LC). The vagus nerve projects to the nucleus tractus solitarius, which projects both directly and indirectly to the LC (George & Aston-Jones, 2010; Nemeroff et al., 2006; Vonck et al., 2014). Transcutaneous VNS can be achieved by delivering electrical impulses to the cervical or the auricular branches of the vagus nerve, which are situated close to the surface of the skin of the neck and outer ear respectively (Ellrich, 2011). Functional magnetic resonance imaging (fMRI) studies in healthy humans demonstrate that the more commonly applied transcutaneous aurical VNS (taVNS) elicits widespread changes in cortical and brainstem activity (Frangos et al., 2015; Kraus et al., 2007; Kraus et al., 2013; Yakunina et al., 2017). In light of the clinical potential of taVNS, it would be valuable to establish if taVNS, like invasive VNS, affects NE, using relatively inexpensive and easy-to-use biomarkers of NE. Here we evaluated the effect of taVNS on NE levels using three accepted biomarkers and one putative biomarker of central NE activity: salivary alpha amylase (SAA), salivary cortisol, pupil size, and the P3 component of the event-related brain potential (ERP), respectively.

SAA is a digestive enzyme that is released by the saliva glands in response to local sympathetic nervous system activity (Bosch et al., 2011). SAA secretion is increased during stress and correlates with blood plasma NE during exercise (Bosch et al., 1996; Chatterton et al., 1996). SAA is a proxy marker of sympathetic-adreno-medullary activation (Bosch et al., 2009; Bosch et al., 2011), which is driven by central NE, leading to the assumption that SAA marks central NE activity (Ehlert et al., 2006; Speirs et al., 1974; van Stegeren et al., 2006; Warren, Wilson, et al., 2017). One preliminary study (Ventura-Bort et al., 2018) has reported suggestive evidence that taVNS increases SAA relative to sham stimulation—reason to be optimistic that a larger study with a more targeted methodology might reveal a robust effect of taVNS on SAA.

Salivary cortisol is a glucocorticoid stress hormone that correlates with hypothalamo-pituitary-adrenal axis activation (Bosch et al., 2009; Hill et al., 2003). Salivary cortisol may likewise be a reliable index of central NE activity, mediated in part by noradrenergic inputs to the hypothalamus (Bosch et al., 2009; Dunn et al., 2004; Hill et al., 2003). Salivary cortisol is sensitive to pharmacologically induced changes in central NE activity (Chamberlain et al., 2007; Warren, Wilson, et al., 2017).

Pupil size is correlated with activity of NE-releasing neurons in the LC (Joshi et al., 2016; Murphy, Vandekerckhove, et al., 2014; Reimer et al., 2014; Varazzani et al., 2015). This relationship may be mediated by activity in the rostral ventrolateral medulla, which projects to the LC and also innervates the peripheral sympathetic ganglia regulating the pupil (Nieuwenhuis, Forstmann, & Wagenmakers, 2011). Studies of primates and rodents show that LC activity correlates with baseline pupil diameter (Joshi et al., 2016; Reimer

et al., 2014) and the magnitude of task-evoked pupil dilations (Joshi et al., 2016; Varazzani et al., 2015). In human participants, BOLD activity in the LC covaries with pupil size at rest and during simple decision-making tasks (de Gee et al., 2017; Murphy, Vandekerckhove, et al., 2014). In rats, direct stimulation of the central stump of the vagus nerve provokes pupil dilation (Bianca & Komisaruk, 2007), but results in humans have been mixed (Desbeaumes Jodoin, Lesperance, Nguyen, Fournier-Gosselin, & Richer, 2015; Schevernels et al., 2016).

Phasic changes in cortical NE levels are associated with the scalp-recorded P3 component (Chmielewski et al., 2017; De Taeye et al., 2014; Murphy et al., 2011; Neuhaus et al., 2007; Nieuwenhuis et al., 2005; Warren & Holroyd, 2012; Warren et al., 2011; Wolff et al., 2018). Events that lead to increased phasic firing of the LC also lead to increased P3 amplitude (Nieuwenhuis et al., 2005). Noradrenergic drugs influence P3 amplitude in both animals (Swick et al., 1994) and humans (Brown et al., 2016; Brown, van der Wee, et al., 2015; de Rover et al., 2015), and lesion of the LC eliminates the P3 in monkeys (Pineda et al., 1987). Of interest here, the amplitude of the P3 is increased by invasive VNS (De Taeye et al., 2014; Neuhaus et al., 2007; Schevernels et al., 2016).

Although LC-NE activity is associated with changes in SAA, salivary cortisol, pupil size and the P3, these psychophysiological measures are not exclusively diagnostic of changes in LC-NE activity. For example, fluctuations in pupil size have been shown to track activity in a number of neuromodulatory brainstem centers, including the LC, the dopaminergic ventral tegmental area, and the cholinergic basal forebrain (de Gee et al., 2017; Reimer et al., 2014). Also, P3 amplitude can be modulated by dopaminergic and cholinergic pharmacological manipulations, suggesting a role for those systems in P3 generation (Nieuwenhuis et al., 2005). Thus, although our study is well-equipped to pick up converging evidence for taVNS effects on the noradrenergic system, it does not allow us to fully discriminate between noradrenergic and other neuromodulatory and hormonal effects of taVNS.

To explore the claim that taVNS increases central NE, we assayed SAA, salivary cortisol, pupil size and P3 amplitude across three experiments. In Experiments 1A and 2, we collected saliva samples and analyzed these samples all together. In Experiment 2, we also recorded pupil size. Experiment 1B was a partial replication of 1A, wherein we recorded EEG data during a classic oddball task, the seminal task for eliciting a P3 (Sutton, Braren, Zubin, & John, 1965).

## EXPERIMENT 1A

### Method

#### *Participants*

Twenty-four students at Leiden University (6 male, mean age 22.6) participated in return for €30. We used the following exclusion criteria: history of psychiatric or neurological

disorders, head trauma, migraine, current use of psychoactive drugs, pregnancy, active implants (cochlear implant, pacemaker) and a permanent ear-piercing.

### *Procedure*

The study was a participant-blind cross-over design consisting of two sessions, separated by at least three days. In one session participants received taVNS, and in the other they received sham stimulation. Time of day, recent exercise, mental effort, and time since last meal are all factors that can affect SAA and salivary cortisol levels. Accordingly, participants performed the same tasks in each session at the same time of day, and participants were asked to refrain from excessive exercise, alcohol, caffeine and meals within 3h prior to the examination. Task order and treatment order were counterbalanced across participants. Figure 1A shows the timeline of all three experiments reported here.

The taVNS device was attached during EEG set-up, but not turned on until set-up was almost complete. Set-up was paused to obtain a baseline saliva sample before turning on the device. Participants did not begin the task until the device had been active for 20 minutes. A second saliva sample was taken halfway through the task, and a final sample taken after task completion. Participants did not report any notable adverse after-effects of taVNS.

### *Stimulation*

We applied taVNS (NEMOS®, Cerbomed, Germany) with an intensity of 0.5 mA and a pulse width of 200–300 μs at 25 Hz, alternating between on and off periods every 30 s (Beste et al., 2016; Sellaro et al., 2015; Steenbergen, Sellaro, Stock, et al., 2015). In the taVNS condition, the electrodes were applied to the cymba conchae region, which is heavily innervated by the aurical branch of the vagus nerve (Badran, Brown, et al., 2018; Peuker & Filler, 2002) (**Fig. 1B**). In the sham condition, the electrodes were placed on the left ear lobe (**Fig. 1C**), which should not induce any significant brainstem or cortical activation (Beste et al., 2016; Kraus et al., 2013; Sellaro et al., 2015; Steenbergen, Sellaro, Stock, et al., 2015).

### *Saliva sample collection*

Saliva samples were collected at three points in time: five minutes before taVNS began (baseline, t=-5), at t=45 and t=75 minutes after taVNS began. Whole saliva was collected by instructing participants to let saliva collect passively in their mouth and spit the accumulated saliva into a polypropylene tube once per minute, over a three-minute period (Beltzer et al., 2010; Nagy et al., 2015; Strahler, Skoluda, Kappert, & Nater, 2017). We calculated SAA and salivary cortisol secretion as the flow rate multiplied by the concentration values, as in our previous work (Warren, Wilson, et al., 2017) and as is considered the "gold standard" in the field (Bosch et al., 2011; Strahler et al., 2017).

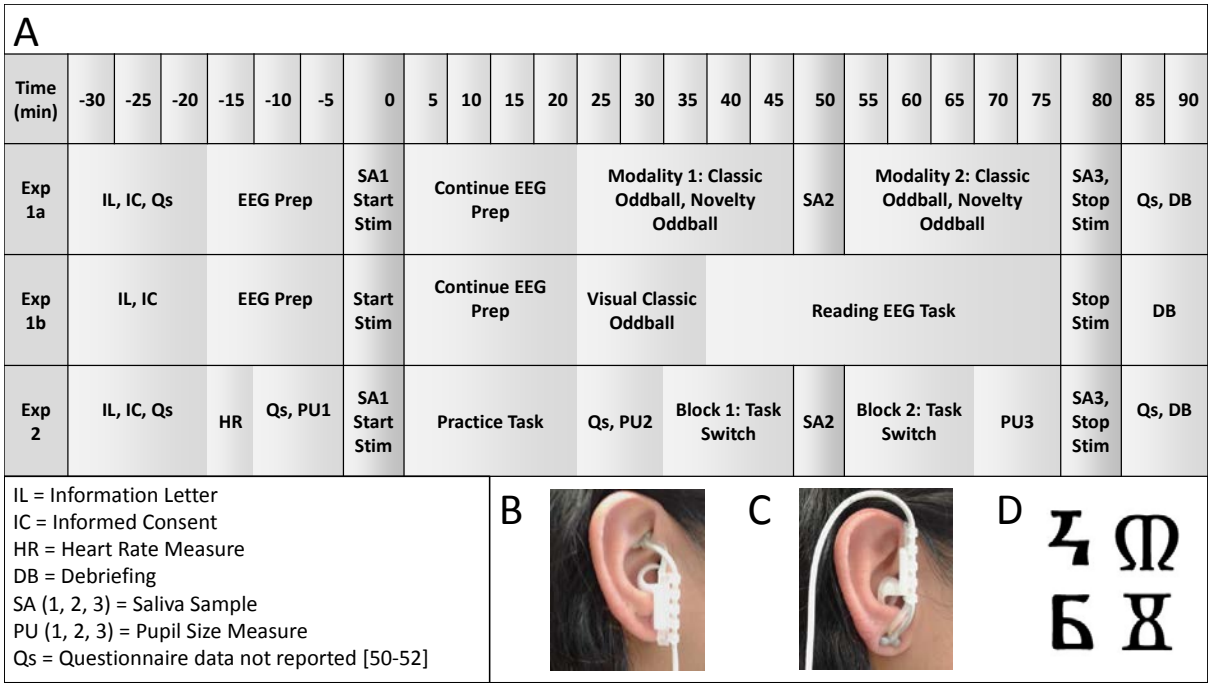


**Figure 1.** A) Depiction of the timing of each experiment. B) Position of the taVNS device that gives targeted stimulation to auricular branch of the vagus nerve. C) Position of the taVNS device for "sham" stimulation, that putatively does not impact activity in the vagus nerve. D) Examples of the visual novelty stimuli used in the novelty oddball P3 task in Experiment 1A.

### *Task*

Participants performed "classic oddball" and "novelty oddball" tasks in both the visual and auditory modality, in which they had to respond with a key press on rare target oddball trials (12% of trials) interspersed among frequent standards/distracters (as well as rare novels in the novelty oddball task). In the classic oddball, there were 36 oddball trials and 264 standard trials. In the novelty oddball there were 36 oddball trials, 36 novel trials, and 228 standard trials. In both the visual and auditory modality, the stimulus was presented for 400 ms with an interstimulus interval of 1000 ms.

In the visual modality, targets and standards consisted of black *X*s and *O*s on a white background. The novel stimuli were symbols derived from the Glagolitic and Cyrillic scripts (**Fig. 1D**). Participants were seated at a viewing distance of 70 cm, such that target and standard stimuli subtended 1.2° of visual angle, and novels subtended 1.7° of visual angle. A black-on-white fixation cross was presented during the interstimulus interval.

In the auditory modality, the fixation cross remained on-screen constantly. The auditory stimuli were tones of high (500 Hz) or low pitch (350 HZ), presented at 70 dB through speakers. Target frequency was counterbalanced across participants. The novel stimuli consisted of unusual noises pulled from the set of Fabiani and Friedman (Fabiani & Friedman, 1995).

### *EEG collection and processing*

EEG was recorded from 64 channels (ActiveTwo system, Biosemi B.V., Netherlands) in the standard 10-20 configuration. Data were pre-amplified at the electrode site and recorded with a sampling rate of 512 Hz with reference to a common mode sense. Impedances were kept below 32 kΩ. EEG recordings were processed using Brain Vision Analyzer 2 (Brain Products GmbH, Germany). Data were re-referenced offline to the right mastoid, and band-pass filtered (0.1 Hz-20.0 Hz). Ocular artifacts were (Gratton, Coles, & Donchin, 1983). Epochs were extracted from the EEG from -200 ms to 800 ms relative to stimulus onset, using the first 200 ms for baseline correction. Trials in which the change in voltage at any channel exceeded 35µV per sampling point were removed as were trials with slow drifts (>300 µV/200 ms) and low activity (<.5µV/100 ms).

We created difference waves to simplify figures and analyses, to isolate the topography of the P3, and to distinguish the P3 to oddballs ("oddball P3") and the P3 to novel stimuli ("novelty P3"). To isolate the oddball P3 we subtracted the standard ERP from the oddball ERP, and to isolate the novelty P3 we subtracted the standard ERP from the novelty ERP. In each case P3 amplitude was quantified as the most positive mean amplitude from a 200-ms sliding window across the entire difference wave.

The oddball P3 was analyzed using an ANOVA including the factors treatment (taVNS vs sham), modality (visual vs auditory), task (classic oddball vs novelty oddball) and electrode (Fz, Cz, Pz). The novelty P3 obtained in the novelty oddball task was analyzed using an ANOVA including the factors treatment (taVNS vs sham), modality (visual vs auditory) and electrode (Fz, Cz, Pz). In addition, treatment order was added as a between-subjects variable-of-no-interest, to account for additional error variance.

## Results

### *Oddball P3*

The amplitude of the oddball P3 showed significant main effects of electrode, indicating a typical parietal distribution (**Fig. 2**), $F(2,44)=60.82$, $p<.001$, task (classic oddball: 7.7 µV; novelty oddball: 7.0 µV; **Fig. 3**), $F(1,22)=13.36$, $p=.001$, and modality (visual: 7.7 µV; auditory: 6.4 µV), $F(1,22)=28.65$, $p<.001$. In addition, electrode interacted with task, $F(2,44)=5.15$, $p=.010$, and exhibited a three-way interaction with task and modality, $F(2,44)=3.56$, $p=.037$. Treatment did not significantly affect oddball P3 amplitude (taVNS: 7.1 µV; sham: 7.0 µV), $F(1,22)=.020$, $p=.89$. Treatment did not interact with electrode, task, or modality.

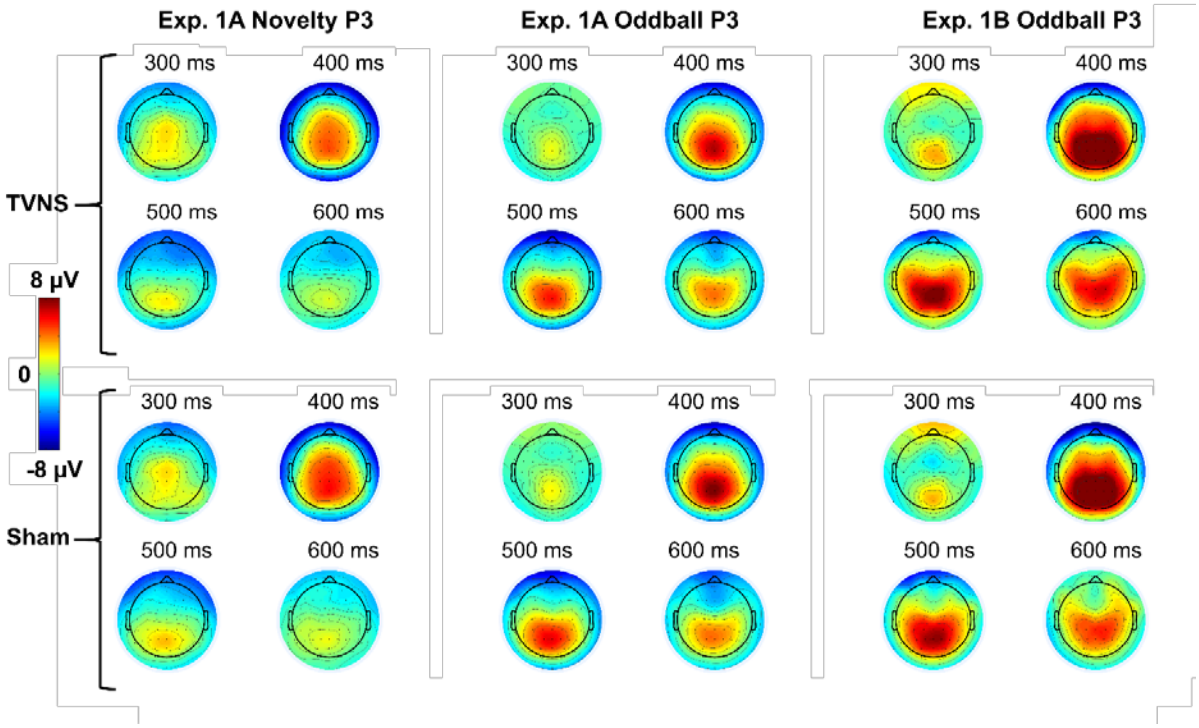


**Figure 2.** Scalp distribution of the oddball P3 and novelty P3 for taVNS (top row) and sham stimulation (bottom row), for the novelty and classic oddball tasks in Exp. 1A, and the classic oddball task in Exp. 1B. For Exp. 1A, scalp distributions are collapsed across the visual and auditory modalities, and for the oddball P3 they are collapsed across tasks as well.

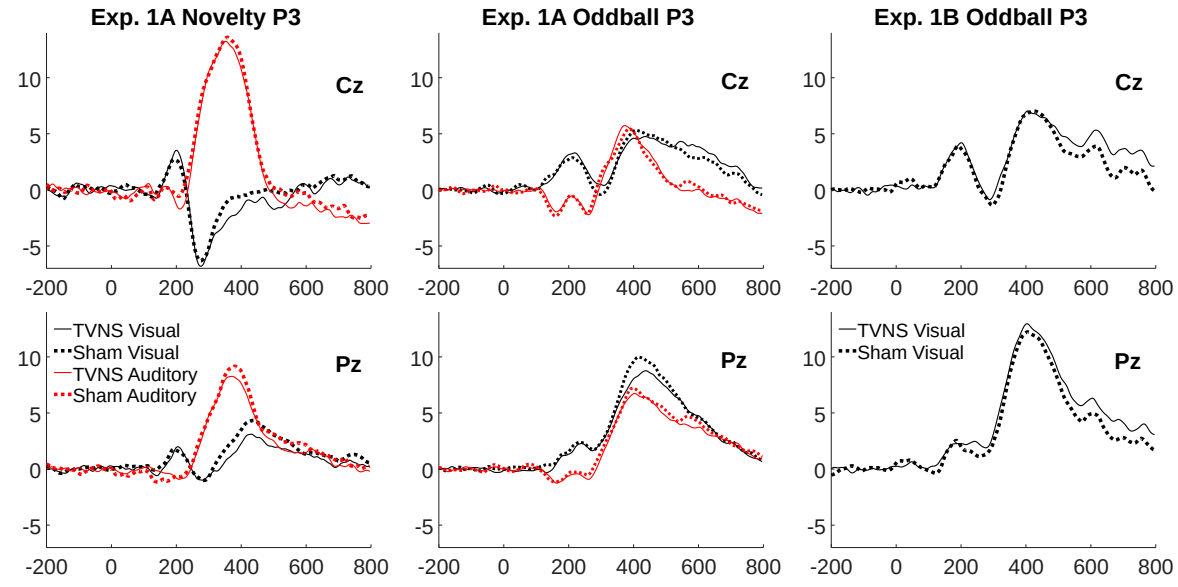


**Figure 3.** ERP waveforms from Experiments 1A and 1B for electrodes Cz (top) and Pz (bottom) were not affected by taVNS. Exp. 1A included both a novelty oddball task and a classic oddball task, in both the visual and auditory modality. Experiment 1B included only a classic oddball task in the visual modality.

### *Novelty P3*

As expected, the novelty P3 had a more frontal distribution than the oddball P3, with largest amplitude at electrode Cz, $F(2,44)=14.05$, $p<.001$ (**Fig. 2**). The novelty P3 was larger in the auditory modality (10.5 μV), than in the visual modality (2.8 μV), $F(1,22)=82.36$, $p<.001$ (**Fig. 3**). In addition, the effect of modality on novelty P3 amplitude was larger at Fz and Cz than at Pz, $F(2,44)=34.17$, $p<.001$. Treatment did not significantly affect novelty P3 amplitude (taVNS: 6.4 μV; sham: 6.8 μV), $F(1,22)=0.65$, $p=.43$.

## EXPERIMENT 1B

Our task in Experiment 1A yielded a typical oddball P3 and novelty P3, exhibiting characteristic effects of electrode, task and modality. There were no effects of treatment on the oddball P3 or novelty P3. Given that P3 amplitude was shown to be increased by invasive VNS, we considered the possibility that our null effect of treatment on P3 amplitude was a type-2 error, and followed up with a simplified experiment on new participants, composed of a single classic oddball task with a greater number of trials, and with the exact same stimulation protocol.

### Method

#### *Participants*

Twenty Leiden University students (11 males, mean age 23.6) participated in return for €25. Exclusion criteria were the same as Experiment 1A.

#### *Task and Procedure*

The task was an abbreviated version of the task used in Experiment 1A. Experiment 1B included only the visual version of the classic oddball paradigm. We increased the number of trials from 300 to 400 (352 standards, 48 targets). The materials (*X*s and *O*s) were the same, as were all the timing parameters.

The exact same stimulation protocol was used as in Experiment 1A. The first 55 minutes of each session in Experiment 1B were identical to Experiment 1A, except that participants did not fill out any questionnaires, and participants did not provide saliva samples (**Fig. 1A**).

#### *EEG collection and processing*

EEG collection and processing methods as well as statistical analysis were identical as described for Experiment 1A, except as follows. Recordings for five participants had noisy signals at one electrode. For these participants the bad electrode was removed before ocular correction, and its signal interpolated from the remaining electrodes using a spline-based method.

## Results

The oddball P3 in Experiment 1B exhibited a parietal distribution (**Fig. 2**), with largest amplitude at Pz, $F(2,34)=32.54$, $p<.001$. The oddball P3 was larger in the taVNS condition (7.6 μV) than in the sham condition (6.5 μV). This difference was not significant, $F(1,17)=2.32$, $p=.15$ (**Fig. 3**).

## BAYESIAN ANALYSES

In Experiment 1A taVNS did not affect the size of the oddball P3 or novelty P3. We ran Experiment 1B to perform a second examination of this potential effect, and found no effect ($p=.15$). The combined results suggest that taVNS does not affect P3 amplitude, but such a conclusion cannot be firm under the rules of null hypothesis statistical testing. In order to quantify evidence for the null hypothesis, we ran a Bayesian-evidence synthesis analysis (Scheibehenne, Jamil, & Wagenmakers, 2016) on the visual oddball P3 data from Experiments 1A and 1B.

### Method

Data were analyzed using JASP (JASP Team, 2016), which yields Bayes factors that give the relative probability of competing models of the data. We ran a Bayesian repeated-measures ANOVA with treatment as the repeated factor, and two between-subjects factors: treatment order and experiment.

### Results

Bayes factor comparisons favored the null model over a model including an effect of treatment ($BF_{01}=4.53$). This quantity means no effect of treatment is 4.53 times more probable, given the data, than an effect of treatment, which constitutes "substantial evidence" for the null hypothesis (Jeffreys, 1961). The null model was also superior to a model including an interaction of treatment with experiment ($BF_{01}=13.48$). This Bayes factor constitutes "strong evidence" in favor of the null model (Jeffreys, 1961). Taken together with the frequentist methods reported above, the appropriate conclusion is that taVNS does not affect the (visual) oddball P3.

## EXPERIMENT 2

### Method

#### *Participants*

Seventeen young adults (all males, mean age 22.1) participated in Experiment 2. One participant gave saliva samples but did not have his pupil data recorded. Exclusion criteria were the same as for Experiment 1A.

### *Procedure*

The timeline of Experiment 2 is displayed in Figure 1A. Pupil data were recorded at three time points during each session. Saliva samples were collected with the exact same methodology and timing relative to taVNS as described in Experiment 1A. taVNS was applied with the exact same timing, positioning and parameters as in Experiments 1A and 1B. Participants performed a cued task-switching task (Monsell & Mizon, 2006) and other tests from which data will be reported elsewhere (See Chapter 6).

### *Pupil size recording and analysis*

Participants sat in a dimly lit room with head held steady in a chin rest, and fixated on a luminance-controlled, salmon-colored fixation cross on a slate blue computer screen. Pupil diameter was recorded for 96 seconds at 60 Hz using a Tobii T120 eye tracker (Tobii Technology, Stockholm, Sweden). Recordings were made roughly 10 minutes before stimulation began (t=-10), between practice and critical task-switching trials (t=25) and upon completion of the task (t=70). Pupil data were analyzed using custom-made macros in BrainVision Analyzer 2.0 (Brain Products GmbH). Linear interpolation was applied to artifacts such as blinks and missing data.

## Results

We analyzed mean pupil size across the 96-second epoch at each time point. Treatment did not significantly affect pupil size ($p$=0.37), nor interact with time ($p$=0.79, Greenhouse-Geisser corrected). There was an effect of time on pupil size whereby pupil size increased from baseline during task performance, $F(1,15)=9.78$, $p$=.007 (Greenhouse-Geisser corrected) (**Fig. 4**).

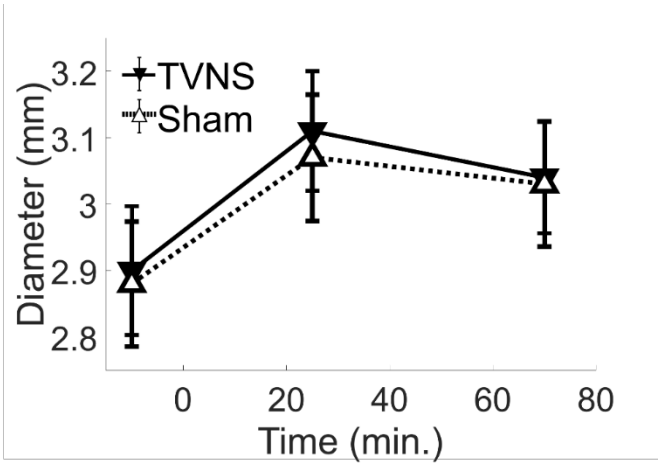


**Figure 4.** Pupil size increased over time but was not affected by taVNS. Error bars reflect SEM.

## ANALYSIS OF SALIVA DATA

### Method

#### *Participants*

Experiments 1a and 2 were run simultaneously with identical taVNS protocol and identical saliva collection, processing and analysis protocol. Saliva samples were collected from twenty participants in Experiment 1a, and seventeen participants in Experiment 2. Twenty-five participants provided SAA samples with concentrations within the sensitivity range of our assay in all six cells of the design (3 samples x 2 treatment conditions). In the follow-up analyses of the effect of sampling time in each treatment condition, thirty-three participants provided utilizable samples in all 3 cells of the taVNS condition, and twenty-seven participants provided utilizable samples in all 3 cells of the sham condition. Salivary cortisol was determined only for the saliva samples from Experiment 2. All seventeen participants provided sufficient samples to include cortisol secretion data in every cell of the design.

#### Saliva sample processing (Experiments 1A and 2)

Fresh saliva samples were stored in ice for a maximum of 2.5 hours. Before freezing, samples were centrifuged at room temperature for 4 min at 4000 x *g* to force debris and bacteria to the bottom of the tube. The clear supernatant was pipetted into a smaller polypropylene tube and frozen at −60◦C until the assay procedure.

#### *Hormonal analyses*

SAA was assayed using a quantitative kinetic determination kit (IBL, Hamburg, Germany) (Nagy et al., 2015). The assay has a sensitivity of 12.5 U/ml. The CV% was 2.5. Each participant's samples were assayed for SAA at the same time. 25/222 samples gave values outside the sensitivity range of the SAA assay on two successive attempts. These samples were considered outliers and not assayed a third time.

Cortisol was assayed using a competitive enzyme-linked immunosorbent assay, according to the manufacturer's instructions (IBL, Hamburg, Germany), with a sensitivity of 0.045 µg/mL, and intra-assay variability (CV%) was 2.4. All samples of the same participant were assayed for cortisol simultaneously. Treatment order and experiment (1a vs. 2) were included as between-subjects variables. Here we report statistical terms involving treatment order because it allows us to deconstruct the omnibus ANOVA in a way that demonstrates a potentially important effect of treatment on this measure.

### Results

#### *Saliva alpha amylase secretion*

An analysis of the pooled data from Experiments 1A and 2 indicated that taVNS affected SAA, exhibited as an interaction of treatment with treatment order and sampling time, $F(2,42)=4.1$, $p=.023$. Other main effects or interactions, including the interaction of

treatment with sampling time, $F(2,42)=0.3$, $p=.73$, were not significant in the omnibus ANOVA. We decomposed the significant three-way interaction by running mixed ANOVAs (including treatment order and sampling time) for the taVNS and sham conditions separately. This analysis indicated that SAA increased from baseline to later samples in the taVNS condition, $F(2,58)=7.1$, $p=.002$, but not in the sham condition, $F(2,46)=1.2$, $p=.31$ (**Fig. 5A**).

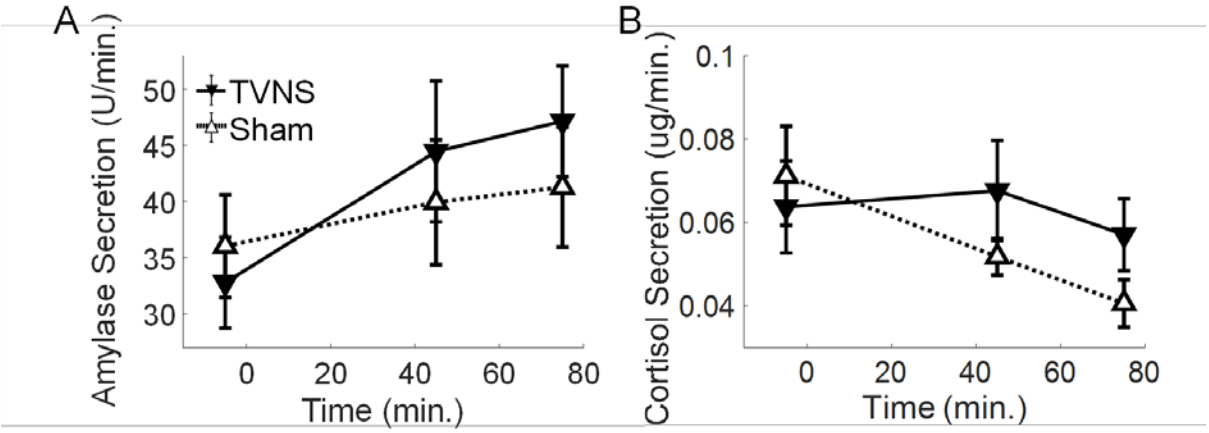


**Figure 5.** Effects of treatment on SAA and cortisol. SAA increased from baseline in the taVNS condition (p = .002) but not the sham condition (p = .31). Cortisol dropped from baseline in the sham condition (p = .020) but not in the taVNS condition (p=.63). Error bars reflect SEM. Means and SEM for the SAA data points come from variable sample sizes due to missing data points (taVNS: n=34, 36, 34; sham: n=34, 30, 29).

### *Salivary cortisol secretion*

Treatment affected salivary cortisol secretion, exhibited as an interaction of treatment with sampling time, $F(2,30)=3.6$, $p=.040$. There were no other significant effects in the omnibus ANOVA. Separate ANOVAs for each treatment revealed that salivary cortisol did not change from baseline in the taVNS condition, $F(2,30)=0.5$, $p=.63$, but significantly *decreased* in the sham condition, $F(2,30)=4.5$, $p=.020$, (**Fig. 5B**). This suggests that taVNS worked against a general tendency for salivary cortisol secretion to decrease over the course of a session.

### *Salivary flow rate*

As with the SAA analysis, we pooled flow rate data from Experiments 1a and 2 for a single analysis**.** Participants tended to provide more saliva as they became practiced and comfortable with the collection method, both within sessions ($M_{t1}=.35$, $M_{t2}=.39$, $M_{t3}=.40$), $F(2,68)=6.5$, $p=.003$, and between sessions ($M_{s1}$ = .36, $M_{s2}=.40$), $F(1,34)=4.5$, $p=.042$. There was no significant effect of treatment on flow rate ($p=.46$).

## General Discussion

We examined the neuromodulatory and hormonal effects of taVNS, analyzing several putative markers of central NE activity. Relative to baseline, taVNS increased SAA and attenuated a decrease in salivary cortisol that was observed with sham stimulation. We also found that baseline pupil size was not affected by taVNS, and that taVNS did not affect P3 amplitude. Thus, two of our four physiological markers responded sensitively to taVNS, consistent with increases in central NE.

Our results compliment work by Ventura-Bort and colleagues (Ventura-Bort et al., 2018), who reported preliminary evidence that taVNS increases SAA. We demonstrate a more robust effect, using a larger sample size (25 vs. 18 participants), more post-stimulation saliva samples (2 vs. 1), and a superior method of saliva collection (whole saliva method vs. absorbent cotton sponges) (Bosch et al., 2011; Strahler et al., 2017). In addition, we report the first evidence that taVNS influences salivary cortisol. Together, these hormonal analyses add to an accumulating pharmacological literature suggesting that SAA and salivary cortisol might be effective markers of central NE activity (Chamberlain et al., 2007; Ehlert et al., 2006; Speirs et al., 1974; van Stegeren et al., 2006; Warren, van den Brink, et al., 2017).

The relationship between pupil size and NE activity has been supported by direct recordings from the LC (Joshi et al., 2016; Varazzani et al., 2015), direct stimulation of the LC (Reimer et al., 2014), and by fMRI data from human participants (de Gee et al., 2017; Murphy, Vandekerckhove, et al., 2014). We found no effect of taVNS on pupil size, suggesting that taVNS might not increase NE. An alternative possibility is that our pupil experiment was underpowered in terms of sample size or recording duration, or otherwise not sensitive enough to the taVNS manipulation. Our null result resonates with Schevernels and colleagues (Schevernels et al., 2016), who found no effect on pupil size of invasive VNS. Although two other invasive VNS studies found significant pupil effects, we know of no other taVNS study that has measured pupil data. Thus, our work serves as a first exploration that should be revisited with methods adjusted accordingly.

The LC-P3 hypothesis proposes that the P3 reflects the change in neural gain produced by a phasic burst of NE release (Nieuwenhuis et al., 2005). Only one research group has reported an effect of taVNS on P3 amplitude (Fischer, Ventura-Bort, Hamm, & Weymar, 2018; Ventura-Bort et al., 2018). In one study (Fischer et al., 2018) these researchers analyzed data from a Simon task and report that taVNS increased both conflict adaptation and N2 amplitude on incompatible trials, but not P3 amplitude. In a separate study they found taVNS increased P3 amplitude (Ventura-Bort et al., 2018). This study was exploratory, reporting significant simple effects in specific cells of their design, without justification from interactions in the omnibus ANOVA. In light of their other null effect, and our Bayesian evidence in favor of no effect, we must acknowledge that the evidence that the P3 is directly affected by invasive or transcutaneous VNS is mixed at best.

We note some limitations to this work. Saliva data was pooled across two experiments. In Experiment 1a participants were being set up with EEG between the baseline sample and subsequent samples, whereas in Experiment 2 participants were practicing the task-switching experiment. The stimulation protocols and collection methods were identical, and no statistical tests were interpreted between experiments, but the difference likely introduced some variability to the data. This could have contributed to the relatively weak statistical support for the effect of taVNS on SAA. That is, the two-way interaction of treatment with sampling time was not significant so we relied on the three-way interaction of treatment with sampling time and treatment order to justify decomposing the omnibus ANOVA. The salivary cortisol results gave more straightforward evidence of an effect of taVNS, but the sample size was smallish (n= 17), though still within an appropriate range of sample sizes for investigating phasic changes in salivary cortisol (for a review see for a review see Strahler et al., 2017). An additional limitation of this work concerns the general parameters and targets used for taVNS. We used a stimulation intensity of 0.5 mA for all participants. In contrast, some studies titrate stimulus intensity to the participant's perceptual threshold (e.g. Badran, Dowdle, et al., 2018) titrated to an intensity of 3.14 mA). In addition, we pre-treated participants with taVNS for 25 minutes before the EEG task began, whereas pre-treating for longer could be more effective. Finally, there is an unresolved question as to whether the cymba conchae is the best target for taVNS, though both sites yield significant changes in cortical activity (Badran, Brown, et al., 2018; Burger & Verkuil, 2018; Fallgatter et al., 2003). It is possible that some of our null effects were due to our use of a weak current, short pre-treatment time, or a sub-optimal target. Nevertheless, our entire protocol was based on previous work (Beste et al., 2016; Sellaro et al., 2015; Steenbergen, Sellaro, Stock, et al., 2015) and use of this protocol lead to significant effects on salivary markers of NE activity. Keeping the discussed null effects and limitations in mind, our results provide support for the clinical and experimental use of taVNS.

# Chapter 6

# Noradrenergic regulation of cognitive flexibility: No effects of stress, transcutaneous vagus nerve stimulation and atomoxetine on task-switching in humans

This chapter is based on: Tona, K.D., Revers, H., Verkuil, B., & Nieuwenhuis, S. (under review). Noradrenergic regulation of cognitive flexibility: no effects of stress, transcutaneous vagus nerve stimulation and atomoxetine on task-switching.

**Abstract**

Cognitive flexibility allows us to adaptively switch between different responsibilities in important domains of our daily life. Previous work has elucidated the neurochemical basis underlying the ability to switch responses to a previously non-reinforced exemplar, and to switch between attentional sets. However, the role of neuromodulators in task switching, the ability to rapidly switch between two or more cognitive tasks afforded by the same stimuli, is still poorly understood. We attempted to fill this gap by manipulating norepinephrine (NE) levels using a stress manipulation (Study 1a, N=48; between-group design), transcutaneous vagus nerve stimulation (tVNS) at two different intensities (Study 1b, N=48; sham-controlled between-group design), and a pharmacological manipulation (Study 2, N=24, double-blind crossover design), all of which increased salivary cortisol measures. Participants repeatedly switched between two cognitive tasks (classifying a digit as high/low (task 1) or as odd/even (task 2)), depending on the preceding cue. On each trial, a cue indicated the task to be performed. The cue-stimulus interval (CSI) was varied to manipulate the time to prepare for the switch. Participants showed typical switch costs, which decreased with the time available for preparation. None of the manipulations modulated the size of the switch costs or the preparation effect. Task-switching performance reflects a complex mix of cognitive control and bottom-up dynamics of task-set representations. Our findings suggest that NE does not affect either of these aspects of cognitive flexibility.

## General Introduction

Cognitive flexibility, the ability to learn associations between stimuli, actions and outcomes and to quickly adapt ongoing behavior to salient changes in the environment, is very important for human survival (Kehagia et al., 2010). It allows us to "juggle" between different responsibilities in important domains of our daily life, and allows species to face new and unexpected conditions in the environment, including threatening conditions (Canas, Quesada, Antoli, & Fajardo, 2003). Cognitive flexibility is a multifaceted construct. Two examples of lower-order cognitive flexibility are basic reinforcement learning and reversal learning—responding to a previously non-reinforced exemplar within the same dimension. These cognitive functions are critically dependent on environmental signals or feedback, allowing us to flexibly learn and unlearn goal-directed behaviors (Kehagia et al., 2010). Two examples of higher-order cognitive flexibility are extra-dimensional attentional set shifting and task switching. Extra-dimensional set-shifting concerns the ability to adapt behavior flexibly following feedback, but pertains to broader stimulus dimensions rather than a specific exemplar. Task switching is a purer form of cognitive flexibility because it is uncontaminated by learning and feedback processing (Kehagia et al., 2010). Instead, people rely on implicit or explicit cues that indicate frequent shifts between two or more tasks afforded by the same stimuli; for example to classify a digit as odd–even or as high–low with a left or right button press (Fischer, Plessow, & Kiesel, 2010; Monsell & Mizon, 2006; Monsell, Sumner, & Waters, 2003).

Previous literature shows that neuromodulators such as dopamine, serotonin and NE modulate several forms of cognitive flexibility. Dopamine modulation in the striatum and prefrontal cortex is critical for basic reinforcement learning and the integration of negative feedback during reversal learning, while serotonin appears to play an important role in inhibiting perseverative responding after reversal of cue–outcome contingencies (Kehagia et al., 2010; Matias, Lottem, Dugué, & Mainen, 2017; Walker, Robbins, & Roberts, 2009). In contrast, NE plays a crucial role in extra-dimensional set shifting and adaptive updating of beliefs about the environment (Janitzky et al., 2015; Jepma et al., 2018; Lapiz & Morilak, 2006; Pajkossy, Szollosi, Demeter, & Racsmany, 2018; Sales, Friston, Jones, Pickering, & Moran, 2019; Tait et al., 2007). Building on such findings, Kehagia and colleagues (2009, 2010) proposed that NE may also be critical for task switching: flexibly shifting between task sets on the basis of trial-to-trial instruction cues. However, surprisingly little research has investigated the role of NE in task switching (Steenbergen, Sellaro, de Rover, Hommel, & Colzato, 2015; Wolff et al., 2018). Here we addressed this question by examining task-switching performance after manipulating activity of the locus coeruleus-norepinephrine (LC-NE) system using stress induction, transcutaneous auricular vagus nerve stimulation (tVNS), and administration of the drug atomoxetine.

The relationship between stress and LC activation is well-documented, and the LC is an important component of the central stress circuitry (for reviews see Aston-Jones, Rajkowski, Kubiak, & Alexinsky, 1994; Itoi & Sugimoto, 2010; Sara & Bouret, 2012). Most environmental stressors increase the spontaneous discharge rate of the LC. Several brain areas involved in the typical stress response, including the central nucleus of the amygdala and paraventricular nucleus of the hypothalamus, provide inputs to the LC. Corticotropin-releasing hormone is an important mediator of this stress-induced LC activation and ensuing effects throughout the brain, which prepare the organism for a rapid and appropriate behavioral response to the stressor. Indeed, blockade of noradrenergic beta receptors diminishes the effect of stress on emotional memory (Cahill & McGaugh, 1998; Kroes et al., 2016) and global brain state (Hermans et al., 2011). In the present research, we used an effective, standardized protocol for experimental stress induction in humans (Schwabe & Schachinger, 2018).

The vagus nerve is the longest nerve in our body and communicates the state of the viscera to the brain and vice versa. Importantly, the vagus nerve projects to the nucleus tractus solitarius which in turn projects directly and indirectly to the LC, the main source of NE in the brain (Berridge & Waterhouse, 2003). External stimulation of the vagus nerve (VNS, used usually to suppress epileptic seizures) can be achieved either invasively, with a surgical procedure involving vagus nerve stimulator implantation within the chest cavity; or transcutaneously, with an iPod-like device delivering electrical impulses to the auricular branch of the vagus nerve, which is situated close to the surface of the skin of the outer ear. Animal studies have found that VNS increased the firing rate of NE neurons in the LC (Dorr & Debonnel, 2006; Raedt et al., 2011; Roosevelt et al., 2006), and increased extracellular NE levels in the prefrontal cortex (Follesa et al., 2007), basolateral amygdala (Hassert et al., 2004), and cerebrospinal fluid (Martlé et al., 2015). Importantly, this increase in NE levels occurred in a dose-dependent manner, and returned to baseline after termination of VNS (Raedt et al., 2011; Roosevelt et al., 2006). Although there is no direct evidence that tVNS has similar effects on the LC-NE system, functional magnetic resonance imaging studies in healthy humans have demonstrated that tVNS elicits widespread changes in cortical and brainstem activity (Frangos et al., 2014; Kraus et al., 2007). Other recent work has shown that tVNS modulates hormonal (Fischer et al., 2018; Warren et al., 2019) and psychophysiological (Fischer et al., 2018; but see Warren et al., 2019) indices of noradrenergic function in human subjects. In the current research, we examined the effects on cognitive flexibility of tVNS at two levels of intensity.

Although the above-mentioned methods of tVNS and stress induction allow examination of NE effects on cognition, psychopharmacological manipulation provides a more robust method for directly manipulating NE levels and for establishing a causal role for NE. To this end, we also manipulated brain-wide NE levels via administration of the NE transporter blocker atomoxetine, a compound usually prescribed to treat attention-deficit hyperactivity disorder (Pringsheim, Hirsch, Gardner, & Gorman, 2015; Sharma & Couture, 2014). In cortical areas, the NE transporter is responsible for the reuptake of not

only NE but also dopamine from the synaptic cleft (Devoto & Flore, 2006). Thus, atomoxetine increases both central NE and cortical dopamine levels (Bymaster et al., 2002; Koda et al., 2010). Finally, in human subjects atomoxetine administration has been shown to affect NE biomarkers such as alpha-amylase (Chamberlain et al., 2007; Warren, van den Brink, et al., 2017).

We studied higher-order cognitive flexibility using a task switching paradigm (Monsell et al., 2003) in which the task to be performed on each trial was indicated by a cue presented at the start of the trial. This paradigm distinguishes between trials on which the task changes (“ switch trials”) and trials on which the task stays the same (“repeat trials”). The finding of interest is that reaction time is longer, and error rate greater, on switch trials (the “switch cost”); and as the cue–stimulus interval is prolonged—allowing more opportunity for advance preparation—the switch cost is reduced (the “preparation effect”). Switch costs are attributable to a combination of the time required for resolving interference from residual activation of the previous, no-longer relevant task set (“task-set inertia”) and of the time required for retrieving the newly cued task set (“task-set reconfiguration”; “task-set reconfiguration”; “task-set reconfiguration”; “task-set reconfiguration”; Monsell et al., 2003). The cognitive flexibility required to switch between tasks depends on the dynamic transformation of neural task-set representations from trial to trial (Qiao, Zhang, Chen, & Egner, 2017; Yeung, Nystrom, Aronson, & Cohen, 2006). In order to ensure that the observed switch costs and preparation effect would accurately reflect this type of cognitive flexibility instead of a cue-repetition effect, we used two cues per task, which allowed us to avoid direct cue repetitions between trials (Logan & Bundesen, 2003; Monsell & Mizon, 2006).

In Study 1 we tested three groups of participants. All participants performed the task on two separate occasions in which either tVNS or sham stimulation was applied according to a single-blind counterbalanced design. Two of the groups received common, medium-intensity (0.5 mA) tVNS. One of those groups underwent also a stress induction procedure, the other group underwent a control procedure. Comparison of those two groups allowed us to examine the effect of stress (in the context of tVNS) on task switching, as reported under ‘Results Study 1a: Effects of tVNS and stress’. The third group received tVNS (versus sham) at a higher intensity (1.0 mA). Comparison of this group with the medium-intensity/no-stress group allowed us to examine the relatively unknown dose-dependent effects of tVNS. This can be seen as an initial step toward establishing a linear or curvilinear relationship between tVNS intensity and cognitive flexibility, or other aspects of cognitive task performance (Dietrich et al., 2008; Frangos et al., 2014; Ghacibeh, Shenker, Shenal, Uthman, & Heilman, 2006; Hulsey et al., 2017). These results are reported under ‘Results Study 1b: effects of tVNS intensity’. In Study 2 we examined the effect of our psychopharmacological manipulation on task switching, using a double-blind placebo-controlled cross-over design.

Note that we do not claim that stress induction, tVNS and atomoxetine selectively affect NE levels. Stress causes a myriad of adaptive neurochemical changes. VNS can affect levels of dopamine and serotonin, although these effects may require chronic stimulation

or reflect indirect effects of the change in NE levels (Manta, El Mansari, Debonnel, & Blier, 2013; Martlé et al., 2015). And as mentioned above, atomoxetine also increases cortical dopamine levels. We also do not intend to suggest that the three manipulations affect the LC-NE system in a similar way. However, if task switching is crucially dependent on activity of the LC-NE system, one would expect effects of (some of) these manipulations on task switching performance. To foreshadow the results, we did not find such effects.

## STUDY 1

### Methods

#### *Participants*

Seventy-two Dutch native-speaking volunteers (18-29 years old; mean age: 21.4) participated in this study. All had normal or corrected-to-normal vision. To avoid menstrual cycle effects on cortisol responses (Kirschbaum, Kudielka, Gaab, Schommer, & Hellhammer, 1999), only male participants were included. Exclusion criteria were: neurological or psychiatric disorder, bradycardia, cardiac arrhythmia, cardiovascular disease, psychoactive medication or drug use, active implants (e.g., cochlear implant), and skin disorder such as eczema. Participants were asked to refrain from alcohol intake within 24 hours prior to the study, and to refrain from excessive exercise, caffeine and heavy meals within 3 hours prior to the study. To ensure that the participants were blind to the active stimulation/sham condition, prior participation in other tVNS studies was an additional exclusion criterion. All participants gave written informed consent prior to their participation, and, based on their preference, were compensated with 24 euros or course credits. The study was approved by the ethics committee of the Institute of Psychology at Leiden University.

#### *Design*

tVNS was applied according to a single-blind, sham-controlled, cross-over design. The study consisted of two sessions, scheduled one week apart at the same time of the day. To control for circadian fluctuations in cortisol levels (Lupien, Maheu, Tu, Fiocco, & Schramek, 2007), all sessions were conducted between 12.00 and 6.00 pm. Participants received either tVNS or sham stimulation, in a counterbalanced order. Participants were randomly assigned to one of three groups (each with N = 24):

- medium-intensity tVNS (0.5 mA)
- medium-intensity tVNS (0.5 mA) and stress induction
- high-intensity tVNS (1.0 mA)

The study design and procedure were exactly the same for all groups, with the following exceptions. The intensity of tVNS differed between the medium- and high-intensity groups. Additionally, in the stress group, stress was induced using a socially evaluated cold pressor test (SECPT), while the other two groups received a control treatment that involved a similar procedure but without social, psychological and physical stress induction (see below).

***Task***

*Experimental phase*

To assess cognitive flexibility, we used an unpredictable cued task-switching paradigm (Monsell et al., 2003), implemented in E-Prime (Psychology Software tools, Pittsburgh, PA). Participants were asked to classify a digit (1-4, 6-9) as high/low (task 1) or as odd/even (task 2), depending on the preceding cue. The cue was a colored circle (pink or yellow) or an outline shape (diamond or square, see Figure 1), displayed on a grey background. The diamond-shaped and pink-colored cues indicated that task 1 should be performed, while the square-shaped and yellow-colored cues indicated that task 2 should be performed. The probability of a task switch was 25%.

Digits were displayed in a black Courier New 24-pt font with a height of 1 cm centered on the cue of side 3 cm, which was displayed in the center of the screen (Figure 1). Each trial started with a blank screen for 750 ms, followed by a fixation cross of 500 ms. After a preparation interval of 150 ms or 800 ms, the digit appeared in the center of the cue until the participant's response. A response triggered the immediate onset of the next trial, unless a wrong key was pressed, in which case an error message appeared for 2 sec to allow the participant to recover before onset of the next trial.

To unconfound the effects of task switching and cue change (Monsell & Mizon, 2006), the cue changed on every trial, alternating between shape and color. The cue-stimulus interval (CSI) was manipulated in such a way that the participants had little time for advance preparation (CSI=150 ms) or more time (CSI=800 ms). Participants performed the tasks by pressing the letters "Q" (odd, high) or "P" (even, low) on a keyboard with their left and right index fingers. They were instructed to respond as quickly as possible while minimizing the number of errors and to use the available preparation time effectively.

The experiment consisted of 768 trials that were presented in six blocks of 128 trials. Each block started with four warm-up trials and consisted of trials with only a long or a short CSI. Blocks with long and short CSI alternated in an ABABAB order for half of the participants and a BABABA order for the other half of the participants. This factor was stratified with treatment order to ensure that the order of the CSIs across blocks was orthogonal to the order of treatments (tVNS/sham in first session for Study 1 and placebo/atomoxetine in first session for Study 2). In between the blocks, there were subject-paced breaks with a maximum duration of 15 sec, and at the end of each block participants received written feedback about their mean RT and error rate for that block. Participants were challenged to beat this performance in the remaining blocks. The task-switching experiment lasted approximately 30 minutes.

*Practice phase*

Prior to the actual experiment, participants received extensive practice to ensure that they learnt the cue-stimulus mapping well. The practice task consisted of four blocks and lasted approximately 20 min. During the first block, participants learnt the first task by

practicing 32 trials of the odd-even task with the digit displayed inside the appropriate cue. During the second block, participants practiced 32 trials of the high-low task, using the same procedure. In the third block, participants performed 64 trials with a long CSI and random switches between task 1 and task 2. The last block consisted of 64 trials with a short RSI and random switches between task 1 and task 2.

To ensure proper learning of the cue-task mapping, the cue-task mapping was displayed in the top-right corner of the screen throughout the practice phase. Additionally, before the initiation of the third practice block, the experimenter ran through the learned tasks together with the participant, to make sure the cue-task mappings were properly represented. To mitigate learning effects, the practice phase of session 2 was half as long as the practice phase of session 1.

***Data analysis***

We performed repeated-measures ANOVAs with mean correct RT and accuracy (% errors) as dependent variables, treatment (tVNS/sham), CSI (150 ms/800 ms), trial type (switch/repeat) and task (odd/even or high/low) as within-subject independent variables, and group (stress vs no-stress) and treatment order as between-subject variables (Study 1a), or tVNS intensity (0.5/1.0 mA) and treatment order as between-subject variables (Study 1b). Treatment order and task were factors of no interest, so we do not report any statistical terms involving these factors. The following trials were excluded from the analyses: all practice trials, warm-up trials, trials following errors, incorrect trials and trials with RTs longer than 2 sec.

Data was analyzed with IBM SPSS Statistics for Windows, version 25 (IBM Corp., Armonk, N.Y., USA). A significance level of $p<.05$ was adopted for all statistical tests. Significant results were followed by t-tests to clarify the direction of the effect. Greenhouse-Geisser correction was used whenever the assumption of sphericity was violated.

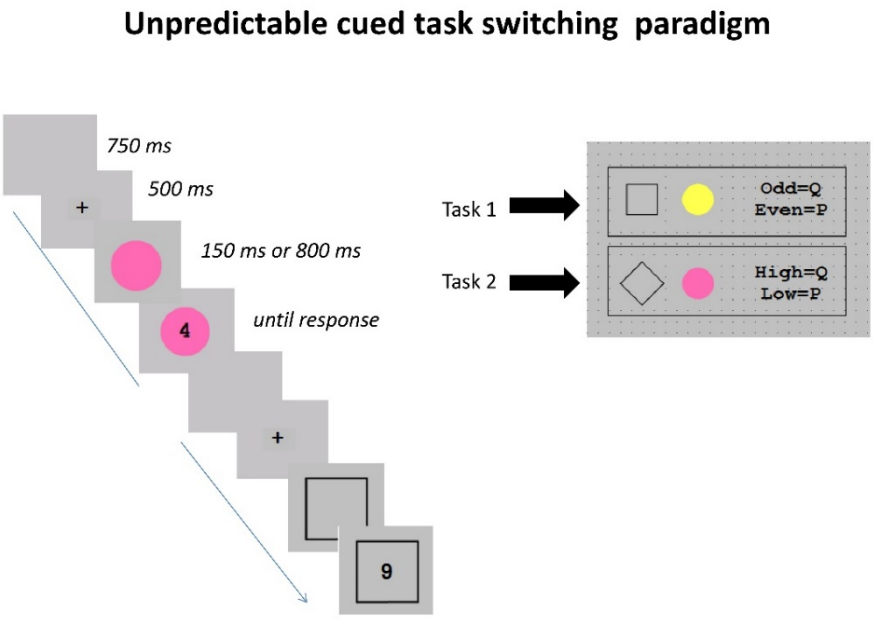


**Figure 1**: Illustration of the task switching paradigm. The same paradigm was used in all the studies reported in this manuscript.

***Procedure***

The timeline of each experimental session is illustrated in Figure 2. The tVNS or sham stimulation started before the practice phase of the task switching experiment. After the practice, which took about twenty minutes, the participant underwent an assessment of their mood. Then the stress induction (or control procedure) took place, followed by the actual task switching paradigm.

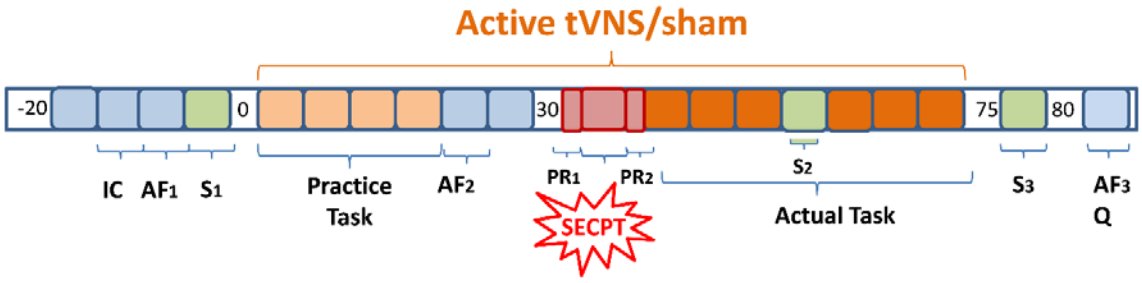


**Figure 2.** Timeline of procedures in Study 1. IC= informed consent, $S_{(1,2,3)}$ = saliva measurement, AF $_{(1,2,3,)}$ = Affect Grid, PR $_{(1,2)}$ = pain rating, Q= after-effect questionnaire

***tVNS***

We used a tVNS device to stimulate the vagus nerve (NEMOS®, Cerbomed, Erlangen, Germany). The device was switched on for a period of 75 minutes, with a frequency of 25 Hz, and stimulation intensity set at 0.5 mA for the medium-intensity groups or 1.0 mA for the high-intensity group. The stimulation followed a pattern set by the manufacturer, alternating between 30 seconds on and 30 seconds off. In one of the sessions the participant received tVNS on the left concha, at the inner side of the ear where the afferent auricular branch of the vagus nerve can be stimulated. In the other session, participants received sham stimulation on the left ear lobe. Administering sham stimulation in this manner has proven to produce no significant activation in the brainstem and cortex (Kraus et al., 2013).

At the end of each session, an after-effect questionnaire was used to assess possible side effects of tVNS and how the participants experienced the stimulation (Sellaro et al., 2015). The participants were asked to indicate on a 5-point scale the extent to which specific possible tVNS side effects/experiences applied to them. The included complaints were: headache, neck pain, uncomfortable feeling, nausea, muscle constructions, tingling sensation, burning feeling under electrodes, and open question “other” where participants could mention complains missing from the list.

Mean ratings of uncomfortable feeling were 2.0 for the 0.5 mA (sham: 1.6) versus 2.1 for the 1.0 mA (sham: 1.7) group, and 1.9 (sham: 1.9) for the stress group respectively. Scores for tingling feeling were 2.7 for the 0.5 mA (sham: 2.4) versus 3.1 for the 1.0 mA (sham: 3.4) group, and 3.1 for the stress group (sham: 2.1). Finally, scores of feeling of

burning sensation were 2.3 for the 1.0 mA (sham: 1.7) group but below 2.0 for the other groups. Ratings for other scales were all below 2.0.

***Stress Induction***

To manipulate stress, we used the socially evaluated cold pressor test (SECPT), which combines induction of physiological (cold pressor) and psychological (negative social evaluation) stress. The SECPT has been shown to be a robust stressor, leading to increased levels of the stress hormone cortisol (Schwabe, Haddad, & Schachinger, 2008).

The participant was instructed to submerge his right hand until the wrist into a bucket of ice water (4°C), to not move this hand, and to keep it in the water until he could not bear it anymore. Although no time restriction was revealed to the participant, in line with ethical and safety restrictions, he was told by the experimenter to take his hand out of the water after three minutes. To ensure induction of psychological stress, instructions were given in a strict manner by an experimenter who was wearing a white coat, and the participant was evaluated by a committee of two members while having his hand in cold water. The evaluation included visual observation, mock notes and negative feedback by the committee members and simultaneous videotaping of the participant. The participant was told that the camera was recording his facial expressions, which would be evaluated at a later time point.

In the control condition, the same procedure was followed but the participant submerged his hand in room temperature water (22-25 $^{o}$C) and the evaluators did not induce any psychological/social stress. To be consistent, the same instructions were given to the participant as during the stress manipulation but not in a strict manner. Although the participant was told to keep his hand in the water until he could not bear it anymore and no time restriction was revealed to him, the experimenter asked him to take his hand out of the water when the three minutes had passed. Throughout the control condition, the control social evaluators avoided looking at the participant, and acted in a neutral manner. Also, it was clear that the camera that was in the room was turned off and pointing towards the wall instead of the participant.

***Validation of stress manipulation***

To test the effectiveness of the stress manipulation, we assessed psychological and physiological distress by means of subjective pain ratings and salivary cortisol levels. Pain ratings were collected immediately before and after the stress induction. Participants indicated on a visual scale ranging from 0-100 how much pain they felt at the moment. Changes in pain perception were assessed by subtracting the values reported after the SECPT/control manipulation from those reported immediately before. The difference values for the stress and non-stress group were compared using independent *t*-tests.

To assess cortisol levels, saliva samples were collected at three time points (see Figure 2): at baseline, soon after the stress or control manipulation and after completion of the task. Samples were assayed for cortisol using a competitive enzyme-linked immunosorbent assay, according to the manufacturer's instructions (IBL, Hamburg, Germany). All

samples of a given participant were assayed simultaneously. For additional information about saliva sample collection and processing methods see (Warren et al., 2019; Warren, van den Brink, et al., 2017). Cortisol data were analyzed using a 3x2 mixed ANOVA with time point (first vs. second vs. third measurement) as a within-subjects factor and group (stress vs. no stress) as between-subjects factor.

**Results Study 1a: Effects of tVNS and stress**

***Effects of stress on subjective pain and salivary cortisol***

Stress led to increased pain perception and elevated salivary cortisol levels (cortisol levels are reported in μg/dl unit). Exposure to the SECPT increased mean subjective pain ratings (stress group: 29.65, no-stress group: 3.79, $t(32) = 7.94$, $p < 0.001$). The stress-induction procedure increased cortisol levels over time, as compared to the control procedure, yielding a significant main effect of stress ($F(1,42) = 4.45$, $p = .041$), and a time point x stress interaction, ($F(2,84) = 5.540$, $p = .017$ after Greenhouse-Geisser correction). While baseline cortisol levels did not differ between the groups (stress group mean: 0.39, no-stress group mean: 0.32; $t(45) = 0.82$, $p = .42$), cortisol levels were significantly higher in the stress group at 15 minutes and 70 minutes after the end of stress induction (stress group mean: 0.41, no-stress group mean: 0.22; $t(43) = 3.38$, $p = 0.002$; and stress group mean: 0.37, no-stress group mean: 0.18; $t(29) = 3.14$, $p = 0.004$, respectively).

***Reaction times***

Mean reaction times (RTs) are presented in Figure 3. Participants showed a typical switch cost of 60 ms ($F(1,44) = 39.8$, $p < .001$; switch 786 ms, repeat 726 ms), which decreased with the time available for preparation ($F(1,44) = 14.45$, $p < .001$). The switch cost was smaller in long CSI blocks (39 ms) than in short CSI blocks (79 ms). There was also a main effect of CSI ($F(1,44) = 160$, $p < .001$). These are well-established findings in task switching research.

Treatment ($F(1,44) < 1$, $p = .97$) and stress ($F(1,44) < 1$ , $p = .73$) did not have a main effect on RT (stress 749 ms, no stress 763 ms), and there was no significant interaction between treatment and stress ($F(1,44) = .24$, $p = .62$). Importantly, the switch cost and the preparation effect were not modulated by tVNS ($F(1,44) = 1.55$, $p = .22$; $F(1,44) = 3.19$, $p = .08$) or stress ($F(1,44) = 2.39$, $p = .13$; $F(1,44) = 1.19$, $p = .28$) and there were no interactions between those factors and other factors of interest.

***Accuracy***

Percentages of errors are presented in Figure 3. Participants showed a typical switch cost of 4.2% ($F(1,44) = 67.23$, $p < .001$; switch: 91.2%, repeat: 95.4%), which decreased with the time available for preparation ($F(1,44) = 12.75$, $p = .001$). The switch cost was smaller in long CSI blocks (3.1%) than in short CSI blocks (5.1%). There was also a main effect of CSI ($F(1,44) = 17.25$, $p < .001$).

Treatment ($F(1,44) < 1$, $p = .97$) and stress ($F(1,44) = 0.48$, $p = .55$) did not have a main effect on accuracy. There was no significant interaction between treatment and stress ($F(1,44) < 1$, $p = .67$). The switch cost and the preparation effect were not modulated by

tVNS ($F(1,44) < 1$, $p = .58$; $F(1,44) < 1$, $p = .71$) or stress ($F(1,44) < 1$, $p = .82$; $F(1,44) < 1$, $p = .41$), and there were no interactions between these factors and other factors of interest.

***Exploratory analysis: effect of stress in sham condition only***

It is possible that stress did not affect task switching performance because it was manipulated in the context of tVNS—perhaps tVNS somehow suppressed the effect of stress (Lerman et al., 2019; Tobaldini et al., 2019). To examine this scenario, we carried out an ANOVA comparing the stress and non-stress groups (0.5 mV), including only data from the sham condition. With regard to RT, stress did not have a main effect ($F(1,44) < 1$, $p = .59$), and did not modulate the switch cost ($F(1,44) = 2.75$, $p = .10$) and the preparation effect ($F(1,44) < 1$, $p = .33$). Similarly, with regard to accuracy, stress did not have a main effect ($F(1,44) = 0.37$, $p = .55$), and did not modulate the switch cost ($F(1,44) < 1$, $p = .89$) or the preparation effect ($F(1,44) = 3,38$, $p = .07$). There was a significant stress x CSI interaction ($F(1,44) = 4.65$, $p = .037$), with the effect of CSI on overall accuracy (i.e., regardless of trial type) being smaller in the stress group (mean: 0.6%) than in the non-stress group (mean: 1.8%). This result was driven by a difference in accuracy at the long CSI. Interpretations of this finding must remain tentative, given the post hoc nature of this analysis, the large number of statistical tests performed in the present studies, and the fact that the RT data did not show a similar interaction.

**Results study 1b: effects of tVNS intensity**

***Effects of tVNS on mood***

Elsewhere we show that for a subset of the participants in this study, from whom we collected and analyzed saliva measurements tVNS treatment (0.5 mA) significantly increased salivary levels of cortisol and α-amylase compared to sham stimulation (Warren et al., 2018), thus confirming the effect of tVNS. Here we examine the effects of tVNS on mood. Mood was assessed at three time points (Figure 2) using the Affect Grid (Russell, Weiss, & Mendelsohn, 1989), a quick means of assessing affect along the dimensions of pleasure-displeasure and arousal-sleepiness. Pleasure and arousal scores were analyzed separately by means of repeated-measures ANOVAs with time point (first vs. second vs. third measurement) and treatment (tVNS vs. sham) as within-participants factors, and tVNS intensity (0.5/1.0 mA) and treatment order as between-subject factors. There was an effect of time point on pleasure ($F(2,88) = 7.77$, $p = 0.001$), with pleasure decreasing over time, but there was no effect of treatment or tVNS intensity on arousal ($F(1,44) = 1.78$, $p = 0.18$; $F(1,44) = 0.44$, $p = 0.51$) and pleasure ($F(1,44) = 0.46$, $p = 0.60$; $F(1,44) = 0.006$ $p = 0.94$).

***Reaction times***

Mean RTs are presented in Figure 3. Participants showed a typical switch cost of 66 ms ($F(1,44) = 49.5$, $p < .001$; switch 760 ms, repeat 694 ms), which decreased with the time available for preparation ($F(1,44) = 35.7$, $p < .001$). The switch cost was smaller in long CSI blocks (37 ms) than in short CSI blocks (96 ms). There was also a main effect of CSI ($F(1, 44) = 177.4$, $p < .001$).

Treatment ($F(1,44) = 2.8$, $p = .10$) and tVNS intensity ($F(1,44) = 3.2$, $p = .08$) did not have a main effect on RT, but the means indicated faster responses for the high-intensity group (0.5 mA: 763 ms, 1.0 mA: 690 ms). There was no significant interaction between treatment and tVNS intensity ($F(1,44) = 1.3$, $p = .25$). Importantly, the switch costs and the preparation effect were not modulated by treatment or tVNS intensity and there were no interactions between these factors and other factors of interest.

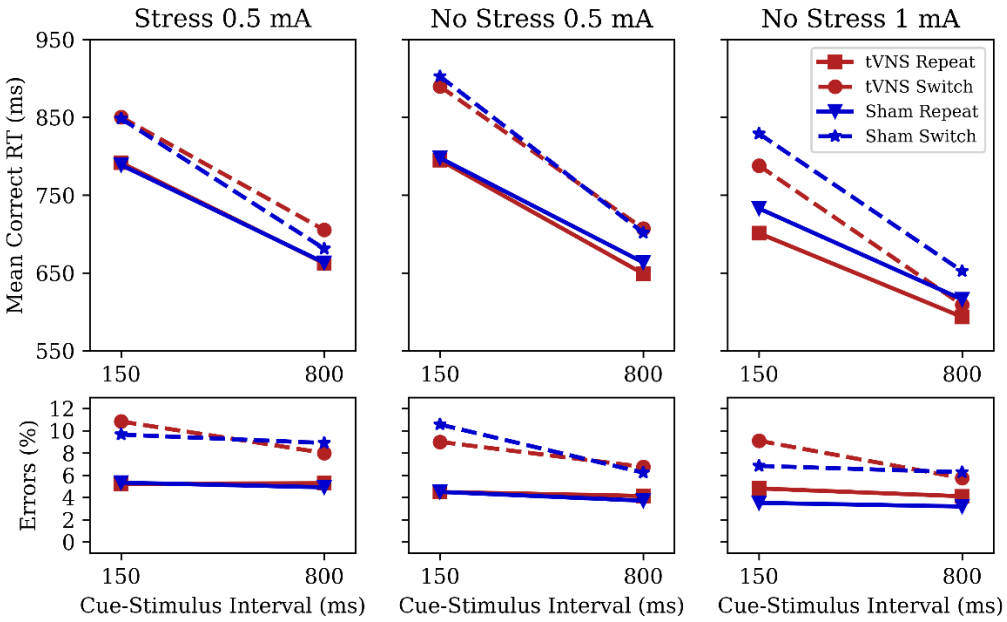


**Figure 3**: Effects of stress, tVNS (vs sham) and tVNS intensity on mean correct RT (top) and error rate (bottom).

### *Accuracy*

Participants' accuracy scores showed a typical switch cost of 3.5% ($F(1,44) = 50.43$, $p < .001$; switch 92.5%, repeat 96.0%), which decreased with the time available for preparation ($F(1,44) = 15.12$, $p < .001$). The switch cost was smaller in long CSI blocks (2.5%) than in short CSI blocks (4.6%). There was also a main effect of CSI ($F(1,44) = 24.53$, $p < .001$). Treatment ($F(1,44) = 1.60$, $p = .21$) and tVNS intensity ($F(1,44) = .46$, $p = .50$) did not have a significant main effect on accuracy. Finally, there was no significant interaction between treatment and tVNS intensity ($F(1,44) < 2.87$, $p = .09$.

### *Exploratory analysis: tVNS at 1.0 mA intensity causes speed-accuracy tradeoff*

Although the omnibus ANOVA did not yield significant main effects of treatment and tVNS intensity, the right panel of Figure 3 suggests that tVNS at 1.0 mA intensity decreased RTs at the expense of more errors. To examine the robustness of this finding, we carried out an ANOVA that included only the 1.0 mA group. While high-intensity tVNS did not affect the switch cost and the preparation effect ($F(1, 22) = 1.89$, $p = .18$; $F(1, 22) < 1$, $p = .55$, respectively), it had a main effect on RT ($F(1,22) = 5.30$, $p = .03$),

indicating that overall responses were faster in the tVNS condition (673 ms) than in the sham condition (708 ms).

Regarding accuracy, while high-intensity tVNS did not affect the switch cost ($F(1,22) < 1$, $p = .79$) and the preparation effect ($F(1,22) < 1$, $p = .35$), it had a main effect on error rate ($F(1,22) = 5.16$, $p = .03$), indicating an overall decrease in accuracy in the tVNS condition (94.1%) compared to the sham condition (95.1%). For completeness we report a significant two-way interaction between tVNS intensity and CSI, ($F(1,22) = 5.56$, $p = .03$), but that interaction was largely driven by a spurious difference in the effect of CSI between low and high sham stimulation intensity. Together, these findings suggest that tVNS at 1.0 mA caused a change in the participants' speed-accuracy tradeoff.

## STUDY 2

## Effects of atomoxetine

### Methods

#### *Participants*

Twenty-four young volunteers (six male; 18-25 years old; mean age: 21.7) participated as part of a larger pharmacological neuroimaging study (van den Brink et al., 2016). Participants were screened by a physician for the following exclusion criteria: standard contraindications for MRI; current use of psychoactive or cardiovascular medication; a history of psychiatric illness or head trauma; cardiovascular disease; renal failure; hepatic insufficiency; glaucoma; hypertension; drug or alcohol abuse; learning disabilities; poor eyesight (myopia $\leq -6$ diopters); smoking $> 5$ cigarettes a day; and pregnancy. All participants gave written informed consent prior to their participation, and were compensated with €135. The study was approved by the Leiden University medical ethics committee.

#### *Design and Procedure*

The task performed by participants was identical to that used in Study 1. As in Study 1, blocks with long and short CSI alternated in an ABABAB or BABABA fashion, and this between-subject factor was stratified with treatment order. The study was conducted according to a double-blind placebo-controlled cross-over design. In each of the two sessions, scheduled one week apart at the same time of the day, participants received either a single oral dose of atomoxetine (40 mg) or placebo (125 mg of lactose monohydrate with 1% magnesium stearate, visually identical to the drug), in counterbalanced order. Data reported elsewhere show that for these participants the atomoxetine treatment significantly increased salivary levels of cortisol and α-amylase, reliable markers of sympathetic nervous system and hypothalamus-pituitary-adrenal axis activation, respectively (Warren, van den Brink, Nieuwenhuis, & Bosch, 2017).

The procedure of Study 2 is illustrated in Figure 4. The practice of the task switching paradigm started immediately after the pill ingestion, when the drug did not have any effects yet ($t = 0$ min; see Warren et al., 2016). The actual experiment was conducted

when atomoxetine plasma levels were at their peak ($t$ = 140-170 min; Sauer, Ring, & Witcher, 2005). Between the practice phase and the experimental phase, participants underwent resting-state functional neuroimaging.

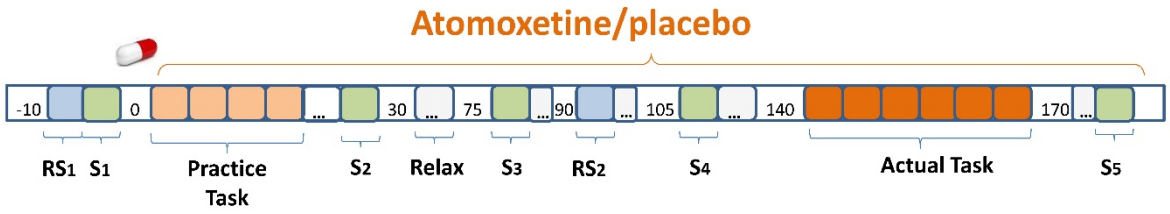


**Figure 4.** Timeline of procedures in Study 2. $RS_{(1,2)}$ = resting-state MRI, $S_{(1,2,3,4,5)}$ = saliva measurement

### *Analysis*

We performed repeated-measures ANOVAs with correct RT and accuracy (% errors) as dependent variables, treatment (atomoxetine/placebo), CSI (150 ms/800 ms), trial type (switch/repeat) and task (odd/even or high/low) as within-subject independent variables and treatment order as a between-subject variable. As in Study 1, treatment order and task were factors of no interest, so we do not report any statistical terms involving these factors. Trial exclusion criteria were the same as in Study 1.

## Results

### *Reaction times*

Mean RTs are presented in Figure 5. The pattern of findings was similar to that in Study 1. Participants showed a typical switch cost of 85 ms ($F$(1,22) = 47.21, $p$ < .001; switch 733 ms, repeat 818 ms), which decreased with the time available for preparation ($F$(1,22) = 24.68, $p$ < .001). The switch cost was smaller in long CSI blocks (44 ms) than in short CSI blocks (127 ms). There was also a main effect of CSI ($F$(1,22) = 128.63, $p$ < .001).

Treatment ($F$(1,22) = 1.24, $p$ = .27) did not have a main effect on RT, but the means indicated somewhat slower responses in the atomoxetine condition (785 ms) than in the placebo condition (765 ms). Importantly, the switch costs ($F$(1,22) = 2.88, $p$ =.10) and the preparation effect ($F$(1, 22) < 1, $p$ =.62) were not modulated by atomoxetine and there were no interactions between treatment and other factors of interest.

### *Accuracy*

As shown in Figure 5, the pattern of mean accuracy scores was also similar to that in Study 1. Participants showed a typical switch cost of 3.8% ($F$(1,22) = 49.8, $p$ < .001; switch 91.2%, repeat 95.0%), which decreased with the time available for preparation ($F$(1,22) = 9.8, $p$ = .005). The switch cost was smaller in long CSI blocks (2.1%) than in short CSI blocks (5.4%). There was also a main effect of CSI ($F$(1,22) = 17.9, $p$ < .001).

Treatment ($F$(1,22) < 1, $p$ = .78) did not have a main effect on accuracy (atomoxetine 93.2%, placebo 93.0%). Importantly, the switch costs ($F$(1,22) < 1, $p$ = .92) and the

preparation effect ($F(1,22) < 1$, $p = .43$) were not modulated by atomoxetine and there were no interactions between treatment and other factors of interest.

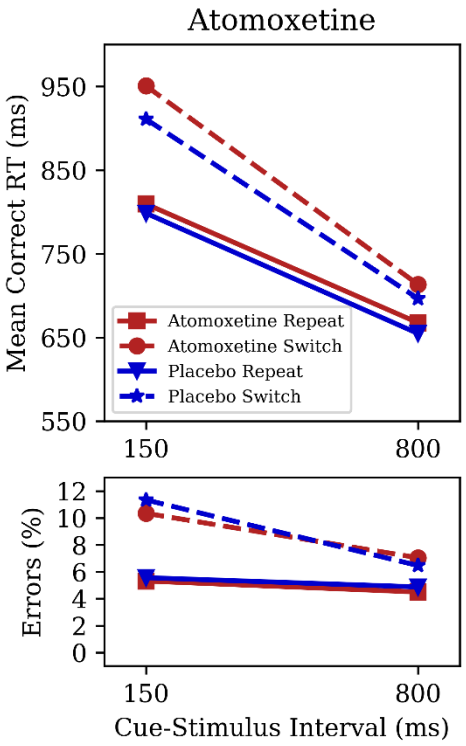


**Figure 5**. Effects of atomoxetine. Mean correct RT (top) and error rate (bottom) as a function of treatment, CSI and trial type.

## General Discussion

Previous work has suggested an important role for the LC-NE system in modulating several forms of cognitive flexibility, possibly by global modulation of gain and corresponding levels of decision noise (Aston-Jones & Cohen, 2005; Kane et al., 2017; Warren, van den Brink, et al., 2017). However, it is still unknown whether NE levels are also critical for task switching (Kehagia et al., 2009; Kehagia et al., 2010), which requires the dynamic transformation of task-set representations from trial to trial. We addressed this question by examining cued task-switching performance after manipulating activity of the LC-NE system using stress induction, tVNS, and administration of atomoxetine. Our findings were highly consistent: none of these manipulations affected measures of task-switching performance, suggesting that NE is not involved in the cognitive flexibility required to switch between relatively abstract rules and sets of stimulus-response mappings.

A potential explanation for these findings is that our manipulations of the noradrenergic system were unsuccessful. However, this explanation is implausible. First, we used an effective, standardized protocol for experimental stress induction (Schwabe & Schachinger, 2018), which led to increased pain perception and elevated salivary cortisol levels in our participants. And as argued above, the relationship between stress and noradrenergic activity has been well-documented. The success of our tVNS manipulation

is less clear. Invasive VNS in rodents results in increased NE levels. Elsewhere we report that our 0.5-mA tVNS manipulation significantly increased salivary cortisol and α-amylase, two indirect hormonal markers of noradrenergic function, in a partially overlapping group of participants (Warren et al., 2018). However, reported effects of tVNS on psychophysiological markers of noradrenergic function in humans (pupil size and P3 amplitude) are mixed (Fischer et al., 2018; Warren et al., 2019), perhaps due to differences in stimulation intensity or choice of sham stimulation location. It is also worth noting that our tVNS manipulation did not affect subjective (psychological, declarative) arousal levels as assed with affect grid questionnaire; this dissociation between subjective (psychological) and physiological arousal/ stress levels has been reported in prior literature (Kindt, Soeter, & Vervliet, 2009). Finally, there is a wealth of evidence that atomoxetine has dose-dependent effects on LC firing rate and synaptic NE levels (Bari & Aston-Jones, 2013), and we previously reported data obtained in the same study and participants, showing that our manipulation increased salivary cortisol and α-amylase (Warren, van den Brink, et al., 2017). Taken together, there is little doubt that at least two of our manipulations were successful at manipulating noradrenergic activity.

What do our null findings mean? The two tasks our participants had to perform involved the same inputs (digits 1-4, 6-9) and outputs (keys Q and P) but differed in the mappings from input to output. The difficulty of combining these tasks lies in the brain's propensity to use the same representations for different purposes. That is, although in general this "multiplexing" offers an efficient way of encoding information, mutual interference, or cross-talk, arises when two tasks make simultaneous demands on the same representations (Feng, Schwemmer, Gershman, & Cohen, 2014). In principle, task switching is different from multitasking, in that the two sets of stimulus-response rules need not be active at the same time. However, it takes long for an irrelevant task-set representation to dissipate. In a typical, fast-paced task-switching experiment, this task-set inertia causes interference between the relevant and irrelevant task sets (Monsell et al., 2003; Yeung et al., 2006), which is reflected in the switch cost (i.e., a main effect of trial type). In such circumstances cognitive control can be used to reduce cross-talk in the service of overall task performance (Feng et al., 2014). In a task-switching experiment, participants can -to some extent- actively prepare for the upcoming switch trial by proactively reconfiguring the task set. This process is reflected in the preparation effect—the reduction of switch costs with growing CSI (i.e., an interaction between CSI and trial type). Importantly, the present findings suggest that our manipulations affected neither task-set inertia nor proactive task-set reconfiguration.

We studied higher-order cognitive flexibility using a task switching paradigm (Monsell et al., 2003) in which the task to be performed on each trial was indicated by a cue presented at the start of the trial. This paradigm distinguishes between trials on which the task changes (" switch trials") and trials on which the task stays the same ("repeat trials"). The finding of interest is that reaction time is longer, and error rate greater, on switch trials (the "switch cost"); and as the cue–stimulus interval is prolonged—allowing more opportunity for advance preparation—the switch cost is reduced (the "preparation

effect"). Switch costs are attributable to a combination of the time required for resolving interference from residual activation of the previous, no-longer relevant task set ("task-set inertia") and of the time required for retrieving the newly cued task set ("task-set reconfiguration"; Monsell et al., 2003). The cognitive flexibility required to switch between tasks depends on the dynamic transformation of neural task-set representations from trial to trial (Qiao et al., 2017; Yeung et al., 2006). In order to ensure that the observed switch costs and preparation effect would accurately reflect this type of cognitive flexibility instead of a cue-repetition effect, we used two cues per task, which allowed us to avoid direct cue repetitions between trials (Logan & Bundesen, 2003; Monsell & Mizon, 2006).

We are aware of two published studies on the effect of acute stress on task switching, which produced mixed results. Steinhauser and colleagues found that stress modulated the preparation effect (for response times, not error rates), but not the switch costs itself (Steinhauser, Maier, & Hübner, 2007). Their control group showed the typical reduction in switch costs at a long CSI, their stress group did not, which led the authors to conclude that stress induces a change in task-set reconfiguration strategy. Plessow and colleagues, using the same tasks as our study, found no effect of stress on the preparation effect and no effect on the RT switch cost; stress only led to a significant but small increase in the accuracy switch cost (stress group: 2.9%, control group: 1.4%; Plessow, Kiesel, & Kirschbaum, 2012). Both studies used a stress-induction procedure that involved a psychological component (social evaluation and increased cognitive load), but not a physiological component such as our cold pressor test. Plessow and colleagues confirmed the success of their stress manipulation by examining salivary cortisol levels; Steinhauser and colleagues report no cortisol data. Neither study controlled for cue-repetition effects and hence examined a confounded measure of task switching ability. More research is needed to fully understand the effect of acute stress on task switching.

We found no effects of tVNS (versus sham) and tVNS intensity on measures of task switching. A previous study found that invasive VNS (versus sham) impaired cognitive flexibility of epilepsy patients on an anagram task (Ghacibeh et al., 2006), so more research is needed in this area. In a post hoc exploratory analysis we found that tVNS at a higher intensity was associated with a speed-accuracy tradeoff: Stimulation at 1.0 mA resulted in faster (Δ 35 ms) but less accurate responses (Δ 1.0%). This finding seems at odds with findings that invasive VNS *decreases* excitability of the motor cortex in active rats (Mollet et al., 2013), even at mild stimulation intensities, which would predict slower and more accurate responses. One study examined effects of tVNS on excitability of the motor cortex in healthy human volunteers (Capone et al., 2015). However, this study was underpowered (N=10), used an unusually high stimulation intensity (8.0 mA), and did not find significant effects after correction for multiple statistical comparisons. Thus, our finding that 1.0 mA changes the speed-accuracy tradeoff requires replication, preferably augmented with measurements of motor cortex excitability.

Finally, although we used a drug (atomoxetine) and dose (40 mg) known to influence various aspects of cognitive task performance and cortical state (Jepma et al., 2016;

Pfeffer et al., 2018; van den Brink, Nieuwenhuis, & Donner, 2018; Warren, van den Brink, et al., 2017), even our pharmacological manipulation failed to modulate task switching performance. Two other pharmacological studies have yielded consistent results. One study found no effect of the beta-adrenergic antagonist propranolol (80 mg) on switch costs (Steenbergen, Sellaro, de Rover, et al., 2015). However, there is some evidence that higher-order cognitive flexibility is mediated by alpha receptors, not beta receptors (Lapiz & Morilak, 2006). Another study found no effect on switch costs of the dopamine and norepinephrine transporter blocker methylphenidate (20 mg (Frobose et al., 2017). Neither study was designed to examine the preparation effect.

While the cortical areas involved in task switching are rather well-known (Worringer et al., 2019), very little is known about the neurochemical basis supporting efficient task switching. In a much-cited review, Kehagia and colleagues (Kehagia et al., 2010) hypothesized that task switching may have a noradrenergic substrate, similar to extra-dimensional set-shifting, another example of higher-order cognitive flexibility. However, the present findings suggest that norepinephrine does not play an important role in task switching. This has applications for everyday life activities given that cognitive flexibility allows us to quickly adapt ongoing behavior to salient changes in the environment and is important for human success (e.g. at work) and survival (e.g. threatening conditions). It also has clinical applications related to disorders such as ADHD, anxiety disorders, epilepsy and Parkinson's disease where pharmacological administration of noradrenaline is the most common treatment or excessive flexibility/rigidity is one of the main symptom.

# Chapter 7

## Lay summary in English:

## A scientific journey in simple words

**This PhD dissertation: an explorer's journey**

In the 21st century humans have created very detailed maps of planet Earth, have mapped other planets, and are even in search of extraterrestrial life. However, surprisingly enough, they have not yet succeeded at mapping the structures that are inside their own brain, or understanding their behavior and cognition. Surprising that we don't know what is in our brain, isn't it? This PhD dissertation is a journey in understanding parts of our brain, cognition, physiological functions and behavior and it does so by investigating the locus coeruleus-norepinephrine (LC-NE) system in humans *in vivo* (in living humans, not brains of dead donors as it has been usually done until now).

To make the content of this PhD dissertation more clear for the layman reader, the research of this thesis is likened to the journey of 13$^{th}$ and 15$^{th}$ century explorers. Explorers like Marco Polo and Christopher Columbus tried to map and understand planet "Earth", while we try to map and understand planet "Brain and Cognition" by concentrating on the LC-NE system.

**What is the locus coeruleus-noradrenergic system?**

The locus coeruleus, a small brainstem nucleus, is the main source of the chemical norepineprine in the brain and is involved in a number of cognitive functions as well as several neurological and psychiatric disorders. In this dissertation we study the human LC-NE system, the anatomy of this tiny brainstem nucleus and the involvement of the LC-NE system in stress, arousal, cognitive flexibility and physiology (hormones & pupil responses).

**The LC-NE system in the brain & the periphery: Functions**

The LC-NE system exerts its action in the brain and body via neuronal (electrical) but also neurochemical and hormonal pathways. It influences the brain via the connections it has with multiple brain regions, and it influences the periphery via the connections it has with other brainstem nuclei, the spinal cord, and the vagus nerve; but also due to the involvement of the LC-NE system in two systems that are well studied in the stress literature: the fast and rapidly activated peripheral autonomic nervous system and the slower activated hypothalamic- pituitary- adrenergic axis (HPA-axis).

The LC-NE system is put into action to face environmental challenges, in parallel with the recruitment of the autonomic nervous system, which responds to homeostatic challenges, stressors, and other stimuli that are important for the organism, and in turn determines general arousal level. The autonomic activation promotes the physiological response, whereas the LC promotes an efficient and appropriate cognitive response through its action in the forebrain. In this way, the LC-NE system plays an important role in cognition and in the orienting reflex, which includes physiological responses such as changes in pupil dilation and heart rate, activated by arousing or motivationally significant stimuli or unexpected changes in the environment (Sara & Bouret 2012; Nieuwenhuis et al., 2011; Pfaff et al., 2012). Thus, the LC mobilizes the brain for action

while the (sympathetic) autonomic nervous system mobilizes the body; therefore, the LC-NE system as a whole is involved in mobilization of both the brain and the periphery.

A significant number of studies have aimed to illuminate these functions of the LC-NE system, but due to technical and anatomical challenges, a large part of this research has been limited to animal subjects or computational models. Research conducted in the context of this PhD dissertation aimed to bridge the gap between animal studies and theoretical work by acquiring data in living human subjects.

**This PhD dissertation: Holistic approach**

When studying planet "Earth", explorers of the 15$^{th}$ century were interested in learning about geography and mapping methods in order to reach new lands (e.g., new paths to the Indies), the treasures that they expected to find there, the flora, and the civilizations. One can imagine that depending on their knowledge, different members of the crew would concentrate on different tasks in order to realize the exploration. One member would concentrate on creating a map, another on navigating the boat, another on examining the trade winds, another on exploring the expected treasures. However, after this segregation of tasks, they needed to come together and bridge their knowledge in order to make the trip possible and to survive in the new land. Thus, for making the exploration a success, it was important to always return to the holistic level and have a good overview of the broad picture.

In a similar way, when studying the planet "Brain and Cognition", researchers tend to segregate the different parts in order to be able to deeply study the system of interest, but it is important to always return to the holistic level in the end. The beauty of human cognition is that it is based on different levels of brain and body functions that act together in harmony: from cell, to synapse, from neuron to neuromodulatory networks, from central neuromodulators to hormones that are secreted in the body, from anatomy to physiology and cognition. Therefore, this dissertation approaches human cognition and the study of the LC-NE system in a holistic manner.

To this end, all chapters were written by taking into consideration theoretical knowledge about the LC-NE system with regard to brain anatomy, cognitive functions, neuromodulation (mainly NE), physiological responses, and clinical applications. **Chapters 2 and 3** deal mainly with the anatomy of the LC, while **Chapters 4, 5 and 6** concentrate on cognition and human physiology. Additionally, **Chapters 5 and 6** take a clinical approach and collectively deal with clinical applications of tVNS (medical device), the hormones alpha-amylase and cortisol, bodily physiological responses, stress, and pharmacology.

Below there is a brief description of the chapters and studies performed for this PhD dissertation, where a holistic approach in cognitive and clinical neuroscience is applied.

**Anatomical Chapters (Chapters 2 & 3)- Creating and assessing robustness of a brain atlas**

**Chapter 2 and 3** of this PhD dissertation describe anatomical studies that provided methodological developments in the visualization of the LC in living humans.

***What prevents us from looking inside our brainstem?***

The challenges are of two kinds: technical and anatomical. Regarding the technical challenges, there is a need for specific technological advancements, and these have only recently taken place. This means that no matter how hard the researcher-explorers of the past tried to map these structures in living humans, such an enterprise was simply impossible because the timing was not right: one is dependent on technological advances that take quite some time to become feasible and be implemented in brain research. Regarding the anatomical challenges, some structures are difficult to map because they are small, their location and size varies a lot among different individuals, and also in some cases are located in parts of the brain that cannot be easily visualized in living humans within the MRI scanner due to motion artifacts (e.g., they are located in brain tissue close to the vessels or the fourth ventricle and pulsate when blood or cerebrospinal fluid is rushing). The individual differences in the location and size of these structures signify that in different people these brain structures can be a bit higher or lower, and the size and shape can also differ. Under these circumstances, the explorer-researcher, like a modern Christopher Columbus, starts a journey to explore West Indies (i.e., the LC in her case) but runs the risk of accidentally ending up in America (i.e., another, nearby brain nucleus).

***What might be the solution?***

***Solution Nr 1: assess if your map is trustworthy and create a better map***

To avoid mixing the Indies with America in the brain, you need to know if your map is trustworthy. For this, you need to practically assess if the map that was created does indeed lead to Indies and not somewhere else. This can be done by letting different explorers use the same map: will all of them end up in the same region with 100% accuracy? It can also be done by using the same map at different time points: will one explorer end up in the same region with 100% accuracy if she makes the voyage several times? This is exactly what we did in **Chapter 2** but we did so for the brain**.**

Additionally, to avoid mixing the Indies with America in the brain, one could create a better map, this can be a probabilistic map. This is exactly what we did in **Chapter 2.** Contrary to the common practice where human brain maps are created only from donors after their death, our probabilistic brain map is based on MRI images of living humans (called "*in vivo*" in scientific jargon).

Our probabilistic map is also more accurate compared to simple brain maps because it aligns all the different images of the LC, one on top of the other, and quantifies the similarities and the differences. In this way the final output is a map that shows a representative image of the core of the LC but also some extra borders around it in order

to quantify the certainty of the structure localization (e.g., how certain are you that you are in the LC?).

To compare this with an explorer's trip, our probabilistic map is also more accurate compared to simple maps because it aligns and takes into consideration not only one single map, but all the different maps depicting Indies (e.g., the one created by cartographer Toscanelli, another one by Henricus Martellus etc). In this way, the final output is a map that shows a more representative, accurate image of the Indies: it provides the core of the land but also some extra borders around it in order to quantify the certainty of the structure localization—that is, how certain are you that you are indeed in the Indies?

Finally, we measured the reliability of imaging the LC in humans: is the trip to Indies and the related activities reliable? Does it even make sense to try to make a map and embark to this trip? We also made the LC brain atlas publicly available, so it can be used for free (http://www.nitrc.org/projects/prob_lc_3t). Give it a try!

***Solution Nr 2: compare the available maps and start using higher-resolution camera***

A second solution would be to compare the available maps and start using technological improvements such as a higher-resolution camera (7 Tesla MRI scanner). This is what we did in **Chapter 3**. We used special MRI sequences that prior literature indicated as promising for imaging structures like the LC. We assessed the effectiveness of these MRI sequences in visualizing the LC by comparing them with each other and by comparing them with scans made with a "low-resolution camera" (3 Tesla MRI scanner).

In sum, in **Chapter 2** we assessed if the map is trustworthy and created a better map to increase the chances that travelers end up in the Indies (LC) and not in America (another brainstem nucleus). In **Chapter 3** we compared the available maps (special scans for LC visualization) and started using a higher-resolution camera (7T MRI scanner), which should in theory improve the visualization of the desired structure.

**Explore an alternative route to reach the Indies**

***Psychophysiological chapter (Chapter 5) - Exploring an alternative, less invasive, inexpensive route to reach the desired destination (LC-NE system)***

Apart from designing a map, assessing the map's robustness, and using state-of-the-art technology to further improve a map, a good explorer is also interested in finding alternative, cheaper, easier, less dangerous, and more accessible routes to reach their destination. Indeed, based on the theories of Greek scholars like Pythagoras, Aristotle and Ptolemy that the planet is actually a sphere, Christopher Columbus trusted astronomer Toscanelli's map and theory that sailing west across the Atlantic would be a quicker way to reach the Indies (Spice Islands). Columbus hypothesized that by traveling west, he'd open up new trade routes and he would be able to reach the Indies via an alternative route. He started his journey to test this hypothesis. We did the same in **Chapter 5**. Given the anatomical connections between the LC-NE system and the vagus nerve (the longest

nerve of the human body, connecting the brain with the gut), and findings that transcutaneous vagus nerve stimulation can be a new, non-invasive, cheaper, and easier to use method to stimulate the vagus nerve, we hypothesized that we could use this method to modulate the LC-NE system. So we started a journey to test this hypothesis.

**You have reached your destination. What treasures can this land offer?**

***LC-NE system, cognition, physiology, & hormones (Chapter 4 and 6) - What kind of cognitive functions is the LC-NE system involved in?***

Suppose you assessed the risks and reliability of the trip, you created the map and you tried to improve it **(Chapter 2 & 3),** you found some signs to support an alternative, not dangerous route to your destination (**Chapter 5)** and now you are ready to reach this destination. What do you expect to find there? Based on prior knowledge, Columbus was expecting his destination (Indies) to be a land of spices. In the same way, we expected the LC-NE system to be involved in specific cognitive phenomena: a) the accessory stimulus effect (improved performance caused by a loud noise irrelevant to the task at hand), and b) switching between tasks (cognitive flexibility). In Columbus' case, those who reached India, confirmed that India has spices. However, Columbus reached America, a land full of gold and cotton instead of spices. Similarly, we found evidence that the LC-NE is involved in the accessory stimulus affect (spices, bingo!), but is not involved in task switching (cotton, oops!).

**Results of this PhD project - What did we find?**

***Chapter 2: Is your map trustworthy and can you create a better map?***

***Title of the chapter in scientific jargon*:** *In vivo* visualization of the locus coeruleus in humans: Quantifying the test-retest reliability

We found moderate reproducibility and scan-rescan stability, indicating that the localization and segmentation of the LC in vivo is a challenging, but reliable enterprise. However, clinical or longitudinal studies should be carried out carefully. Thus the voyage to the Indies is an enterprise worth trying, but you should be careful and be prepared for the dangers you will face during the trip.

Our probabilistic atlas results show substantial variability in the spatial location of the LC and this map is freely available (http://www.nitrc.org/projects/prob_lc_3t). This atlas is the first probabilistic atlas for the LC and one of the few attempts to map the brainstem, a field that deserves more attention and promises to turn the brainstem from a "tera incognita" into a fully mapped and understood region in the future (Forstmann et al., 2017). We provide the first probabilistic map. Enjoy the voyage!

***Chapter 3: How do the available maps perform and does it make sense to use higher-resolution camera?***

***Title of the chapter in scientific jargon:*** Quantifying the contrast of the human locus coeruleus *in vivo* at 7 Tesla MRI

In Chapter 3, we made a first step towards the improvement of visualization of LC in an ultra-high-field (7 Tesla) MRI scanner. We are the first ones to compare these scan sequences at 7T and develop a version of the TSE scan sequence for use at 7T. Future work can utilize this work and proceed to further development and improvement of MRI scans in order to achieve better visualization of the LC at 3T, 7T and maybe higher magnetic field scanners.

It should be noted that choosing the correct lenses and resolution is important in enterprise of atlas creation. If you use lenses strong enough to visualize planets, these will not work when you want to visualize the Indies, which is just part of Earth. Some locations are sufficiently visualized with a low- to medium-resolution camera. The LC is visualized decently at low resolution (3T); however, better visualization is needed and high-resolution camera can be promising in improving visualization of the LC. Still some work is needed to achieve perfect visualization. Future work can build on the work done in this chapter.

***Chapter 5: Exploring an alternative, less invasive, inexpensive route to reach the desired destination (LC-NE system)***

***Title of the chapter in scientific jargon:*** The neuromodulatory and hormonal effects of transcutaneous vagus nerve stimulation as evidenced by salivary alpha-amylase, salivary cortisol, pupil diameter, and the P3 event-related potential

In Chapter 5, we evaluate the effect of tVNS on NE levels using three accepted biomarkers and one putative biomarker of central NE activity: the hormone alpha-amylase, the hormone cortisol, pupil size, and the P3 component of the event-related brain potential (these are brainwaves that are assessed using electroencephalography), respectively. Results show that tVNS significantly increased salivary alpha-amylase and salivary cortisol, but did not affect P3 amplitude or pupil size. These findings suggest that salivary alpha-amylase and cortisol, but not pupil size and P3 amplitude, can be used to monitor the arousal-related effects of tVNS.

***Chapter 4: You have reached your destination. Bingo! Your destination is a land full of spices***

***Title of the chapter in scientific jargon:*** The accessory stimulus effect is mediated by phasic arousal: a pupillometry study

As highlighted in Chapter 1, the LC-NE system plays an important role in regulating arousal. A phenomenon that has been linked with arousal and enhanced cognitive performance is the accessory stimulus effect (AS effect). The AS effect refers to the phenomenon where people show improved performance when -while they are performing a visual task- they hear an irregular, loud noise from time to time. Importantly, this noise leads to better performance compared to when doing the task alone, despite the fact that it does not provide any information about the task at hand.

Despite the common inference that the AS effect is mediated by a phasic arousal response, there is only some indirect evidence to support this idea. In this chapter we provide the first evidence for this long-standing assumption and we demonstrate that the LC-NE system is involved in the accessory stimulus effect.

***Chapter 6: You have reached your destination. Oups! Your destination is not a land of spices- how about some cotton?***

***Title of the chapter in scientific jargon:*** Noradrenergic regulation of cognitive flexibility: No effects of stress, transcutaneous vagus nerve stimulation and atomoxetine on task-switching in humans

Cognitive flexibility allows us to adaptively switch between different responsibilities in important domains of our daily life and is a multifaceted construct containing learning, updating, cognitive control, decision making and switching between tasks. Previous work has suggested an important role for the LC-NE system in modulating several forms of cognitive flexibility, possibly by modulation of gain and corresponding levels of decision noise. However, it is still unknown whether NE levels are also critical for the task switching, an aspect of cognitive flexibility which requires the dynamic transformation of task-set representations from trial to trial.

In Chapter 6, we addressed this question by examining cued task-switching performance after manipulating activity of the LC-NE system using stress induction, tVNS at moderate and high intensity, and pharmacological administration of the selective NE blocker atomoxetine. None of the manipulations affected task switching. Our findings suggest that NE does not affect this aspect of cognitive flexibility.

**Did they live happily ever after and what comes next?**

I don't know if they lived happily ever after, but I do know what should come next: The exploration of the brain should continue. And of course this journey will have higher impact and will be much more fun if cognitive neuroscientists (explorers) join powers. In the end, a "modern Christopher Columbus" researcher will always benefit from a colleague who – like a "modern Amerigo Vespucci" – would demonstrate that she was wrong to believe that she reached the Indies; she had actually reached an unexplored, wholly new continent previously unknown to Eurasians, a "New World" that would be called "America". Importantly, modern explorers know that those who do not read history are doomed to repeat it, and can take lessons from 15th century's explorers in order to avoid mistakes of the past. Therefore, they ought to treat their discoveries in an ethical and respectful manner, promote "fair trade" and open science, embrace a collaborative atmosphere instead of a "rich-get-richer" competitive approach. They should also provide the relevant credits to the relevant people, always remain open to critique and alternative perspectives and, above all, have as their main goal the contribution to knowledge and to a better society instead of self-interest and an accumulation of publications. Amen!

# Chapter 8

## Short lay summary translated in

## Greek, Albanian and Dutch

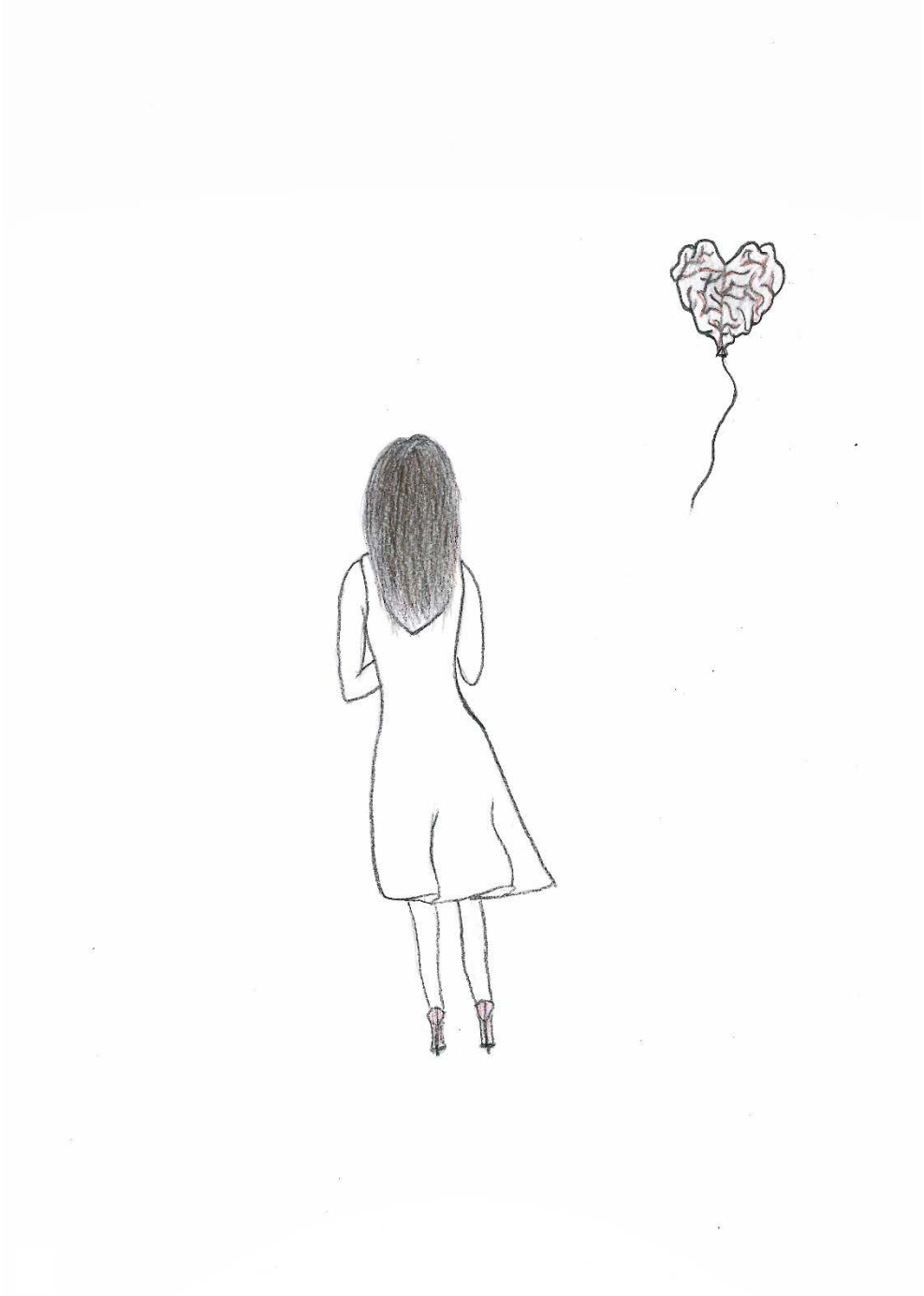

## ΣΥΝΟΠΤΙΚΗ ΠΕΡΙΛΗΨΗ ΣΤΑ ΕΛΛΗΝΙΚΑ – ΑΥΤΟ ΤΟ ΕΠΙΣΤΗΜΟΝΙΚΟ ΤΑΞΙΔΙ ΜΕ ΑΠΛΑ ΛΟΓΙΑ

### Αυτή η διδακτορική διατριβή: σαν το ταξίδι ενός θαλασσοπόρου - εξερευνητή

Τον 21ο αιώνα οι άνθρωποι έχουν δημιουργήσει λεπτομερείς χάρτες του πλανήτη Γη, έχουν χαρτογραφήσει και άλλους πλανήτες και μάλιστα αναζητούν με επιστημονικές μεθόδους ακόμη και την ύπαρξη εξωγήινης ζωής. Ωστόσο, παραδόξως, οι άνθρωποι δεν έχουν καταφέρει ακόμη να χαρτογραφήσουν πλήρως τις περιοχές του εγκεφάλου τους ή να κατανοήσουν την συμπεριφορά τους. Δεν είναι περίεργο που ακόμη δεν έχουμε καταφέρει να μάθουμε τί βρίσκεται μέσα στον ίδιο μας τον εγκέφαλο; Η διδακτορική διατριβή που διαβάζετε αυτή τη στιγμή είναι ένα ταξίδι που επιδιώκει την χαρτογράφηση τμημάτων του ανθρώπινου εγκεφάλου, και την κατανόηση των γνωσιακών λειτουργιών, της φυσιολογίας και της συμπεριφοράς του ανθρώπου. Επικεντρώνεται στην διερεύνηση του συστήματος Υπόμελα Τόπου- Νορεπινεφρίνης (ΥΤ-ΝΕ, στα αγγλικά: locus coeruleus - norepinephrine, LC-NE) σε *"εν ζωή"* (*in vivo)* υποκείμενα, δηλαδή σε ζωντανούς ανθρώπους, όχι στον εγκέφαλο των νεκρών δοτών όπως συνηθίζονταν μέχρι σήμερα ("*μετά θάνατον*" μεθοδολογία).

Για να καταστεί το περιεχόμενο αυτής της διδακτορικής διατριβής πιο σαφές για το μη επιστημονικό κοινό, η έρευνα αυτής της διατριβής παρομοιάζεται με το ταξίδι των εξερευνητών του 13ου και του 15ου αιώνα. Εξερευνητές όπως ο Μάρκο Πόλο και ο Χριστόφορος Κολόμβος προσπάθησαν να χαρτογραφήσουν και να κατανοήσουν τον πλανήτη "Γη", ενώ εμείς προσπαθούμε να χαρτογραφήσουμε και να κατανοήσουμε τον πλανήτη "Εγκέφαλο και Νού» επικεντρώνοντας το ενδιαφέρον μας στο σύστημα υπόμελα τόπου- νορεπινεφρίνης (ΥΤ-ΝΕ, στα αγγλικά: LC-NE).

### Τι είναι το σύστημα Υπόμελα τόπου- Νορεπινεφρίνης;

Ο υπόμελας τοπος, ένας μικρός πυρήνας του εγκεφάλου, είναι η κύρια πηγή της ουσίας νορεπινεφρίνης στον εγκέφαλο και εμπλέκεται σε διάφορες γνωστικές λειτουργίες καθώς και σε αρκετές νευρολογικές και ψυχιατρικές διαταραχές (διαταραχή έλλειψης προσοχής, νόσος Αλτζχάιμερ, διαταραχές του στρες, κατάθλιψη κ.λ.π.). Η νορεπινεφρίνη λειτουργεί ως νευροδιαβιβαστής στον εγκέφαλο και το κεντρικό νευρικό σύστημα και ως ορμόνη σε άλλα μέρη του σώματος. Σε αυτήν την διδακτορική διατριβή μελετάμε το ανθρώπινο σύστημα ΥΠ-ΝΕ, την ανατομία αυτού του μικροσκοπικού πυρήνα του εγκεφάλου, και τη συμμετοχή του συστήματος ΥΤ-ΝΕ στο άγχος, τη διέγερση, τη γνωστική ευελιξία και τη φυσιολογία (ορμόνες και αντανακλαστικά της κόρης του ματιού).

### Το σύστημα ΥΤ-ΝΕ στον εγκέφαλο και την περιφέρεια: λειτουργίες

Το σύστημα ΥΤ-ΝΕ ασκεί τη δράση του στον εγκέφαλο και το σώμα μέσω της χρήσης νευρωνικών (ηλεκτρικών) αλλά και νευροχημικών και ορμονικών οδών. Επηρεάζει τον εγκέφαλο μέσω των συνδέσεων που έχει με περιοχές του εγκεφάλου και επηρεάζει το υπόλοιπο σώμα χάρη στις συνδέσεις που έχει με άλλους πυρήνες του εγκεφάλου, του νωτιαίου μυελού, του πνευμονογαστρικού νεύρου, και λόγω της συμμετοχής του

συστήματος ΥΤ-ΝΕ σε δύο συστήματα που έχουν μελετηθεί καλά στη βιβλιογραφία του άγχους : το γρήγορο και ταχέως ενεργοποιούμενο αυτόνομο νευρικό σύστημα και ο βραδύτερος ενεργοποιούμενος άξονας υποθαλάμου-υπόφυσης- επινεφριδίων (ΥΥΕ, στα αγγλικά: HPA- axis).

Σε καταστάσεις όπου απαιτείται υψηλή εγρήγορση, όπως σε καταστάσεις κινδύνου ή άγχους, το σύστημα ΥΤ-ΝΕ τίθεται σε δράση παράλληλα με το αυτόνομο νευρικό σύστημα για να αντιμετωπίσει περιβαλλοντικές προκλήσεις (π.χ. μία τίγρη ή έναν απαιτητικό εργοδότη). Έτσι, το σύστημα ΥΤ - ΝΕ , σε συνέργεια με το (συμπαθητικό) αυτόνομο νευρικό σύστημα, κινητοποιεί τον εγκέφαλο και το υπόλοιπο σώμα για δράση.

Ένας σημαντικός αριθμός μελετών στοχεύει στην κατανόηση των λειτουργιών του συστήματος ΥΤ-ΝΕ, αλλά λόγω τεχνικών και ανατομικών προκλήσεων, μεγάλο μέρος αυτής της έρευνας περιορίστηκε σε πειραματόζωα, θεωρητικά μοντέλα, ή υπολογιστική μοντελοποίηση. Η έρευνα που πραγματοποιήθηκε στο πλαίσιο αυτής της διδακτορικής διατριβής είχε ως στόχο να γεφυρώσει το χάσμα μεταξύ των μελετών σε πειραματόζωα (μελέτη σε βασικό επίπεδο) και των θεωρητικών μοντέλων (μελέτη σε θεωριτικό επίπεδο), αποκτώντας δεδομένα σε ζωντανούς, *"εν ζωή"* ανθρώπους (μελέτη σε ενδιάμεσο επίπεδο) και με πολύπλευρο, ολιστικό τρόπο.

**Αυτή η διδακτορική διατριβή: Ολιστική προσέγγιση**

Όταν μελετούσαν τον πλανήτη "Γη", οι εξερευνητές του 15ου αιώνα ενδιαφέρθηκαν να μάθουν για τη γεωγραφία και τις μεθόδους χαρτογράφησης για να φτάσουν σε νέα εδάφη (π.χ., νέα μονοπάτια προς τις Ινδίες), τους θησαυρούς που περίμεναν να βρουν εκεί, τη χλωρίδα και τους πολιτισμούς. Ανάλογα με τις γνώσεις του καθενός, διαφορετικά μέλη του πληρώματος επικεντρώνονταν σε διαφορετικά καθήκοντα προκειμένου να πραγματοποιήσουν την εξερεύνηση (δημιουργία χάρτη, μελέτη του καιρού, εξασφάλιση ασφάλειας κ.λ.π.). Ωστόσο, μετά από αυτόν τον διαχωρισμό των καθηκόντων, έπρεπε να συνεργαστούν και να ενώσουν τις γνώσεις τους μέσω μιας ολιστικής προσέγγισης έτσι ώστε να πραγματοποιήσουν το ταξίδι και να επιβιώσουν στη νέα γη.

Με παρόμοιο τρόπο, όταν μελετούν τον πλανήτη "Γή και Νού", οι επιστήμονες - εξερευνητές τείνουν να διαχωρίζουν τα διάφορα μέρη του συστήματος προκειμένου να μελετήσουν καλά το σύστημα ενδιαφέροντος. Όμως είναι σημαντικό στο τέλος να επιστρέφουμε πάντα στο ολιστικό επίπεδο. Η ομορφιά της ανθρώπινης γνώσης είναι ότι βασίζεται σε διαφορετικά επίπεδα λειτουργιών του εγκεφάλου και του σώματος τα οποία δρουν μαζί σε αρμονία: από το κύτταρο, στη σύναψη, από τον νευρώνα στα νευρωνικά δίκτυα, από τους νευροδιαβιβαστές του εγκεφάλου έως τις ορμόνες που εκκρίνονται στο σώμα, από την ανατομία στη φυσιολογία και τις γνωσιακές λειτουργίες. Επομένως, αυτή η διατριβή προσεγγίζει την ανθρώπινη νόηση και τη μελέτη του συστήματος ΥΤ- ΝΕ με ολιστικό τρόπο.

Για το σκοπό αυτό, όλα τα κεφάλαια γράφτηκαν λαμβάνοντας υπόψη τα πολλαπλά επίπεδα της ανθρώπινης νόησης και μελέτες του συστήματος ΥΤ-ΝΕ σχετικά με την ανατομία του εγκεφάλου, τις γνωσιακές λειτουργίες, τους νευροδιαβιβαστές (κυρίως

ΝΕ), τις αντιδράσεις του σώματος/φυσιολογίας, και τις κλινικές εφαρμογές. **Τα κεφάλαια 2 και 3** ασχολούνται κυρίως με την ανατομία του ΥΤ, ενώ **τα κεφάλαια 4, 5 και 6** επικεντρώνονται στη γνώση και την ανθρώπινη φυσιολογία. Επιπλέον, τα **Κεφάλαια 5 και 6** ακολουθούν μια κλινική προσέγγιση και ασχολούνται συλλογικά με κλινικές εφαρμογές της μεθοδολογίας της επιδερμικής διέγερσης πνευμονογαστρικού νεύρου (transcutaneous vagus nerve stimulation, tVNS), των ορμονών άλφα-αμυλάσης και κορτιζόλης, των αντιδράσεων του σώματος/φυσιολογίας , του άγχους και της φαρμακολογίας.

Παρακάτω υπάρχει μια σύντομη περιγραφή των κεφαλαίων και των μελετών που πραγματοποιήθηκαν στα πλαίσια αυτής της διδακτορικής διατριβής, όπου εφαρμόζεται μια ολιστική προσέγγιση στη γνωσιακή και κλινική νευροεπιστήμη.

**Ανατομικά Κεφάλαια (Κεφάλαια 2 & 3) - Δημιουργία και αξιολόγηση της αξιοπιστίας ενός εγκεφαλικού άτλαντα**

**Τα κεφάλαια 2 και 3** αυτής της διδακτορικής διατριβής περιγράφουν ανατομικές μελέτες και ν μεθοδολογικές εξελίξεις σχετικά με την οπτικοποίηση της ΥΤ σε ζωντανούς ανθρώπους.

***Τι μας εμποδίζει να κοιτάξουμε μέσα στον εγκέφαλό μας;***

Οι προκλήσεις είναι δύο ειδών: τεχνικές και ανατομικές. Όσον αφορά τις τεχνικές προκλήσεις, ` χρειαζόμαστε συγκεκριμένες τεχνολογικές εξελίξεις, και αυτές έχουν πραγματοποιηθεί πρόσφατα. Όσον αφορά τις ανατομικές προκλήσεις, ορισμένες δομές είναι δύσκολο να χαρτογραφηθούν επειδή είναι μικρές, η θέση και το μέγεθός τους ποικίλλει πολύ μεταξύ διαφορετικών ατόμων, και επίσης σε ορισμένες περιπτώσεις βρίσκονται σε μέρη του εγκεφάλου που δεν μπορούν εύκολα να απεικονιστούν σε ζωντανούς ανθρώπους μέσω της μαγνητικής τομογραφίας (βρίσκονται σε μέρη του εγκεφάλου που πάλλονται λόγω της ροής του εγκεφαλονωτιαίου υγρού). Οι ατομικές διαφορές στη θέση και το μέγεθος αυτών των δομών υποδηλώνουν ότι σε διαφορετικούς ανθρώπους αυτές οι εγκεφαλικές δομές μπορεί να είναι βρίσκονται λίγο πιο ψηλά ή πιο χαμηλά, και το μέγεθος και το σχήμα μπορεί επίσης να διαφέρουν. Υπό αυτές τις συνθήκες, ο επιστήμονας – εξερευνητής, σαν σύγχρονος Χριστόφορος Κολόμβος, ξεκινά ένα ταξίδι για να εξερευνήσει τις Ινδίες (δηλαδή το ΥΤ στην περίπτωσή μας), αλλά διατρέχει τον κίνδυνο να φτάσει κατά λάθος στην Αμερική (δηλαδή μια άλλη, κοντινή περιοχή του εγκεφάλου στην περίπτωση μας) .

***Ποια θα μπορούσε να είναι η λύση;***

***Λύση Nr 1: αξιολόγησε εάν ο χάρτης σου είναι αξιόπιστος και δημιούργησε έναν καλύτερο χάρτη***

Για να αποφύγετε το μπέρδεμα των Ινδιών με την Αμερική στον εγκέφαλο, πρέπει να γνωρίζετε εάν ο χάρτης σας είναι αξιόπιστος. Αυτό ακριβώς κάναμε στο Κεφάλαιο 2, αλλά το κάναμε για τον εγκέφαλο. Επιπλέον, κάποιος θα μπορούσε να δημιουργήσει έναν καλύτερο χάρτη, π.χ. έναν πιθανολογικό χάρτη (αγγλικά: probabilistic atlas). Αυτό

ακριβώς κάναμε στο **Κεφάλαιο 2**. Σε αντίθεση με την κοινή πρακτική όπου οι χάρτες ανθρώπινου εγκεφάλου δημιουργούνται μόνο από δότες μετά το θάνατό τους, ο πιθανολογικός χάρτης μας βασίζεται σε μαγνητικές τομογραφίες ζωντανών ανθρώπων.

Για να συγκρίνουμε τον πιθανολογικό χάρτη ΥΤ με το ταξίδι ενός θαλασσοπόρου - εξερευνητή, ο πιθανολογικός χάρτης μας είναι πιο ακριβής σε σύγκριση με τους απλούς χάρτες, επειδή ευθυγραμμίζει και λαμβάνει υπόψη όχι μόνο έναν χάρτη, αλλά και όλους τους διαφορετικούς χάρτες που απεικονίζουν τις Ινδίες (π.χ. τον χάρτη του χαρτογράφου Toscanelli, του Henricus Martellus και άλλους). Με αυτόν τον τρόπο, το τελικό αποτέλεσμα είναι ένας χάρτης που δείχνει μια πιο αντιπροσωπευτική, ακριβή εικόνα των Ινδιών: περιέχει το κέντρο της χώρας αλλά και πολλαπλές συνοριογραμμές της χώρας, προκειμένου να ποσοτικοποιηθεί η βεβαιότητα της δομής, δηλαδή, πόσο σίγουροι είστε ότι βρίσκεστε πράγματι στις Ινδίες και όχι σε γειτονική ή (ακόμη χειρότερα) μία πιο απομακρυσμένη χώρα;

Δημοσιεύσαμε τον πιθανολογικό άτλαντα ΥΤ, οπότε μπορεί να χρησιμοποιηθεί δωρεάν από όλους (http://www.nitrc.org/projects/prob_lc_3t). Δοκίμασε το!

***Λύση Nr 2: Σύγκρινε τους διαθέσιμους χάρτες και άρχισε να χρησιμοποιείς κάμερα υψηλότερης ανάλυσης***

Μια δεύτερη λύση θα μπορούσε να είναι η σύγκριση των διαθέσιμων χαρτών και χρήσης τεχνολογίας αιχμής, όπως π.χ. μια κάμερα υψηλότερης ανάλυσης (7 Tesla μαγνητικό τομογράφο, 7T- MRI). Αυτό κάναμε στο **Κεφάλαιο 3**. Χρησιμοποιήσαμε ειδικές ακολουθίες μαγνητικού τομογράφου (αγγλικά: MRI sequences) που η βιβλιογραφία έδειχνε να είναι υποσχόμενη για δομές απεικόνισης όπως τον ΥΤ. Ποσοτικοποιήσαμε την αποτελεσματικότητα αυτών των ακολουθιών στην οπτικοποίηση του ΥΤ συγκρίνοντάς τα μεταξύ τους και συγκρίνοντάς τα με ακολουθίες που έγιναν με «κάμερα χαμηλής ανάλυσης» (3 Tesla μαγνητικό τομογράφο, 3T- MRI).

Εν ολίγοις, στο **Κεφάλαιο 2** αξιολογήσαμε εάν ο χάρτης είναι αξιόπιστος και δημιουργήσαμε έναν καλύτερο χάρτη για να αυξήσουμε τις πιθανότητες να καταλήξουν οι ταξιδιώτες στις Ινδίες (ΥΤ) και όχι στην Αμερική (δηλαδή μία άλλη περιοχή του εγκεφάλου στην περίπτωσή μας). **Στο Κεφάλαιο 3** συγκρίναμε τους διαθέσιμους χάρτες (ειδικές ακολουθίες για οπτικοποίηση ΥΤ) και ξεκινήσαμε να χρησιμοποιούμε κάμερα υψηλότερης ανάλυσης (μαγνητικός τομογράφος 7Τ), η οποία θεωρητικά πρέπει να μας δείξει καλύτερη εικόνα της επιθυμητής περιοχής (ΥΤ).

**Εξερεύνησε μια εναλλακτική διαδρομή για να φτάσεις στις Ινδίες**

***Κεφάλαιο φυσιολογίας (Κεφάλαιο 5) - Εξερεύνηση μιας εναλλακτικής, λιγότερο επεμβατικής, φθηνής διαδρομής για να φτάσουμε στον επιθυμητό προορισμό (σύστημα ΥΤ-ΝΕ)***

Εκτός από τον σχεδιασμό ενός χάρτη, την αξιολόγηση της αξιοπιστίας του χάρτη και τη χρήση τεχνολογίας αιχμής για την περαιτέρω βελτίωση ενός χάρτη **(Κεφάλαιο 2 & 3),** ένας καλός θαλασσοπόρος - εξερευνητής ενδιαφέρεται επίσης να βρει εναλλακτικά,

φθηνότερα, ευκολότερα, λιγότερο επικίνδυνα, και πιο προσιτά μονοπάτια για να φτάσει στον προορισμό του. Πράγματι, ο Κολόμβος υπέθεσε ότι ταξιδεύοντας δυτικά, θα άνοιγε νέες εμπορικές διαδρομές και θα μπορούσε να φτάσει στις Ινδίες μέσω μιας εναλλακτικής διαδρομής. Ξεκίνησε, λοιπόν, το ταξίδι του για να δοκιμάσει αυτήν την υπόθεση. Κάναμε και εμείς το ίδιο στο **Κεφάλαιο 5.** Δεδομένου των ανατομικών συνδέσεων μεταξύ του συστήματος ΥΤ-ΝΕ και του πνευμονογαστρικού νεύρου (το μακρύτερο νεύρο του ανθρώπινου σώματος που συνδέει τον εγκέφαλο με τα εντόσθια), και ευρήματα ότι η νέα μεθοδολογία της επιδερμικής διέγερσης του πνευμονογαστρικού νεύρου (transcutaneous vagus nerve stimulation, tVNS) μπορεί να αποδειχθεί μία μη επεμβατική, φθηνότερη, και ευκολότερη στη χρήση μέθοδο για τη διέγερση του πνευμονογαστρικού νεύρου, υποθέσαμε ότι θα μπορούσαμε να χρησιμοποιήσουμε αυτήν τη μέθοδο για να διεγείρουμε το σύστημα ΥΤ-ΝΕ. Ξεκινήσαμε, λοιπόν, ένα ταξίδι για να δοκιμάσουμε αυτήν την υπόθεση.

**Φτάσατε στον προορισμό σας. Τί θησαυρούς προσφέρει αυτή η χώρα;**

***Σύστημα ΥΤ-ΝΕ, γνωσιακό σύστημα, φυσιολογία και ορμόνες (Κεφάλαια 4 και 6) - Σε τι είδους γνωστικές λειτουργίες εμπλέκεται το σύστημα ΥΤ-ΝΕ;***

Ας υποθέσουμε ότι αξιολογήσατε τους κινδύνους και την αξιοπιστία του ταξιδιού, δημιουργήσατε τον χάρτη και προσπαθήσατε να τον βελτιώσετε **(Κεφάλαιο 2 & 3),** βρήκατε κάποια στοιχεία που υποστηρίζουν μία πιθανή, εναλλακτική, λιγότερο επικίνδυνη διαδρομή προς τον προορισμό σας **(Κεφάλαιο 5)** και τώρα είσαστε έτοιμοι να φτάσετε σε αυτόν τον προορισμό. Τι περιμένετε να βρείτε εκεί; Με βάση τα δεδομένα που είχε από άλλους, ο Κολόμβος ανέμενε οτι ο προορισμό του (Ινδίες) θα ήταν μια χώρα γεμάτο μπαχαρικά. Κατά τον ίδιο τρόπο, περιμέναμε το σύστημα ΥΤ-ΝΕ να εμπλέκεται σε συγκεκριμένα γνωσιακά φαινόμενα: α) στην επίδραση βοηθητικού ερεθίσματος (αγγλικά: accessory stimulus effect, δηλαδή το φαινόμενο όπου ένας θόρυβος στο φόντο βελτιώνει την απόδοσή μας κατά τη εκτέλεση μιας εργασίας παρά το γεγονός ότι δεν παρέχει καμία πληροφορίες για την εργασία), και β) στην γνωστική ευελιξία (αγγλικά: cognitive flexibilty, δηλαδή η γνωστική ικανότητα διανοητικής εναλλαγής μεταξύ δύο διαφορετικών εννοιών ή εργασιών). Στο παράδειγμα της εποχής του Κολόμβου, όσοι έφτασαν στις Ινδίες, επιβεβαίωσαν ότι οι Ινδίες έχουν μπαχαρικά. Ωστόσο, ο Κολόμβος είχε φτάσει στην Αμερική, μια χώρα γεμάτη χρυσό και βαμβάκι αντί για μπαχαρικά. Ομοίως και εμείς, βρήκαμε ενδείξεις ότι το σύστημα ΥΤ-ΝΕ εμπλέκεται στην επίδραση βοηθητικού ερεθίσματος: μπαχαρικά, μπίνγκο! Αλλά δεν εμπλέκεται στην εναλλαγή εργασιών : βαμβάκι, ουπς!

**«Έζησαν αυτοί καλά και εμείς καλύτερα» και τί έπεται στη συνέχεια;**

Δεν ξέρω αν έζησαν αυτοί καλά, αλλά ξέρω τί έπεται στη συνέχεια: η εξερεύνηση του εγκεφάλου πρέπει να συνεχιστεί. Και φυσικά αυτό το ταξίδι θα έχει μεγαλύτερο αντίκτυπο και θα είναι πολύ πιο διασκεδαστικό εάν οι γνωστικοί νευροεπιστήμονες (επιστήμονες -εξερευνητές) ένωναν στις δυνάμεις τους. Στην τελική, ένας ερευνητής «σύγχρονος Χριστόφορος Κολόμβος» θα επωφελούνταν από έναν συνάδελφο ο οποίος -

όπως ένας «σύγχρονος Αμέριγκο Βεσπούτσι» - θα απεδείκνυε ότι έκανε λάθος να πιστεύει πως έφτασε στις Ινδίες. Στην πραγματικότητα είχε φτάσει σε μια ανεξερεύνητη ήπειρο που ήταν ως τότε άγνωστη στους Ευρασιάτες, έναν «Νέο Κόσμο» που θα ονομαζόταν «Αμερική». Είναι σημαντικό για τους σύγχρονους επιστήμονες- εξερευνητές να γνωρίζουν ότι όσοι δεν διαβάζουν την ιστορία είναι καταδικασμένοι να την επαναλάβουν και οτι πρέπει να παίρνουν μαθήματα από τους θαλασσοπόρους - εξερευνητές του 15ου αιώνα για να αποφύγουν λάθη του παρελθόντος. Επομένως, πρέπει να αντιμετωπίσουν τις ανακαλύψεις τους όχι με αποικιοκρατική διάθεση αλλά με ηθική και σεβασμό, με διάθεση προάσπισης ενός «δίκαιου εμπορίου» και της δωρεάν, ανοικτής πρόσβασης σε επιστημονικές δημοσιεύσεις. Να ενστερνιστούν μια ατμόσφαιρα αξιοκρατίας και συνεργασίας αντί μιας ανταγωνιστικής προσέγγισης τύπου «ο πλούσιος γίνεται πλουσιότερος και ο φτωχός φτωχότερος». Θα πρέπει επίσης να δίνουν τα απαραίτητα εύσημα στους ανθρώπους που το αξίζουν, να παραμένουν πάντα ανοιχτοί σε κριτικές και οπτικές που είναι διαφορετικές από την δική τους και - πάνω απ' όλα - να έχουν ως κύριο στόχο τους τη συμβολή στη γνώση και στην βελτίωση της κοινωνίας αντί για την προώθηση προσωπικών συμφερόντων και τη συσσώρευση δημοσιεύσεων. Αμήν!

## PERMBLEDHJE E SHKURTUAR NE SHQIP

### Kjo disertacion i doktoratës: si rrugëtimi i një eksploruesi

Në shekullin e 21 njerëzit kanë krijuar harta shumë të hollësishme të planetit Tokë, kanë hartografuar planetë të tjerë dhe madje janë në kërkim të jetës jashtëtokësore. Sidoqoftë, çuditërisht njerezit nuk kanë arritur ende të hartografojnë strukturat që janë brenda trurit të tyre, ose të kuptojnë nga burojnë sjellja dhe aftësia e të menduarit. A nuk është e çuditshme që nuk kemi arritur të kuptojmë se çfarë gjendet në trurin tonë? Ky disertacion i doktoratës është një udhëtim për të kuptuar pjesët e trurit tonë, njohjes, funksioneve fiziologjike dhe sjelljes së njeriut. Këtë e bën duke shqyrtuar sistemin locus coeruleus-norepinephrine (LC-NE, norepinefrina quhet gjithashtu noradrenalinë) te njerëzit *in vivo* (tek njerëzit e gjallë, jo trurin e dhuruesve të vdekur siç është bërë zakonisht deri më tani).

Për të bërë përmbajtjen e këtij disertacionit të doktoraturës më të qartë edhe për lexuesit që nuk kanë kualifikimet shkencore, studimi i kësaj teze krahasohet me udhëtimin e eksploruesve te shekujve te 13$^{të}$ dhe 15$^{të}$ . Eksplorues si Marko Polo dhe Kristofor Kolombi u përpoqën të hartografojnë dhe të kuptojnë planetin "Tokë", ndërsa ne përpiqemi të hartografojmë dhe kuptojmë planetin “Tru dhe Njohja” duke u përqëndruar në sistemin LC-NE.

### Cili është sistemi locus coeruleus-noradrenergjik?

Locus coeruleus, një bërthamë e vogël e trurit, është burimi kryesor i norepineprinës kimike në tru dhe është i përfshirë në një numër funksionesh konjitive, si dhe disa çrregullime neurologjike dhe psikiatrike (çrregullim i vëmendjes, sëmundja e Alzheimerit, çrregullime stresi, depresioni etj.) Në këtë disertacion ne studojmë sistemin LC-NE të njeriut, anatominë e kësaj bërthamë të vogël të sistemit të trurit dhe përfshirjen e sistemit LC-NE në stres, në stimulim, në fleksibilitetin konjitiv dhe fiziologji (hormonet dhe reflekset e bebes së syrit).

### Sistemi LC-NE në tru dhe periferi: Funksionet

Sistemi LC-NE ushtron veprimin e tij në tru dhe trup përmes rrugëve neuronale (elektrike) por edhe neurokimike dhe hormonale. Ndikon në tru përmes lidhjeve që ka me rajone të shumta të trurit, dhe ndikon në periferi përmes lidhjeve që ka me bërthama të tjera të sistemit të trurit, palcës kurrizore dhe nervit vagus; por edhe për shkak të përfshirjes së sistemit LC-NE në dy sisteme që janë studiuar mirë në literaturën e stresit: sistemi nervor autonom periferik i aktivizuar me shpejtësi, si dhe boshti me aktivizim më të ngadaltë boshti hipotalamik-hipofizë-adrenergjik (boshti hypothalamic-pituitary-adrenal, boshti HPA).

Në situata kur nevojitet gatishmëri e lartë, si në situata rreziku ose stresi, sistemi LC-NE vihet në veprim paralelisht me sistemin nervor autonom, për t'u përballur me sfidat mjedisore (per shembull nje tigër ose kërkesat e një bosi). Kështu që sistemi LC-NE – së bashku me sistemin nervor autonom (simpatik) - mobilizon trurin dhe si rrjedhojë gjithë trupin për veprim.

Një numër i konsiderueshëm studimesh kanë synuar të kuptojne funksionet e sistemit LC-NE, por për shkak të sfidave teknike dhe anatomike, një pjesë e madhe e këtij studimi ka qenë i kufizuar në kafshë laboratorike, në modele teorike, ose në llogaritje kompjuterike. Studimi i kryer në kontekstin e kesaj doktorature kishte si qëllim të zvogeloi hendekun midis punës që bëhet mbi studimin e kafshëve nga njëra anë, dhe punës teorike nga ana tjeter, duke marrë të dhëna nga njerëz të gjallë, me mënyra gjithperfshirese.

**Ky disertacion PhD: trajtim holistik**

Kur studionin planetin "Tokë", eksploruesit e shekullit te 15$^{të}$ ishin të interesuar për të mësuar në lidhje me gjeografinë dhe metoda hartografike për të arritur toka të reja (p.sh., rrugë të reja për ne Indi), thesaret që prisnin të gjeni atje, florën dhe qytetërimet. Në varësi të njohurive të secilit, anëtarët e ndryshëm të ekuipazhit do të përqendroheshin në detyra të ndryshme për të realizuar hulumtimin (krijimin e një harte, studimin e motit, sigurine nga rreziqet etj). Sidoqoftë, pas kësaj ndarjeje të detyrave, atyre u duhej të mblidheshin dhe të kombinonin njohuritë e tyre nëpërmjet një mënyre holistike (gjithperfshirese) për të bërë të mundur udhëtimin dhe për të mbijetuar në tokën e re.

Në një mënyrë të ngjashme, kur studiojnë planetin "Truri dhe Njohja", studiuesit priren të veçojnë pjesët e ndryshme në mënyrë që të jenë në gjendje të studiojnë thellësisht sistemin e interesit, por është e rëndësishme që gjithmonë të rikthehemi në nivelin holistik. Bukuria e aftësise se njohjes njerëzore është se bazohet në nivele të ndryshme të funksioneve të trurit dhe trupit, të cilat veprojnë së bashku në harmoni: nga qeliza, në sinapset, nga neuroni në rrjetet neuromoduluese, nga neuromoduluesit qendrorë në tru tek hormonet që sekretohen në trup, nga anatomia në fiziologji dhe funksionet e njohjes. Prandaj, ky disertacion i afrohet njohjes njerëzore dhe studimit të sistemit LC-NE në mënyrë holistike.

Për këtë qëllim, të gjithë kapitujt janë shkruar duke marrë parasysh njohuritë teorike në lidhje me sistemin LC-NE në lidhje me anatominë e trurit, funksionet konjitive, neuromodulimin (kryesisht NE), përgjigjet fiziologjike dhe aplikimet klinike. **Kapitujt 2 dhe 3** merren kryesisht me anatominë e LC, ndërsa **kapitujt 4, 5 dhe 6** përqendrohen në njohje dhe fiziologji njerëzore. Për më tepër, **kapitujt 5 dhe 6** kanë një kendveshtrim klinik dhe merren kolektivisht me aplikimet klinike të tVNS (pajisje mjekësore), të hormoneve alfa-amylaza dhe kortizol, përgjigjet fiziologjike trupore, të stresit dhe farmakologjisë.

Më poshtë jepet një përshkrim i shkurtër i kapitujve dhe studimeve të kryera për këtë disertacion të doktoratës, ku aplikohet një kendveshtrim me i gjëre holistik në neuroshkencën konjitive dhe klinike.

**Kapitujt Anatomikë (Kapitujt 2 & 3) - Krijimi dhe vlerësimi i qëndrueshmërisë së një atlasi të trurit**

**Kapitulli 2 dhe 3** i këtij disertacioni doktorature përshkruajnë studime anatomike që siguruan zhvillime metodologjike në vizualizimin e LC në njerëz të gjallë.

***Cfarë na pengon të shikojmë brenda trurit tonë?***

Sfidat janë të dy llojeve: teknike dhe anatomike. Sa i përket sfidave teknike, ka nevojë për përparime specifike teknologjike, të cilat kanë ndodhur vetëm kohët e fundit. Për sa i përket sfidave anatomike, disa struktura janë të vështira për t'u hartuar, sepse ato janë të vogla, vendndodhja dhe madhësia e tyre ndryshon shumë midis individëve të ndryshëm, dhe gjithashtu në disa raste ndodhen në pjesë të trurit ku është e vështirë të vizualizohen në njerëz të gjalle nepermjet MRI skanerit, për shkak të lëvizjes (ato janë të vendosura në pjesë të trurit që pulsojnë për shkak të nxitimit të lëngut cerebrospinal). Dallimet individuale në vendndodhjen dhe madhësinë e këtyre strukturave tregojnë se në njerëz të ndryshëm këto struktura të trurit mund të ndodhen pak më lartë ose më të poshtë, dhe gjithashtu mund të ndryshojnë nga madhësia dhe forma. Në këto rrethana, shkencëtari-studiues, si një Kristofor Kolomb modern, fillon një udhëtim për të eksploruar Inditë (d.m.th., LC në këtë rast), por rrezikon të përfundojë aksidentalisht në Amerikë (d.m.th., një bërthamë tjetër e trurit aty pranë).

***Cila do mund të ishte zgjidhja?***

***Zgjidhja Nr 1: vlerësoni nëse harta juaj është e besueshme dhe krijoni një hartë më të mirë***

Për të shmangur përzierjen e Indise me Amerikën në tru, duhet të dini nëse harta juaj është e qartë. Kjo është pikërisht ajo që kemi bërë në **Kapitullin 2** por ne e bëmë atë për trurin**.** Për më tepër, mund të krijohet një hartë më e mirë, kjo mund të jetë një hartë probabiliteti. Kjo është saktësisht ajo që ne bëmë në **Kapitullin 2.** Në kundërshtim me praktikën e zakonshme ku hartat e trurit të njeriut krijohen vetëm nga dhuruesit pas vdekjes së tyre, harta jonë probabiliste bazohet në imazhet MRI të njerëzve të gjallë.

Për të krahasuar hartën probabilistike të LC me udhëtimin e një eksploruesi, harta jonë probabilistike është më e saktë në krahasim me hartat e thjeshta, sepse përafrohet dhe merr parasysh jo vetëm një hartë të vetme, por të gjitha hartat e ndryshme që përshkruajnë Inditë (p.sh., ajo e krijuar nga hartograf Toscanelli, një tjetër nga Henricus Martellus etj). Në këtë mënyrë, rezultati përfundimtar është një hartë që tregon një imazh më përfaqësues, më të saktë të Indise: ai siguron pozicionin e qendrës se vendit, por edhe disa kufij shtesë përreth tij, në mënyrë që të saktesohet siguria e lokalizimit të strukturës - d.m.th. sa të sigurt jeni që arritet me të vërtetë në Indi, dhe jo ne nje shtet tjeter?

Ne e bëmë Atlasin probabilistik të trurit të LC publik, dhe kështu që mund të përdoret gratis nga kushdo (http://www.nitrc.org/projects/prob_lc_3t). Provojeni!

***Zgjidhja Nr 2: krahasoni hartat e disponueshme dhe filloni të përdorni kamera me rezolucion më të lartë***

Një zgjidhje e dytë do të ishte krahasimi i hartave në dispozicion dhe fillimi i përdorimit të përmirësimeve teknologjike siç është një aparat fotografik me rezolucion më të lartë (skanues MRI 7 Tesla). Kjo është ajo që bëmë në **Kapitullin 3**. Ne kemi përdorur

sekuenca të veçanta MRI që literatura e mëparshme kishte shenja premtuese për strukturat e imazhit si LC. Ne vlerësuam efektivitetin e këtyre sekuencave të MRI në vizualizimin e LC duke i krahasuar ato me njëri-tjetrin dhe duke i krahasuar ato me skanime të bëra me një "aparat fotografik me rezolucion të ulët" (skanues MRI 3 Tesla).

Si përmbledhje, në **Kapitullin 2** kemi vlerësuar nëse harta është e besueshme dhe kemi krijuar një hartë më të mirë për të rritur shanset që udhëtarët të përfundojnë në Indi (LC) dhe jo në Amerikë (një bërthamë tjetër e sistemit të trurit). Në **Kapitullin 3** kemi krahasuar hartat e disponueshme (skanime speciale për vizualizimin LC) dhe filluam të përdorim një aparat fotografik me rezolucion më të lartë (skanues MRI 7 Tesla), i cili në teori duhet të përmirësojë vizualizimin e strukturës së dëshiruar.

**Eksploroni një rrugë alternative për të arritur në Indi**

***Kapitullin Psikofiziologjik (Kapitulli 5) - Eksplorimi i një rruge alternative, me invazim minimal dhe kosto të ulët për të arritur në destinacionin e dëshiruar (sistemi LC-NE)***

Përveç konstruktimit të një harte, vlerësimit të qëndrueshmërisë së hartës dhe përdorimit të teknologjisë më të lartë për të përmirësuar më tej një hartë **(Kapitulli 2 & 3)**, një eksplorues i mirë është gjithashtu i interesuar të gjejë rrugë alternative, me kosto më të ulët, më të lehta, me më pak rreziqe dhe më të arritshme për të arritur në destinacionin e tyre. Në të vërtetë, Kolombi hipotezoi se duke udhëtuar në perëndim, ai do të hapte rrugë të reja tregtare dhe do të ishte në gjendje të arrinte në Indi përmes një rruge alternative. Kështu dhe ai filloi udhëtimin e tij për të provuar këtë hipotezë. Ne bëmë të njëjtën gjë në **Kapitullin 5**. Duke pasur parasysh lidhjet anatomike midis sistemit LC-NE dhe nervit vagus (nervi më i gjatë i trupit të njeriut, që lidh trurin me zorrët), si edhe gjetjet që stimulimi nervor transkutan i nervit mund të jetë një metode e re, jo-invazive, më e lirë dhe më e lehtë qe mund te perdoret për të stimuluar nervin vagus, kemi hipotezuar se mund të përdorim këtë metodë për të moduluar sistemin LC-NE. Kështu që filluam një udhëtim për të testuar këtë hipotezë.

**Ju keni arritur destinacionin tuaj. Cfarë thesare mund të ofrojë kjo tokë?**

***Sistemi LC-NE, njohja, fiziologjia dhe hormonet (Kapitulli 4 dhe 6) - Në çfarë lloj funksionesh njohëse është përfshirë sistemi LC-NE?***

Supozoni se keni vlerësuar rreziqet dhe besueshmërinë e udhëtimit, keni krijuar hartën dhe jeni përpjekur ta përmirësoni atë **(Kapitulli 2 & 3),** keni gjetur disa shenja për të mbështetur hipotezën e një rruge alternative, më pak të rrezikshme për në destinacionin tuaj (**Kapitulli 5)** dhe tani ju janë gati për të arritur këtë destinacion. Cfarë prisni të gjeni atje? Bazuar në njohuritë e mëparshme, Kolombi po priste që destinacioni i tij (India) të ishte një tokë me erëza. Në të njëjtën mënyrë, ne prisnim që sistemi LC-NE të përfshihej në fenomene specifike njohëse: a) efektin stimulues aksesor (fenomene ku një zhurmë e larte ne sfond përmirëson performancën tuaj gjatë një detyre, edhe pse nuk jep ndonjë informacion në lidhje me detyrën), dhe b) fleksibilitet konjitiv (aftësi njohëse për të kaluar mendërisht midis dy koncepteve të ndryshme) ose detyrave). Në rastin e Kolombit,

ata që arritën në Indi, konfirmuan që India ka erëza. Sidoqoftë, Kolombi arriti në Amerikë, një vend plot me ar dhe pambuk në vend të erëzave. Në mënyrë të ngjashme, ne gjetëm prova që LC-NE është e përfshirë në ndikimin e stimulit aksesor (erëza, bingo!), Por nuk është i përfshirë në aspektin komutues të detyrave të fleksibilitetit konjitiv (pambuk, ups!).

**A ishte ky fundi i ketij udhetimi, dhe çfarë do të vijë më pas?**

Nuk e di nëse ky udhetim ndalon ketu, por e di se çfarë duhet të vijë më tej: eksplorimi i trurit duhet të vazhdojë. Dhe sigurisht që ky udhëtim do të ketë ndikim më të madh dhe do të jetë shumë më interesant nëse neuroshkencëtarët njohës (eksploruesit) bashkojne fuqitë. Në fund të fundit, një studiues si "Kristofor Kolombi modern" do të përfitojë gjithmonë nga një koleg i cili - si një "Amerigo Vespuçi modern" - do të tregonte se e kishte gabim që besonte se ai arriti në Indi; ai kishte arritur faktikisht në një kontinent të pashpjeguar, tërësisht të ri më parë të panjohur për Euroaziatët, një "Botë e Re" që do të quhej "Amerikë". Eshtë e rëndësishme për eksploruesit modernë të dinë që ata që nuk lexojnë histori janë të dënuar ta përsërisin atë dhe mund të marrin mësime nga eksploruesit e shekullit të 15$^{të}$ me qëllim që të shmangin gabimet e së kaluarës. Prandaj, ata duhet të trajtojnë zbulimet e tyre jo si kolonizues, por në një mënyrë etike dhe respektuese, të promovojnë "tregti të ndershme" dhe shkencë të hapur, të përqafojnë një atmosferë bashkëpunuese në vend të një gare konkurruese ku "të pasurit pasurohen dhe te varfërit varfërohen". Ata gjithashtu duhet të sigurojnë kreditë përkatëse për personat qe u perkasin, të qëndrojnë gjithmonë të hapur ndaj kritikave dhe perspektivave alternative dhe, mbi të gjitha, të kenë si synimin e tyre kryesor kontributin për dijen dhe për një shoqëri më të mire, në vend të interesit vetiak dhe grumbullimi të botimeve. Amin!

## KORTE SAMENVATTING IN HET ENGELS - DEZE WETENSCHAPPELIJKE REIS IN EENVOUDIGE WOORDEN

### Dit proefschrift: een ontdekkingsreis

In de 21e eeuw heeft de mensheid gedetailleerde kaarten van de planeet Aarde gemaakt, heeft ze andere planeten in kaart gebracht, en is ze op zoek gegaan naar buitenaards leven. Verrassend genoeg zijn ze er nog niet in geslaagd de structuren in hun eigen hersenen in kaart te brengen of hun gedrag en cognitie te begrijpen. Eigenaardig dat we niet weten wat er in onze hersenen zit, toch? Dit proefschrift is een reis om de delen van onze hersenen, cognitie, fysiologische functies en gedrag te begrijpen en doet dit door het locus coeruleus-norepinephrine (LC-NE) systeem in mensen in vivo te onderzoeken (bij levende mensen, niet bij hersenen van dode donoren zoals tot nu toe gebruikelijk was).

Om de inhoud van dit proefschrift duidelijker te maken voor de leek, is het onderzoek voor dit proefschrift vergeleken met de reis van de 13e en 15e eeuwse ontdekkingsreizigers. Waar ontdekkingsreizigers zoals Marco Polo en Christopher Columbus probeerden de planeet "Aarde" in kaart te brengen en te begrijpen, probeerden wij de planeet "Hersenen en cognitie" in kaart te brengen en te begrijpen door ons te concentreren op het LC-NE-systeem.

### Wat is het locus coeruleus-noradrenergisch systeem?

De locus coeruleus, een kleine hersenstamkern, is de belangrijkste bron van de chemische boodschapperstof norepineprine in de hersenen, en is betrokken bij een aantal cognitieve functies en bij verschillende neurologische en psychiatrische stoornissen (ADHD, de ziekte van Alzheimer, stressstoornissen, depressie et cetera). In dit proefschrift bestuderen we het menselijke LC-NE-systeem, de anatomie van deze kleine hersenstamkern en de betrokkenheid van het LC-NE-systeem bij stress, opwinding, cognitieve flexibiliteit en fysiologie (hormonen en pupilreacties).

### Het LC-NE-systeem in de hersenen en de periferie: functies

Het LC-NE-systeem oefent zijn werking uit in de hersenen en het lichaam via neuronale (elektrische) maar ook neurochemische en hormonale routes. Het beïnvloedt de hersenen via de verbindingen die het heeft met meerdere hersengebieden, en het beïnvloedt de periferie via de verbindingen die het heeft met andere hersenstamkernen, het ruggenmerg en de nervus vagus; maar ook door de betrokkenheid van het LC-NE systeem in twee systemen die goed bestudeerd zijn in de stressliteratuur: het snelle en snel geactiveerde perifere autonome zenuwstelsel en de langzaam geactiveerde hypothalamus-hypofyse-adrenerge as (HPA-as).

In situaties waar hoge alertheid vereist is, zoals in situaties van gevaar of stress, wordt het LC-NE-systeem ingezet om deze situaties aan te gaan, parallel met de activering van het autonome zenuwstelsel. Zo mobiliseert het LC-NE-systeem - in samenwerking met het (sympathische) autonome zenuwstelsel - de hersenen en de periferie voor actie.

Een groot aantal onderzoeken heeft zich gericht op de functies van het LC-NE-systeem, maar vanwege technische en anatomische uitdagingen heeft een groot deel van deze onderzoeken zich beperkt tot diermodellen of computermodellen. Onderzoek uitgevoerd in het kader van dit proefschrift was gericht op het overbruggen van de kloof tussen dierstudies en theoretisch werk door gegevens te verzamelen bij levende menselijke proefpersonen met een holistische aanpak.

**Dit proefschrift: holistische benadering**

De ontdekkingsreizigers uit de 15e eeuw waren bij het bestuderen van planeet Aarde geïnteresseerd in geografie en het in kaart brengen van methoden om nieuwe gebieden te bereiken (bijvoorbeeld nieuwe routes naar Indië), de schatten die ze dachten daar te vinden en de flora en bevolkingen. Afhankelijk van hun kennis concentreerden verschillende leden van de bemanning zich op verschillende taken om de exploratie te realiseren (het creëren van een kaart, het bestuderen van het weer, zorgen voor veiligheid et cetera). Na deze opsplitsing in taken moesten ze echter samenkomen en hun kennis samenvoegen om de reis mogelijk te maken en te overleven in het nieuwe land.

Op een vergelijkbare manier hebben onderzoekers bij het bestuderen van de planeet "Hersenen en Cognitie" de neiging om de verschillende delen te scheiden om hun eigen onderwerp diepgaand te kunnen bestuderen, maar het is belangrijk om uiteindelijk altijd terug te keren naar het holistische niveau. Het mooie van menselijke cognitie is dat het gebaseerd is op verschillende niveaus van hersen- en lichaamsfuncties die in harmonie samenwerken: van cel tot synaps, van neuron tot neuromodulerende netwerken, van centrale neuromodulatoren in de hersenen tot hormonen die worden uitgescheiden in de lichaam, van anatomie tot fysiologie en cognitie. Daarom benadert dit proefschrift de menselijke cognitie en de studie van het LC-NE-systeem op een holistische manier.

Daartoe werd tijdens het schrijven van alle hoofdstukken rekening gehouden met theoretische kennis over het LC-NE-systeem met betrekking tot de anatomie van de hersenen, cognitieve functies, neuromodulatie (voornamelijk NE), fysiologische reacties en klinische toepassingen. **Hoofdstukken 2 en 3** behandelen voornamelijk de anatomie van de LC, terwijl de **hoofdstukken 4, 5 en 6** zich richten op cognitie en menselijke fysiologie. Daarnaast hebben **hoofdstukken 5 en 6** een klinische benadering en gaan ze gezamenlijk in op klinische toepassingen van tVNS (medisch hulpmiddel), de hormonen alpha-amylase en cortisol, lichamelijke fysiologische reacties, stress en farmacologie.

Hieronder volgt een korte beschrijving van de hoofdstukken en onderzoeken die zijn uitgevoerd voor dit proefschrift, waarbij een holistische benadering in de cognitieve en klinische neurowetenschappen wordt toegepast.

**Anatomische hoofdstukken (hoofdstukken 2 en 3) - Het creëren en beoordelen van de robuustheid van een hersenatlas**

**Hoofdstuk 2 en 3** van dit proefschrift beschrijven anatomische studies die methodologische ontwikkelingen leverden in de visualisatie van de LC bij levende mensen.

Wat weerhoudt ons ervan om in onze hersenen te kijken ?

Er zijn twee soorten uitdagingen: technische en anatomische. Wat de technische uitdagingen betreft is er behoefte aan specifieke technologische vooruitgang en deze heeft pas recentelijk plaatsgevonden. Wat betreft de anatomische uitdagingen: sommige structuren zijn moeilijk in kaart te brengen omdat ze klein zijn, en hun locatie en grootte sterk varieert tussen verschillende individuen. In sommige gevallen bevinden ze zich ook in delen van de hersenen die met een MRI-scanner niet gemakkelijk kunnen worden gevisualiseerd bij levende mensen als gevolg van beweging (ze zijn in delen van de hersenen die pulseren als gevolg van cerebrospinale vloeistofdoorstroom). De individuele verschillen in de locatie en grootte van deze structuren hebben als gevolg dat bij verschillende mensen deze hersenstructuren iets hoger of lager kunnen liggen, en ook de grootte en vorm kunnen verschillen. Onder deze omstandigheden start de ontdekkingsreiziger-onderzoeker, net als een moderne Christopher Columbus, een reis om Indië te verkennen (dwz de LC in haar geval), maar loopt het risico per ongeluk in Amerika terecht te komen (dwz een andere nabijgelegen hersenkern).

**Wat is de oplossing?**

***Oplossing nr. 1: beoordeel of uw kaart betrouwbaar is en maak een betere kaart***

Om te voorkomen dat Indië met Amerika in de hersenen wordt verwisseld, moet je weten of je kaart betrouwbaar is. Dit is precies wat we deden in **hoofdstuk 2,** maar we deden het voor de hersenen. Daarnaast zou men een betere kaart kunnen ontwikkelen, bijvoorbeeld een probabilistische kaart. Dit is precies wat we deden in **hoofdstuk 2**. In tegenstelling tot de gangbare praktijk waarbij menselijke hersenkaarten alleen worden gemaakt van donoren na hun dood, is onze probabilistische kaart gebaseerd op MRI-afbeeldingen van levende mensen (in wetenschappelijk jargon "in vivo" genoemd) .

Om de probabilistische kaart van de LC met een ontdekkingsreis te vergelijken: onze probabilistische kaart is nauwkeuriger in vergelijking met eenvoudige kaarten omdat deze uitgelijnd is en met meerdere kaarten van Indië is vergeleken (bijvoorbeeld een kaart cartograaf Toscanelli en een van Henricus Martellus, et cetera). Op deze wijze is het uiteindelijke resultaat een kaart met een representatiever, accurater beeld van Indië: het toont de kern van het land, maar ook enkele omringende extra grenzen om de betrouwbaarheid van de juiste locatie te bepalen - dat wil zeggen, hoe zeker ben je dat je inderdaad in Indië bent?

We hebben de probabilistische atlas van de LC voor iedereen gratis beschikbaar gemaakt (http://www.nitrc.org/projects/prob_lc_3t). Probeer het eens.

***Oplossing Nr 2: vergelijk de beschikbare kaarten en gebruik een camera met een hogere resolutie***

Een tweede oplossing zou zijn om de beschikbare kaarten te vergelijken en technologische verbeteringen te gebruiken, zoals een camera met een hogere resolutie (7 Tesla MRI-scanner). Dit is wat we in **hoofdstuk 3** hebben gedaan. We gebruikten speciale MRI-sequenties die volgens eerdere literatuur veelbelovend waren om structuren zoals de LC in kaart te brengen. We beoordeelden de effectiviteit van deze MRI-sequenties bij het visualiseren van de LC door ze met elkaar te vergelijken en door ze te vergelijken met scans gemaakt met een "camera met lage resolutie" (3 Tesla MRI-scanner).

Samenvattend hebben we in **hoofdstuk 2** beoordeeld of de kaart betrouwbaar is en hebben we een betere kaart gemaakt om de kans te vergroten dat reizigers in Indië (LC) terechtkomen en niet in Amerika (een andere hersenstamkern). In **hoofdstuk 3** vergeleken we de beschikbare kaarten (speciale scans voor LC-visualisatie) en gebruikten we een camera met een hogere resolutie (7T MRI-scanner), die in theorie de visualisatie van de gewenste structuur zou moeten verbeteren.

**Verken een alternatieve route om Indië te bereiken**

***Psychofysiologisch hoofdstuk (hoofdstuk 5) - Verkenning van een alternatieve, minder invasieve, goedkope route om de gewenste bestemming te bereiken (LC-NE-systeem )***

Naast het ontwerpen van een kaart, het beoordelen van de robuustheid van de kaart en het gebruik van de modernste technologie om een kaart verder te verbeteren (**hoofdstuk 2 en 3**) , is een goede ontdekkingsreiziger ook geïnteresseerd in het vinden van alternatief, goedkoper, gemakkelijker, minder gevaarlijk, en meer toegankelijke routes om zijn bestemming te bereiken. Columbus veronderstelde inderdaad dat hij door naar het westen te reizen nieuwe handelsroutes zou openen en dat hij Indië via een alternatieve route zou kunnen bereiken. Hij begon zijn reis om deze hypothese te testen. We hebben hetzelfde gedaan in **hoofdstuk 5**. Gezien de anatomische verbindingen tussen het LC-NE-systeem en de nervus vagus (de langste zenuw van het menselijk lichaam, die de hersenen met de darmen verbindt), en de mogelijkheid van transcutane stimulatie van de nervus vagus (een nieuwe, niet-invasieve, goedkope en gemakkelijke methode om de nervus vagus te stimuleren), veronderstelden we dat we deze methode zouden kunnen gebruiken om het LC-NE-systeem te moduleren. Dus begonnen we aan een reis om deze hypothese te toetsen.

**Je hebt je bestemming bereikt. Welke schatten kan dit land bieden?**

***LC-NE-systeem, cognitie, fysiologie en hormonen (hoofdstuk 4 en 6) - Bij welke cognitieve functies is het LC-NE-systeem betrokken?***

Stel, je hebt de risico's en betrouwbaarheid van de reis beoordeeld, je hebt de kaart gemaakt en je hebt geprobeerd deze te verbeteren **(hoofdstuk 2 en 3)**, je hebt een aantal borden gevonden die een alternatieve, minder gevaarlijke route naar je bestemming ondersteunen **(hoofdstuk 5)** en nu ben je klaar om deze bestemming te bereiken. Wat verwacht je daar te vinden? Op basis van eerdere kennis verwachtte Columbus dat zijn

bestemming (Indië) een land van specerijen zou zijn. Op dezelfde manier hadden we verwacht dat het LC-NE-systeem betrokken zou zijn bij specifieke cognitieve verschijnselen: a) het accessory stimulus effect: het verschijnsel dat een hard achtergrondgeluid de prestaties tijdens een taak verbetert, ondanks dat het achtergrondgeluid geen informatie voor de taak bevat;, en b) cognitieve flexibiliteit: het cognitief vermogen om mentaal te schakelen tussen twee verschillende concepten of taken. In het geval van Columbus bevestigden degenen die Indië bereikten dat Indië kruiden heeft. Columbus bereikte echter Amerika, een land vol goud en katoen in plaats van kruiden. Zo vonden wij het bewijs dat de LC-NE is betrokken bij het accessory stimulus effect (specerijen, bingo!), maar niet betrokken bij de cognitieve flexibiliteit om te schakelen tussen twee taken (katoen, oops!).

**Leefden ze nog lang en gelukkig en wat komt daarna?**

Ik weet niet of ze nog lang en gelukkig leefden, maar ik weet wel wat er daarna zou moeten komen: de verkenning van de hersenen moet doorgaan. En natuurlijk zal deze reis een grotere impact hebben en veel leuker zijn als cognitieve neurowetenschappers (ontdekkingsreizigers) de krachten bundelen. Uiteindelijk zal een 'moderne Christopher Columbus' onderzoeker altijd baat hebben bij een collega die - net als een' moderne Amerigo Vespucci '- zou aantonen dat ze ongelijk had om te geloven dat ze Indië had bereikt; ze had zelfs een onontgonnen, geheel nieuw continent bereikt dat voorheen onbekend was bij Euraziaten, een 'Nieuwe Wereld' die 'Amerika' zou worden genoemd. Belangrijk is dat moderne ontdekkingsreizigers weten dat degenen die de geschiedenis niet lezen gedoemd zijn om het te herhalen, en kunnen leren van de ontdekkingsreizigers uit de 15e eeuw om fouten uit het verleden te voorkomen. Daarom moeten ze hun ontdekkingen op een ethische en respectvolle manier behandelen, "eerlijke handel" en open wetenschap bevorderen, een sfeer van samenwerking omarmen in plaats van een concurrerende "de rijken-worden-rijker" benadering. Daarnaast moeten ze de bijdragen van anderen erkennen, open blijven staan voor kritiek en alternatieve perspectieven, en vooral het doel hebben om bij te dragen aan kennis en aan een betere samenleving in plaats van eigenbelang en een opeenstapeling van publicaties. Amen!

## References


Afshar, F., Watkins, E. S., & Yap, J. C. (1978). *Stereotaxic Atlas of the Human Brainstem and Cerebellar Nuclei: A Variability Study*: Raven Press.

Arnsten, A. F., Steere, J. C., & Hunt, R. D. (1996). The contribution of alpha 2-noradrenergic mechanisms of prefrontal cortical cognitive function. Potential significance for attention-deficit hyperactivity disorder. *Archives of General Psychiatry, 53*(5), 448-455 doi:http://dx.doi.org/410.1001/archpsyc.1996.01830050084013.

Astafiev, S. V., Snyder, A. Z., Shulman, G. L., & Corbetta, M. (2010). Comment on "Modafinil shifts human locus coeruleus to low-tonic, high-phasic activity during functional MRI" and "Homeostatic sleep pressure and responses to sustained attention in the suprachiasmatic area". *Science, 328*(5976), 309; author reply 309. doi:10.1126/science.1177200

Aston-Jones, G., & Cohen, J. D. (2005). An integrative theory of locus coeruleus-norepinephrine function: adaptive gain and optimal performance. *Annual Review Neuroscience, 28*, 403-450. doi:10.1146/annurev.neuro.28.061604.135709

Aston-Jones, G., Foote, S., & Bloom, F. (1984). Anatomy and physiology of locus coeruleus neurons: Functional implications. In M. Ziegler & C. Lake (Eds.), *In: Norepinephrine* (pp. pp 92–116): Baltimore: Williams & Wilkins.

Aston-Jones, G., Rajkowski, J., & Cohen, J. (1999). Role of locus coeruleus in attention and behavioral flexibility. *Biol Psychiatry, 46*(9), 1309-1320.

Aston-Jones, G., Rajkowski, J., & Cohen, J. (2000). Locus coeruleus and regulation of behavioral flexibility and attention. *Prog Brain Res, 126*, 165-182. doi:10.1016/s0079-6123(00)26013-5

Aston-Jones, G., Rajkowski, J., Kubiak, P., & Alexinsky, T. (1994). Locus coeruleus neurons in monkey are selectively activated by attended cues in a vigilance task. *The Journal of Neuroscience, 14*(7), 4467-4480.

Baas, D., Aleman, A., & Kahn, R. S. (2004). Lateralization of amygdala activation: a systematic review of functional neuroimaging studies. *Brain Res Brain Res Rev, 45*(2), 96-103. doi:10.1016/j.brainresrev.2004.02.004

Badran, B. W., Brown, J. C., Dowdle, L. T., Mithoefer, O. J., LaBate, N. T., Coatsworth, J., . . . George, M. S. (2018). Tragus or cymba conchae? Investigating the anatomical foundation of transcutaneous auricular vagus nerve stimulation (taVNS). *Brain Stimul, 11*(4), 947-948. doi:10.1016/j.brs.2018.06.003

Badran, B. W., Dowdle, L. T., Mithoefer, O. J., LaBate, N. T., Coatsworth, J., Brown, J. C., . . . George, M. S. (2018). Neurophysiologic effects of transcutaneous auricular vagus nerve stimulation (taVNS) via electrical stimulation of the tragus: A concurrent taVNS/fMRI study and review. *Brain Stimul, 11*(3), 492-500. doi:10.1016/j.brs.2017.12.009

Bari, A., & Aston-Jones, G. (2013). Atomoxetine modulates spontaneous and sensory-evoked discharge of locus coeruleus noradrenergic neurons. *Neuropharmacology, 64*, 53-64. doi:10.1016/j.neuropharm.2012.07.020

Bartzokis, G., Mintz, J., Marx, P., Osborn, D., Gutkind, D., Chiang, F., . . . Marder, S. R. (1993). Reliability of in vivo volume measures of hippocampus and other brain structures using MRI. *Magn Reson Imaging, 11*(7), 993-1006.

Beatty, J., & Lucero-Wagoner, B. (2000). The pupillary system. In J. T. Cacioppo, Tassinary, L.G., & Bertntson, G.G (Ed.), *Handbook of psychophysiology* (2nd ed., pp. 142-182). New York: Cambridge University Press.

Beltzer, E. K., Fortunato, C. K., Guaderrama, M. M., Peckins, M. K., Garramone, B. M., & Granger, D. A. (2010). Salivary flow and alpha-amylase: collection technique, duration, and oral fluid type. *Physiol Behav, 101*(2), 289-296. doi:10.1016/j.physbeh.2010.05.016

Bernstein, I. H., Chu, P. K., Briggs, P., & Schurman, D. L. (1973). Stimulus intensity and foreperiod effects in intersensory facilitation. *Quarterly Journal of Experimental Psychology, 25*(2), 171-181. doi:10.1080/14640747308400336

Bernstein, I. H., Clark, M. H., & Edelstein, B. A. (1969). Effects of an auditory signal on visual reaction time. *Journal of Experimental Psychology, 80*(3), 567-569.doi: http://dx.doi.org/510.1037/h0027444.

Bernstein, I. H., Rose, R., & Ashe, V. (1970). Preparatory state effects in intersensory facilitation. *Psychonomic Science, 19*(2), 113-114. doi:10.3758/BF03337448

Berridge, C. W., & Waterhouse, B. D. (2003). The locus coeruleus–noradrenergic system: modulation of behavioral state and state-dependent cognitive processes. *Brain Research Reviews, 42*(1), 33-84. doi:http://dx.doi.org/10.1016/S0165-0173(03)00143-7

Bertelson, P., & Tisseyre, F. (1969). The time-course of preparation: Confirmatory results with visual and auditory warning signals. *Acta Psychologica, 30*, 145-154. doi:http://dx.doi.org/10.1016/0001-6918(69)90047-X

Berthoud, H. R., & Neuhuber, W. L. (2000). Functional and chemical anatomy of the afferent vagal system. *Auton Neurosci, 85*(1-3), 1-17. doi:10.1016/s1566-0702(00)00215-0

Beste, C., Steenbergen, L., Sellaro, R., Grigoriadou, S., Zhang, R., Chmielewski, W., . . . Colzato, L. (2016). Effects of Concomitant Stimulation of the GABAergic and Norepinephrine System on Inhibitory Control - A Study Using Transcutaneous Vagus Nerve Stimulation. *Brain Stimul, 9*(6), 811-818. doi:10.1016/j.brs.2016.07.004

Betts, M. J., Cardenas-Blanco, A., Kanowski, M., Jessen, F., & Düzel, E. (2017). In vivo MRI assessment of the human locus coeruleus along its rostrocaudal extent in young and older adults. *NeuroImage, 163*(Supplement C), 150-159. doi:https://doi.org/10.1016/j.neuroimage.2017.09.042

Bianca, R., & Komisaruk, B. R. (2007). Pupil dilatation in response to vagal afferent electrical stimulation is mediated by inhibition of parasympathetic outflow in the rat. *Brain Res, 1177*, 29-36. doi:10.1016/j.brainres.2007.06.104

Blazejewska, A. I., Schwarz, S. T., Pitiot, A., Stephenson, M. C., Lowe, J., Bajaj, N., . . . Gowland, P. A. (2013). Visualization of nigrosome 1 and its loss in PD: pathoanatomical correlation and in vivo 7 T MRI. *Neurology, 81*(6), 534-540. doi:10.1212/WNL.0b013e31829e6fd2

Bolding, M. S., Reid, M. A., Avsar, K. B., Roberts, R. C., Gamlin, P. D., Gawne, T. J., . . . Lahti, A. C. (2013). Magnetic Transfer Contrast Accurately Localizes Substantia Nigra Confirmed by Histology. *Biological Psychiatry, 73*(3), 289-294. doi:10.1016/j.biopsych.2012.07.035

Bosch, J. A., Brand, H. S., Ligtenberg, T. J., Bermond, B., Hoogstraten, J., & Nieuw Amerongen, A. V. (1996). Psychological stress as a determinant of protein levels and salivary-induced aggregation of Streptococcus gordonii in human whole saliva. *Psychosom Med, 58*(4), 374-382. doi:10.1097/00006842-199607000-00010

Bosch, J. A., de Geus, E. J., Carroll, D., Goedhart, A. D., Anane, L. A., van Zanten, J. J., . . . Edwards, K. M. (2009). A general enhancement of autonomic and cortisol responses during social evaluative threat. *Psychosom Med, 71*(8), 877-885. doi:10.1097/PSY.0b013e3181baef05

Bosch, J. A., Veerman, E. C., de Geus, E. J., & Proctor, G. B. (2011). alpha-Amylase as a reliable and convenient measure of sympathetic activity: don't start salivating just yet! *Psychoneuroendocrinology, 36*(4), 449-453. doi:10.1016/j.psyneuen.2010.12.019

Bouret, S., & Sara, S. J. (2004). Reward expectation, orientation of attention and locus coeruleus-medial frontal cortex interplay during learning. *European Journal of Neuroscience, 20*(3), 791-802. doi:10.1111/j.1460-9568.2004.03526.x

Bremner, J. D. (2006). Traumatic stress: effects on the brain. *Dialogues Clin Neurosci, 8*(4), 445-461.

Brown, S. B., Slagter, H. A., van Noorden, M. S., Giltay, E. J., van der Wee, N. J., & Nieuwenhuis, S. (2016). Effects of clonidine and scopolamine on multiple target detection in rapid serial

visual presentation. *Psychopharmacology (Berl), 233*(2), 341-350. doi:10.1007/s00213-015-4111-y

Brown, S. B., Tona, K. D., van Noorden, M. S., Giltay, E. J., van der Wee, N. J., & Nieuwenhuis, S. (2015). Noradrenergic and cholinergic effects on speed and sensitivity measures of phasic alerting. *Behavioral Neuroscience, 129*(1), 42-49. doi:10.1037/bne0000030

Brown, S. B., van der Wee, N. J., van Noorden, M. S., Giltay, E. J., & Nieuwenhuis, S. (2015). Noradrenergic and cholinergic modulation of late ERP responses to deviant stimuli. *Psychophysiology, 52*(12), 1620-1631. doi:10.1111/psyp.12544

Brown, S. B., van Steenbergen, H., Kedar, T., & Nieuwenhuis, S. (2014). Effects of arousal on cognitive control: empirical tests of the conflict-modulated Hebbian-learning hypothesis. *Frontiers in Human Neuroscience, 8*, 23. doi:10.3389/fnhum.2014.00023

Burger, A. M., & Verkuil, B. (2018). Transcutaneous nerve stimulation via the tragus: are we really stimulating the vagus nerve? *Brain Stimul, 11*(4), 945-946. doi:10.1016/j.brs.2018.03.018

Bymaster, F. P., Katner, J. S., Nelson, D. L., Hemrick-Luecke, S. K., Threlkeld, P. G., Heiligenstein, J. H., . . . Perry, K. W. (2002). Atomoxetine increases extracellular levels of norepinephrine and dopamine in prefrontal cortex of rat: a potential mechanism for efficacy in attention deficit/hyperactivity disorder. *Neuropsychopharmacology, 27*(5), 699-711. doi:10.1016/s0893-133x(02)00346-9

Cahill, L., & McGaugh, J. L. (1998). Mechanisms of emotional arousal and lasting declarative memory. *Trends Neurosci, 21*(7), 294-299.

Cahill, L., Uncapher, M., Kilpatrick, L., Alkire, M. T., & Turner, J. (2004). Sex-Related Hemispheric Lateralization of Amygdala Function in Emotionally Influenced Memory: An fMRI Investigation. *Learning & Memory, 11*(3), 261-266. doi:10.1101/lm.70504

Canas, J., Quesada, J. F., Antoli, A., & Fajardo, I. (2003). Cognitive flexibility and adaptability to environmental changes in dynamic complex problem-solving tasks. *Ergonomics, 46*(5), 482-501. doi:10.1080/0014013031000061640

Capone, F., Assenza, G., Di Pino, G., Musumeci, G., Ranieri, F., Florio, L., . . . Di Lazzaro, V. (2015). The effect of transcutaneous vagus nerve stimulation on cortical excitability. *J Neural Transm, 122*(5), 679-685. doi:10.1007/s00702-014-1299-7

Cedarbaum, J. M., & Aghajanian, G. K. (1978). Afferent projections to the rat locus coeruleus as determined by a retrograde tracing technique. *The Journal of Comparative Neurology, 178*(1), 1-15. doi:10.1002/cne.901780102

Chamberlain, S. R., Muller, U., Cleary, S., Robbins, T. W., & Sahakian, B. J. (2007). Atomoxetine increases salivary cortisol in healthy volunteers. *J Psychopharmacol, 21*(5), 545-549. doi:10.1177/0269881106075274

Chan-Palay, V., & Asan, E. (1989). Alterations in catecholamine neurons of the locus coeruleus in senile dementia of the Alzheimer type and in Parkinson's disease with and without dementia and depression. *The Journal of Comparative Neurology, 287*(3), 373-392. doi:10.1002/cne.902870308

Chatterton, R. T., Jr., Vogelsong, K. M., Lu, Y. C., Ellman, A. B., & Hudgens, G. A. (1996). Salivary alpha-amylase as a measure of endogenous adrenergic activity. *Clin Physiol, 16*(4), 433-448. doi:10.1111/j.1475-097x.1996.tb00731.x

Chen, X., Huddleston, D. E., Langley, J., Ahn, S., Barnum, C. J., Factor, S. A., . . . Hu, X. (2014). Simultaneous imaging of locus coeruleus and substantia nigra with a quantitative neuromelanin MRI approach. *Magnetic Resonance Imaging, 32*(10), 1301-1306. doi:https://doi.org/10.1016/j.mri.2014.07.003

Chiao, J. Y. (2009). Cultural neuroscience: a once and future discipline. *Prog Brain Res, 178*, 287-304. doi:10.1016/s0079-6123(09)17821-4

Chmielewski, W. X., Muckschel, M., Ziemssen, T., & Beste, C. (2017). The norepinephrine system affects specific neurophysiological subprocesses in the modulation of inhibitory control

by working memory demands. *Human brain mapping, 38*(1), 68-81. doi:10.1002/hbm.23344
Cho, Z. H., Kang, C. K., Son, Y. D., Choi, S. H., Lee, Y. B., Paek, S. H., . . . Kim, Y. B. (2014). Pictorial review of in vivo human brain: from anatomy to molecular imaging. *World Neurosurg, 82*(1-2), 72-95. doi:10.1016/j.wneu.2012.10.020
Clewett, D. V., Lee, T. H., Greening, S., Ponzio, A., Margalit, E., & Mather, M. (2016). Neuromelanin marks the spot: identifying a locus coeruleus biomarker of cognitive reserve in healthy aging. *Neurobiol Aging, 37*, 117-126. doi:10.1016/j.neurobiolaging.2015.09.019
Dahl, M. J., Mather, M., Duezel, S., Bodammer, N. C., Lindenberger, U., Kuehn, S., & Werkle-Bergner, M. (2018). Locus coeruleus integrity preserves memory performance across the adult life span. *bioRxiv*.
de Gee, J. W., Colizoli, O., Kloosterman, N. A., Knapen, T., Nieuwenhuis, S., & Donner, T. H. (2017). Dynamic modulation of decision biases by brainstem arousal systems. *eLife, 6*, e23232. doi:10.7554/eLife.23232
de Hollander, G., Keuken, M. C., & Forstmann, B. U. (2015). The subcortical cocktail problem; mixed signals from the subthalamic nucleus and substantia nigra. *PLoS One, 10*(3), e0120572. doi:10.1371/journal.pone.0120572
de Rover, M., Brown, S. B., Band, G. P., Giltay, E. J., van Noorden, M. S., van der Wee, N. J., & Nieuwenhuis, S. (2015). Beta receptor-mediated modulation of the oddball P3 but not error-related ERP components in humans. *Psychopharmacology (Berl), 232*(17), 3161-3172. doi:10.1007/s00213-015-3966-2
De Taeye, L., Vonck, K., van Bochove, M., Boon, P., Van Roost, D., Mollet, L., . . . Raedt, R. (2014). The P3 event-related potential is a biomarker for the efficacy of vagus nerve stimulation in patients with epilepsy. *Neurotherapeutics, 11*(3), 612-622. doi:10.1007/s13311-014-0272-3
DeArmond, S. J., Fusco, M. M., & Dewey, M. M. (1974). *Structure of the human brain: a photographic atlas*: Oxford University Press.
Del Grande, F., Santini, F., Herzka, D. A., Aro, M. R., Dean, C. W., Gold, G. E., & Carrino, J. A. (2014). Fat-suppression techniques for 3-T MR imaging of the musculoskeletal system. *Radiographics, 34*(1), 217-233. doi:10.1148/rg.341135130
Desbeaumes Jodoin, V., Lesperance, P., Nguyen, D. K., Fournier-Gosselin, M. P., & Richer, F. (2015). Effects of vagus nerve stimulation on pupillary function. *Int J Psychophysiol, 98*(3 Pt 1), 455-459. doi:10.1016/j.ijpsycho.2015.10.001
Devoto, P., & Flore, G. (2006). On the origin of cortical dopamine: is it a co-transmitter in noradrenergic neurons? *Curr Neuropharmacol, 4*(2), 115-125.
Dice, L. R. (1945). Measures of the Amount of Ecologic Association Between Species. *Ecology, 26*(3), 297-302. doi:10.2307/1932409
Diederich, A., Schomburg, A., & Colonius, H. (2012). Saccadic reaction times to audiovisual stimuli show effects of oscillatory phase reset. *PLoS One, 7*(10), e44910. doi:10.1371/journal.pone.0044910
Diedrichsen, J., Maderwald, S., Kuper, M., Thurling, M., Rabe, K., Gizewski, E. R., . . . Timmann, D. (2011). Imaging the deep cerebellar nuclei: a probabilistic atlas and normalization procedure. *NeuroImage, 54*(3), 1786-1794. doi:10.1016/j.neuroimage.2010.10.035
Dietrich, S., Smith, J., Scherzinger, C., Hofmann-Preiß, K., Freitag, T., Eisenkolb, A., & Ringler, R. (2008). A novel transcutaneous vagus nerve stimulation leads to brainstem and cerebral activations measured by functional MRI / Funktionelle Magnetresonanztomographie zeigt Aktivierungen des Hirnstamms und weiterer zerebraler Strukturen unter transkutaner Vagusnervstimulation. In *Biomedizinische Technik/Biomedical Engineering* (Vol. 53, pp. 104).

Dorr, A. E., & Debonnel, G. (2006). Effect of vagus nerve stimulation on serotonergic and noradrenergic transmission. *J Pharmacol Exp Ther, 318*(2), 890-898. doi:10.1124/jpet.106.104166

Duchin, Y., Abosch, A., Yacoub, E., Sapiro, G., & Harel, N. (2012). Feasibility of Using Ultra-High Field (7 T) MRI for Clinical Surgical Targeting. *PLoS One, 7*(5), e37328. doi:10.1371/journal.pone.0037328

Dunn, A. J., Swiergiel, A. H., & Palamarchouk, V. (2004). Brain circuits involved in corticotropin-releasing factor-norepinephrine interactions during stress. *Ann N Y Acad Sci, 1018*, 25-34. doi:10.1196/annals.1296.003

Duyn, J. H., van Gelderen, P., Li, T.-Q., de Zwart, J. A., Koretsky, A. P., & Fukunaga, M. (2007). High-field MRI of brain cortical substructure based on signal phase. *Proceedings of the National Academy of Sciences, 104*(28), 11796-11801. doi:10.1073/pnas.0610821104

Ehlert, U., Erni, K., Hebisch, G., & Nater, U. (2006). Salivary alpha-amylase levels after yohimbine challenge in healthy men. *J Clin Endocrinol Metab, 91*(12), 5130-5133. doi:10.1210/jc.2006-0461

Ehrminger, M., Latimier, A., Pyatigorskaya, N., Garcia-Lorenzo, D., Leu-Semenescu, S., Vidailhet, M., . . . Arnulf, I. (2016). The coeruleus/subcoeruleus complex in idiopathic rapid eye movement sleep behaviour disorder. *Brain, 139*(Pt 4), 1180-1188. doi:10.1093/brain/aww006

Einhäuser, W., Stout, J., Koch, C., & Carter, O. (2008). Pupil dilation reflects perceptual selection and predicts subsequent stability in perceptual rivalry. *Proceedings of the National Academy of Sciences, 105*(5), 1704-1709. doi:10.1073/pnas.0707727105

Eldar, E., Cohen, J. D., & Niv, Y. (2013). The effects of neural gain on attention and learning. *Nature Neuroscience, 16*(8), 1146-1153. doi:10.1038/nn.3428

Ellrich, J. J. E. N. R. (2011). Transcutaneous vagus nerve stimulation. *6*(4), 254-256.

Fabiani, M., & Friedman, D. (1995). Changes in brain activity patterns in aging: the novelty oddball. *Psychophysiology, 32*(6), 579-594. doi:10.1111/j.1469-8986.1995.tb01234.x

Fallgatter, A. J., Neuhauser, B., Herrmann, M. J., Ehlis, A. C., Wagener, A., Scheuerpflug, P., . . . Riederer, P. (2003). Far field potentials from the brain stem after transcutaneous vagus nerve stimulation. *J Neural Transm (Vienna), 110*(12), 1437-1443. doi:10.1007/s00702-003-0087-6

Fedorow, H., Tribl, F., Halliday, G., Gerlach, M., Riederer, P., & Double, K. L. (2005). Neuromelanin in human dopamine neurons: comparison with peripheral melanins and relevance to Parkinson's disease. *Prog Neurobiol, 75*(2), 109-124. doi:10.1016/j.pneurobio.2005.02.001

Feng, S. F., Schwemmer, M., Gershman, S. J., & Cohen, J. D. (2014). Multitasking versus multiplexing: Toward a normative account of limitations in the simultaneous execution of control-demanding behaviors. *Cogn Affect Behav Neurosci, 14*(1), 129-146. doi:10.3758/s13415-013-0236-9

Fernandes, P., Regala, J., Correia, F., & Goncalves-Ferreira, A. J. (2012). The human locus coeruleus 3-D stereotactic anatomy. *Surg Radiol Anat, 34*(10), 879-885. doi:10.1007/s00276-012-0979-y

Fernandez-Duque, D., & Posner, M. I. (1997). Relating the mechanisms of orienting and alerting. *Neuropsychologia, 35*(4), 477-486. doi: http://dx.doi.org/410.1016/S0028-3932(1096)00103-00100.

Fischer, R., Plessow, F., & Kiesel, A. (2010). Auditory warning signals affect mechanisms of response selection: evidence from a Simon task. *Experimental psychology, 57*(2), 89-97. doi:10.1027/1618-3169/a000012

Fischer, R., Ventura-Bort, C., Hamm, A., & Weymar, M. (2018). Transcutaneous vagus nerve stimulation (tVNS) enhances conflict-triggered adjustment of cognitive control. *Cogn Affect Behav Neurosci, 18*(4), 680-693. doi:10.3758/s13415-018-0596-2

Follesa, P., Biggio, F., Gorini, G., Caria, S., Talani, G., Dazzi, L., . . . Biggio, G. (2007). Vagus nerve stimulation increases norepinephrine concentration and the gene expression of BDNF and bFGF in the rat brain. *Brain Res, 1179*, 28-34. doi:10.1016/j.brainres.2007.08.045

Forstmann, B. U., de Hollander, G., van Maanen, L., Alkemade, A., & Keuken, M. C. (2017). Towards a mechanistic understanding of the human subcortex. *Nat Rev Neurosci, 18*(1), 57-65. doi:10.1038/nrn.2016.163

Frangos, E., Ellrich, J., & Komisaruk, B. R. (2014). Non-invasive Access to the Vagus Nerve Central Projections via Electrical Stimulation of the External Ear: fMRI Evidence in Humans. *Brain Stimul*. doi:10.1016/j.brs.2014.11.018

Frangos, E., Ellrich, J., & Komisaruk, B. R. (2015). Non-invasive Access to the Vagus Nerve Central Projections via Electrical Stimulation of the External Ear: fMRI Evidence in Humans. *Brain Stimul, 8*(3), 624-636. doi:10.1016/j.brs.2014.11.018

Frings, L., Wagner, K., Unterrainer, J., Spreer, J., Halsband, U., & Schulze-Bonhage, A. (2006). Gender-related differences in lateralization of hippocampal activation and cognitive strategy. *Neuroreport, 17*(4), 417-421. doi:10.1097/01.wnr.0000203623.02082.e3

Frobose, M. I., Swart, J. C., Cook, J. L., Geurts, D. E., den Ouden, H. E., & Cools, R. (2017). Catecholaminergic modulation of the avoidance of cognitive control. *bioRxiv*. doi:10.1101/191015

George, M. S., & Aston-Jones, G. (2010). Noninvasive techniques for probing neurocircuitry and treating illness: vagus nerve stimulation (VNS), transcranial magnetic stimulation (TMS) and transcranial direct current stimulation (tDCS). *Neuropsychopharmacology, 35*(1), 301-316. doi:10.1038/npp.2009.87

German, D., Walker, B., Manaye, K., Smith, W., Woodward, D., & North, A. (1988). The human locus coeruleus: computer reconstruction of cellular distribution. *The Journal of Neuroscience, 8*(5), 1776-1788.

Gesi, M., Soldani, P., Giorgi, F. S., Santinami, A., Bonaccorsi, I., & Fornai, F. (2000). The role of the locus coeruleus in the development of Parkinson's disease. *Neurosci Biobehav Rev, 24*(6), 655-668.

Geva, R., Zivan, M., Warsha, A., & Olchik, D. (2013). Alerting, Orienting or Executive Attention Networks: Differential Patters of Pupil Dilations. *Frontiers in Behavioral Neuroscience, 7*. doi:10.3389/fnbeh.2013.00145

Ghacibeh, G. A., Shenker, J. I., Shenal, B., Uthman, B. M., & Heilman, K. M. (2006). Effect of vagus nerve stimulation on creativity and cognitive flexibility. *Epilepsy Behav, 8*(4), 720-725. doi:10.1016/j.yebeh.2006.03.008

Gilzenrat, M. S., Nieuwenhuis, S., Jepma, M., & Cohen, J. D. (2010). Pupil diameter tracks changes in control state predicted by the adaptive gain theory of locus coeruleus function. *Cogn Affect Behav Neurosci, 10*(2), 252-269.

Grabner, G., Janke, A. L., Budge, M. M., Smith, D., Pruessner, J., & Collins, D. L. (2006). Symmetric atlasing and model based segmentation: an application to the hippocampus in older adults. *Med Image Comput Comput Assist Interv, 9*(Pt 2), 58-66.

Grant, S. J., Aston-Jones, G., & Redmond, D. E., Jr. (1988). Responses of primate locus coeruleus neurons to simple and complex sensory stimuli. *Brain Research Bulletin, 21*(3), 401-410. doi: http://dx.doi.org/410.1016/0361-9230(1088)90152-90159.

Gratton, G., Coles, M. G., & Donchin, E. (1983). A new method for off-line removal of ocular artifact. *Electroencephalogr Clin Neurophysiol, 55*(4), 468-484. doi:10.1016/0013-4694(83)90135-9

Grudzien, A., Shaw, P., Weintraub, S., Bigio, E., Mash, D. C., & Mesulam, M. M. (2007). Locus coeruleus neurofibrillary degeneration in aging, mild cognitive impairment and early Alzheimer's disease. *Neurobiol Aging, 28*(3), 327-335. doi:10.1016/j.neurobiolaging.2006.02.007

Haacke, E. M., & Brown, R. W. (2014). *Signal, contrast, and noise; CH 15. In Magnetic resonance imaging: physical principles and sequence design*: J. Wiley & Sons; New York, Chicester, Weinheim.

Haacke, E. M., Mittal, S., Wu, Z., Neelavalli, J., & Cheng, Y.-C. N. (2009). Susceptibility-Weighted Imaging: Technical Aspects and Clinical Applications, Part 1. *American Journal of Neuroradiology, 30*(1), 19-30. doi:10.3174/ajnr.A1400

Hackley, S. A., Langner, R., Rolke, B., Erb, M., Grodd, W., & Ulrich, R. (2009). Separation of phasic arousal and expectancy effects in a speeded reaction time task via fMRI. *Psychophysiology, 46*(1), 163-171. doi:10.1111/j.1469-8986.2008.00722.x

Hackley, S. A., & Valle-Inclan, F. (1998). Automatic alerting does not speed late motoric processes in a reaction-time task. *Nature, 391*(6669), 786-788 doi: http://dx.doi.org/710.1038/35849.

Hackley, S. A., & Valle-Inclán, F. (1999). Accessory Stimulus Effects on Response Selection: Does Arousal Speed Decision Making? *Journal of cognitive neuroscience, 11*(3), 321-329. doi:10.1162/089892999563427

Hackley, S. A., & Valle-Inclán, F. (2003). Which stages of processing are speeded by a warning signal? *Biological Psychology, 64*(1–2), 27-45. doi:http://dx.doi.org/10.1016/S0301-0511(03)00101-7

Hajcak, G., McDonald, N., & Simons, R. F. (2003). To err is autonomic: error-related brain potentials, ANS activity, and post-error compensatory behavior. *Psychophysiology, 40*(6), 895-903 doi: http://dx.doi.org/810.1111/1469-8986.00107.

Hamill, R. W., Shapiro, R. E., & Vizzard, M. A. (2012). Chapter 4 - Peripheral Autonomic Nervous System. In D. Robertson, I. Biaggioni, G. Burnstock, P. A. Low, & J. F. R. Paton (Eds.), *Primer on the Autonomic Nervous System (Third Edition)* (pp. 17-26). San Diego: Academic Press.

Hancock, M. B., & Fougerousse, C. L. (1976). Spinal projections from the nucleus locus coeruleus and nucleus subcoeruleus in the cat and monkey as demonstrated by the retrograde transport of horseradish peroxidase. *Brain Research Bulletin, 1*(2), 229-234. doi:10.1016/0361-9230(76)90072-1

Hassert, D. L., Miyashita, T., & Williams, C. L. (2004). The effects of peripheral vagal nerve stimulation at a memory-modulating intensity on norepinephrine output in the basolateral amygdala. *Behavioral Neuroscience, 118*(1), 79-88. doi:10.1037/0735-7044.118.1.79

Hennig, J., Nauerth, A., & Friedburg, H. (1986). RARE imaging: A fast imaging method for clinical MR. *Magnetic Resonance in Medicine, 3*(6), 823-833. doi:10.1002/mrm.1910030602

Henrich, J., Heine, S. J., & Norenzayan, A. (2010). The weirdest people in the world? *Behav Brain Sci, 33*(2-3), 61-83; discussion 83-135. doi:10.1017/s0140525x0999152x

Hermans, E. J., van Marle, H. J., Ossewaarde, L., Henckens, M. J., Qin, S., van Kesteren, M. T., . . . Fernandez, G. (2011). Stress-related noradrenergic activity prompts large-scale neural network reconfiguration. *Science, 334*(6059), 1151-1153. doi:10.1126/science.1209603

Hill, S. A., Taylor, M. J., Harmer, C. J., & Cowen, P. J. (2003). Acute reboxetine administration increases plasma and salivary cortisol. *J Psychopharmacol, 17*(3), 273-275. doi:10.1177/02698811030173008

Hoffman, E. J., Huang, S. C., & Phelps, M. E. (1979). Quantitation in positron emission computed tomography: 1. Effect of object size. *J Comput Assist Tomogr, 3*(3), 299-308.

Hulsey, D. R., Riley, J. R., Loerwald, K. W., Rennaker, R. L., Kilgard, M. P., & Hays, S. A. (2017). Parametric characterization of neural activity in the locus coeruleus in response to vagus nerve stimulation. *Experimental Neurology, 289*, 21-30. doi:https://doi.org/10.1016/j.expneurol.2016.12.005

Iglói, K., Doeller, C. F., Berthoz, A., Rondi-Reig, L., & Burgess, N. (2010). Lateralized human hippocampal activity predicts navigation based on sequence or place memory.

*Proceedings of the National Academy of Sciences, 107*(32), 14466-14471. doi:10.1073/pnas.1004243107

Ishimatsu, M., & Williams, J. T. (1996). Synchronous activity in locus coeruleus results from dendritic interactions in pericoerulear regions. *The Journal of Neuroscience, 16*(16), 5196-5204.

Itoi, K., & Sugimoto, N. (2010). The Brainstem Noradrenergic Systems in Stress, Anxiety and Depression. *Journal of Neuroendocrinology, 22*(5), 355-361. doi:10.1111/j.1365-2826.2010.01988.x

Janitzky, K., Lippert, M. T., Engelhorn, A., Tegtmeier, J., Goldschmidt, J., Heinze, H. J., & Ohl, F. W. (2015). Optogenetic silencing of locus coeruleus activity in mice impairs cognitive flexibility in an attentional set-shifting task. *Front Behav Neurosci, 9*, 286. doi:10.3389/fnbeh.2015.00286

Jeffreys, H. (1961). *The theory of probability*: OUP Oxford.

Jenkinson, M., Beckmann, C. F., Behrens, T. E., Woolrich, M. W., & Smith, S. M. (2012). FSL. *NeuroImage, 62*(2), 782-790. doi:10.1016/j.neuroimage.2011.09.015

Jepma, M., Brown, S., Murphy, P. R., Koelewijn, S. C., de Vries, B., van den Maagdenberg, A. M., & Nieuwenhuis, S. (2018). Noradrenergic and Cholinergic Modulation of Belief Updating. *Journal of cognitive neuroscience*, 1-18. doi:10.1162/jocn_a_01317

Jepma, M., Murphy, P. R., Nassar, M. R., Rangel-Gomez, M., Meeter, M., & Nieuwenhuis, S. (2016). Catecholaminergic Regulation of Learning Rate in a Dynamic Environment. *PLoS Comput Biol, 12*(10), e1005171. doi:10.1371/journal.pcbi.1005171

Jepma, M., & Nieuwenhuis, S. (2010). Pupil Diameter Predicts Changes in the Exploration–Exploitation Trade-off: Evidence for the Adaptive Gain Theory. *Journal of cognitive neuroscience, 23*(7), 1587-1596. doi:10.1162/jocn.2010.21548

Jepma, M., Wagenmakers, E. J., Band, G. P., & Nieuwenhuis, S. (2009). The effects of accessory stimuli on information processing: evidence from electrophysiology and a diffusion model analysis. *Journal of cognitive neuroscience, 21*(5), 847-864. doi:10.1162/jocn.2009.21063

Jones, B. E., & Yang, T. Z. (1985). The efferent projections from the reticular formation and the locus coeruleus studied by anterograde and retrograde axonal transport in the rat. *J Comp Neurol, 242*(1), 56-92. doi:10.1002/cne.902420105

Joshi, S., Li, Y., Kalwani, Rishi M., & Gold, Joshua I. (2016). Relationships between Pupil Diameter and Neuronal Activity in the Locus Coeruleus, Colliculi, and Cingulate Cortex. *Neuron, 89*(1), 221-234. doi:http://dx.doi.org/10.1016/j.neuron.2015.11.028

Kane, G. A., Vazey, E. M., Wilson, R. C., Shenhav, A., Daw, N. D., Aston-Jones, G., & Cohen, J. D. (2017). Increased locus coeruleus tonic activity causes disengagement from a patch-foraging task. *Cogn Affect Behav Neurosci*. doi:10.3758/s13415-017-0531-y

Kehagia, A. A., Cools, R., Barker, R. A., & Robbins, T. W. (2009). Switching between abstract rules reflects disease severity but not dopaminergic status in Parkinson's disease. *Neuropsychologia, 47*(4), 1117-1127. doi:http://dx.doi.org/10.1016/j.neuropsychologia.2009.01.002

Kehagia, A. A., Murray, G. K., & Robbins, T. W. (2010). Learning and cognitive flexibility: frontostriatal function and monoaminergic modulation. *Curr Opin Neurobiol, 20*(2), 199-204. doi:10.1016/j.conb.2010.01.007

Kelly, S. C., He, B., Perez, S. E., Ginsberg, S. D., Mufson, E. J., & Counts, S. E. (2017). Locus coeruleus cellular and molecular pathology during the progression of Alzheimer's disease. *Acta Neuropathologica Communications, 5*, 8. doi:10.1186/s40478-017-0411-2

Keren, N. I., Lozar, C. T., Harris, K. C., Morgan, P. S., & Eckert, M. A. (2009). In vivo mapping of the human locus coeruleus. *NeuroImage, 47*(4), 1261-1267. doi:http://dx.doi.org/10.1016/j.neuroimage.2009.06.012

Keren, N. I., Taheri, S., Vazey, E. M., Morgan, P. S., Granholm, A. C., Aston-Jones, G. S., & Eckert, M. A. (2015). Histologic Validation of Locus Coeruleus MRI Contrast in Post-mortem Tissue. *NeuroImage*. doi:10.1016/j.neuroimage.2015.03.020

Keuken, M. C., & Forstmann, B. U. (2015). A probabilistic atlas of the basal ganglia using 7 T MRI. *Data in Brief, 4*, 577-582. doi:10.1016/j.dib.2015.07.028

Keuken, M. C., Isaacs, B. R., Trampel, R., van der Zwaag, W., & & Forstmann, B. U. (in press). Visualizing the human subcortex using ultra-high field magnetic resonance imaging. *Brain Topography*.

Kiesel, A., & Miller, J. (2007). Impact of contingency manipulations on accessory stimulus effects. *Perception & Psychophysics, 69*(7), 1117-1125. doi:10.3758/BF03193949

Kindt, M., Soeter, M., & Vervliet, B. (2009). Beyond extinction: erasing human fear responses and preventing the return of fear. *Nature Neuroscience, 12*(3), 256-258. doi:10.1038/nn.2271

Kneeland, J. B., Shimakawa, A., & Wehrli, F. W. (1986). Effect of intersection spacing on MR image contrast and study time. *Radiology, 158*(3), 819-822. doi:10.1148/radiology.158.3.3945757

Koda, K., Ago, Y., Cong, Y., Kita, Y., Takuma, K., & Matsuda, T. (2010). Effects of acute and chronic administration of atomoxetine and methylphenidate on extracellular levels of noradrenaline, dopamine and serotonin in the prefrontal cortex and striatum of mice. *J Neurochem, 114*(1), 259-270. doi:10.1111/j.1471-4159.2010.06750.x

Kraus, T., Hosl, K., Kiess, O., Schanze, A., Kornhuber, J., & Forster, C. (2007). BOLD fMRI deactivation of limbic and temporal brain structures and mood enhancing effect by transcutaneous vagus nerve stimulation. *J Neural Transm (Vienna), 114*(11), 1485-1493. doi:10.1007/s00702-007-0755-z

Kraus, T., Kiess, O., Hosl, K., Terekhin, P., Kornhuber, J., & Forster, C. (2013). CNS BOLD fMRI effects of sham-controlled transcutaneous electrical nerve stimulation in the left outer auditory canal - a pilot study. *Brain Stimul, 6*(5), 798-804. doi:10.1016/j.brs.2013.01.011

Kroes, M. C., Tona, K. D., den Ouden, H. E., Vogel, S., van Wingen, G. A., & Fernandez, G. (2016). How Administration of the Beta-Blocker Propranolol Before Extinction can Prevent the Return of Fear. *Neuropsychopharmacology, 41*(6), 1569-1578. doi:10.1038/npp.2015.315

Lakatos, P., Karmos, G., Mehta, A. D., Ulbert, I., & Schroeder, C. E. (2008). Entrainment of neuronal oscillations as a mechanism of attentional selection. *Science, 320*(5872), 110-113. doi:10.1126/science.1154735

Langley, J., Huddleston, D. E., Liu, C. J., & Hu, X. (2016). Reproducibility of locus coeruleus and substantia nigra imaging with neuromelanin sensitive MRI. *MAGMA*. doi:10.1007/s10334-016-0590-z

Lapiz, M. D., & Morilak, D. A. (2006). Noradrenergic modulation of cognitive function in rat medial prefrontal cortex as measured by attentional set shifting capability. *Neuroscience, 137*(3), 1039-1049. doi:10.1016/j.neuroscience.2005.09.031

Lawrence, M. A., & Klein, R. M. (2013). Isolating exogenous and endogenous modes of temporal attention. *Journal of Experimental Psychology: General, 142*(2), 560-572. doi:10.1037/a0029023

Lee, J. H., Baek, S. Y., Song, Y., Lim, S., Lee, H., Nguyen, M. P., . . . Cho, H. (2016). The Neuromelanin-related T2* Contrast in Postmortem Human Substantia Nigra with 7T MRI. *Sci Rep, 6*, 32647. doi:10.1038/srep32647

Leong, S. K., Shieh, J. Y., & Wong, W. C. (1984). Localizing spinal-cord-projecting neurons in neonatal and immature albino rats. *J Comp Neurol, 228*(1), 18-23. doi:10.1002/cne.902280104

Lerman, I., Davis, B., Huang, M., Huang, C., Sorkin, L., Proudfoot, J., . . . Simmons, A. N. (2019). Noninvasive vagus nerve stimulation alters neural response and physiological autonomic

tone to noxious thermal challenge. *PLoS One, 14*(2), e0201212. doi:10.1371/journal.pone.0201212

Liu, K. Y., Marijatta, F., Hämmerer, D., Acosta-Cabronero, J., Düzel, E., & Howard, R. J. (2017). Magnetic resonance imaging of the human locus coeruleus: A systematic review. *Neuroscience & Biobehavioral Reviews, 83*(Supplement C), 325-355. doi:https://doi.org/10.1016/j.neubiorev.2017.10.023

Logan, G. D., & Bundesen, C. (2003). Clever homunculus: is there an endogenous act of control in the explicit task-cuing procedure? *Journal of Experimental Psychology: Human Perception and Performance, 29*(3), 575-599.

Lohr, J. B., & Jeste, D. V. (1988). Locus ceruleus morphometry in aging and schizophrenia. *Acta Psychiatr Scand, 77*(6), 689-697.

Lonergan, M. H., Olivera-Figueroa, L. A., Pitman, R. K., & Brunet, A. (2013). Propranolol's effects on the consolidation and reconsolidation of long-term emotional memory in healthy participants: a meta-analysis. *Journal of psychiatry & neuroscience : JPN, 38*(4), 222-231. doi:10.1503/jpn.120111

Lupien, S. J., Maheu, F., Tu, M., Fiocco, A., & Schramek, T. E. (2007). The effects of stress and stress hormones on human cognition: Implications for the field of brain and cognition. *Brain Cogn, 65*(3), 209-237. doi:10.1016/j.bandc.2007.02.007

Manaye, K. F., McIntire, D. D., Mann, D. M., & German, D. C. (1995). Locus coeruleus cell loss in the aging human brain: a non-random process. *J Comp Neurol, 358*(1), 79-87. doi:10.1002/cne.903580105

Mann, D. M., & Yates, P. O. (1974). Lipoprotein pigments--their relationship to ageing in the human nervous system. II. The melanin content of pigmented nerve cells. *Brain, 97*(3), 489-498.

Manta, S., El Mansari, M., Debonnel, G., & Blier, P. (2013). Electrophysiological and neurochemical effects of long-term vagus nerve stimulation on the rat monoaminergic systems. *International Journal of Neuropsychopharmacology, 16*(2), 459-470. doi:10.1017/s1461145712000387

Martlé, V., Raedt, R., Waelbers, T., Smolders, I., Vonck, K., Boon, P., . . . Bhatti, S. (2015). The Effect of Vagus Nerve Stimulation on CSF Monoamines and the PTZ Seizure Threshold in Dogs. *Brain Stimul, 8*(1), 1-6. doi:https://doi.org/10.1016/j.brs.2014.07.032

Mather, M., Clewett, D., Sakaki, M., & Harley, C. W. (2015). Norepinephrine ignites local hot spots of neuronal excitation: How arousal amplifies selectivity in perception and memory. *Behavioral and Brain Sciences, FirstView*, 1-100. doi:doi:10.1017/S0140525X15000667

Mather, M., Clewett, D., Sakaki, M., & Harley, C. W. (2016). Norepinephrine ignites local hotspots of neuronal excitation: How arousal amplifies selectivity in perception and memory. *Behav Brain Sci, 39*, e200. doi:10.1017/s0140525x15000667

Mather, M., Joo Yoo, H., Clewett, D. V., Lee, T.-H., Greening, S. G., Ponzio, A., . . . Thayer, J. F. (2017). Higher locus coeruleus MRI contrast is associated with lower parasympathetic influence over heart rate variability. *NeuroImage, 150*, 329-335. doi:https://doi.org/10.1016/j.neuroimage.2017.02.025

Matias, S., Lottem, E., Dugué, G. P., & Mainen, Z. F. (2017). Activity patterns of serotonin neurons underlying cognitive flexibility. *eLife, 6*, e20552. doi:10.7554/eLife.20552

Matsuura, K., Maeda, M., Yata, K., Ichiba, Y., Yamaguchi, T., Kanamaru, K., & Tomimoto, H. (2013). Neuromelanin Magnetic Resonance Imaging in Parkinson's Disease and Multiple System Atrophy. *European Neurology, 70*(1-2), 70-77.

McGraw, K. O., & Wong, S. P. (1996). Forming inferences about some intraclass correlation coefficients. *Psychological Methods, 1*(1), 30-46. doi:10.1037/1082-989X.1.1.30

McRobbie, D. W., Moore, E. A., Graves, M. J., & Prince, M. R. (2017). *MRI from Picture to Proton* (3 ed.). Cambridge: Cambridge University Press.

Miyoshi, F., Ogawa, T., Kitao, S.-i., Kitayama, M., Shinohara, Y., Takasugi, M., . . . Kaminou, T. (2013). Evaluation of Parkinson Disease and Alzheimer Disease with the Use of Neuromelanin MR Imaging and <sup>123</sup>I-Metaiodobenzylguanidine Scintigraphy. *American Journal of Neuroradiology, 34*(11), 2113-2118. doi:10.3174/ajnr.A3567

Mollet, L., Grimonprez, A., Raedt, R., Delbeke, J., El Tahry, R., De Herdt, V., . . . Vonck, K. (2013). Intensity-dependent modulatory effects of vagus nerve stimulation on cortical excitability. *Acta Neurol Scand, 128*(6), 391-396. doi:10.1111/ane.12135

Monsell, S., & Mizon, G. A. (2006). Can the task-cuing paradigm measure an endogenous task-set reconfiguration process? *Journal of Experimental Psychology: Human Perception and Performance, 32*(3), 493-516. doi:10.1037/0096-1523.32.3.493

Monsell, S., Sumner, P., & Waters, H. (2003). Task-set reconfiguration with predictable and unpredictable task switches. *Mem Cognit, 31*(3), 327-342.

Morey, R. A., Selgrade, E. S., Wagner, H. R., 2nd, Huettel, S. A., Wang, L., & McCarthy, G. (2010). Scan-rescan reliability of subcortical brain volumes derived from automated segmentation. *Human brain mapping, 31*(11), 1751-1762. doi:10.1002/hbm.20973

Morey, R. D., & Rouder, J. N. (2013). Package "BayesFactor". R package version 0.9.7.

Morey, R. D., & Rouder, J. N. (2015). BayesFactor (Version 0.9.10-2)[Windows].

Mouton, P. R., Pakkenberg, B., Gundersen, H. J. G., & Price, D. L. (1994). Absolute number and size of pigmented locus coeruleus neurons in young and aged individuals. *Journal of Chemical Neuroanatomy, 7*(3), 185-190. doi:http://dx.doi.org/10.1016/0891-0618(94)90028-0

Mravec, B., Lejavova, K., & Cubinkova, V. (2014). Locus (coeruleus) minoris resistentiae in pathogenesis of Alzheimer's disease. *Curr Alzheimer Res, 11*(10), 992-1001.

Murphy, P. R., O'Connell, R. G., O'Sullivan, M., Robertson, I. H., & Balsters, J. H. (2014). Pupil diameter covaries with BOLD activity in human locus coeruleus. *Human brain mapping, 35*(8), 4140-4154. doi:10.1002/hbm.22466

Murphy, P. R., Robertson, I. H., Balsters, J. H., & O'Connell R, G. (2011). Pupillometry and P3 index the locus coeruleus-noradrenergic arousal function in humans. *Psychophysiology, 48*(11), 1532-1543. doi:10.1111/j.1469-8986.2011.01226.x

Murphy, P. R., van Moort, M. L., & Nieuwenhuis, S. (2016). The Pupillary Orienting Response Predicts Adaptive Behavioral Adjustment after Errors. *PLoS One, 11*(3), e0151763. doi:10.1371/journal.pone.0151763

Murphy, P. R., Vandekerckhove, J., & Nieuwenhuis, S. (2014). Pupil-linked arousal determines variability in perceptual decision making. *PLoS Comput Biol, 10*(9), e1003854. doi:10.1371/journal.pcbi.1003854

Musacchio, J. M. (1975). Enzymes Involved in the Biosynthesis and Degradation of Catecholamines. In L. L. Iversen, S. D. Iversen, & S. H. Snyder (Eds.), *Biochemistry of Biogenic Amines* (pp. 1-35). Boston, MA: Springer US.

Nagy, T., van Lien, R., Willemsen, G., Proctor, G., Efting, M., Fulop, M., . . . Bosch, J. A. (2015). A fluid response: Alpha-amylase reactions to acute laboratory stress are related to sample timing and saliva flow rate. *Biol Psychol, 109*, 111-119. doi:10.1016/j.biopsycho.2015.04.012

Naidich, T. P., Duvernoy, H. M., Delman, B. N., Sorensen, A. G., Kollias, S. S., & Haacke, E. M. (2009). *Duvernoy's atlas of the human brain stem and cerebellum* Wien: SpringerWienNewYork.

Nakane, T., Nihashi, T., Kawai, H., & Naganawa, S. (2008). Visualization of Neuromelanin in the Substantia Nigra and Locus Ceruleus at 1.5T Using a 3D-gradient Echo Sequence with Magnetization Transfer Contrast. *Magnetic Resonance in Medical Sciences, 7*(4), 205-210. doi:10.2463/mrms.7.205

Nemeroff, C. B., Mayberg, H. S., Krahl, S. E., McNamara, J., Frazer, A., Henry, T. R., . . . Brannan, S. K. (2006). VNS therapy in treatment-resistant depression: clinical evidence and putative neurobiological mechanisms. *Neuropsychopharmacology, 31*(7), 1345-1355. doi:10.1038/sj.npp.1301082

Neuhaus, A. H., Luborzewski, A., Rentzsch, J., Brakemeier, E. L., Opgen-Rhein, C., Gallinat, J., & Bajbouj, M. (2007). P300 is enhanced in responders to vagus nerve stimulation for treatment of major depressive disorder. *J Affect Disord, 100*(1-3), 123-128. doi:10.1016/j.jad.2006.10.005

Nieuwenhuis, S., Aston-Jones, G., & Cohen, J. D. (2005). Decision making, the P3, and the locus coeruleus-norepinephrine system. *Psychol Bull, 131*(4), 510-532. doi:10.1037/0033-2909.131.4.510

Nieuwenhuis, S., De Geus, E. J., & Aston-Jones, G. (2011). The anatomical and functional relationship between the P3 and autonomic components of the orienting response. *Psychophysiology, 48*(2), 162-175. doi:10.1111/j.1469-8986.2010.01057.x

Nieuwenhuis, S., & de Kleijn, R. (2013). The impact of alertness on cognitive control. *Journal of Experimental Psychology: Human Perception and Performance, 39*(6), 1797-1801. doi:10.1037/a0033980

Nieuwenhuis, S., Forstmann, B. U., & Wagenmakers, E.-J. (2011). Erroneous analyses of interactions in neuroscience: a problem of significance. *Nature Neuroscience, 14*(9), 1105-1107.

Nieuwenhuys, R., Voogd, J., & van Huijzen, C. (2013). *The Human Central Nervous System: A Synopsis and Atlas*: Springer Berlin Heidelberg.

Ogisu, K., Kudo, K., Sasaki, M., Sakushima, K., Yabe, I., Sasaki, H., . . . Shirato, H. (2013). 3D neuromelanin-sensitive magnetic resonance imaging with semi-automated volume measurement of the substantia nigra pars compacta for diagnosis of Parkinson's disease. *Neuroradiology, 55*(6), 719-724. doi:10.1007/s00234-013-1171-8

Ohm, T. G., Busch, C., & Bohl, J. (1997). Unbiased Estimation of Neuronal Numbers in the Human Nucleus Coeruleus during Aging. *Neurobiology of Aging, 18*(4), 393-399. doi:http://dx.doi.org/10.1016/S0197-4580(97)00034-1

Ohtsuka, C., Sasaki, M., Konno, K., Koide, M., Kato, K., Takahashi, J., . . . Terayama, Y. (2013). Changes in substantia nigra and locus coeruleus in patients with early-stage Parkinson's disease using neuromelanin-sensitive MR imaging. *Neuroscience Letters, 541*(0), 93-98. doi:http://dx.doi.org/10.1016/j.neulet.2013.02.012

Oyola, M. G., & Handa, R. J. (2017). Hypothalamic-pituitary-adrenal and hypothalamic-pituitary-gonadal axes: sex differences in regulation of stress responsivity. *Stress, 20*(5), 476-494. doi:10.1080/10253890.2017.1369523

Pajkossy, P., Szollosi, A., Demeter, G., & Racsmany, M. (2018). Physiological Measures of Dopaminergic and Noradrenergic Activity During Attentional Set Shifting and Reversal. *Frontiers in psychology, 9*, 506. doi:10.3389/fpsyg.2018.00506

Paxinos, G., & Feng Huang, X. ( c1995). *Atlas of the human brainstem*: Academic Press.

Peuker, E. T., & Filler, T. J. (2002). The nerve supply of the human auricle. *Clinical Anatomy, 15*(1), 35-37. doi:10.1002/ca.1089

Pfaff, D. W., Martin, E. M., & Faber, D. (2012). Origins of arousal: roles for medullary reticular neurons. *Trends Neurosci, 35*(8), 468-476. doi:10.1016/j.tins.2012.04.008

Pfeffer, T., Avramiea, A. E., Nolte, G., Engel, A. K., Linkenkaer-Hansen, K., & Donner, T. H. (2018). Catecholamines alter the intrinsic variability of cortical population activity and perception. *PLoS Biol, 16*(2), e2003453. doi:10.1371/journal.pbio.2003453

Pineda, J. A., Foote, S. L., & Neville, H. J. (1987). The effects of locus coeruleus lesions on a squirrel monkey late positive component: a preliminary study. *Electroencephalogr Clin Neurophysiol Suppl, 40*, 481-486.

Plessow, F., Kiesel, A., & Kirschbaum, C. (2012). The stressed prefrontal cortex and goal-directed behaviour: acute psychosocial stress impairs the flexible implementation of task goals. *Exp Brain Res, 216*(3), 397-408. doi:10.1007/s00221-011-2943-1

Posner, M. I. (1978). *Chronometric explorations of mind*. Oxford, England: Lawrence Erlbaum.

Posner, M. I., Klein, R., Summers, J., & Buggie, S. (1973). On the selection of signals. *Memory & Cognition, 1*(1), 2-12. doi:10.3758/BF03198062

Pringsheim, T., Hirsch, L., Gardner, D., & Gorman, D. A. (2015). The pharmacological management of oppositional behaviour, conduct problems, and aggression in children and adolescents with attention-deficit hyperactivity disorder, oppositional defiant disorder, and conduct disorder: a systematic review and meta-analysis. Part 1: psychostimulants, alpha-2 agonists, and atomoxetine. *Can J Psychiatry, 60*(2), 42-51. doi:10.1177/070674371506000202

Priovoulos, N., Jacobs, H. I. L., Ivanov, D., Uludag, K., Verhey, F. R. J., & Poser, B. A. (2017). High-resolution in vivo imaging of human locus coeruleus by magnetization transfer MRI at 3T and 7T. *NeuroImage*. doi:http://dx.doi.org/10.1016/j.neuroimage.2017.07.045

Qiao, L., Zhang, L., Chen, A., & Egner, T. (2017). Dynamic Trial-by-Trial Recoding of Task-Set Representations in the Frontoparietal Cortex Mediates Behavioral Flexibility. *The Journal of Neuroscience, 37*(45), 11037-11050. doi:10.1523/jneurosci.0935-17.2017

R-Development_Core_Team. (2013). R: A Language and Environment for Statistical Computing. *R Foundation for Statistical Computing; Vienna, Austria; http://www.R-project.org/*.

R Development Core Team. (2008). R: A language and environment for statistical computing (Version version 3.2.4). Vienna, Austria: R Foundation for Statistical Computing. Retrieved from https://www.R-project.org/

Raedt, R., Clinckers, R., Mollet, L., Vonck, K., El Tahry, R., Wyckhuys, T., . . . Meurs, A. (2011). Increased hippocampal noradrenaline is a biomarker for efficacy of vagus nerve stimulation in a limbic seizure model. *J Neurochem, 117*(3), 461-469. doi:10.1111/j.1471-4159.2011.07214.x

Reimer, J., Froudarakis, E., Cadwell, Cathryn R., Yatsenko, D., Denfield, George H., & Tolias, Andreas S. (2014). Pupil Fluctuations Track Fast Switching of Cortical States during Quiet Wakefulness. *Neuron, 84*(2), 355-362. doi:http://dx.doi.org/10.1016/j.neuron.2014.09.033

Ressler, K. J., & Nemeroff, C. B. (1999). Role of norepinephrine in the pathophysiology and treatment of mood disorders. *Biological Psychiatry, 46*(9), 1219-1233. doi:http://dx.doi.org/10.1016/S0006-3223(99)00127-4

Roosevelt, R. W., Smith, D. C., Clough, R. W., Jensen, R. A., & Browning, R. A. (2006). Increased extracellular concentrations of norepinephrine in cortex and hippocampus following vagus nerve stimulation in the rat. *Brain Research, 1119*(1), 124-132. doi:http://dx.doi.org/10.1016/j.brainres.2006.08.048

Rorden, C., & Brett, M. (2000). Stereotaxic display of brain lesions. *Behav Neurol, 12*(4), 191-200.

Rouder, J. N., Morey, R. D., Speckman, P. L., & Province, J. M. (2012). Default Bayes factors for ANOVA designs. *Journal of Mathematical Psychology, 56*(5), 356-374.

Ruffoli, R., Giorgi, F. S., Pizzanelli, C., Murri, L., Paparelli, A., & Fornai, F. (2011). The chemical neuroanatomy of vagus nerve stimulation. *J Chem Neuroanat, 42*(4), 288-296. doi:10.1016/j.jchemneu.2010.12.002

Safaai, H., Neves, R., Eschenko, O., Logothetis, N. K., & Panzeri, S. (2015). Modeling the effect of locus coeruleus firing on cortical state dynamics and single-trial sensory processing. *Proceedings of the National Academy of Sciences of the United States of America, 112*(41), 12834-12839. doi:10.1073/pnas.1516539112

Sales, A. C., Friston, K. J., Jones, M. W., Pickering, A. E., & Moran, R. J. (2019). Locus Coeruleus tracking of prediction errors optimises cognitive flexibility: An Active Inference model. *PLoS Comput Biol, 15*(1), e1006267. doi:10.1371/journal.pcbi.1006267

Samuels, E. R., & Szabadi, E. (2008a). Functional neuroanatomy of the noradrenergic locus coeruleus: its roles in the regulation of arousal and autonomic function part I: principles of functional organisation. *Current neuropharmacology, 6*(3), 235-253. doi:10.2174/157015908785777229

Samuels, E. R., & Szabadi, E. (2008b). Functional neuroanatomy of the noradrenergic locus coeruleus: its roles in the regulation of arousal and autonomic function part II: physiological and pharmacological manipulations and pathological alterations of locus coeruleus activity in humans. *Current neuropharmacology, 6*(3), 254-285. doi:10.2174/157015908785777193

Sanders, A. F. (1975). The foreperiod effect revisited. *Quarterly Journal of Experimental Psychology, 27*(4), 591-598. doi:10.1080/14640747508400522

Sanders, A. F. (1980). 20 Stage Analysis of Reaction Processes. In E. S. George & R. Jean (Eds.), *Advances in Psychology* (Vol. Volume 1, pp. 331-354): North-Holland.

Sara, S. J. (2009). The locus coeruleus and noradrenergic modulation of cognition. *Nat Rev Neurosci, 10*(3), 211-223. doi:10.1038/nrn2573

Sara, S. J., & Bouret, S. (2012). Orienting and Reorienting: The Locus Coeruleus Mediates Cognition through Arousal. *Neuron, 76*(1), 130-141.

Sasaki, M., Shibata, E., Tohyama, K., Kudo, K., Endoh, J., Otsuka, K., & Sakai, A. (2008). Monoamine neurons in the human brain stem: anatomy, magnetic resonance imaging findings, and clinical implications. *Neuroreport, 19*(17), 1649-1654. doi:10.1097/WNR.0b013e328315a637

Sasaki, M., Shibata, E., Tohyama, K., Takahashi, J., Otsuka, K., Tsuchiya, K., . . . Sakai, A. (2006). Neuromelanin magnetic resonance imaging of locus ceruleus and substantia nigra in Parkinson's disease. *Neuroreport, 17*(11), 1215-1218. doi:10.1097/01.wnr.0000227984.84927.a7

Scheibehenne, B., Jamil, T., & Wagenmakers, E. J. (2016). Bayesian Evidence Synthesis Can Reconcile Seemingly Inconsistent Results: The Case of Hotel Towel Reuse. *Psychol Sci, 27*(7), 1043-1046. doi:10.1177/0956797616644081

Schevernels, H., van Bochove, M. E., De Taeye, L., Bombeke, K., Vonck, K., Van Roost, D., . . . Boehler, C. N. (2016). The effect of vagus nerve stimulation on response inhibition. *Epilepsy Behav, 64*(Pt A), 171-179. doi:10.1016/j.yebeh.2016.09.014

Schramm, N. L., McDonald, M. P., & Limbird, L. E. (2001). The α2A-Adrenergic Receptor Plays a Protective Role in Mouse Behavioral Models of Depression and Anxiety. *The Journal of Neuroscience, 21*(13), 4875-4882.

Schwabe, L., & Schachinger, H. (2018). Ten years of research with the Socially Evaluated Cold Pressor Test: Data from the past and guidelines for the future. *Psychoneuroendocrinology, 92*, 155-161. doi:10.1016/j.psyneuen.2018.03.010

Sclocco, R., Beissner, F., Bianciardi, M., Polimeni, J. R., & Napadow, V. (2017). Challenges and opportunities for brainstem neuroimaging with ultrahigh field MRI. *NeuroImage*. doi:10.1016/j.neuroimage.2017.02.052

Seibold, V. C., Bausenhart, K. M., Rolke, B., & Ulrich, R. (2011). Does temporal preparation increase the rate of sensory information accumulation? *Acta Psychologica, 137*(1), 56-64. doi:10.1016/j.actpsy.2011.02.006

Seifried, T., Ulrich, R., Bausenhart, K. M., Rolke, B., & Osman, A. (2010). Temporal preparation decreases perceptual latency: evidence from a clock paradigm. *The Quarterly journal of experimental psychology, 63*(12), 2432-2451. doi:10.1080/17470218.2010.485354

Sellaro, R., van Leusden, J. W., Tona, K. D., Verkuil, B., Nieuwenhuis, S., & Colzato, L. S. (2015). Transcutaneous Vagus Nerve Stimulation Enhances Post-error Slowing. *Journal of cognitive neuroscience, 27*(11), 2126-2132. doi:10.1162/jocn_a_00851

Servan-Schreiber, D., Printz, H., & Cohen, J. D. (1990). A network model of catecholamine effects: gain, signal-to-noise ratio, and behavior. *Science, 249*(4971), 892-895 doi: http://dx.doi.org/810.1126/science.2392679.

Sharma, A., & Couture, J. (2014). A review of the pathophysiology, etiology, and treatment of attention-deficit hyperactivity disorder (ADHD). *Ann Pharmacother, 48*(2), 209-225. doi:10.1177/1060028013510699

Shibata, E., Sasaki, M., Tohyama, K., Kanbara, Y., Otsuka, K., Ehara, S., & Sakai, A. (2006). Age-related changes in locus ceruleus on neuromelanin magnetic resonance imaging at 3 Tesla. *Magn Reson Med Sci, 5*(4), 197-200.

Smith, S. M., Jenkinson, M., Woolrich, M. W., Beckmann, C. F., Behrens, T. E., Johansen-Berg, H., . . . Matthews, P. M. (2004). Advances in functional and structural MR image analysis and implementation as FSL. *NeuroImage, 23 Suppl 1*, S208-219. doi:10.1016/j.neuroimage.2004.07.051

Speirs, R. L., Herring, J., Cooper, W. D., Hardy, C. C., & Hind, C. R. (1974). The influence of sympathetic activity and isoprenaline on the secretion of amylase from the human parotid gland. *Arch Oral Biol, 19*(9), 747-752. doi:10.1016/0003-9969(74)90161-7

Stahl, J., & Rammsayer, T. H. (2005). Accessory stimulation in the time course of visuomotor information processing: stimulus intensity effects on reaction time and response force. *Acta Psychologica, 120*(1), 1-18. doi:10.1016/j.actpsy.2005.02.003

Steenbergen, L., Sellaro, R., de Rover, M., Hommel, B., & Colzato, L. S. (2015). No role of beta receptors in cognitive flexibility: Evidence from a task-switching paradigm in a randomized controlled trial. *Neuroscience, 295*, 237-242. doi:https://doi.org/10.1016/j.neuroscience.2015.03.049

Steenbergen, L., Sellaro, R., Stock, A. K., Verkuil, B., Beste, C., & Colzato, L. S. (2015). Transcutaneous vagus nerve stimulation (tVNS) enhances response selection during action cascading processes. *Eur Neuropsychopharmacol, 25*(6), 773-778. doi:10.1016/j.euroneuro.2015.03.015

Steinhauser, M., Maier, M., & Hübner, R. (2007). Cognitive Control Under Stress: How Stress Affects Strategies of Task-Set Reconfiguration. *Psychological Science, 18*(6), 540-545. doi:10.1111/j.1467-9280.2007.01935.x

Strahler, J., Skoluda, N., Kappert, M. B., & Nater, U. M. (2017). Simultaneous measurement of salivary cortisol and alpha-amylase: Application and recommendations. *Neurosci Biobehav Rev, 83*, 657-677. doi:10.1016/j.neubiorev.2017.08.015

Sutton, S., Braren, M., Zubin, J., & John, E. R. (1965). Evoked-potential correlates of stimulus uncertainty. *Science, 150*(3700), 1187-1188. doi:10.1126/science.150.3700.1187

Swick, D., Pineda, J. A., & Foote, S. L. (1994). Effects of systemic clonidine on auditory event-related potentials in squirrel monkeys. *Brain Research Bulletin, 33*(1), 79-86.

Tait, D. S., Brown, V. J., Farovik, A., Theobald, D. E., Dalley, J. W., & Robbins, T. W. (2007). Lesions of the dorsal noradrenergic bundle impair attentional set-shifting in the rat. *European Journal of Neuroscience, 25*(12), 3719-3724. doi:10.1111/j.1460-9568.2007.05612.x

Takahashi, J., Shibata, T., Sasaki, M., Kudo, M., Yanezawa, H., Obara, S., . . . Terayama, Y. (2015). Detection of changes in the locus coeruleus in patients with mild cognitive impairment and Alzheimer's disease: high-resolution fast spin-echo T1-weighted imaging. *Geriatr Gerontol Int, 15*(3), 334-340. doi:10.1111/ggi.12280

Tobaldini, E., Toschi-Dias, E., Appratto de Souza, L., Rabello Casali, K., Vicenzi, M., Sandrone, G., . . . Montano, N. (2019). Cardiac and Peripheral Autonomic Responses to Orthostatic Stress During Transcutaneous Vagus Nerve Stimulation in Healthy Subjects. *J Clin Med, 8*(4). doi:10.3390/jcm8040496

Tona, K.-D., Keuken, M. C., de Rover, M., Lakke, E., Forstmann, B. U., Nieuwenhuis, S., & van Osch, M. J. P. (2017). In vivo visualization of the locus coeruleus in humans: quantifying the test–retest reliability. *Brain Structure and Function*. doi:10.1007/s00429-017-1464-5

Trujillo, P., Summers, P. E., Ferrari, E., Zucca, F. A., Sturini, M., Mainardi, L. T., . . . Costa, A. (2016). Contrast mechanisms associated with neuromelanin-MRI. *Magnetic Resonance in Medicine*, n/a-n/a. doi:10.1002/mrm.26584

Usher, M., Cohen, J. D., Servan-Schreiber, D., Rajkowski, J., & Aston-Jones, G. (1999). The Role of Locus Coeruleus in the Regulation of Cognitive Performance. *Science, 283*(5401), 549-554. doi:10.1126/science.283.5401.549

Valentino, R. J., & Van Bockstaele, E. (2008). Convergent regulation of locus coeruleus activity as an adaptive response to stress. *European Journal of Pharmacology, 583*(2–3), 194-203. doi:http://dx.doi.org/10.1016/j.ejphar.2007.11.062

van Bodegom, M., Homberg, J. R., & Henckens, M. (2017). Modulation of the Hypothalamic-Pituitary-Adrenal Axis by Early Life Stress Exposure. *Front Cell Neurosci, 11*, 87. doi:10.3389/fncel.2017.00087

van den Brink, R. L., Nieuwenhuis, S., & Donner, T. H. (2018). Amplification and Suppression of Distinct Brainwide Activity Patterns by Catecholamines. *The Journal of Neuroscience, 38*(34), 7476-7491. doi:10.1523/jneurosci.0514-18.2018

van den Brink, R. L., Wynn, S. C., & Nieuwenhuis, S. (2014). Post-error slowing as a consequence of disturbed low-frequency oscillatory phase entrainment. *The Journal of Neuroscience, 34*(33), 11096-11105. doi:10.1523/jneurosci.4991-13.2014

van der Zwaag, W., Schafer, A., Marques, J. P., Turner, R., & Trampel, R. (2016). Recent applications of UHF-MRI in the study of human brain function and structure: a review. *NMR Biomed, 29*(9), 1274-1288. doi:10.1002/nbm.3275

van Kammen, D. P., & Kelley, M. (1991). Dopamine and norepinephrine activity in schizophrenia. An integrative perspective. *Schizophr Res, 4*(2), 173-191.

Van Rullen, R., Busch, N. A., Drewes, J., & Dubois, J. (2011). Ongoing EEG Phase as a Trial-by-Trial Predictor of Perceptual and Attentional Variability. *Frontiers in psychology, 2*, 60. doi:10.3389/fpsyg.2011.00060

van Steenbergen, H., & Band, G. P. (2013). Pupil dilation in the Simon task as a marker of conflict processing. *Frontiers in Human Neuroscience, 7*, 215. doi:10.3389/fnhum.2013.00215

van Stegeren, A., Rohleder, N., Everaerd, W., & Wolf, O. T. (2006). Salivary alpha amylase as marker for adrenergic activity during stress: Effect of betablockade. *Psychoneuroendocrinology, 31*(1), 137-141. doi:http://dx.doi.org/10.1016/j.psyneuen.2005.05.012

Varazzani, C., San-Galli, A., Gilardeau, S., & Bouret, S. (2015). Noradrenaline and dopamine neurons in the reward/effort trade-off: a direct electrophysiological comparison in behaving monkeys. *The Journal of Neuroscience, 35*(20), 7866-7877. doi:10.1523/jneurosci.0454-15.2015

Ventura-Bort, C., Wirkner, J., Genheimer, H., Wendt, J., Hamm, A. O., & Weymar, M. (2018). Effects of Transcutaneous Vagus Nerve Stimulation (tVNS) on the P300 and Alpha-Amylase Level: A Pilot Study. *Frontiers in Human Neuroscience, 12*, 202. doi:10.3389/fnhum.2018.00202

Versluis, M. J., Peeters, J. M., van Rooden, S., van der Grond, J., van Buchem, M. A., Webb, A. G., & van Osch, M. J. P. (2010). Origin and reduction of motion and f0 artifacts in high resolution T2*-weighted magnetic resonance imaging: Application in Alzheimer's disease patients. *NeuroImage, 51*(3), 1082-1088. doi:http://dx.doi.org/10.1016/j.neuroimage.2010.03.048

Vijayashankar, N., & Brody, H. (1979). A Quantitative Study of the Pigmented Neurons in the Nuclei Locus Coeruleus and Subcoeruleus in Man as Related to Aging. *Journal of Neuropathology & Experimental Neurology, 38*(5), 490-497. doi:10.1097/00005072-197909000-00004

Vinck, M., Batista-Brito, R., Knoblich, U., & Cardin, J. A. (2015). Arousal and locomotion make distinct contributions to cortical activity patterns and visual encoding. *Neuron, 86*(3), 740-754. doi:10.1016/j.neuron.2015.03.028

Vonck, K., Raedt, R., Naulaerts, J., De Vogelaere, F., Thiery, E., Van Roost, D., . . . Boon, P. (2014). Vagus nerve stimulation...25 years later! What do we know about the effects on cognition? *Neurosci Biobehav Rev, 45*, 63-71. doi:10.1016/j.neubiorev.2014.05.005

Vos, S. B., Jones, D. K., Viergever, M. A., & Leemans, A. (2011). Partial volume effect as a hidden covariate in DTI analyses. *NeuroImage, 55*(4), 1566-1576. doi:10.1016/j.neuroimage.2011.01.048

Waldman, S. (2009). Chapter 11 - The Vagus Nerve—Cranial Nerve X. In (pp. p. 29–34): Pain Rev.

Walker, S. C., Robbins, T. W., & Roberts, A. C. (2009). Differential contributions of dopamine and serotonin to orbitofrontal cortex function in the marmoset. *Cereb Cortex, 19*(4), 889-898. doi:10.1093/cercor/bhn136

Warren, C. M., & Holroyd, C. B. (2012). The Impact of Deliberative Strategy Dissociates ERP Components Related to Conflict Processing vs. Reinforcement Learning. *Front Neurosci, 6*, 43. doi:10.3389/fnins.2012.00043

Warren, C. M., Tanaka, J. W., & Holroyd, C. B. (2011). What can topology changes in the oddball N2 reveal about underlying processes? *Neuroreport, 22*(17), 870-874. doi:10.1097/WNR.0b013e32834bbe1f

Warren, C. M., Tona, K. D., Ouwerkerk, L., van Paridon, J., Poletiek, F., van Steenbergen, H., . . . Nieuwenhuis, S. (2019). The neuromodulatory and hormonal effects of transcutaneous vagus nerve stimulation as evidenced by salivary alpha amylase, salivary cortisol, pupil diameter, and the P3 event-related potential. *Brain Stimul, 12*(3), 635-642. doi:10.1016/j.brs.2018.12.224

Warren, C. M., van den Brink, R. L., Nieuwenhuis, S., & Bosch, J. A. (2017). Norepinephrine transporter blocker atomoxetine increases salivary alpha amylase. *Psychoneuroendocrinology, 78*, 233-236. doi:10.1016/j.psyneuen.2017.01.029

Warren, C. M., Wilson, R. C., van der Wee, N. J., Giltay, E. J., van Noorden, M. S., Cohen, J. D., & Nieuwenhuis, S. (2017). The effect of atomoxetine on random and directed exploration in humans. *PLoS One, 12*(4), e0176034. doi:10.1371/journal.pone.0176034

Weiskopf, N., Mohammadi, S., Lutti, A., & Callaghan, M. F. (2015). Advances in MRI-based computational neuroanatomy: from morphometry to in-vivo histology. *Curr Opin Neurol, 28*(4), 313-322. doi:10.1097/wco.0000000000000222

Weiskopf, N., Suckling, J., Williams, G., Correia, M. M., Inkster, B., Tait, R., . . . Lutti, A. (2013). Quantitative multi-parameter mapping of R1, PD(*), MT, and R2(*) at 3T: a multi-center validation. *Front Neurosci, 7*, 95. doi:10.3389/fnins.2013.00095

Wetzels, R., & Wagenmakers, E. J. (2012). A default Bayesian hypothesis test for correlations and partial correlations. *Psychon Bull Rev, 19*(6), 1057-1064. doi:10.3758/s13423-012-0295-x

Wolff, N., Mückschel, M., Ziemssen, T., & Beste, C. (2018). The role of phasic norepinephrine modulations during task switching: evidence for specific effects in parietal areas. *Brain Structure and Function, 223*(2), 925-940. doi:10.1007/s00429-017-1531-y

Wonderlick, J. S., Ziegler, D. A., Hosseini-Varnamkhasti, P., Locascio, J. J., Bakkour, A., van der Kouwe, A., . . . Dickerson, B. C. (2009). Reliability of MRI-derived cortical and subcortical morphometric measures: effects of pulse sequence, voxel geometry, and parallel imaging. *NeuroImage, 44*(4), 1324-1333. doi:10.1016/j.neuroimage.2008.10.037

Worringer, B., Langner, R., Koch, I., Eickhoff, S. B., Eickhoff, C. R., & Binkofski, F. C. (2019). Common and distinct neural correlates of dual-tasking and task-switching: a meta-analytic review and a neuro-cognitive processing model of human multitasking. *Brain Struct Funct, 224*(5), 1845-1869. doi:10.1007/s00429-019-01870-4

Yakunina, N., Kim, S. S., & Nam, E. C. (2017). Optimization of Transcutaneous Vagus Nerve Stimulation Using Functional MRI. *Neuromodulation, 20*(3), 290-300. doi:10.1111/ner.12541

Yerkes, R. M., & Dodson, J. D. (1908). The relation of strength of stimulus to rapidity of habit-formation. *Journal of comparative neurology and psychology, 18*(5), 459-482.

Yeung, N., Nystrom, L. E., Aronson, J. A., & Cohen, J. D. (2006). Between-task competition and cognitive control in task switching. *The Journal of Neuroscience, 26*(5), 1429-1438. doi:10.1523/jneurosci.3109-05.2006

Yuan, H., & Silberstein, S. D. (2016). Vagus Nerve and Vagus Nerve Stimulation, a Comprehensive Review: Part I. *Headache, 56*(1), 71-78. doi:10.1111/head.12647

Zecca, L., Stroppolo, A., Gatti, A., Tampellini, D., Toscani, M., Gallorini, M., . . . Zucca, F. A. (2004). The role of iron and copper molecules in the neuronal vulnerability of locus coeruleus and substantia nigra during aging. *Proceedings of the National Academy of Sciences of the United States of America, 101*(26), 9843-9848. doi:10.1073/pnas.0403495101

Zwanenburg, J. J. M., Visser, F., Hendrikse, J., & Luijten, P. R. (2013). Unexpected lateral asymmetry in TSE image contrast explained: tissues with short T2 show extreme sensitivity to B1 inhomogeneity. *Poster presented at the ISMRM 21st Annual Meeting. Salt Lake City, Utah, USA*.

# Acknowledgments

**Acknowledgments**

The journey that led to this Phd dissertation has been one of the most exciting in my life, therefore I would like to acknowledge those who made this journey possible and stood by me. The university has strict limitations regarding the number of words, so I have to keep this section short.

First of all, I would like to thank my supervisors Sander and Birte for making an umbrella under which I could do my research with great freedom. Many thanks for supporting my perfectionistic approach, allowing me to perform additional experiments and for your perspicacious approach in research. It has been an amazing and inspiring journey!

Max, thank you very much for teaching me the stunning technical aspects of brain mapping. But above all, thank you for all the positive energy during our collaborative work and for our inspiring discussions about open science and making research available to the public.

Thijs, thank you for encouraging me to unleash my potential. I started with little knowledge on MRI physics but your calming attitude and guidance helped me to explore the amazing treasures of MRI physics and solve my puzzles.

This journey was made more fun thanks to the LC- NE research group. Arni, Chris, Peter, Rudi and Stephen, thank you for the nice lunch breaks, conferences, collaborations, scientific discussions, and all the screams over the foosball table. It taught me in practice something that I took long to accept: that breaks are refreshing for the brain and essential for high performance.

My colleagues at the Cognitive Psychology unit created an inspiring atmosphere during the years of my Phd, so I would like to thank all of them and express my gratitude. Gezinus, Wido, Eva, Pauline, Marieke, Roberta, Alessandra, Roy, Kerwin, Henk, Guido, Laura, Roel, Evy, Roderik, Pascal, Saskia, Claudia, Lorenza, Bernhard, Mariska, Eliska, Iliana, Zsuzsika, Anne, Szymon, Luisa, Eliska, and Bryant thanks for the lab meetings, debates, unit outings, collaborations, social events and guidance. I would also like to thank ***all*** my friends and colleagues at the units of clinical, social and health psychology, at the LIBC center, the Gorter Center for High Field MRI (LUMC), Curium-LUMC, and the "Integrative Model-based Cognitive Neuroscience (IMCN) research unit" (UvA) who made this journey so interdisciplinary and fun.

Academia is a marathon, not a sprint, and this long run would not have been possible without the support of friends, extracurricular groups and family members. I would therefore like to thank the Phd advisors, my friends from the "ISN theater group" and those from the group "2pR- dances". Particular thanks go to Christos, Andreas and Mary who contributed to my "dance your Phd" video (contest for the scientific journal "Science").

Ilia, Theodore and Job many thanks for translating the layman abstract of the dissertation in Albanian and Dutch language. Sofia, thanks for designing the cover page of this thesis.

Zisi, Christina, Teo, Malvina, Kiki, Elina, Victoria, Vaso, Efi, Javi, Manuel, Perikli, Thaleia, Lieneke, Alessio, Christina, Eleni, Gio, Job, Marieke and Antonia, your support and friendship have been valuable to me during this trip. Χίλια ευχαριστώ!

Words cannot express how grateful I am to my family, therefore in the following section I would like to thank them (in Greek) for their support. My grandpa Apostolis, who was the first one to teach me how to write and become a person of virtue who helps his fellow man. My grandpa Manolis and grandma Frosyna, for their love and discussions in the vineyard about philosophy and the effects of (nor) adrenaline. My parents for their sweetness and trust. I have always admired their strength and virtue. Finally, my gratitude is also addressed to Zisoulis, my uncles, aunts and cousins who make me feel a member of a strong and protective network. This helps me to welcome with pleasure every challenge that life and research bring to my path.

Παππού Αποστόλη, ήσουν ο πρώτος που μου έμαθε γράμματα και επέμενε να απαγγέλνω όλα τα ποιήματα απ' έξω, κι ας έλεγαν οι δάσκαλοι πως δεν χρειάζεται. Η αγάπη σου για την μόρφωση και την ανατροφή ενός ανθρώπου ώστε να γίνει ένας Σωστός Άνθρωπος, «με μυαλό», αρετή, αξιοπρέπεια, ο οποίος να σέβεται και να βοηθάει τον συνάνθρωπό του, αποτέλεσαν φάρο για εμένα όλα αυτά τα χρόνια. Οι συμβουλές σου θα με ακολουθούν για πάντα.

Παππού Μανόλη και γιαγιά Φροσύνα, σας ευχαριστώ για την αγάπη και την έγνοια σας κάθε φορά που μιλούσαμε για τα νέα μου και για την έρευνα. Παππού, οι συζητήσεις μας στο αμπέλι περί φιλοσοφίας και τις επιδράσεις της (νορ)αδρεναλίνης εύφραιναν την ψυχή μου και ανυπομονώ να τις συνεχίσουμε (κάτω από την δροσερή σκιά των δέντρων πάντα). Ous ni videm di apropia trore!

Πατερούλη, η γλύκα του χαρακτήρα σου, η κατανόηση, και η εμπιστοσύνη που μου δείχνεις μου δίνουν πάντα δύναμη. Μάνα, η ικανότητα, η οξυδέρκεια, και η πολυπραγμοσύνη σου με κάνουν να αναρωτιέμαι εάν ποτέ θα καταφέρω να σε φτάσω έστω και στο μικρό σου δαχτυλάκι. Πάντοτε θαύμαζα το πόσο δυνατοί και ταυτοχρόνως πόσο σωστοί άνθρωποι είσαστε. Αποτελείτε παράδειγμα για μένα σε όλους τους τομείς της ζωής.

Τέλος, η ευγνωμοσύνη μου απευθύνεται και στον Ζησούλη, στους θείους, θείες και τα ξαδέρφια μου. Με κάνετε να αισθάνομαι πάντα αποδεκτή και μέλος ενός δυνατού και προστατευτικού δικτύου. Αυτό με βοηθάει να καλωσορίζω με ευχαρίστηση και δύναμη κάθε πρόκληση που φέρνουν στην πορεία μου η έρευνα και και η ζωή. Σας ευχαριστώ μέσα από την καρδιά μου!

# About the author

Klodiana - Daphne Tona was born in 1985 in Kamenitsa, Albania. She completed her elementary school in Greece (Macedonia region), and her secondary school and high school in Athens in 2004. She received her Diploma in Psychology from the National and Kapodestrian University of Athens (4 years programme; summa cum laude). During her studies, she spent one semester at Utrecht University in the Netherlands as a recipient of the Erasmus scholarship grant. She also performed two clinical internships in mental health units in Athens and – at an extracurricular basis – an additional training as an assistant neuropsychologist in a unit with demented patients (Department of Neurology, Aeginition hospital, Athens). This is where she "fell in love with brains", and decided to move back to the Netherlands to acquire a research master's degree in Cognitive Neuroscience (at Radboud University, Nijmegen; graduated in 2012). Here she did her research internship in the lab of Prof. Guillén Fernández at Donders Center for Cognitive Neuroimaging. After that, she moved to Leiden to do her doctoral research under the supervision of Prof. Sander Nieuwenhuis and Prof. Birte Forstmann (Cognitive Psychology Unit, Leiden University). Here she applied an interdisciplinary approach combining the fields of cognitive & clinical neuroscience and methodologies such as pharmacology, psychophysiology, and ultra-high resolution 7T MRI. As part of this research, Daphne also visited the University of Amsterdam for MRI analysis of brainstem data (in close collaboration with dr. Max. Keuken) and for analysis of alpha-amylse and salivary cortisol data (at the lab of dr. Jos Bosch). The results of her doctoral work are outlined in this dissertation.

During her PhD project Daphne has been involved in the organization of several symposia & meetings and also served as board member of several initiatives. She served as the Social Events Officer for the Leiden PhD Association (Leids Promovendi Overleg; LEO). She also served as the local representative for the March for Science Event (2017), given that she believes in evidence-based, science-informed public policies. Finally, she joined powers with 10 PhD candidates from 5 Dutch Universities to do research that provide solutions to wicked societal challenges (i.e. enhance sustainability of the healthcare system) in collaboration with business experts (extracurricular initiative "SMO-Promovendi"). Currently she is one of the coordinators of the Stress and Emotion Hotspot at Leiden Institute for Brain and Cognition (LIBC).

Upon the completion of her doctorate research, Daphne started working as a researcher and lecturer at the Clinical Psychology Unit at Leiden University and as a post-doctoral researcher at Curium-LUMC, a mental health unit for children and adolescents. Here she uses her interdisciplinary knowledge to create a better future for the young generation.

Her passion is to combine cognitive and clinical neuroscience and to put scientific knowledge at the service of society in order to a) enhance resilience, b) promote healthcare, c) advance social justice, and d) contribute to a better society. She is enough of a realist to understand that this is not an easy enterprise, but she is more of a stubborn to die trying.

## List of publications

***Peer reviewed scientific articles:***

Tona, K.D., Revers, H., Verkuil, B., & Nieuwenhuis, S. (in press). Noradrenergic regulation of cognitive flexibility: no effects of stress, transcutaneous vagus nerve stimulation and atomoxetine on task-switching.

Odintsova V.V., Roetman P.J, Ip H.F., Pool R., Van der Laan C.M., Tona K.D., Vermeiren R.R.J.M. & Boomsma D.I. (2019), Genomics of human aggression: current state of genome-wide studies and an automated systematic review tool., Psychiatric Genetics 29(5): 170–190.

Tona, K.D., van Osch, M.J.P., Nieuwenhuis, S., & Keuken, M.C. (2019). Visualizing the human locus coeruleus in vivo at 7 Tesla MRI. PLoS ONE, 14: e0209842.

Warren, C.M., Tona, K.D., Ouwerkerk, L., van Paridon, J., Poletiek, F., van Steenbergen, H., Bosch, J.A., & Nieuwenhuis, S. (2019). The neuromodulatory and hormonal effects of transcutaneous vagus nerve stimulation as evidenced by salivary alpha amylase, salivary cortisol, pupil diameter, and the P3 event-related potential. Brain Stimulation, 12, 635-642.

Tona, K.D., Keuken, M.C., de Rover, M., Lakke, E., Forstmann, B.U., Nieuwenhuis, S., & van Osch, M.J.P. (2017). In vivo visualization of the locus coeruleus in humans: Quantifying the test-retest reliability. Brain Structure and Function, 222, 4203-4217.

van den Brink, R.L., Pfeffer, T., Warren, C.M., Murphy, P.R., Tona, K.D. van der Wee, N.J., Giltay, E.J., van Noorden, M.S., Rombouts, S.A., Donner, T.H., & Nieuwenhuis, S. (2016). Catecholaminergic neuromodulation shapes intrinsic MRI functional connectivity in the human brain. Journal of Neuroscience, 36, 7865-7876.

Warren, C.M., Eldar, E., van den Brink, R.L., Tona, K.D., van der Wee, N.J., Giltay, E.J., van Noorden, M.S., Bosch, J.A., Wilson, R.C., Cohen, J.D., & Nieuwenhuis, S. (2016). Catecholamine-mediated increases in gain enhance the precision of cortical representations. Journal of Neuroscience, 36, 5699-5708.

Kroes M.C.W., Tona K.D., Den Ouden H.E.M., Vogel S., Van Wingen G.A. & Fernandez G. (2016), How administration of the beta-blocker propranolol prior to extinction can prevent the return of fear, Neuropsychopharmacology 41: 1569-1578.

Tona, K.D., Murphy, P.R., Brown, S.B., & Nieuwenhuis, S. (2016). The accessory stimulus effect is mediated by phasic arousal: a pupillometry study. Psychophysiology, 53, 1108-1113.

Sellaro, R., van Leusden, J.W., Tona, K.D., Verkuil, B., Nieuwenhuis, S., & Colzato, L.S. (2015). Transcutaneous vagus nerve stimulation (tVNS) enhances post-error slowing. Journal of Cognitive Neuroscience, 27, 2126-2132.

Brown, S.B., Tona, K.D., van Noorden, M.S., Giltay, E.J., van der Wee, N.J., & Nieuwenhuis, S. (2015). Noradrenergic and cholinergic effects on speed and sensitivity measures of phasic alerting. Behavioral Neuroscience, 129, 42-49.

Olde Rikkert M., Tona K.D., Janssen L., Burns A., Lobo A., Robert P., Sartorius N., Stoppe G. & Waldemar G. (2011), Validity, Reliability and Feasibility of Clinical Staging Scales in Dementia: a Systematic Review, American Journal of Alzheimer's Disease & Other Dementia 26(5): 357-365.

***Books:***
Berge J., Blok J., Maldonado C.G., Heckendorf E., Holst-Bernal S., Noten M., Silva C. da, Tona K.D., Truijens D. & Verlinden E. (2018), Riding the techwave in an era of change: The healthcare guide to the future. Rotterdam: Stichting Maatschappij en Onderneming.

***Data & Brain Atlas:***
https://www.nitrc.org/projects/prob_lc_3t

## *Data availability*

All extracted data from the MRI sequences and code used to analyse the data

https://osf.io/83r9j/?view_only=a9e469fac61e4731a5e1cb7ade3ab9a2.

***March for Science :***
https://www.youtube.com/watch?time_continue=59&v=cwoUSG7Sd6o&feature=emb_logo